

THEOPHRASTE, NOUSSI. Ph.D. Defining nanoscale genetic interactions between the bacterium *E. coli* and engineered nanoparticles for biomedical and environmental remediation applications. (2023)

Directed by Dr. Dennis R. LaJeunesse. 293 pp.

The production of engineered nanoparticles is on the rise worldwide. Engineered nanoparticles have distinct physicochemical properties which enable their utilization in a variety of sectors from Biomedicine to Environmental remediation. Engineered nanoparticles interact with biological systems potentially changing the behavior of these systems by inducing specific physiological and metabolic modifications within the exposed organisms; furthermore, these responses to engineered nanoparticles may also differ from one organism to another. While a great deal of work has been done to identify lethal/antimicrobial nanomaterials to control pathogenic microbial biofilm formation, little work has been done to study non-lethal impact of nanomaterials on microbes. Moreover, the genetic impact of this cell-nanoparticle interaction is not well understood. We have defined the transcriptional genetic response of the gram-negative bacterium *Escherichia coli* (*E. coli*) to three different engineered silica, gold, and polystyrene nanoparticles. Screening an *E. coli* reporter gene library that covers 70% of the *E. coli* genome, we have identified eight genes that are upregulated in response to nanoparticle exposure and possibly represent a common nanoparticle response mechanism. These eight genes have been verified using qRT-PCR and include previously identified stress response genes (*rssB*, *evgA*, *sodC*), genes encoding transports (*yhdY*, *yhhT*) and several genes with unknown function (*glcC*, *vacJ/MlaA*, *cysQ*). The gene ontology of the eight genes shows that metabolic pathways, signal transduction pathways, oxidative stress and protein transport systems are significantly affected in response to the three nanoparticle exposures. Interestingly, the growth curves analysis of the single gene knockout of the eight genes reveals that the exposure to nanoparticles likely increase

the cell growth rate in all mutants when compared to control and no growth pattern alterations with the wild type *E. coli* is observed. Furthermore, only the two mutants Δ sodC and Δ CysQ show significant exponential growth rates compared to control. These results demonstrate that there is specific common response of *E. coli* to round-shaped metalloid, metal, and polymeric nanoparticles and suggest that both sodC and cysQ genes are inherent in the bacterial growth mechanism during normal growth conditions. Overall, this research will provide a better understanding of bacteria stress response as well as bacterial resistance to nanoparticle-based antibiotics and identify potential new targets for drugs given that the bacteria-nanoparticle interactions have crucial implications in public health and the environment.

DEFINING NANOSCALE GENETIC INTERACTIONS BETWEEN THE BACTERIUM E.

COLI AND ENGINEERED NANOPARTICLES FOR BIOMEDICAL AND

ENVIRONMENTAL REMEDIATION APPLICATIONS

by

Theophraste Noussi

A Dissertation
Submitted to
the Faculty of The Graduate School at
The University of North Carolina at Greensboro
in Partial Fulfillment
of the Requirements for the Degree
Doctor of Philosophy

Greensboro

2023

Approved by

Dr. Dennis R. LaJeunesse
Committee Chair

DEDICATION

This dissertation is dedicated to my mother Anne Pokam whose dedication to Earth and her unwavering support have been unlimited sources of inspiration for me during this journey. To my siblings, other family members and friends, for their continuous love, support, and advice during the completion of this work.

APPROVAL PAGE

This dissertation written by Theophraste Noussi has been approved by the following committee of the Faculty of The Graduate School at The University of North Carolina at Greensboro.

Committee Chair

Dr. Dennis R. LaJeunesse

Committee Members

Dr. Eric Josephs

Dr. Tetyana Ignatova

Dr. Jeffrey Alston

March 17, 2023

Date of Acceptance by Committee

March 13, 2023

Date of Final Oral Examination

ACKNOWLEDGEMENTS

First, I would like to thank my supervisor Dr. Dennis R. LaJeunesse, for his patience, presence, scientific expertise, constant guidance, shrewdness, and great sense of humor. His tremendous mentorship, dedication to science and enthusiasm inspired me and carried me through all the stages of this dissertation work.

I would also like to express my utmost gratitude to my committee members: Dr. Eric Josephs, Dr. Tetyana Ignatova and Dr. Jeffrey Alston for their invaluable support, availability, and advice that helped me get to this incredible outcome.

Last, a special thank you to the Joint School of Nanoscience and Nanoengineering (JSNN) for providing all the resources and the amazing work environment to do research and to allow me to not only grow as a scientist but also as a good citizen of the world.

TABLE OF CONTENTS

LIST OF TABLES	viii
LIST OF FIGURES	ix
CHAPTER I: INTRODUCTION.....	1
Nanomaterials.....	1
Some prominent type of nanomaterials and their properties.....	1
Metallic nanomaterials.....	3
Metal oxide nanomaterials.....	4
Polymeric nanomaterials.....	5
Semiconductors.....	6
Organic/Carbon-based Nanomaterials.....	7
Beneficial impacts of nanomaterials	8
Impact of nanomaterials on plants	9
Impact of nanomaterial on animal systems.....	10
Impact of nanomaterials on microorganisms.....	11
Research achievements.....	12
Innovation.....	13
CHAPTER II: LITERATURE REVIEW	14
Gram-negative bacterium <i>Escherichia coli</i> (<i>E. coli</i>).....	14
Mechanisms of Bacterial adhesion.....	16
Bacterial Flagella	18
Bacterial Curli.....	19
Bacterial Pili (Fimbriae)	21
Type IV Pili	21
Type I pili.....	21
Stress responses of Gram-Negative bacteria	23
Some environmental stressors and their response mechanisms in Bacteria.....	26
Oxidative stress.....	26
Acid stress.....	28

Temperature stresses	29
Two-component regulatory systems in <i>E. coli</i>	31
Some prominent Two-component regulatory in <i>E. coli</i>	32
EvgS/EvgA system	32
PhoQ/PhoP system.....	33
How bacteria interact with nanoparticles.	34
Conclusion.....	38
CHAPTER III: TRANSCRIPTOMIC RESPONSES OF <i>E. COLI</i> EXPOSED TO ENGINEERED NANOPARTICLES	43
Introduction	43
Materials and methods	46
Materials	46
Methods	47
Characterization of nanoparticles	47
Fixation of <i>E. coli</i> cells with nanoparticles.....	47
Bacteria exposure to nanoparticles	48
Quantitative analysis of the gene expression.....	49
RNA extraction	49
Quantitative PCR of the 8 cluster genes	50
<i>E. coli</i> Mutants' growth curves.....	52
Statistical analysis.....	53
Results and discussion.....	53
Characterization of nanoparticles	53
Bacterial gene screening after exposure to engineered nanoparticles	54
Verification of the gene expression of the common gene response to all three nanoparticles.....	61
<i>E. coli</i> mutants' growth curves.....	66
Discussion	72
The common gene response: Gene expression profile and growth fitness of <i>E. coli</i>	72
Conclusion.....	75
CHAPTER IV: EXPRESSION OF OXIDATIVE STRESS RELATED GENES IN <i>E. COLI</i> AT THE INTERFACE OF CHARGED GALLIUM NITRIDE SURFACES	76

Introduction	76
Experimental section	78
Bacteria and growth conditions	78
qRT-PCR	80
Results and discussion.....	80
Substrate treatment and properties overview	82
Explanation of the pathways probed.....	82
katE expression	84
sodB results	86
oxyS results.....	88
Summary of gene expression results	91
Conclusions	95
CHAPTER V: CONCLUSIONS AND FUTURE DIRECTIONS	96
Conclusions	96
Future research recommendations.....	97
REFERENCES	99
APPENDIX A: FUNCTIONS OF GENES DIFFERENTIALLY EXPRESSED BY THE NANOPARTICLES.....	142
APPENDIX B: LIST OF GENES TESTED FROM THE E. COLI PROMOTER LIBRARY .	145

LIST OF TABLES

Table 1: Alternative sigma factors in <i>E. coli</i>	26
Table 2: Nanoparticle impact on microorganisms	40
Table 3: Primer selection	49
Table 4: Table of mutants	51
Table 5: DLS results of the nanoparticles including average size and zeta potential values.....	54
Table 6: List of the cluster genes activated by all three nanoparticles.	60
Table 7: Parameters of the eight <i>E. coli</i> mutants' growth curves. (*) represents the statistically significant difference between wild type and mutants and (**) represents the statistically significant difference between nontreated (control) and nanoparticle-treated <i>E. coli</i> mutants. ...	69
Table 8: Primer selection for RTPCR.....	80
Table 9: Fold-change in gene expression between the charged and uncharged surfaces	83

LIST OF FIGURES

Figure 1: Schematic representation of the classification of nanomaterials based on dimensionality with some examples.	3
Figure 2: Schematic representation of 2 types of polymeric nanoparticles (nanosphere and nanocapsule) for drug delivery applications.	6
Figure 3: Diagram of the beneficial effects of the nanoparticles on some living organisms.....	9
Figure 4: Cell wall structure of the Gram-negative bacteria <i>E. coli</i>	15
Figure 5: Schematic representation of a bacterial flagellum	18
Figure 6: Schematic representation of a bacterial curli	20
Figure 7: Schematic representation of the <i>fim</i> domains of a matured type I pilus.....	23
Figure 8: Illustration of the general stress response mechanism in Bacteria	25
Figure 9: Oxidative stress response mechanism in bacteria	28
Figure 10: Acid stress responses in bacteria. 1-proton efflux by H ⁺ -ATPase apparatus; 2-decrease in cell membrane fluidity; 3-membrane channel size modification; 4- proton pump....	29
Figure 11: proposed Cold and Heat stress responses in bacteria.	30
Figure 12: Schematic of the two-component regulatory systems (TCS) in Bacteria.	32
Figure 13: Transcriptional cascades initiated by both EvgS/EvgA and PhoQ/PhoP systems. The red arrow represents the connection between the two TCS via the protein B1500.....	34
Figure 14: Proposed common mechanism of action of metal, metal oxide and polymeric nanoparticles.	38
Figure 15: <i>E. coli</i> promoter library description	47
Figure 16: Experimental design of the <i>E. coli</i> promoter library exposure to nanoparticles.	48
Figure 17: <i>E. coli</i> mutants growth curves experiment.	52
Figure 18: SEM images of nanoparticles: (a) Silica, (b) gold, and (c) polystyrene nanoparticles. Size distribution histograms of (d) silica, (e) gold, and (f) polystyrene nanoparticles.	54
Figure 19: Number of genes significantly regulated by all three nanoparticles.	56
Figure 20: Distribution of up-regulated genes at each time point.	57

Figure 21: Venn diagram showing the total number of genes significantly expressed in presence of silica, gold and polystyrene nanoparticles. Blue = up-regulated genes, red = down-regulated genes.	58
Figure 22: SEM images of the <i>E. coli</i> with nanoparticles. (a) Control, (b) silica Nps, (c) polystyrene Nps and (d) gold Nps. the red arrows show the attachment of nanoparticles to the bacteria cell wall.	59
Figure 23: Differential expression of the eight genes after exposure to silica (red), gold (green), and polystyrene (orange) nanoparticles. (*) indicates the statistical significance compared to control.	63
Figure 24: <i>E. coli</i> mutants growth curves from exposure to silica, gold, and polystyrene nanoparticles.	71
Figure 25: Gene ontology of genes activated by Nanoparticles.	73
Figure 26: Proposed model of <i>sodC</i> and <i>cysQ</i> genes in the regulation of normal cell growth in <i>E. coli</i>	74
Figure 27: Relative Ct values of <i>katE</i> expression for the a) WT, b) Δ fliC, and c) Δ csgG <i>E. coli</i>	84
Figure 28: Relative Ct values of <i>sodB</i> expression for the a) WT, b) Δ fliC, and c) Δ csgG <i>E. coli</i>	87
Figure 29: Relative Ct values of <i>oxyS</i> expression for the a) WT, b) Δ fliC, and c) Δ csgG <i>E. coli</i>	89

CHAPTER I: INTRODUCTION

Nanomaterials

The recent years have seen a gigantic increase in production of synthetic/engineering nanomaterials for a vast array of real-world applications especially in fields such as biomedicine, agriculture, electronics, pharmaceuticals, cosmetics, and the manufacturing industry (Saleh, 2020). Nanomaterials are defined as natural or synthetic materials with less than 100 nm in size at least in one dimension which endow these materials with distinctive physical and chemical properties that are different from their bulk counterparts (Kolahalam et al., 2019; Miernicki et al., 2019; Saleh, 2020).

Nanomaterials exist in a variety of morphologies and are categorized based on their dimensionality. For instance, nanomaterials such as quantum dots and nanoparticles are zero-dimensional (0-D) as all three dimensions are in the nanoscale range. One-dimensional nanomaterials (1-D) have one dimension in the nanoscale range and include materials such as nanorods and nanotubes. Two-dimensional nanomaterials (2-D) possess two dimensions in the nanoscale range and one out of it, these include nanolayers and nanofilms. Three-dimensional nanomaterials (3-D) are not in nanoscale dimensions but are made of nanoscale components, these are mostly nanocomposites (Figure 1) (Gleiter, n.d.; Kolahalam et al., 2019).

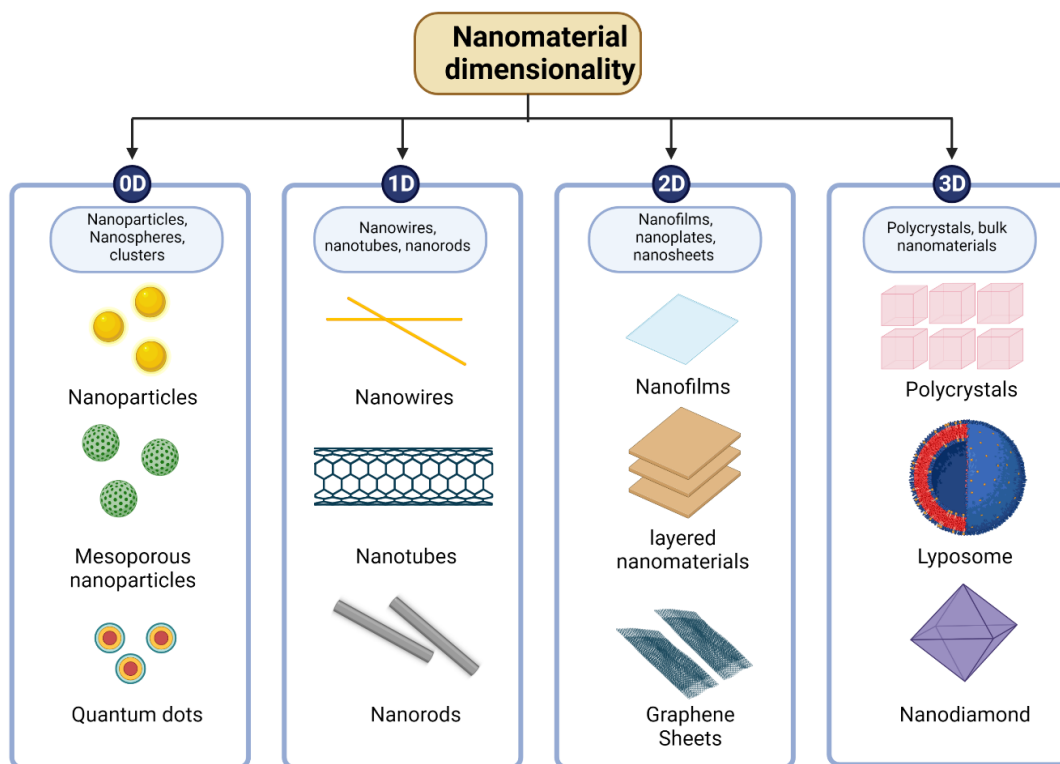
Some prominent type of nanomaterials and their properties

Many nanomaterials exhibit unique, tunable, and/or size- dependable properties (Datta et al., 2008). Because of this, nanomaterials attract a great deal of interest compared to the parent “bulk” materials. For instance, simply changing the size of the nanomaterials often results in changes to mechanical, chemical, electrical, and optical properties (Saleh, 2020). The shape and

size of nanomaterials influence their properties and often result in new physicochemical capabilities.

Another important characteristic of nanomaterials is their chemical composition. The chemical composition plays a key role in defining unique properties in nanomaterials through the nature of the core material, surface reactivities, and the large surface-to-volume area (Dekkers et al., 2019). For instance, metal nanomaterials like gold or copper Nps possess core inorganic materials and shells that could be of inorganic, organic nature (Khan et al., 2019). Nanomaterials have been synthesized from a variety of materials included carbon-based nanomaterials, metals nanomaterials, metal-oxide nanomaterials, polymeric nanomaterials, semiconductors, and lipid-based nanomaterial (Gleiter, n.d.).

Figure 1: Schematic representation of the classification of nanomaterials based on dimensionality with some examples.



Metallic nanomaterials

The core chemical element of metallic nanomaterials is any metallic element including iron, copper, zinc and gold. Various chemicals and photochemical methods have been developed to synthesize metal nanomaterials (Kolahalam et al., 2019). Furthermore, the size and properties of many metal nanomaterials depend heavily on the method used for synthesis. For instance, gold nanoparticles that are synthesized via a combination of sonoelectrochemical and ultrasonic vibration techniques (Saleh, 2020; Shiau et al., 2018) result in nanoparticles that contain reduced size which increases the availability of atoms on the surface of the material making it more active compared to the metal bulk compound; This characteristic provides a high surface area reactivity that has been exploited for applications such as catalysis, biosensing, bioimaging and

absorption processes (Kolahalam et al., 2019). metallic nanomaterials have impressive size dependable optical properties (Kelly et al., 2003). That interaction with light is promoted by the surface plasmon and the quantum confinement of electrons (Saleh, 2020). For instance, gold nanoparticles display different colors in variation of their size, shape and percentage of gold concentrations which influence its absorption properties when interacting with light (Khan et al., 2019).

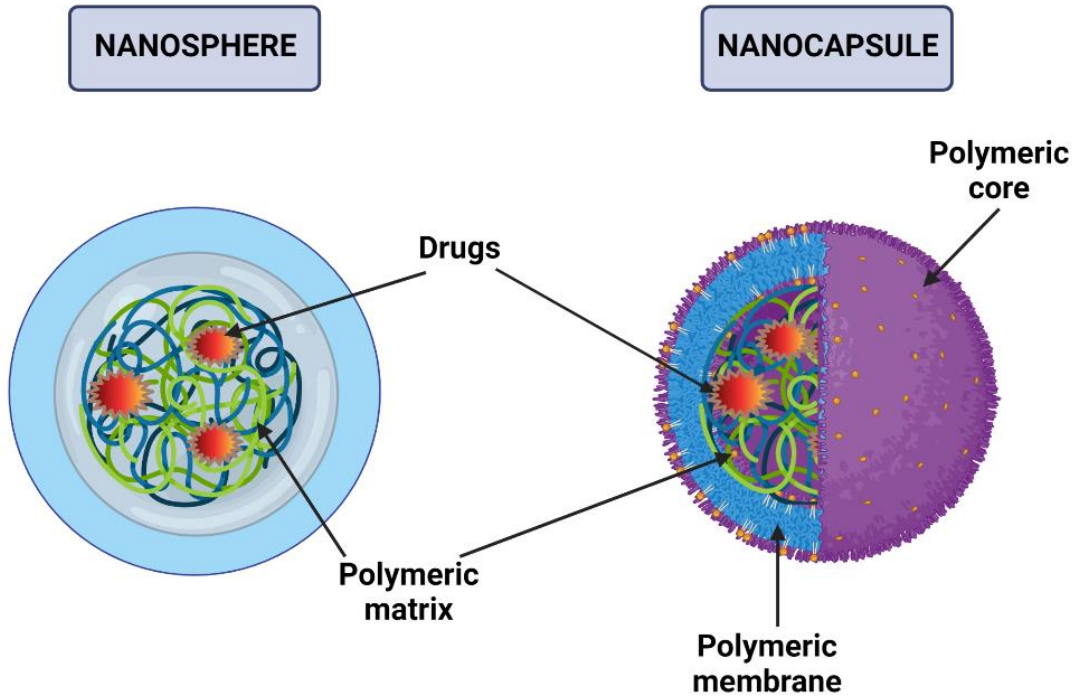
Metal oxide nanomaterials

Metal oxide nanomaterials retain their elemental core and are distinguishable from metallic nanomaterials by their unique physicochemical properties that offer a high density and limited size of corners and edges at their surfaces (Chavali & Nikolova, 2019). Furthermore, the electronic structure defines the conductor, semiconductor and insulator properties of these materials (Yoon et al., 2022). Metal oxides nanomaterials have been synthesized by sol-gel or hydrothermal reactions (Parashar et al., 2020). Similar to metallic nanoparticles, the change in size of metal oxide nanomaterials alter the chemical, magnetic, electrical, and conducting properties (Chavali & Nikolova, 2019; W.-T. Liu, 2006). In addition to specific chemical and physical properties, biocompatibility which is the ability of a material to interact with biological systems without exerting toxic activities to their biological functions, is often major characteristic of these materials. Their biocompatibility come from the fact that most metal oxide nanoparticles have a core inorganic element that is already part of some metabolic processes, and this enables their assimilation into biological systems (Ling & Hyeon, 2013). Because of their biocompatibility, metal-oxide nanoparticles are important in applications such as environmental remediation and biomedicine (Chavali & Nikolova, 2019; Saleh, 2020).

Polymeric nanomaterials

Polymeric nanomaterials are nanoscale materials made of natural or synthetic polymers such as polystyrene nanoparticles (Loos et al., 2014). These materials demonstrate a great potential in pharmaceutical and medical applications as drug carriers in drug delivery processes (Soppimath et al., 2001; Zielińska et al., 2020). The size, shape, biocompatibility, and stability are among the distinctive properties that possess polymeric nanomaterials and can be affected by the type of synthesis methods used (Jawahar & Meyyanathan, 2012). The production methods consist of solvent evaporation, polymerization of monomers, emulsification/solvent diffusion, nanoprecipitation, dispersion of polymers and more (Soppimath et al., 2001; Zielińska et al., 2020). Nanospheres or nanocapsules are obtained at the end of the synthesis process as shown in Figure 2 (Christoforidis et al., 2012).

Figure 2: Schematic representation of 2 types of polymeric nanoparticles (nanosphere and nanocapsule) for drug delivery applications.



Semiconductors

Semiconductors are materials that possess both electrical properties of a conductor and an insulator material. Semiconductor materials have band gaps that are relatively small compared to conductors and insulators. The commonly used inorganic semiconductors exist as single elements like Silicon and Germanium or as compounds of elements like SiC, GaAs and more (Tipler & Llewellyn, 2008). Semiconductors have unique electrical properties. The type of conductivity of inorganic semiconductors resides in the nature of the chemical element known as impurity added to an intrinsic semiconductor material in a process called doping which results in creation of whether the n-type or p-type semiconductors (Tipler & Llewellyn, 2008). The difference between the n-type and the p-type is the charge carrier. The charge carrier in n-type is electrons and holes in p-type semiconductors (Tipler & Llewellyn, 2008). Semiconductor

materials can be inorganic and organic in nature (Tipler & Llewellyn, 2008). Some inorganic semiconductors are biocompatible such as elemental Silicon (Si), Silicon Carbide (SiC), and Gallium Nitride (GaN). For example, GaN is a binary III-V wide bandgap semiconductor with a value of 3.4eV used in power conversion devices and in the fabrication of light-emitting diodes (An et al., 2016). Recently, many studies have been conducted on gallium Nitride interaction with biological organisms such as microbes because of the optoelectronic feature presented as the persistent photoconductivity (PPC) property which is defined as the charge accumulation on GaN surface after exposure to UV light, altering the morphology and the genetic responses of the organism of interest (Snyder, Reddy, et al., 2018).

Organic/Carbon-based Nanomaterials

Nanomaterial composed of carbon and carbon-based compounds, including biological materials fall into this category; many of these nanomaterials display properties found in metallic and metal oxide nanomaterials and recently, this has increased interest in these materials. There are different types of carbon-based nanomaterials, The carbon-based nanomaterials commonly and widely used are Graphite, graphene, fullerene, carbon black, carbon nanotubes, graphite, graphene oxide and reduced graphene oxide (Madannejad et al., 2019).

Due to their composition, shape and size, organic/carbon-based nanomaterials display a range of distinctive physicochemical properties (Mauter & Elimelech, 2008). Organic/Carbon-based Nanomaterials display distinct electrical, mechanical, and physical properties that are intrinsically dependent on the carbon's structure and hybridization state during synthesis processes (Li et al., 2019). For instance, Graphite is a crystalline form of pure carbon present in nature; it can be both naturally and synthetically produced through contact or regional metamorphism of sedimentary organic matter and from coke and pitch respectively (Chehreh

Chelgani et al., 2016). Graphite has great electrical properties and can have both metallic and non-metallic characteristics (Sengupta et al., 2011). Another example is Graphene which is known as the two-dimensional allotropic form of the sp² hybridized carbon and possessed a myriad of properties such as large surface area, thermal stability, high electrical conductivity, optical transparency and more that are currently used for various applications including electronics, biosensing, biomedicine and environmental remediation (Huang et al., 2011; Mbayachi et al., 2021). Carbon nanotubes (CNTs) exhibit impressive mechanical characteristics such as rigidity as well as flexibility (Ajayan, 1999; Li et al., 2019). There are two major CNTs: Single-walled carbon nanotubes (SWNTs) and multiwalled carbon nanotubes (MWNTs). On one hand, SWNTs have a great optical absorption near-infrared range which has attracted a great deal of attention for research in the photo-thermal field and photoacoustic imaging (Tasis et al., 2006). MWNTs are extremely hydrophobic which make them bioincompatible and thus hinder their application in biological and biomedical settings (Li et al., 2019; Saleh, 2020; Tasis et al., 2006).

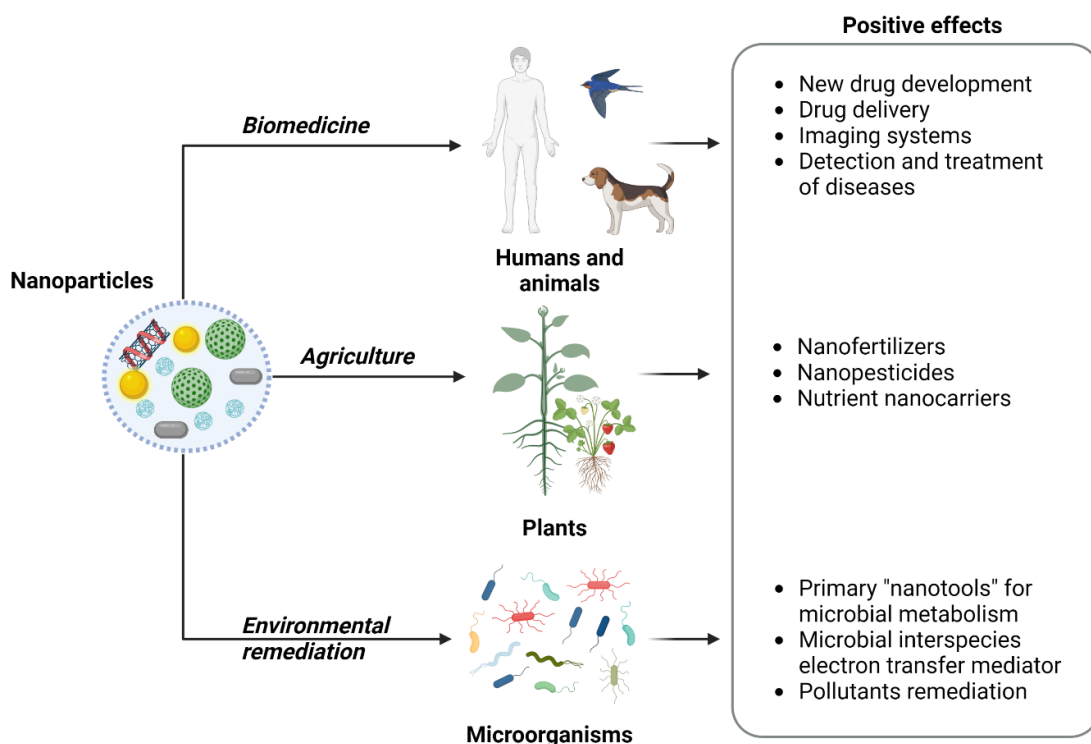
Beneficial impacts of nanomaterials

Engineered nanomaterials play important roles in many industrial processes and are produced through rigorous physical, mechanical, and chemical processes along with sophisticated lab procedures and are present in almost all aspects of everyday life, from telecommunications to personal care products (Hochella et al., 2019). However, anthropogenic activities often lead to the unexpected, intentional, or fortuitous production of synthetic nanoscale materials (Ermolin & Fedotov, 2016; Hochella et al., 2015). Incidental nanomaterials are often formed by unpremeditated man-made activities and are produced from various sources including industrial waste, mining waste, metal corrosion. Despite the differences in origin

between incidental and engineered NMs, incidental nanoscale materials interact with all the environmental compartments and thus, impact the organisms living in the air, marine, and terrestrial ecosystems (Hochella et al., 2019).

Nanotechnology has revolutionized many industries that transformed lives by enhancing the already existing traits of their finished products via usage of nanomaterials. While engineered nanomaterials have proven to be beneficial at many levels of the society, (Figure 3), the impact of these incidental nanomaterials on living systems remains unclear.

Figure 3: Diagram of the beneficial effects of the nanoparticles on some living organisms



Impact of nanomaterials on plants

The application of nanomaterials within the agricultural sector has increased, recent reports have stated that the crop productivity of soybean can be increased by 16.74%, 10.29% for rice, 28.81% for winter wheat, 10.93% for spring maize and 12.34-19.76% for vegetables with

the use of nanofertilizers compared to standard fertilizers (Shang et al., 2019). The overarching goal of the use of nanomaterial in agriculture is to increase the crop yield as well as the quality of crops (Rastogi et al., 2017). Agricultural nanomaterials are produced in the form of nanofertilizers to improve soil quality by increasing the bioaccessibility of nutrients in soils, therefore promote the plant growth (Ahmed et al., 2021; Mejias et al., 2021); nanopesticides to mitigate plant parasite attack; and nano-herbicides to eliminate invasive plant species that hinder the crop growth (Chaud et al., 2021; Deka et al., 2021). For instance, single-walled carbon nanohorns increase the rate of the seed germination in crops like tomato, rice, corn, and soybean (Lahiani et al., 2015). As nanocarriers, mesoporous silicon nanoparticles can efficiently usher targeted molecules to plants (P. Wang et al., 2016). Iron oxide nanoparticles improve root length, height, and biomass of peanut plants (Rui et al., 2016). Encapsulated herbicide in chitosan nanoparticle cores drastically increases the herbicide ability in the soil (Maruyama et al., 2016). In addition, some nanoparticles have been used as nanosensors to monitor the soil geochemical parameters imperative for healthy plant growth (Sharma et al., 2021).

Impact of nanomaterial on animal systems

The recent breakthroughs in biomedicine and in the pharmaceutical industries have been defined by the use and/or incorporation of nanomaterials in devices and drugs to develop sophisticated approaches to disease detection and treatment. Also, establish innovative drug development for the cure of rare diseases and increase precision of drug delivery in biological systems (Biswas et al., 2023). The disease diagnostic is revolutionized by nanobiosensors and their ability to rapidly detect potential causes of a variety of illnesses (Ahangari et al., 2023; Hegde et al., 2022). For example, brucellosis which is a bacterial infection in both humans and livestock caused by *Brucella* can be detected using oligo-gold nanoparticles probes (Ahangari et

al., 2022). Palladium NPs based immune sensors featuring cytotoxin gene antibodies have been developed to detect the Gram-negative bacterium *H. pylori* (Zhu et al., 2022). Nanomaterials that enhanced the active molecule properties in drugs have been developed to facilitate the treatment of some diseases while improving the drug delivery process at the same time (Zhu et al., 2022). For instance, sensitive angiogenesis related disorders like critical limb ischemia that can be treated using cerium oxide Nps (Hoseinzadeh et al., 2022; Park et al., 2020). Tumor treatment of cancer in deep tissues can be efficiently targeted using a nanomaterial-based optical system for drug delivery (Ma et al., 2022; McNeil, 2011).

Impact of nanomaterials on microorganisms

Microbes interact with their world via nanoscale interaction and often produce and interact with nanomaterials of different chemical nature (Chwalibog et al., 2010; Shende et al., 2021). These interactions are driven by specific physicochemical mechanisms that trigger diverse metabolic alteration and responses in the microbial cells. The microbe-nanomaterial interaction has significant ramifications as both exist at high magnitude in every ecosystem on Earth (Hochella et al., 2019). The physiochemical characteristics of nanoparticles such as the size, shape, surface charge and composition enable them to be the primary nutrient source for enhancing microbial life compared to the bulk counterparts (Mansor & Xu, 2020). Nanoparticles can act as mediators in electron transfer processes between microbial cells of the same and different species to ensure cell-cell communication and to strengthen the biofilm structure (Y. Liu et al., 2022; R. Wang et al., 2021). For example, in presence of cadmium sulfide (CdS) nanoparticles, the non-photosynthetic bacterium *Moorella thermoacetica*, engages in a photosynthetic process that drives the formation of acetic acid from carbon dioxide (Sakimoto et al., 2016). In another example, bacteria known as magnetotactic bacteria *magnetovibrio*

blakemorei synthesize and utilize intracellularly embedded iron-based nanoparticles to control their orientation and movement within a magnetic field (Mansor & Xu, 2020).

A plethora of studies have focused on the antimicrobial effects of nanoparticles on microorganisms. While some have demonstrated the antimicrobial effects of nanoparticles at lethal concentrations on microorganisms and the metabolic and physiological alterations as specifically related to cell death (Mammari et al., 2022), little work has been done to elucidate the impact of nanomaterials at non-lethal concentrations. While some nanoparticles have shown to be detrimental to the microbial population from the single cell to the biofilm. Metal and metal oxide nanoparticles are the most intensively studied for their antibacterial, antifungal, and antiviral activities that in most cases, lead to the cell death (Slavin et al., 2017). The contribution of nanoparticles as part of the treatment of infectious diseases has been significant in society. Moreover, New nanoparticles-based drugs have been developed faster to respond to the growing increase in novel microbial infections.

The use of nanoparticles in biomedical and environmental remediation fields are ubiquitous. However, the current research landscape is focusing on the lethal antimicrobial properties of nanoparticles on diverse pathogenic microorganisms. But, the fate, adverse effects and nanotoxicity of these nanoparticles on the microbiome present in the environment are yet to be determined.

Research achievements

My goal was to determine the transcriptomic responses of the Gram-negative bacterium *Escherichia coli* (*E. coli*) to exposure of non-lethal concentrations of three distinct nanoparticles: Silica, gold, and polystyrene nanoparticles. Each of these particles were composed of different material but shared roughly the same size which endowed them with distinct chemical natures. I

found that each particle results in distinct changes to the *E. coli* transcriptome, however, there was a core response of eight genes that was demonstrated by the bacterium against all three particles. These results suggest that this bacterium has evolved a core nanomaterial response and that this core response may control changes to the cells metabolic and physiological processes. This work is critical for providing new knowledge about the nanoscale interaction of nanoparticles with bacteria for environmental remediation and biomedical applications. This work will also provide a better understanding of the genetic bacteria-nanoparticle interface while proposing potential intracellular targets for new drug development to fight against rampant bacterial resistance to nanoparticles-based antibiotics.

Innovation

The keys points of my research work include:

- 1) Determining the specific response genes of the bacterium *E. coli* associated with the exposure of silica (SiO₂), gold (Au), and polystyrene (PS) nanoparticles.
- 2) Identifying the common genetic response (8 upregulated genes) to all the three nanoparticles.
- 3) Determining the essentiality of the eight genes knockouts on the *E. coli* growth fitness.

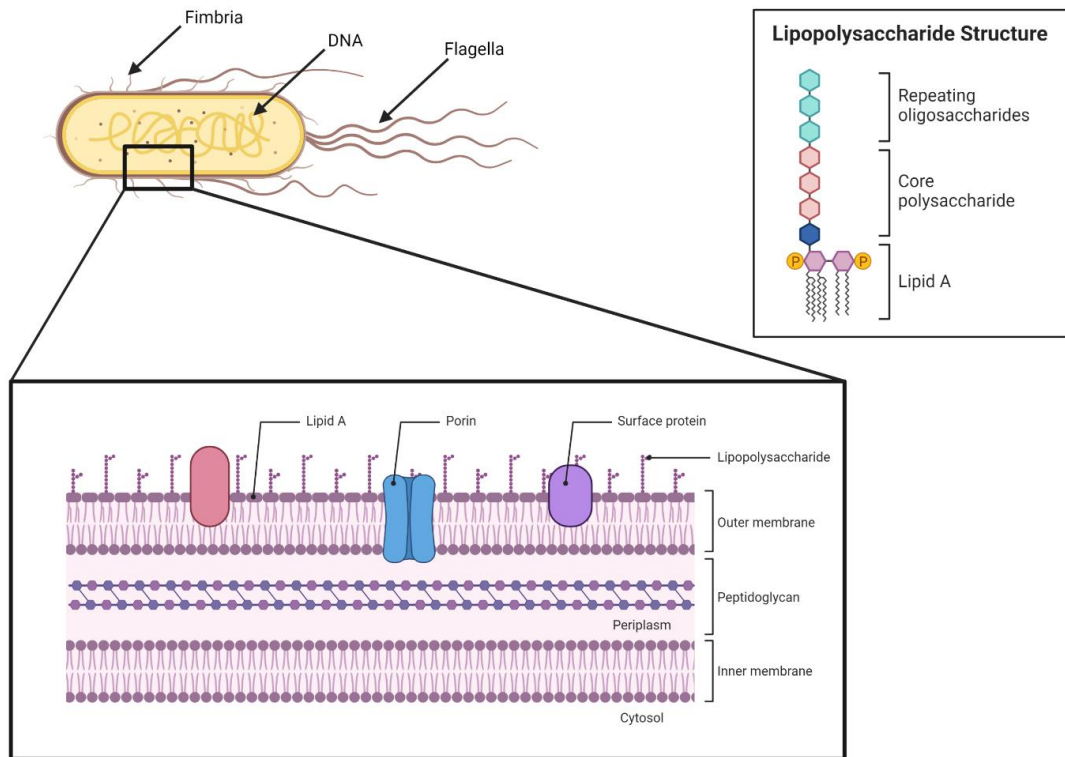
CHAPTER II: LITERATURE REVIEW

Gram-negative bacterium *Escherichia coli* (*E. coli*)

As a member of the family of *Enterobacteriaceae*, *E. coli* is a rod-shape like Gram-negative bacterium that has been intensively studied because of the great characteristics it offers such as the rapid cell growth under optimal growth conditions (cell division approximately every 20 minutes) as well as the majority (more than 70%) of its genome has been sequenced (Jang et al., 2017). The cellular organization of the *E. coli* bacterium structure consists of a cell wall, which comprises 2 membrane bilayers that are the outer membrane and the inner membrane, the periplasm is the space between these two membranes (J. Wang et al., 2021) (Figure 4). The periplasmic peptidoglycan membrane is an important intracellular polymer assuring the integrity of the cell wall from internal and external turbulences (Gumbart et al., 2014; Miller & Salama, 2018). The bacterium *E. coli* is commonly used as preferential model organism for gene manipulation for industrial enzymes production and to understand the basic molecular functions of bacteria cells. Additionally, *E. coli* is mostly known as a commensal bacterium part of the normal microbial flora colonizing in a symbiotic way, the gastrointestinal tract of humans and some animals (Vila et al., 2016). However, *E. coli* can also exist as a pathogenic strain causing a variety of infections in both humans and animals that can lead to death (Kaper et al., 2004). It is estimated that more than 40,000 deaths are registered annually in the USA attributed to serious pathogenic *E. coli* infections like urinary tract infections (UTIs), diarrhoeal disease and meningitis (Russo, 2003). The main difference between the commensal *E. coli* and the pathogenic strain is the presence of specific virulence factors in the pathogenic *E. coli* genome such as toxins, adhesins, polysaccharide substances and more (Braz et al., 2020; Santos et al., 2020). The genetic diversity of the bacterium *E. coli* has enabled its ability to survive and evolve

in the strictest environmental settings while integrating indigenous microbial communities (Braz et al., 2020). This genetic complexity is dictated by the environmental conditions imposed upon the *E. coli* population to assure the long-term survival of the strain in the environment (Braz et al., 2020). In addition, the whole morphological structure of *E. coli* has evolved to assure protection and survival of the cells, the filamentous extracellular components such as flagella, fimbria and curli play a key role in the adaptation, navigation, and colonization of different types of mediums and surfaces (Dörr et al., 2019). Therefore, these bacterial filamentous structures mediate the shift from planktonic state to the sessile state when needed by bacteria for its survival (Dworkin et al., 2006).

Figure 4: Cell wall structure of the Gram-negative bacteria *E. coli*



Mechanisms of Bacterial adhesion

Bacteria have adapted cellular mechanisms that enable them to adhere to a wide variety of surfaces. All bacteria species employ different mechanisms for adhesion, most of which are the product of cell wall composition and other characteristics of their cell surface (Busscher & van der Mei, 2012; Kimkes & Heinemann, 2019; Tuson & Weibel, 2013b).

Bacterial adhesion to surface is initiated by overcoming an energy barrier through morphological and physicochemical transformations of the cells. This process consists of the deformation of the cell membrane upon adhesion to a substratum and/ or the change in movement of bacterial appendages that are triggered by the two-component signal transduction (Busscher & van der Mei, 2012). The cellular attachment process of bacteria to surfaces occurs in two phases. The first phase is reversible and consists of electrostatic and hydrodynamic interactions between the bacteria and the surface. During that process, the adhesion forces are strong. Most bacteria cells are negatively charged, which makes them prompt to strongly bind to positively charged surfaces (Kimkes & Heinemann, 2019). However, charge driven adhesion will vanish in high ionic strength fluids because of charge screening (Tuson & Weibel, 2013).

The second phase takes more time (a couple of hours) and is irreversible. Bacterial adhesion occurs under different conditions depending on the motility state of the cells, the fluid flows in the medium, the physicochemical changes in the liquid environment (i.e. pH., osmolarity, ionic strength and nutrient concentration), and the nature of surfaces (hydrophilic or hydrophobic) (Kimkes & Heinemann, 2019). The adhesion is initiated by bacterial sensing involving biomolecules localization on surfaces using cell membrane receptors and/or surface structures (Kimkes & Heinemann, 2019). The adhesion forces induce cell wall deformation of bacteria upon contact with a substratum surface leading to response from the cells. Gram-

positive bacteria possess a flexible and thick peptidoglycan layer, which is around 30 nm and plays the role of a protective membrane against any extracellular aggressors. Conversely, Gram-negative bacteria have a small peptidoglycan layer of about 10 nm in thickness enabling the cell adhesion through ligand-receptor mechanism and provide a strength support to pili during the adhesion process (Habimana et al., 2014).

Bacterial attachment to surfaces occurs in two distinct phases with one reversible based on electrostatic interactions and the other irreversible that relies on environmental changes. The attachment of the bacterial cells to biotic or abiotic surfaces is mediated by a panoply of extracellular structures such as the cell wall, Flagella, curli and fimbriae that enable an intimate interaction with the surface.

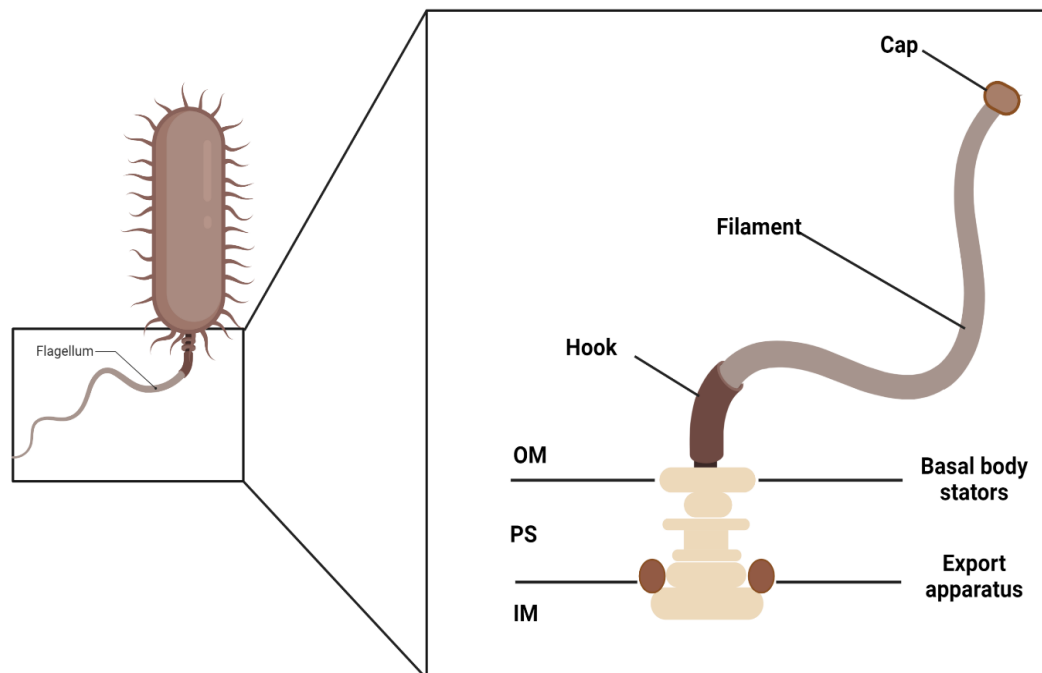
Bacterial cell adhesion involves the interaction of hydrophobic segments of cell wall with abiotic surfaces through van der Waals forces and production of specific biological molecules (Kimkes & Heinemann, 2019). In *E. coli*, the biomolecules expressed on the cell surface include lipopolysaccharides (LPS) and extracellular polymeric substances (EPS) which facilitate the irreversible attachment of cells to surfaces (Tuson & Weibel, 2013). These adhesion mechanisms involve changes in bacterial cell behavior including the passage of bacteria from a planktonic state to a sessile state (Busscher & van der Mei, 2012).

In addition to non-specific interactions, specific interactions are also playing a major role in facilitating the attachment of cells to surfaces, this is also mediated by specific interactions through extracellular organelles present on bacteria surfaces such as flagella, curli and pili (fimbriae) (Kimkes & Heinemann, 2019; Kline et al., 2010a). These bacterial filamentous cell surface structures play distinct yet determining roles in the bacterial adherence process to surfaces (Busscher & van der Mei, 2012; Harapanahalli et al., 2015).

Bacterial Flagella

Flagella are multifunctional extracellular proteinaceous filaments that can be either polar when there is one or several flagella at the same position or peritrichous with flagella are present all over the bacteria surface involve in the motility process, virulence as well as cell adhesion to surfaces (Haiko & Westerlund-Wikström, 2013). The primary step in the cell-surface adhesion process is the motility of the bacteria cells in planktonic state towards the surface driving by the rotation and movement of flagella during a chemotaxis phenomenon or during changes in the environmental conditions. In most *E. coli* strains, a typical flagellum measures up to 10 μm in length and has a diameter of 20 nm. Flagella are composed of over 60 structural proteins with the hollow whip-like filament composed of more than 20,000 flagellin protein subunits, which are critical for its assembly and diverse functions (Haiko & Westerlund-Wikström, 2013). (Figure 5)

Figure 5: Schematic representation of a bacterial flagellum



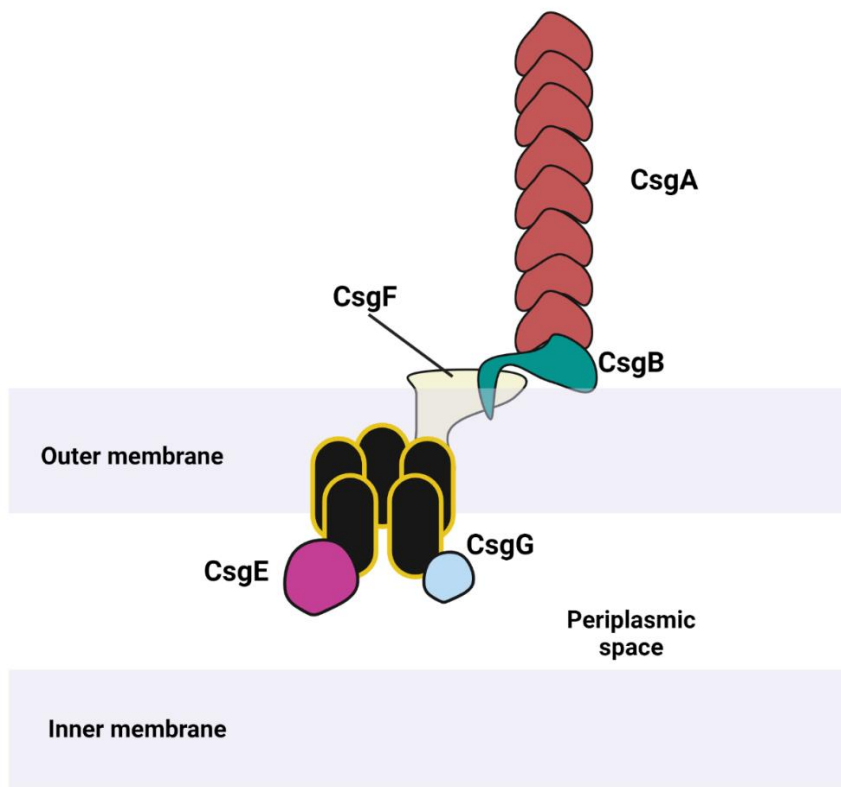
Changes in environmental conditions such as change in PH, osmolarity and temperature dictate bacteria behavior, usually in the transition from motile to sessile behavior (Haiko & Westerlund-Wikström, 2013). This regulates the gene expression of the *flhDC* flagellar operon that triggers the signal transduction as the bacteria adhere to a surface. Flagella reinforce the attachment of the cells on hydrophobic surfaces especially, by sensing the topography of structured surfaces using the flagellar energy vibrations and filling the gaps of the surface geometry to accommodate the cell adhesion (Friedlander et al., 2015). The adhesive properties of flagella are stimulated by hydrophobic nature and degree of the surface and therefore aid strengthening the cell attachment. Besides facilitating adhesion, flagella is also involved in biofilm formation and virulence as these structures also mediate the secretion and export of extracellular non-flagellar proteins (Haiko & Westerlund-Wikström, 2013). Non-specific adhesive properties of flagella differ from bacteria species.

Bacterial Curli

Curli are proteinaceous fibers that are part of the bacteria extracellular matrix produced by enteric bacteria such as *E. coli* and *Salmonella spp* (Barnhart & Chapman, 2006; Evans & Chapman, 2014). Curli fibers measure between 6 to 12 nm wide and are non-branching fibers that are highly resistant to proteases and detergents (Evans & Chapman, 2014). In bacteria such as *E. coli*, curli are differentially expressed at incubation temperatures that are below 30°C and at 37°C depending on the bacterial strains. Curli biogenesis is promoted by the *csgBA* and *csgDEFG* gene operons that encode the six structural proteins that composed curli (Barnhart & Chapman, 2006). The expression and regulation of these operons rely on various environmental signals (Hollenbeck et al., 2018). In bacterial curli structure, *csgA* constitutes the major protein subunit of the curli protein complex formation encoded by the *csgBA* operon (Barnhart &

Chapman, 2006) (Figure 6). It is secreted across the outer membrane as an unstructured peptide and achieved its maturation through nucleation by the minor subunit csgB (Evans & Chapman, 2014). Curli are amyloid fibers that in pathogenic states, are deeply involved in bacterial adhesion to host cells, biofilm formation and maturation and virulence. In the adhesion process, curli fibers have a strong affinity for various proteins on the surface of host cells especially human contact proteins such as fibrinogen, H- kininogen and factor XII as well as extracellular matrix protein like fibronectin and laminin (Barnhart & Chapman, 2006). Curli fibers mediate cell adhesion via extracellular matrix proteins composed by proteoglycans and glycoproteins that favorably prepare surfaces for bacterial attachment through ligand-receptor interactions (Hollenbeck et al., 2018).

Figure 6: Schematic representation of a bacterial curli



Bacterial Pili (Fimbriae)

Type IV Pili

Type IV pili or fimbriae are proteinaceous polymerized filamentous structures that are composed of a major protein called pilin (Imam et al., 2011). Type IV pili are present on the surfaces of most gram-negative bacteria and a few gram-positive bacteria (Imam et al., 2011; Proft & Baker, 2009a). The biogenesis of pili takes place in the inner membrane where the ensemble of pilin monomers is held together as a fimbrial filament from hydrophobic interactions (Melville & Craig, 2013). These fimbrial rod-like fibers are involved in a variety of mechanisms such as specific flagella-independent bacterial motility that are the gliding motility and twitching motility, adhesion and invasion of host cells, biofilm formation and DNA uptake (Proft & Baker, 2009b).

Type I pili

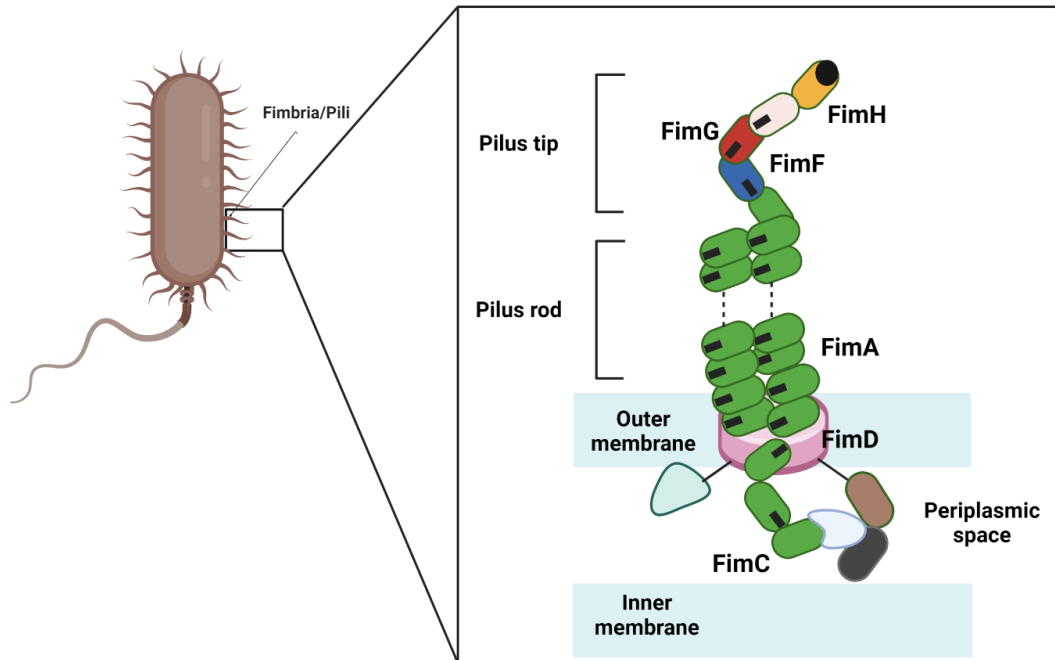
The type I pili protein complex is 6.9 nm thick and 1-2 um long helical rod formed by a right-handed helical array of 500-3000 copies of the subunit fimA (Proft & Baker, 2009b). It is one of the most intensively studied pili for its role in adhesion to host cell surfaces, biofilm formation and virulence (Kline et al., 2010b; Proft & Baker, 2009b). Type I pili of uropathogenic *E. coli* (UPEC) are responsible for the bacterial cell adhesion to epithelial cells of the bladder and the initiation of biofilm formation that leads to urinary tract infections in women (Alonso-Caballero et al., 2018; Connell et al., 1996; Krogfelt et al., n.d.; Miller et al., 2006; Müller et al., 2009; Proft & Baker, 2009; Zeiner et al., 2012).

The biosynthesis of type I Pili is orchestrated by a cluster of genes from the *fim* operon (fimA-fimH) which encodes the hierarchical and organized production of fimbrial protein subunits or pilins (Proft & Baker, 2009b). In the chaperone usher pathway, fimA represents the

major subunit and thousands of fimA form the pilus rod, a helical structure with spring-like properties in the molecular assembly of the type I pili followed in order by fimF, fimG and fimH (Alonso-Caballero et al., 2018; Krogfelt et al., n.d.). fimF and fimG are both minor protein subunits of fimbriae while fimH is involved in the receptor binding to the sugar D-mannose present at the surfaces of host cells.

The biogenesis of the type I pili starts in the cytoplasm where the protein subunits are incompletely formed as immunoglobulin-like structures (Ig) with a β -strand missing causing the formation of a hydrophobic groove. The incomplete subunits migrate into the periplasm thanks to the fimC domain that serve as chaperone that will lead to maturation and protection of the subunits from degradation, aggregation, and premature polymerization (Alonso-Caballero et al., 2018) (Figure 7). This chaperone usher pathway is specific to the biogenesis of type I pili in *E. coli*. The molecular interaction of the fimH and the D-mannose receptor at the epithelial cells surfaces at lower level of the bladder is responsible of the colonization of these cells and the biofilm formation with Mannose bound in a deep negatively charged pocket at the tip of the receptor-binding complex (Alonso-Caballero et al., 2018; Miller et al., 2006; Müller et al., 2009).

Figure 7: Schematic representation of the *fim* domains of a matured type I pilus



In addition, all the FimA subunits interact to one another by β -strand complementation mechanism which resemble an immunoglobulin-like structure that consists of a long β -strand elongating from one domain to the preceding one, establishing a hydrophobic interaction that secures the chain and complements the fold of each domain for full structural stabilization of the complex (Alonso-Caballero et al., 2018). This mechanical stability of these interactions between fimbriae is crucial for the strong adhesion process to epithelial surfaces for the colonization of cells and the initiation of the infection. Structural differences from the quaternary structures of the type I pili assembled *in vitro* and *in vivo* (Hospenthal et al., n.d.).

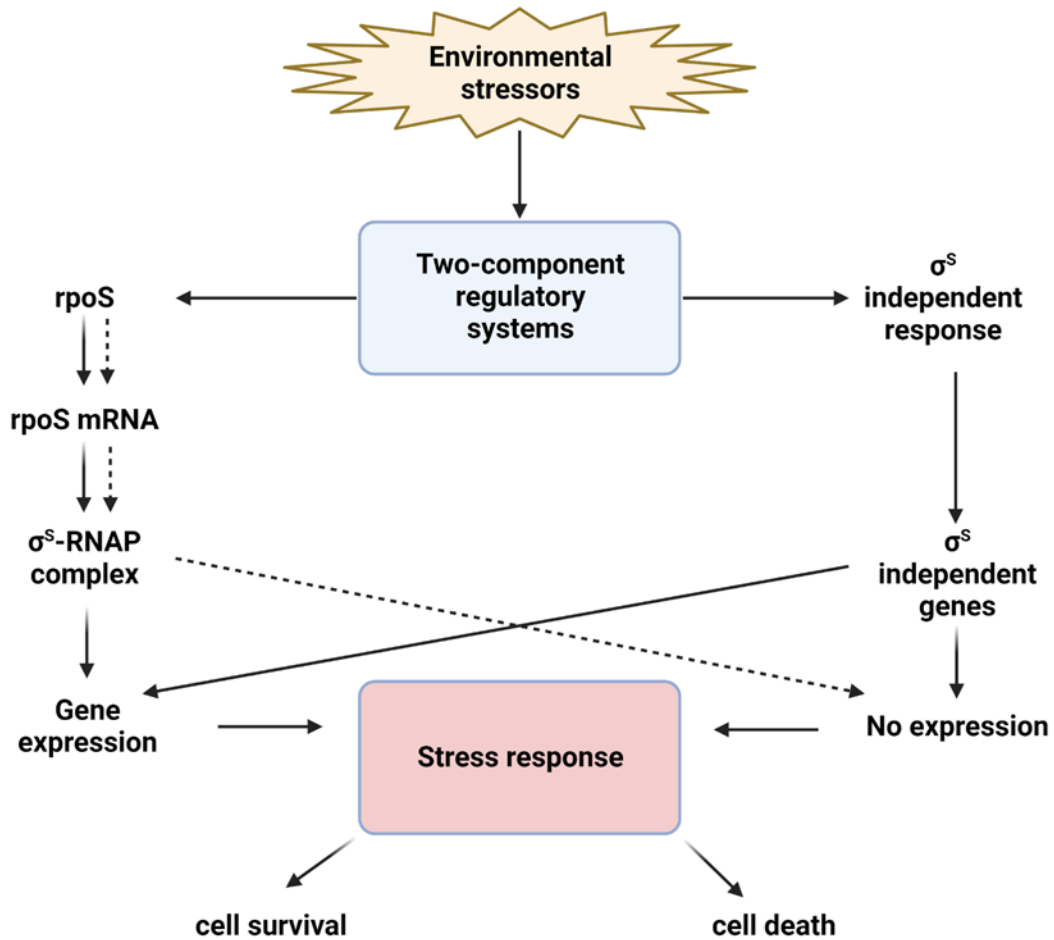
Stress responses of Gram-Negative bacteria

During their life cycle and proliferation in particularly harsh environmental conditions, bacteria are subjected to external aggressions that induce a variety of genetic, morphological, and metabolic changes that allow them to thrive and survive in coarse environments. These external

and internal cellular changes are known as stress responses that are activated when bacteria are sensing environmental cues that could potentially jeopardize the bacteria's homeostasis (Dworkin et al., 2006; Marles-Wright & Lewis, 2007). During their evolution, bacteria are exposed to a wide range of environmental stresses such as physical stress (shear force, irradiation), chemical stress, oxidative stress, heat stress, cold stress, nutrient limitation, pH, toxins, antibiotics and more (Chung et al., 2006; Poole, 2012). To retaliate to these environmental stresses, bacteria have developed sophisticated strategies that consist of large and complex signaling pathways to adapt to changes in their immediate vicinity (Chung et al., 2006; Fang et al., 2016; Rau et al., 2016).

The general stress response in *E. coli* is an elaborated cellular response to environmental assailants that is regulated by the RNA polymerase (RNAP) sigma factor (σ^s) via signal transduction mechanisms and sequence of metabolic reactions that could lead to either the survival or the cell death (Chung et al., 2006; Marles-Wright & Lewis, 2007) (Figure 8). Sigma factors are defined as a class of small proteins that bind to the core RNAP forming a holoenzyme complex that provides recognition and high affinity to specific regions on the promoter sequence that initiate the transcription of genes necessary for a distinct bacterial stress response (Chung et al., 2006; Paget, 2015).

Figure 8: Illustration of the general stress response mechanism in Bacteria



The sigma factor σ^s regulator encoded by *rpoS* is responsible for the transcription of genes involved in the bacteria cell growth and replication through a cascade of molecular reactions (Tripathi et al., 2014). For more specific stress responses in bacteria like *E. coli*, alternative sigma factors are required to help produce distinct bacterial responses tailored to cope with specific environmental stressors as shown in Table 1 (Kazmierczak et al., 2005; Schmid et al., 2012).

Table 1: Alternative sigma factors in *E. coli*

Alternative sigma factors	Genes	Stress response activities	reference
σ^{19}	felC	Iron transport and metabolism	(Dawan & Ahn, 2022)
$\sigma^{24}(\sigma^E)$	rpoE	Heat and cell envelope regulation	(Dawan & Ahn, 2022; Kazmierczak et al., 2005; Marles-Wright & Lewis, 2007)
$\sigma^{28}(\sigma^F)$	flbB, flaL, rpoF	Flagellar synthesis and chemotaxis	(Adnan et al., 2010; Dawan & Ahn, 2022)
$\sigma^{32}(\sigma^H)$	htpT, rpoH	Heat shock	(Dawan & Ahn, 2022; Schmid et al., 2012)
σ^{38}	ropS, katF	Nutrient limitation	(Dawan & Ahn, 2022)
$\sigma^{54}(\sigma^N)$	glnF, nrtA, rpoN	Nitrogen starvation	(Dawan & Ahn, 2022; Kazmierczak et al., 2005)
$\sigma^{70}(\sigma^D)$	rpoD	housekeeping	(Dawan & Ahn, 2022)

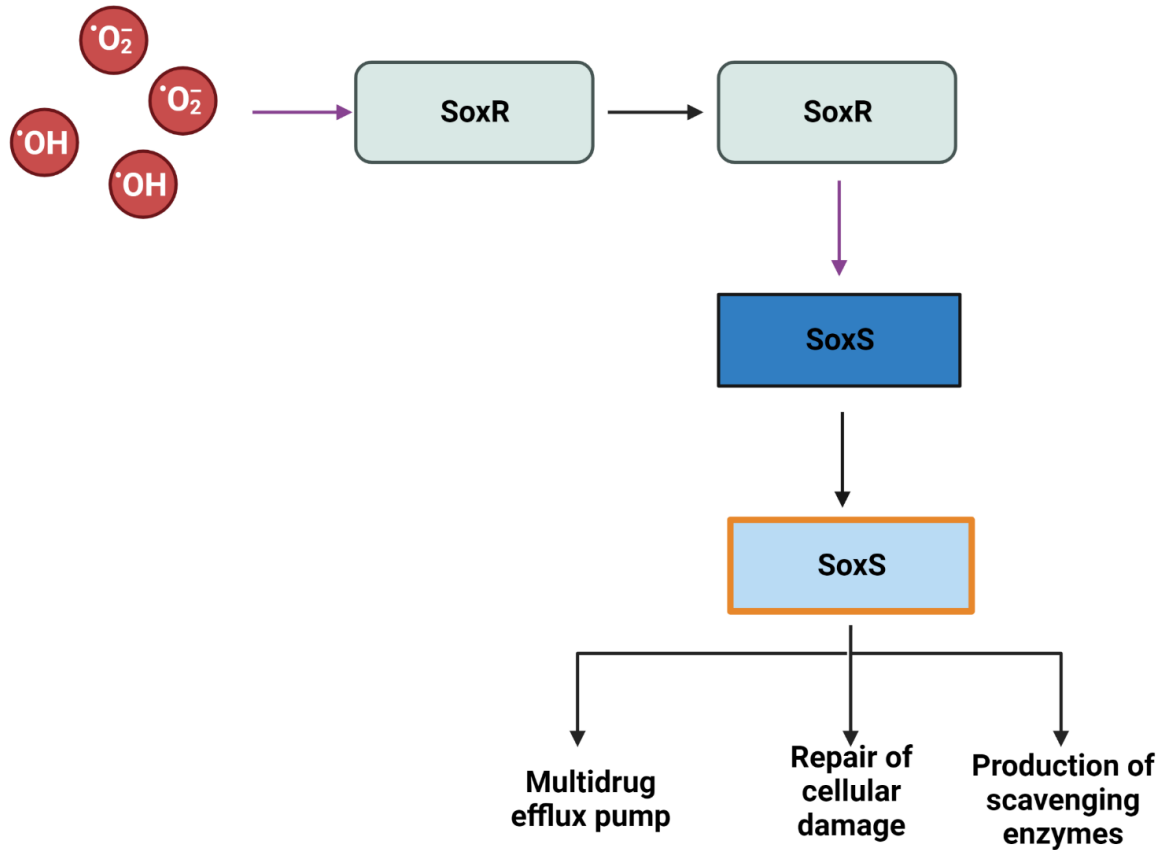
Some environmental stressors and their response mechanisms in Bacteria***Oxidative stress***

The oxidative stress is the most common stress in aerobic bacteria like *E. coli* causing the intracellular production of the harmful Reactive Oxygen Species (ROS) such as hydrogen peroxide and hydroxyl radicals that are byproducts of the aerobic respiration or nutrient

oxidation (Kashmiri & Mankar, 2014). ROS can severely damage a variety of biomolecules like DNA, RNA, Proteins and Lipids and thus elicit defense mechanism responses from the cell to regulate the endogenous concentration of ROS (Kashmiri & Mankar, 2014). When undergoing an oxidative stress attack, bacteria respond by activating one or numerous major ROS-related response mechanisms: Peroxide response, superoxide response and catalases (Figure 9).

The defense mechanism responsible for regulating the concentration of hydrogen peroxide (H_2O_2) in bacteria cells consist of OxyR and OxyS transcriptional regulators. OxyR is an oxidative stress regulator that activates a set of antioxidant genes responsible for the regulation of the hydrogen peroxide H_2O_2 concentration in bacteria cells (Zheng et al., 2001). In both oxidized and reduced form, OxyR is a repressor of its own synthesis (Barshishat et al., 2018). OxyS is another oxidative stress regulator, a small RNA that is expressed downstream in the OxyR regulatory system in hydrogen peroxide detoxification. OxyS expression contributes to the cellular division impairment and enables the cellular repair mechanism (Barshishat et al., 2018).

Figure 9: Oxidative stress response mechanism in bacteria

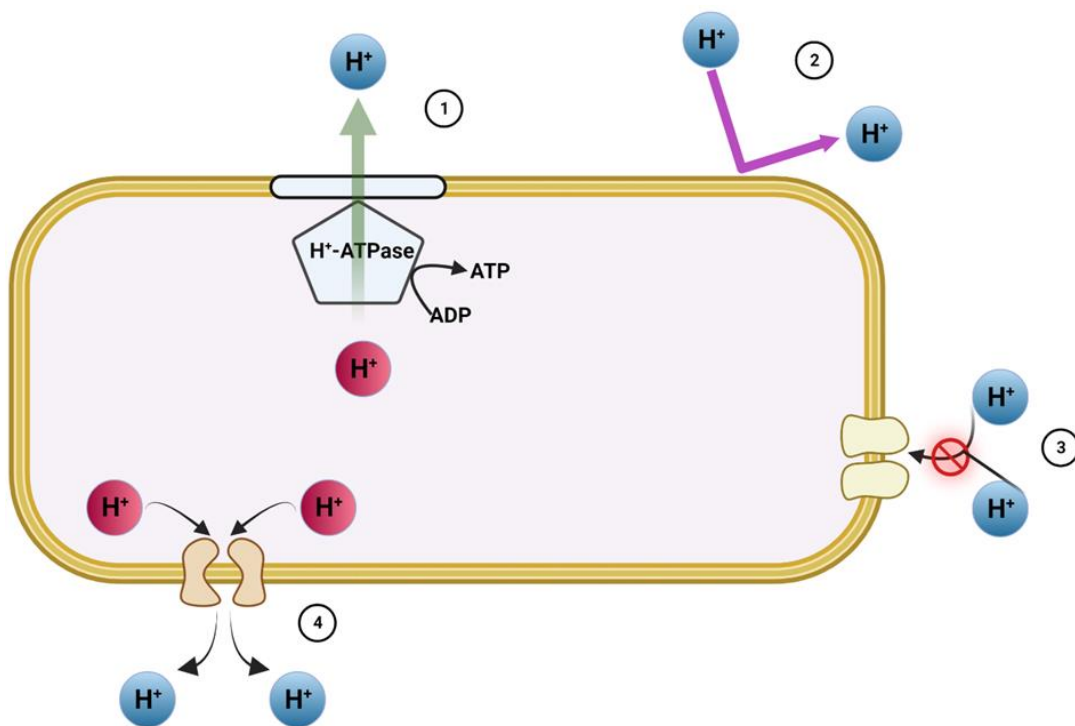


Acid stress

Acid stress is defined by the minor to drastic changes in pH occurring in the environment where bacteria cells are evolving (Xu et al., 2022). The acid stress is promoted by the accumulation of organic acids which for the most part, are products or by-products of bacterial metabolism. The organic acids traverse the cell membrane and reach the cytosol where their dissociation releases protons that acidify the intracellular pH (Guan & Liu, 2020). The combination of the ionized form of organic acids and the constant influx of protons disrupts important cellular biochemical processes causing an inevitable cell death (Chung et al., 2006). However, bacteria have developed acid-tolerant mechanisms that allow them to protect and converse their intracellular pH which is imperative for the cell homeostasis. Restriction of proton

permeation, enhancement of proton efflux pumps to control the transmembrane proton transport, cell membrane modification, and metabolic regulations are other anti-acid stress mechanisms that protect the bacterial cells from acidic stressors in the environment (Figure 10) (Dawan & Ahn, 2022; Guan & Liu, 2020; Xu et al., 2022). These processes enable bacteria cells to resist and thrive in acidic environments. The expression of the operon *gadBC* is intimately responsible for the acid-resistant response in bacteria, conferring the maintenance of intracellular pH (Dawan & Ahn, 2022).

Figure 10: Acid stress responses in bacteria. 1-proton efflux by H⁺-ATPase apparatus; 2-decrease in cell membrane fluidity; 3-membrane channel size modification; 4- proton pump.

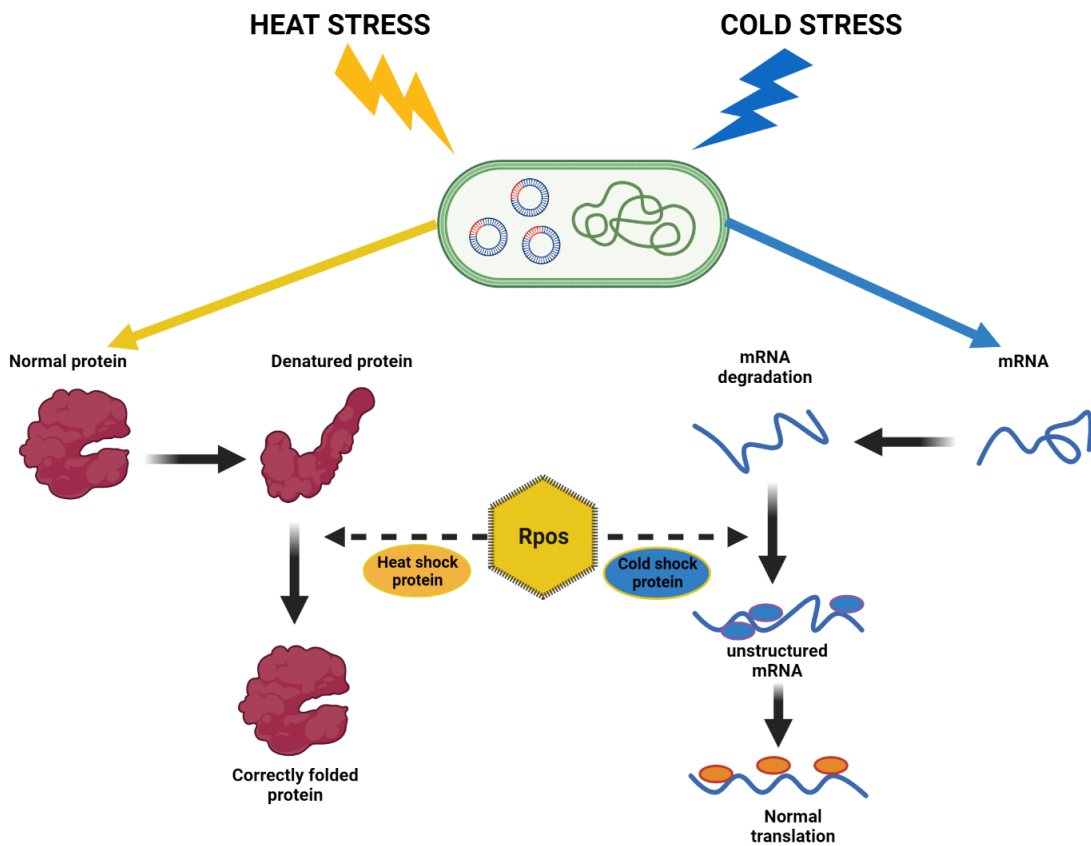


Temperature stresses

Temperature related heat and cold stresses are other common environmental alterations that bacteria are subjected to. They are promoted by the abrupt change in temperature. High temperatures cause heat stress while low temperatures create cold stress (Fang et al., 2016). The

occurrence of heat stress triggers the heat shock response (HSR) and the cold stress initiates the cold shock response (CSR) (Dawan & Ahn, 2022; Ramos et al., 2001). These mechanisms are well regulated and consist of the production of specific proteins that are known as cold shock proteins (CSPs) for the cold stress and heat shock proteins (HSPs) for the heat stress (Figure 11). Under cold stress, CSPs improve bacterial translation and the production of membrane fusion proteins associated with the multidrug efflux pumps that could lead to antibiotic resistance in bacteria (Dawan & Ahn, 2022). *clpL* is a key heat shock protein that is involved in the cell wall biosynthesis. HSPs enable the restoration of unfolded proteins. Moreover, the gene *rpoS* is mainly responsible for the synthesis of both CSPs and HSPs (Dawan & Ahn, 2022; Ramos et al., 2001).

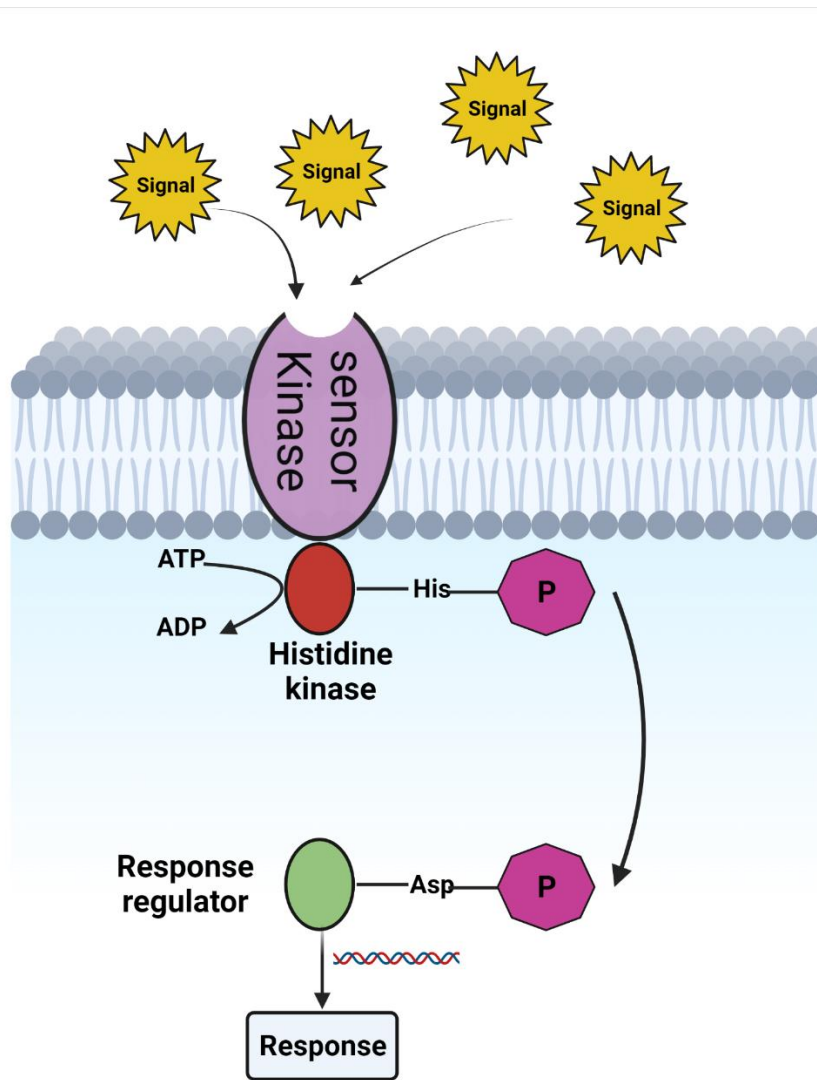
Figure 11: proposed Cold and Heat stress responses in bacteria.



Two-component regulatory systems in *E. coli*

Considered as one of most prominent crosstalk mechanisms between intracellular and extracellular environments in bacteria, the two-component system is a signal transduction apparatus involved in the signaling communication and adaptation to environmental cues that triggers cascade of molecular alterations in bacteria as a response to external stresses (Otto & Silhavy, 2002). In *E. coli*, the two-component signal transduction systems are comprised of a sensor protein Histidine Kinase and a responses regulator protein. The sensor responds to external signals resulting in the activation of the Kinase activity and autophosphorylation of the histidine residue. The activated sensor protein then phosphorylates a response regulator protein that is engaged in physiological and transcriptional changes in the cell regarding the specific signal received (Tiwari et al., 2017) (Figure 12). This mechanism is activated by a variety of environmental stresses including cold stress, heat shock, chemical stress, physical stress (i.e., shear force, irradiation) and oxidative stress (Giuliodori et al., 2007; Poole, 2012; Vorob'eva, 2004).

Figure 12: Schematic of the two-component regulatory systems (TCS) in Bacteria.



Some prominent Two-component regulatory in *E. coli*

EvgS/EvgA system

EvgS/EvgA is a well-characterized two-component regulatory systems (TCS) in *E. coli* (Utsumi, 2017). This signal transduction system has been shown to modulate the expression of the *emrKY* which is a multidrug resistance operon in *E. coli* (Nishino & Yamaguchi, 2002).

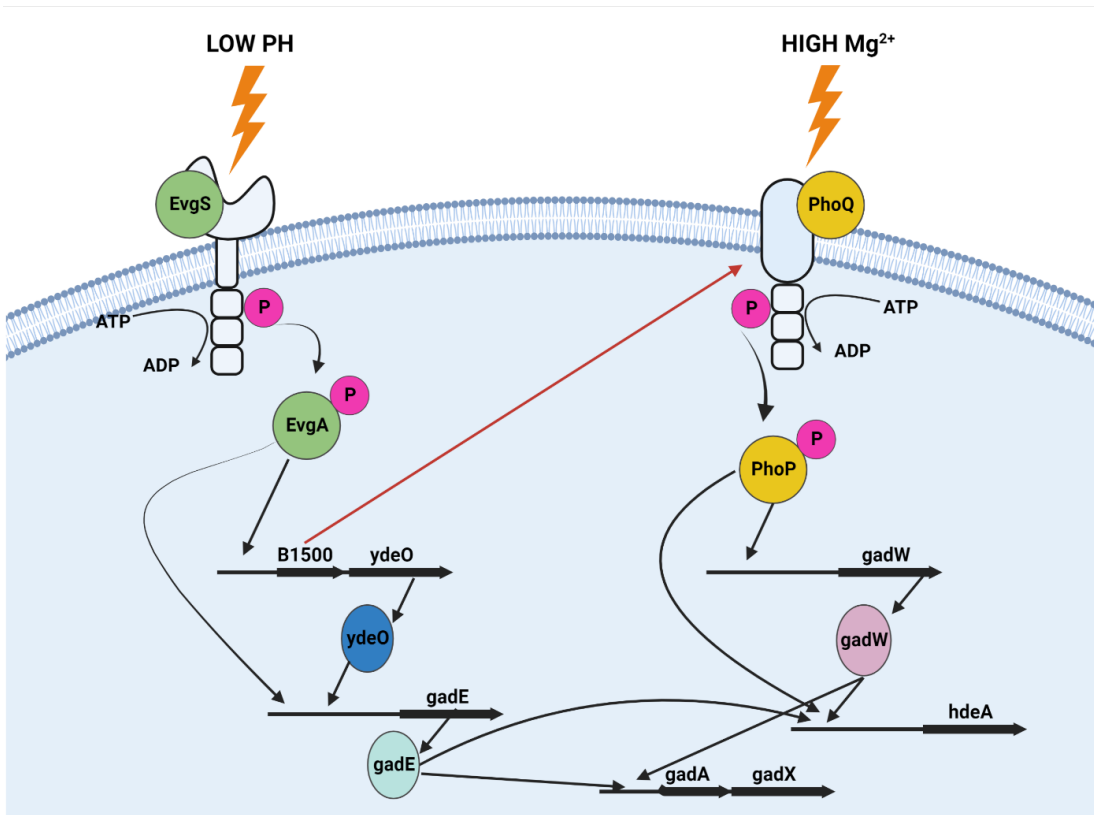
EvgS is the histidine kinase subunit that is prone to be activated by environmental cues such as alkali metals (Na^+ , K^+) and low pH (Itou et al., 2009; Utsumi, 2017). *EvgA* is the response

regulator which overexpression regulated the multidrug resistance transporter genes like yhiUV by increasing its expression and also genes like ydeP and ydeO that are involved in the acid stress response for cells in exponential growth phase (Nishino & Yamaguchi, 2002; Utsumi, 2017) (Figure 13). This EvgS/EvgA signal transduction pathway ensures the survival of the bacteria cells from drug assaults through the activation of multi-drug efflux pump regulated by emrKY gene (Kato et al., 2000).

PhoQ/PhoP system

PhoQ/PhoP is another important two-component regulatory system that has been widely studied and is involved in the extracellular Mg^{2+} and Ca^{2+} starvation stress and antimicrobial peptide stress (Lemmin et al., 2013; Utsumi, 2017). This bacterial regulatory system responds to the extracellular level of both Mg^{2+} and Ca^{2+} by regulating the expression of Mg^{2+} protein transport and lipopolysaccharide synthesis (LPS) genes (Minagawa et al., 2003). Furthermore, the autophosphorylation of the sensor kinase PhoQ is activated by the presence of antibacterial peptide, which leads to the phosphorylation of the response regulator which trigger the expression of genes responsible for the synthesis of proteins implicated in the outer membrane modification (Lemmin et al., 2013). This alteration of the outer membrane protein structure enables the bacterial cells to survive low levels of Mg^{2+} as well as antimicrobial peptide aggressions (Kawasaki et al., 2005; Lemmin et al., 2013). The PhoQ/PhoP signal transduction system is suppressed by high Mg^{2+} concentration in the local environment (Barchiesi et al., 2012). It has been shown that B1500, a small inner membrane protein intimately regulated by evgS/evgA serves as a connector between the evgS/evgA system and the PhoQ/PhoP system by activating the expression of some PhoP-induced genes part of the acid stress response (Eguchi et al., 2007) (Figure 13).

Figure 13: Transcriptional cascades initiated by both EvgS/EvgA and PhoQ/PhoP systems. The red arrow represents the connection between the two TCS via the protein B1500.



How bacteria interact with nanoparticles.

Bacteria can interact and adapt to changes occurring in their immediate vicinity and respond to the presence of environmental components that could either be beneficial or detrimental for the bacterial population (Aruguete & Hochella, 2010). Thus, bacteria can sense and monitor their environment and through genetic and metabolic modification deliver a specific response to the external signals to preserve the bacteria cells homeostasis (Ramos et al., 2001). Among these external components susceptible to perturbation and /or interrupt the bacterial cell cycle, nanoparticles have been widely utilized for that purpose in the field of nanomedicine (Rawashdeh & Haik, n.d.; Tyagi & Kumar, 2020). Nanoparticles exhibit efficient antibacterial properties on both Gram-negative and Gram-positive bacteria (Aruguete & Hochella, 2010). As a

result, they are part of the new drug development and treatment of bacterial infections with the goal of killing the bacteria cells (Tyagi & Kumar, 2020). This lethal interaction of bacteria with nanoparticles depends mainly on the physicochemical properties of the nanoparticles (Neal, 2008) (Table 2) .

The chemical composition influences the behavior of nanoparticles. This characteristic is crucial in understanding the damaging effect on the bacterial cellular organelles that are often targets in bacterial infection remediation (Aruguete & Hochella, 2010; Hochella et al., 2019). Moreover, the size of nanoparticles plays a significant role in the bacteria-nanoparticle interaction. Thus, small nanoscale particles can traverse or be embedded in the bacteria cell wall, reach the intracellular milieu, and then interact with the biomolecules located in the cytosol (Białas et al., 2022; Shaikh et al., 2019; Slavin et al., 2017). While bigger nanoparticles cannot enter the cell membrane but can be actively attached to the bacteria extracellular filaments such as flagella, curli and fimbriae as well as the cell wall (Pajerski et al., 2019; Slavin et al., 2017).

The interaction between bacteria and nanoparticles has been intensively investigated to assess the antibacterial impacts of these nanoscale particles on bacterial cells. The antimicrobial action of nanoparticles is activated upon close contact with extracellular bacterial components, this contact is modulated by forces such as Van Der Waals Forces, electrostatic forces, hydrophobic interactions, and receptor-ligand connection (Shaikh et al., 2019). The precise antibacterial mechanism of some nanoparticles on bacteria is still unknown. However, the adverse effects of that interaction are well studied. Metallic nanoparticles, subjects of intensive research as antimicrobial agents can negatively alter key metabolic processes in bacteria through generation of reactive oxygen species (ROS), change in gene expression levels, inhibition of enzymes and cause electrolyte imbalance (Shaikh et al., 2019; Slavin et al., 2017). Furthermore,

this antimicrobial activity is amplified as the size of the nanoparticle decreases. For instance, silver nanoparticles (AgNps) less than 30 nm in size can readily interact with cell membranes by disrupting the cell permeability that causes cell death (Babayevska et al., 2022; Slavin et al., 2017). Also, the unleash of nano silver ions may be absorbed into the cytoplasm through cation porins that would generate ROS and inhibit the cell growth in bacteria (Yang et al., 2009). Gold nanoparticles (Au Nps) that are deemed chemically inert and “neutral” nanoparticles as they display nontoxic activities in nanomedicine, can exhibit potential antimicrobial behaviors as well (Hashimoto & Honda, 2019). At higher concentrations, Au Nps induce oxidative stress in bacteria cells through ROS formation causing biomolecule damage (Figure 14) (Joshi et al., 2020).

Metal oxide nanoparticles are another class of nanoparticles that have gained a lot of attention for their antimicrobial activities. Several studies suggested that their antimicrobial mechanisms reside in the production of free radicals in aqueous media (Figure14) (Babayevska et al., 2022; Niño-Martínez et al., 2019). When the metal ions are released and absorbed through the cell membrane, they directly interact with functional groups of some enzymes and nucleic acids that lead to a total dysfunction of significant biochemical processes that contribute to cell death (Castellano et al., 2007). Some reports suggested that Unlike metal Nps, some metal oxide Nps such as zinc oxide Nps (ZnO Nps) require a photoactivation to exert strong antibacterial effects(Sivakumar et al., 2018). In presence of UV light, ZnO Nps promote the increase in intracellular ROS concentration in bacterial species such as *E. coli* and *P. aureus* (Niño-Martínez et al., 2019). The synergistic action of both titanium dioxide (TiO₂) and UV light severely damage the outer membrane layer of the *E. coli* cell wall prompting an alteration of *E. coli*

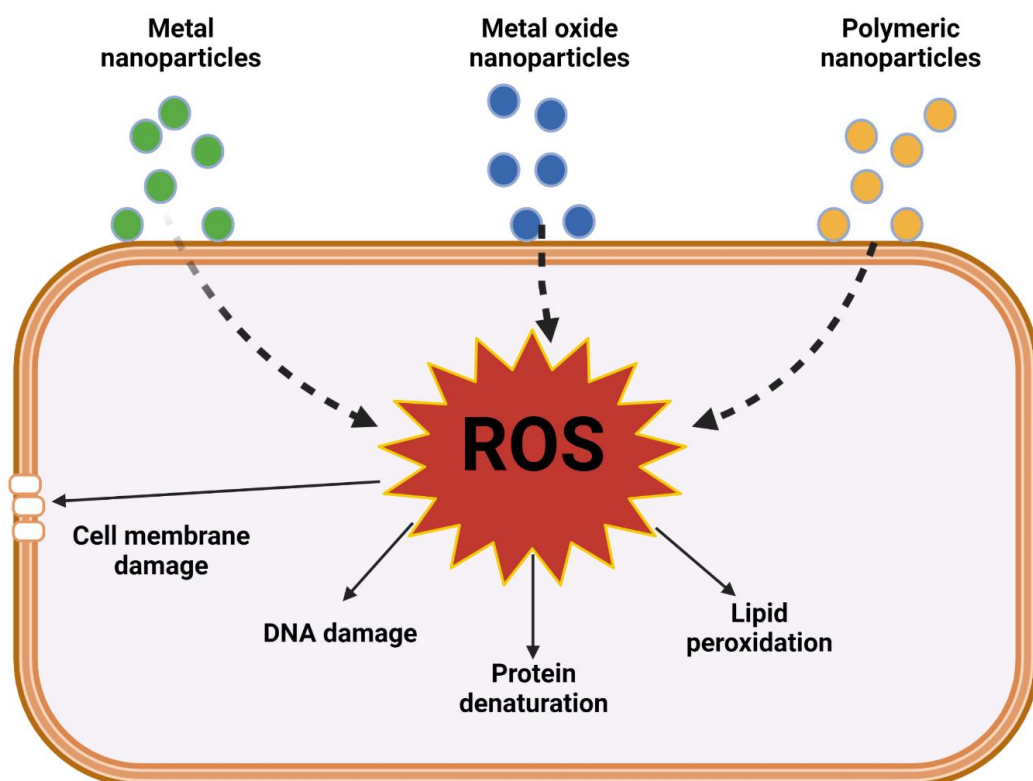
morphology (P. Liu et al., 2010). Similarly, engineered cerium oxide Nps size dependably affect the growth and viability of *E. coli* and *Bacillus subtilis* (Pelletier et al., 2010)

Silica nanoparticles (SiNps) are one of the most used nanoparticles for drug delivery applications (Häffner et al., 2021; Selvarajan et al., 2020). Their physicochemical characteristics like size, shape, large surface area and easy-to-functionalization position them as excellent drug carrier agents (Selvarajan et al., 2020). Mesoporous silica Nanoparticles with modified surface topography as “spikes” cause *E.coli* cell membrane rupture (Häffner et al., 2021). Furthermore, bigger size “inert: SiNps ($\geq 100\text{nm}$) have little to no effects on *E .coli* morphology after exposure and the potential outer membrane disorganization occurs at smaller SiNps sizes (Gammoudi et al., 2013; Mathelié-Guinlet et al., 2017).

Polymeric nanoparticles (PNps) possess beneficial assets in nanomedicine as nanocarriers for drug delivery systems in bacterial infections (Cano et al., 2020). Their chemical properties such as hydrophobicity, surface charge (cationic charge) and biocompatibility are important in their interaction with pathogenic bacteria and that strong affinity for the bacteria cell membrane creates holes on the surface that promote the intracellular leakage (Lam et al., 2018). The antimicrobial activities of PNps depend heavily on the monomer composition and distribution with the polymer chain (Cano et al., 2020). For example, phenol benzoic based polymers specifically disrupt the cell membrane integrity of *Pseudomonas aeruginosa* (J. Liu et al., 2020). However, PNps like polystyrene Nps (nanoplastics) have a greater impact on all living organisms with irreversible consequences especially on significant biogeochemical cycles where bacteria are key components (Kik et al., 2020; Kim et al., 2022). The interaction of Polystyrene Nps (PS Nps) and bacteria result primarily in the increase of intracellular ROS production in *E. coli* and *Bacillus sp* (Kim et al., 2022). Some studies have suggested that the mechanism of action of PS

Nps is through alteration and destruction of the bacteria cell wall as well as promoting potent oxidative stress in bacteria cells (Awet et al., 2018; Kik et al., 2020).

Figure 14: Proposed common mechanism of action of metal, metal oxide and polymeric nanoparticles.



Conclusion

Numerous studies have been conducted to investigate the bacteria-nanoparticle interactions with most of them emphasizing on the lethal antimicrobial effects and potential mechanism of action on bacterial systems. Moreover, these studies revealed the diverse adverse effects triggered by nanoparticle exposure on bacteria cell growth and viability through routine experimental assays limited to a restricted group of specific metabolic products such as ROS induced during bacteria-nanoparticles interplay. Few reports about lethal exposure of bacteria to

nanoparticles have combined these experimental assays with gene expression analysis. However, genetic interactions of non-lethal exposure of bacteria to nanoparticles are yet to be determined. This will provide a better understanding of the hybrid interphase between bacteria and nanoparticles as transcriptomic analysis are best indicators of the nanoscale genetic changes occurring in bacteria cells and subsequently provides a bigger picture about the specific morphological and metabolic alterations in bacteria upon nanoparticles exposure. So, we hypothesized that the non-lethal interactions of bacteria with physico-chemically different nanoparticles: Silica, gold and polystyrene nanoparticles will trigger specific transcriptomic responses in the Gram-negative bacterium *E. coli*. This work defines the genetic foundation that modulate the bacteria response to round-shaped nanoparticles.

Table 2: Nanoparticle impact on microorganisms

NANOPARTICLES	NATURE OF THE NANOMATERIALS	ORGANISMS	MICROBIAL TARGET/RESPONSE SITE	REFERENCES
Fe ₃ O ₄ iron oxide	metal Nps, magnetic Np, size: 8nm	<i>E. coli</i>	cell growth inhibitor	Chatterjee et al.
gold	metal Np, size:5nm	<i>E. coli</i>		Chatterjee et al.
manganese oxide Mn ₂ O ₃	Metal oxide; size: 40-60nm	nitrifying bacteria: Nitrosomonadales, Bradyrhizobiaceae, Rhodocyclaceae, Xanthomonadaceae	ammonia oxidation genes	Phan et al.
copper	metal Nps, size: 40 nm	Moorella thermoacetica	cell membrane, glycolysis and acidification processes	Wu et al.

Silver	metal Nps. 10nm	cyanobacteria	dna replication and repair system.	Lu et al.
Silica	Metal oxide; size: 4nm and 100nm	<i>E. coli</i>	cell membrane	Mathelié-Guinlet et al.
gama-Fe ₂ O ₃	Magnetic NPs, size: 10nm	<i>E. coli</i>	intracellular proteins and DNA strands.	He et al.
Zinc Oxide ZnO ₂	Metal nanoparticles, Size < 20nm	<i>Pseudomonas Aeruginosa</i>	biofilm formation and virulence genes	Abdelraheem et al.
Lithium Cobalt oxide, LiCoO ₂	Metal nanoparticles,	<i>B. subtilis</i>	oxidative stress response genes	Gari et al.
nanoPS	polymer nanoparticles, size: 160nm	<i>Shewanella Oneidensis</i>	cell viability, riboflavin secretion	Fringer et al.
Al ₂ O ₃ , ZnO, CuO Nps	metal oxide Nps 30nm, 30nm and 40nm	feed and inoculum sluge (mostly anaerobic Microorganisms)	mobile genetic elements	Zhang et al.

Ag, ZnO, CuO Nps	metallic Nps 15nm, 20-200nm, <50nm	Acinetobacter Baylyi ADP1	Antimicrobial resistance (AMR) elements	Zhang et al.
PS Nps , PS-NH2, PS-CooH, PS-COC	Polymer Nps, 30nm,100nm,200nm. Modified 200nm	<i>E. coli</i>	cell growth and bacterial resistance mutations	Ning et al.

CHAPTER III: TRANSCRIPTOMIC RESPONSES OF E. COLI EXPOSED TO ENGINEERED NANOPARTICLES

Introduction

The recent years have seen an increasing interest for nanomaterials. Their unique physicochemical properties define by the shape, size, and surface chemistry provide undeniable advantages in many fields like Agriculture, pharmaceuticals, biomedicine, cosmetics, telecommunications and more (Barhoum et al., 2022). In addition, engineered nanoparticles (ENPs) that are nanoscale particles fabricated under sophisticated laboratory protocols for defined purposes are receiving a great deal of attention due to their stability, high reactivities and biocompatibility. As a result, they have infiltrated all sectors of modern life where they are in contact with living organisms. The global production levels of ENPs are estimated at hundreds of tons a year and this production scale is susceptible to increase in the near future as the demand continues to grow (Giese et al., 2018; Keller & Lazareva, 2014). In general, the impacts of ENPs on living organisms have mitigated results. ENPs are useful in nanomedicine for drug delivery and treatment of bacterial infections as well as promoting the bioavailability of nutrients for plants for a greater crop yield in agriculture (Ma et al., 2022; Maruyama et al., 2016; Mejias et al., 2021; Zhu et al., 2022). Other impacts of ENPs are subject of concerns as their nanotoxicity have been extensively investigated among several living beings, but their precise mechanisms of action are still unelucidated. In addition, the lack of resources for innovative exposure assessment makes it harder to evaluate the extent of that nanopollution (Hochella et al., 2015).

During ENPs life cycle, they interact with the different components of the environment. They are present in all ecosystems through intentional or unintentional anthropogenic activities

(Giese et al., 2018; Hochella et al., 2019). Bacteria are among the most affected living organisms by the exposure of ENPs as they form the largest population of living organisms on planet Earth and have been shaping life of the atmospheric, terrestrial, and oceanic ecosystems by playing key role in critical biogeochemical processes such as nitrogen and carbon cycling, electron flux, nutrients bioavailability and mineral growth and dissolution (Aruguete & Hochella, 2010). Therefore, bacteria constitute imperative biological elements to sustain life on Earth, and any disruption of that intrinsic microbial functions by ENPs will have devastating and irreversible effects on the entire environment (Aruguete & Hochella, 2010; Sun et al., 2022).

Several toxicity studies have demonstrated the adverse effects and possible action mechanisms of engineered nanoparticles on some bacteria population (Arakha et al., 2015; Biswas et al., 2023; Dong et al., 2019). The antimicrobial mechanisms include ROS generation, cell membrane disruption, release of metal ions and internalization of nanoparticles (Babayevska et al., 2022). Metallic nanoparticles physicochemical characteristics such as their size, shape and high surface area to volume ratio enable high reactivity and biocompatibility with living organisms which enhance their antimicrobial mechanisms (Shaikh et al., 2019). Moreover, some studies have established that metallic nanoparticles such as silver and gold Nps exhibit antibacterial activities through ROS generation and inhibition of core metabolic enzymes (Ameh et al., 2022; Dong et al., 2019; Hashimoto & Honda, 2019; Joshi et al., 2020; Yang et al., 2009). Silica nanoparticles antibacterial properties are attributed to their sizes, shape, and high surface area (Gammoudi et al., 2013). Their ability to penetrate bacterial cell membrane and disrupt their structure and functions as well as causing genotoxicity, make them desirable as antimicrobial carriers for drug delivery applications in biomedicine (Selvarajan et al., 2020).

The polymeric polystyrene Nps also known as nanoplastics cause a real threat to bacteria communities because of their biocompatibility, persistence, and slow degradation in the environment (Gonçalves & Bebianno, 2021; Matthews et al., 2021). Although, some recent studies reported that polystyrene Nps could drastically alter the inherent microbial population structure and function in the environment as well as enhance beneficial antimicrobial properties as nanocapsule carriers in drug delivery (Gonçalves & Bebianno, 2021; Jawahar & Meyyanathan, 2012; Lam et al., 2018).

The current research landscape has demonstrated that the potent antibacterial activities of nanoparticles control biofilm formation and lead to the bacteria cell death despite the exact antibacterial mechanism of action not being well understood. However, the non-lethal interactions of bacteria with nanoparticles are yet to be established, to better understand the bacteria resistance to nanoparticles-based antibiotics along with the possible consequences on natural transformation processes in the environment.

Herein, we investigated the transcriptional responses of the bacterium *E. coli* to silica, gold and polystyrene Nps using a gene screening technique. And then evaluate the impacts of these nanoparticles on the *E. coli*'s growth fitness. This study will provide an in-depth knowledge of the genetic alterations induced by engineered nanoparticle exposure at nonlethal concentrations.

Materials and methods

Materials

Silica nanoparticles (120 nm, silica nanospheres standard, nanoXact, 10mg/ml, 25ml) were purchased at nanoComposix, USA. Gold nanoparticles (100nm, 0.1mMPBS, reactant free 99% ODI, 572 nm absorption, 100ml. Weight concentration = 0.0389 mg/ml) purchased at Thermo Fisher scientific, inc. And the Polystyrene nanoparticles functionalized with carboxyl groups (100nm, Dio=0.085, SD= 0.0065u CV= 8%, V=15ml.) were purchased at Polysciences, Inc. The stock solutions of the nanoparticles were stored in the fridge at 4C in the dark. The sizes, shapes and zeta potentials of the nanoparticles were measured using Scanning Electron Microscopy (SEM) (Zeiss Auriga Scanning Electron Microscope) and Dynamic Light Scattering (DLS) (malvern zetasizer nano-zs).

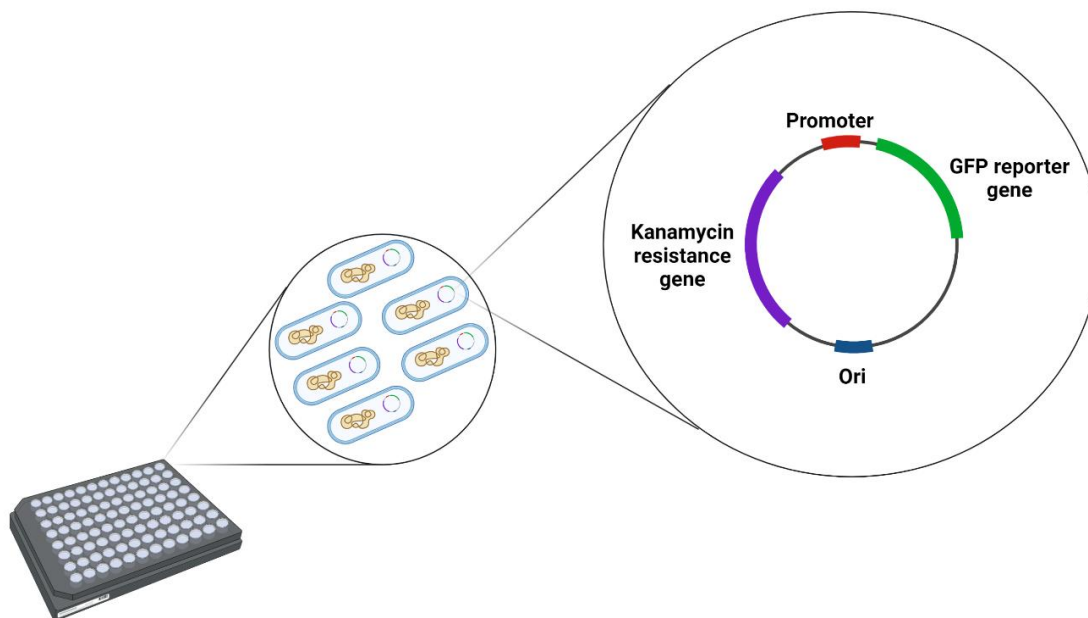
Luria broth (LB) and M9 media low salts (100ml of 5XM9 salts, 1ml Cacl, 1ml Mg, 10ml of 20% glucose, 100ul of Thiamine, 2ml of Amino acid) were utilized for cell culture in this study.

The model organism for this work is the wild type *Escherichia coli* K12 BW25113 and both the *E. coli* promoter library and *E. coli* gene knockouts were purchased at Horizon Discovery Ltd. USA.

The Dharmacon *E. coli* promoter library is a collection of *E. coli* strains containing a fast-folding green fluorescent protein (GFP) as reporter gene that is tethered to an *E. coli* promoter in a low copy plasmid allowing the measurements of gene expression in bacteria with high temporal resolution. It covers more than 70% of the *E. coli* genome (more than 1900 out of 2500 genes) (Zaslaver et al., 2006).

The 96-well and 24-well plates along with the antibiotic kanamycin were purchased at Thermo Fisher scientific, inc.

Figure 15: *E. coli* promoter library description



Methods

Characterization of nanoparticles

The nanoparticles stock solutions were diluted in phosphate Buffer Solution (PBS) to a concentration of 0.1mg/ml. The diluted nanoparticle solutions were stored, protected from light in the fridge at 4°C ready for further experiments. The morphologies and sizes of nanoparticles were measured using SEM. In addition to the size, the zeta potential of the nanoparticles was also determined using Dynamic Light Scattering (DLS) in PBS as solvent.

Fixation of *E. coli* cells with nanoparticles

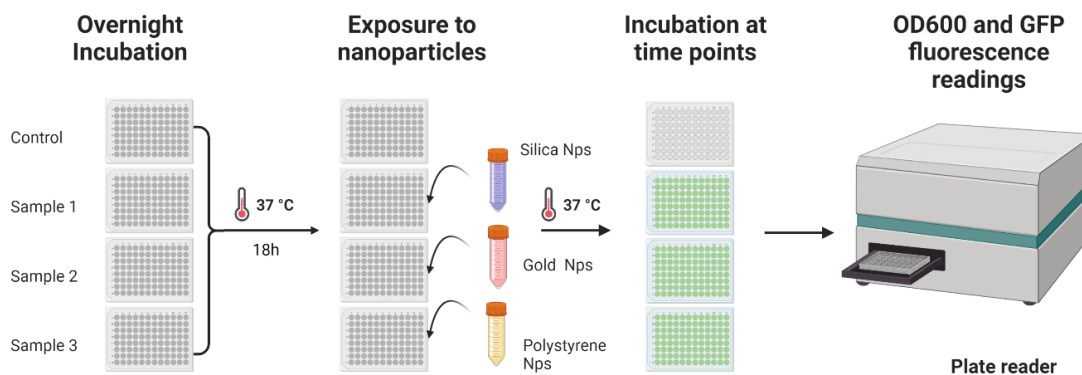
An overnight cell culture of the wild type *E. coli* in LB media were exposed to nanoparticles for 4h. The fix (2mL 25% Glutaraldehyde, 2 ml 16% Paraformaldehyde, 1ml 1x PBS, 5 ml dH₂O) was added to the mixture cell culture with nanoparticles, then incubated at 4°C overnight. The sample was washed several times using purified water and then dehydrated in an

ethanol dehydration series (40%, 60%, 80%, 100%). The dehydrated sample was drop-casted on SEM stubs and dried at room temperature before SEM analysis.

Bacteria exposure to nanoparticles

The frozen Dharmacon *E. coli* promoter library stock stored at -80°C were thawed and 2ul of cells were added to 200 ul of M9 media low salts with kanamycin(50mg/ml). Four 96-well plates were utilized, with three plates for the nanoparticle treatments and one plate serving as the control. The plates were incubated for 18h overnight at 37°C as described by (Zaslaver et al., 2006). Then, 10 ul of the nanoparticle solutions were added to the three plates allocated for the nanoparticle treatments and the measurements of both OD₆₀₀ and GFP fluorescence were performed using a plate reader (BioTek Synergy Mx Microplate Reader) at different increasing time points (15min, 30min, 60min, 120min, 240min). each Dharmacon *E. coli* promoter plate was run in biological triplicates for this experiment.

Figure 16: Experimental design of the *E. coli* promoter library exposure to nanoparticles.



Quantitative analysis of the gene expression

RNA extraction

To extract the RNA, the frozen stock of *E. coli* BW 25113 wild type strain was streaked on a Luria Bertani (LB) agar plate and incubated overnight at 37°C to obtain individual colonies. the next day, a single colony from that cell culture was inoculated in 7 ml of M9 media low salts without antibiotics and incubated overnight for 18h at 37°C, 150 rpm. 1ml of the overnight cell culture was added in four glass tubes, one tube serving as a control and the three others exposed to 50ul of the nanoparticle suspensions of SiO₂, Au and PS Nps respectively. Then, these samples were incubated at the same time intervals as in the gene screening experiment. The total RNA was harvested by following the protocol of the RNA extraction kit (Purelink RNA Mini Kit USA) purchased at Thermo Fisher scientific, inc. The concentrations of the RNA samples collected were measured using the Nanodrop (Thermo Fisher scientific, inc.) and stored in the freezer at -80°C for further experiments.

Table 3: Primer selection

Primers	Sequences F(forward), R(reverse)
glcC	F: 5' GGG CGC GGG ATT ATT GAA AC- 3' R: 5' CGA ACG TCG AGC AGA TCG TA- 3'
rssB	F: 5' CTG GTG CTT GAT ATT GCC GC- 3' R: 5' TCA ATA ACG CGC CCA ACT CT- 3'
cysQ	F: 5' ACA GCT TGG CGA ACA TCA GA- 3' R: 5' TTA CCC TGC CAG TCG TGA AC- 3'
vacJ	F: 5' GGC CGA TGT CTG TGG GTA AA- 3'

	R: 5' CAT CCT GAA TCG CTT GTG CG- 3'
evgA	F: 5' CTG GCG CTA ATG GTT TCG TG- 3' R: 5' TCG AGT TTT TGC TGG TCG GA- 3'
sodC	F: 5' AAT GAC GGC AAA GCT ACC GA- 3' R: 5' TCG GAC ATA TTA TCG CCG CC- 3'
ydhY	F: 5' TGG GTC TTC ATC CAC GAA CG- 3' R: 5' TCA GTG GGT AAA TCA CCG CC- 3'
yhhT	F: 5' GCA CTT AAA GGC GTT TCG CA- 3' R: 5' ATT GGG CAC GTA GTT GAG CA- 3'

Quantitative PCR of the 8 cluster genes

The experiment was performed in a RTPCR specific 96-well plates using the QRTPCR kit (Power SYBR Green RNA-to Ct 1-step Kit) purchased at Thermo Fisher scientific, inc. according to the manufacturer's instructions. All the reagents and RNA samples were kept on ice. Each selected well of the 96-well plate has a total volume of 20ul that contained 2ul of RNA sample, 0.16 ul of enzyme, 1 ul of the forward and reverse primers solution, 10 ul of the reaction mix and 7.04 ul of RNase-free water. The plate was centrifuged briefly to remove any bubbles in the wells then run in an Applied Biosystems 7500 Fast PCR System instrument applied biosystems device with parameters recommended by the qRTPCR kit protocol.

Table 4: Table of mutants

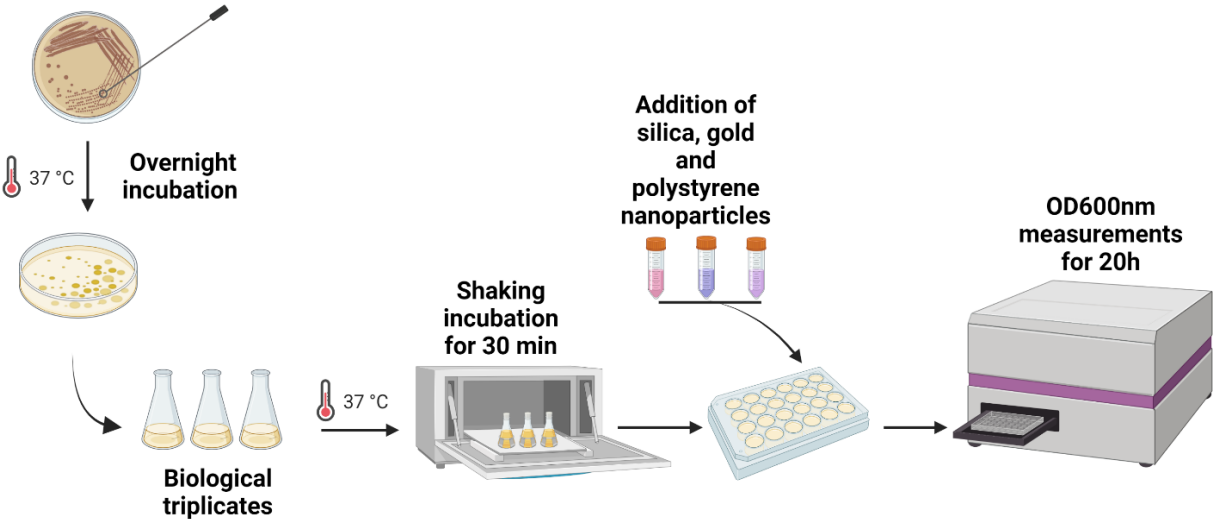
<i>E. coli</i> mutants	Strain identification and Genotype from the <i>E. coli</i> Keio collection
Δ rssB	JW1223; F-, Δ (araD-araB)567, Δ lacZ4787(::rrnB-3), λ -, Δ rssB744::kan, rph-1, Δ (rhaD-rhaB)568, hsdR514
Δ evgA	JW2366 F-, Δ (araD-araB)567, Δ lacZ4787(::rrnB-3), λ -, Δ evgA778::kan, rph-1, Δ (rhaD-rhaB)568, hsdR514
Δ glcC	JW2947 F-, Δ (araD-araB)567, Δ lacZ4787(::rrnB-3), λ -, Δ glcC754::kan, rph-1, Δ (rhaD-rhaB)568, hsdR514
Δ cysQ	JW4172 F-, Δ (araD-araB)567, Δ lacZ4787(::rrnB-3), λ -, rph-1, Δ (rhaD-rhaB)568, Δ cysQ763::kan, hsdR514
Δ yhdY	JW5545 F-, Δ (araD-araB)567, Δ lacZ4787(::rrnB-3), λ -, Δ yhdY788::kan, rph-1, Δ (rhaD-rhaB)568, hsdR514
Δ yhhT	JW5680 F-, Δ (araD-araB)567, Δ lacZ4787(::rrnB-3), λ -, Δ yhhT728::kan, rph-1, Δ (rhaD-rhaB)568, hsdR514

Δ sodC	JW1638 F-, Δ (araD-araB)567, Δ lacZ4787(::rrnB-3), λ -, Δ sodC724::kan, rph-1, Δ (rhaD-rhaB)568, hsdR514
Δ vacJ	JW2343 F-, Δ (araD-araB)567, Δ lacZ4787(::rrnB-3), λ -, Δ m1aA754::kan, rph-1, Δ (rhaD-rhaB)568, hsdR514

***E. coli* Mutants' growth curves**

Each mutant cell line was streaked on a LB agar plate with Kanamycin. Three colonies of each mutant were inoculated in 10 ml of LB with Kanamycin and incubated in a shaker incubator at 37°C, 150 rpm for 30 minutes. Then, 50ul of nanoparticles solutions and 1ml of each cell inoculum were added to a 24-well plate. The cell density OD₆₀₀ measurements was done using a microplate reader with readings at 30-minute intervals for 20h. The wild type *E. coli* BW25113 served as control for this experiment and both Mutant cells and wild type *E. coli* were run as biological triplicates.

Figure 17: *E. coli* mutants growth curves experiment.



Statistical analysis

In this study, all the samples have been run as triplicate and the data are represented as mean \pm standard deviation. For the gene screening analysis, the gene expression folds ≥ 2 and ≤ 0.5 were set as thresholds for significantly up-regulated genes and down-regulated genes respectively. T-test was used to determine the significant differences among nanoparticle treatments and the differences were considered significant when $p < 0.05$.

Results and discussion

Characterization of nanoparticles

According to the manufacturer's description for each nanoparticle, all three nanoparticles have a homogenous spherical shape with gold and polystyrene Nps having an average size of 100 nm while silica nanoparticles have an average size of 120nm. SEM images show that all three engineered nanoparticles are round-shaped (Figure 18) and the SEM analysis of the size distribution revealed that the average diameter size for gold Nps is $90.32 \pm 9.7\text{nm}$ (Figure 18-e), for polystyrene Nps, the average diameter size is $70.43 \pm 7.3\text{nm}$ (Figure 18-f) and silica Nps have an average diameter size of $118.82 \pm 12.5\text{nm}$ (Figure 18-d). In general, these nanoparticle average sizes show to be relatively smaller than the average sizes mentioned by the suppliers. Furthermore, DLS measurements (Table 5) reveal an average hydrodynamic size of $135.13 \pm 5.24\text{ nm}$ for gold Nps, $72.61 \pm 1.01\text{ nm}$ for polystyrene Nps and $139.33 \pm 0.61\text{ nm}$ for silica Nps. The hydrodynamic diameters of both gold and silica nanoparticles were bigger compared to their advertised sizes while polystyrene nanoparticles were smaller than its advertised size value. The zeta potential measurements show that all three nanoparticles have negatively charged surfaces with PS nanoparticles functionalized with carboxyl groups being the more negatively charged - $31.96 \pm 0.57\text{ mV}$ (Table 5). These results suggest that the nanoparticles were relatively close to

the sizes indicated by the manufacturers and factors such as the solvent and/or the aggregation of particles in PBS solution may have influenced the measurements of the nanoparticle sizes.

Figure 18: SEM images of nanoparticles: (a) Silica, (b) gold, and (c) polystyrene nanoparticles. Size distribution histograms of (d) silica, (e) gold, and (f) polystyrene nanoparticles.

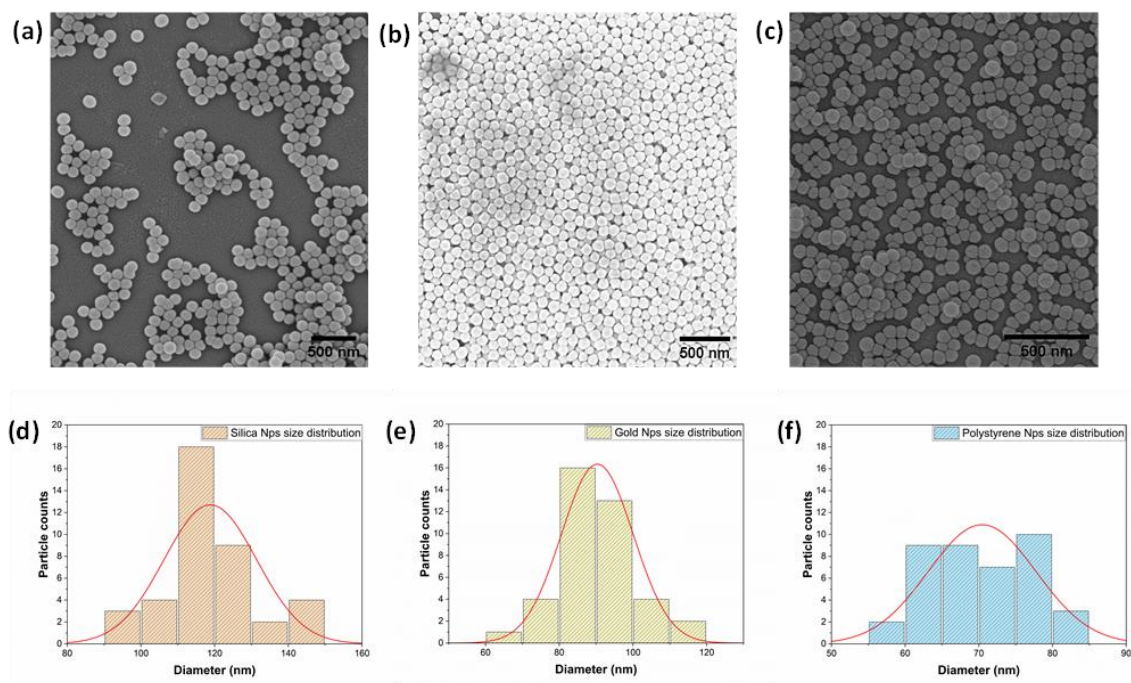


Table 5: DLS results of the nanoparticles including average size and zeta potential values.

Dynamic Light Scattering (DLS)	Size (nm)	Zeta potential (mV)
	PBS	PBS
Silica Nanoparticles	139.33 ± 0.61	-21.43 ± 0.18
Gold Nanoparticles	135.13 ± 5.24	-22.83 ± 0.36
Polystyrene Nanoparticles	72.61 ± 1.01	-31.96 ± 0.57

Bacterial gene screening after exposure to engineered nanoparticles.

In this study, we investigated the bacterial genetic alterations that are triggered by the presence of engineered nanoparticles. We performed an extensive gene screening using an *E.*

coli promoter library. The results of the gene screening were obtained through calculation of the average of the normalized GFP values to OD₆₀₀ which was indicative of the promoter activity and thus the gene expression level. The gene screening revealed that out of the more than 1900 genes tested, 25 genes were upregulated by the silica nanoparticles, 96 genes by gold nanoparticles and polystyrene nanoparticles with the most up regulated genes with 222 genes. However, silica nanoparticles were the only treatment with significantly down-regulated genes with 46 genes (Figure 19). All three nanoparticles showed a dynamic distribution of significantly up-regulated genes over the 4h of exposure time (Figure 20). Among the upregulated genes, polystyrene Nps exhibited the most significant promoter activities at each time point with the highest number of upregulated genes followed by gold Nps and finally, Silica Nps with the least number of gene activated throughout the exposure time.

The Venn diagram suggested that besides the total number of genes specifically activated by each nanoparticle, there are overlaps in up-regulated genes expressed by all three nanoparticles (Figure 21). Therefore, between silica Nps and gold Nps, there are 10 up-regulated genes shared, 13 genes between silica Nps and Polystyrene Nps and 67 genes in common between gold and polystyrene Nps. Interestingly, the Venn diagram revealed that there is a cluster of 8 genes (*glcC*, *rssB*, *cysQ*, *vacJ*, *evgA*, *sodC*, *yhdY*, *yhhT*) that represents the common genetic response for all three nanoparticles (Table 6).

The change in gene expression levels suggested by the gene screening were not the only biological alterations occurring to the bacterium *E. coli*. The SEM images of the interaction of the wild type *E. coli* with the nanoparticles demonstrated morphological changes of the bacterial cell wall with the presence of many pronounced protuberances on the cell wall of nanoparticle-treated *E. coli* compared to control (Figure 22). Furthermore, the SEM images showed the

attachment of the nanoparticles to the cell membrane and in some instances covering the entire bacterium. The nanoparticles were also embedded in the extracellular polymeric matrix.

Figure 19: Number of genes significantly regulated by all three nanoparticles.

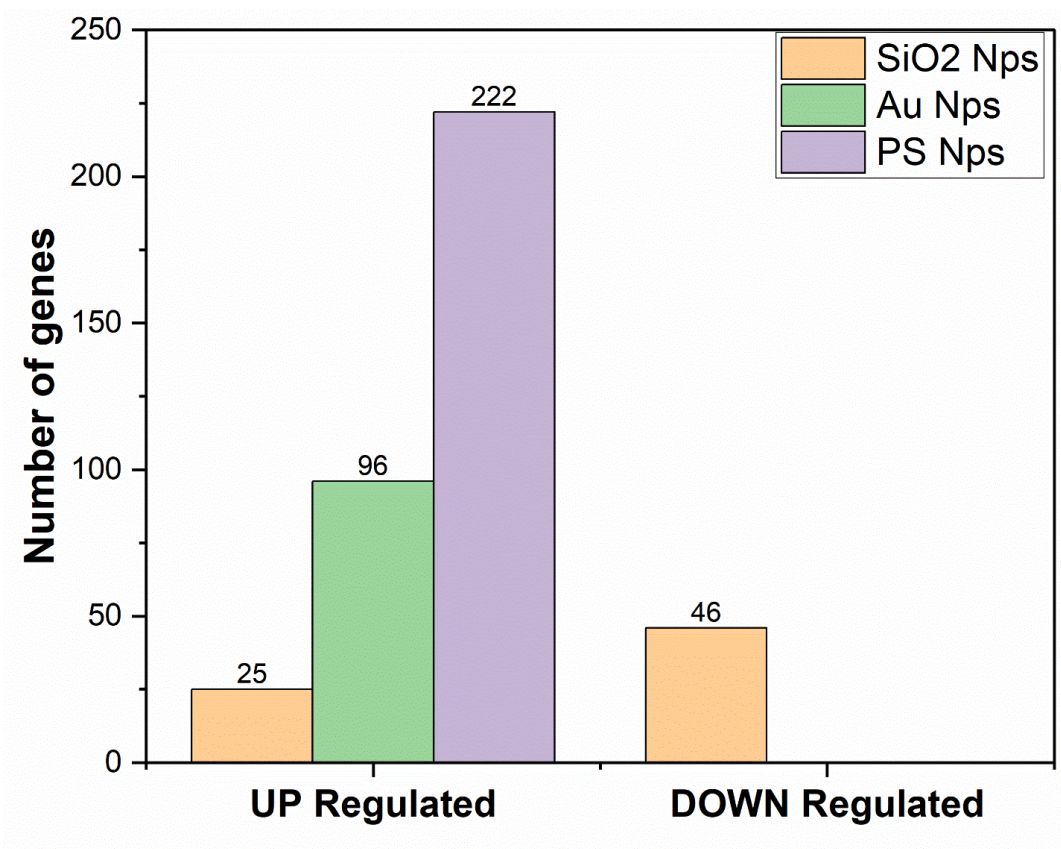


Figure 20: Distribution of up-regulated genes at each time point.

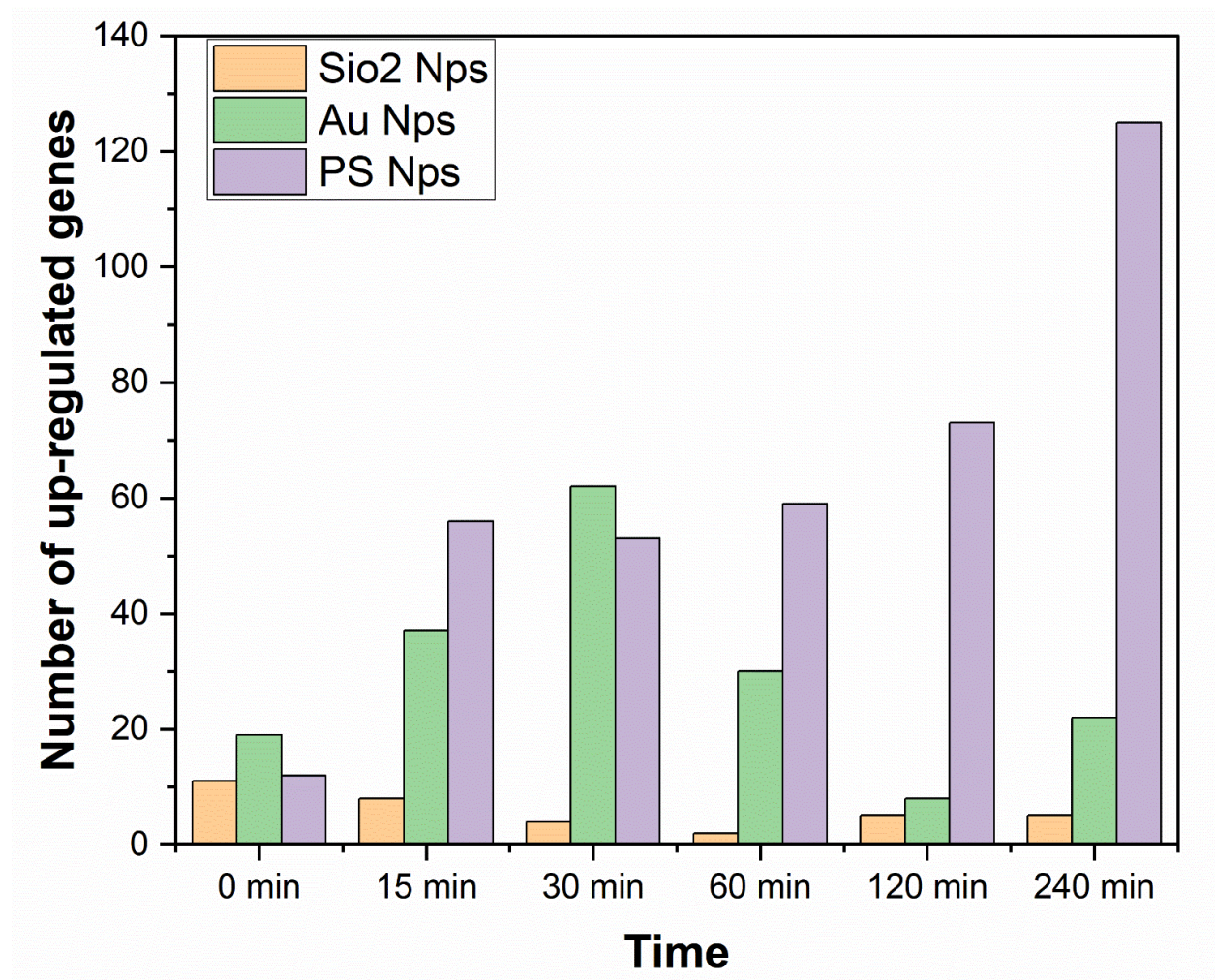


Figure 21: Venn diagram showing the total number of genes significantly expressed in presence of silica, gold and polystyrene nanoparticles. Blue = up-regulated genes, red = down-regulated genes.

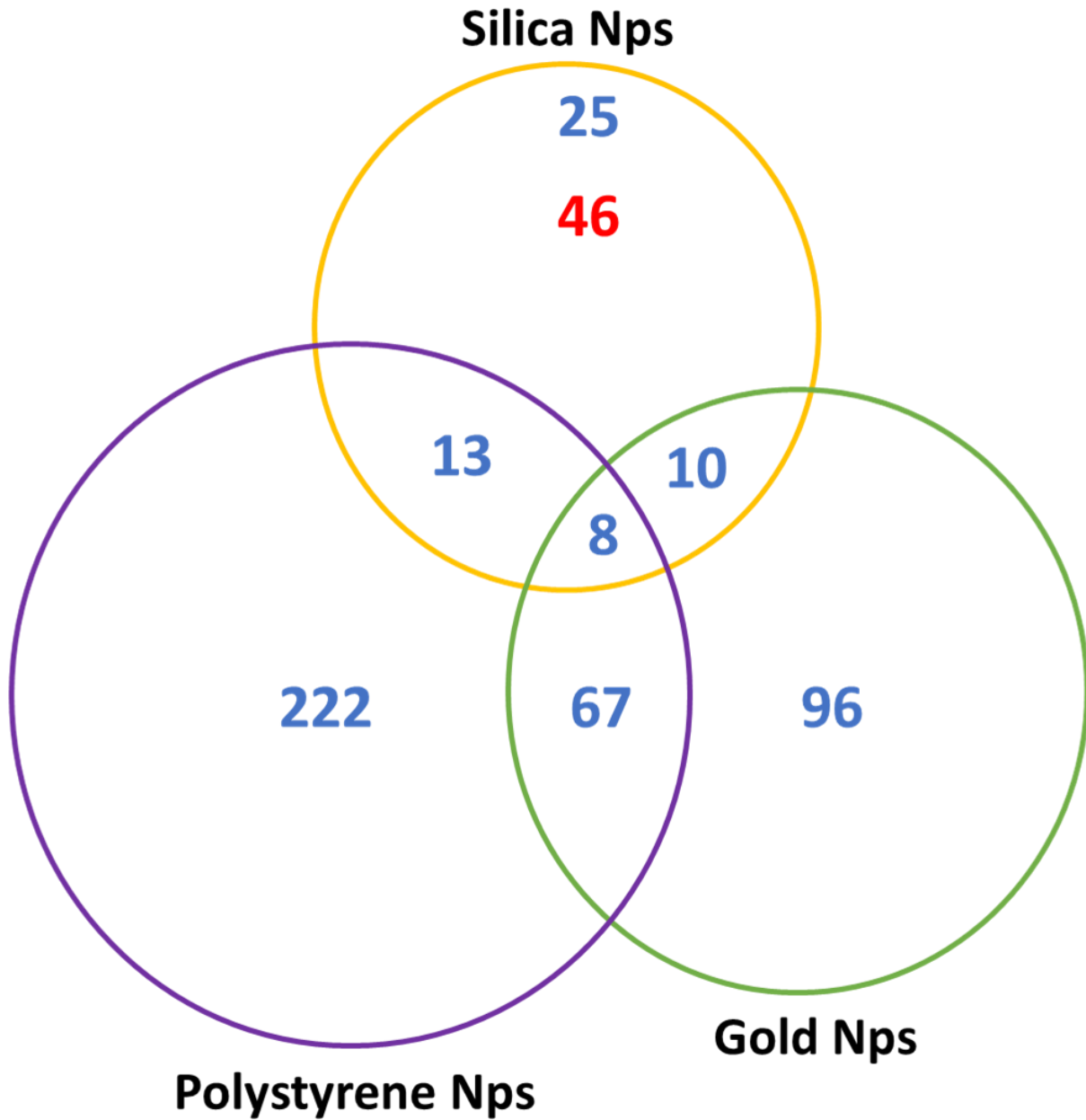


Figure 22: SEM images of the *E. coli* with nanoparticles. (a) Control, (b) silica Nps, (c) polystyrene Nps and (d) gold Nps. the red arrows show the attachment of nanoparticles to the bacteria cell wall.

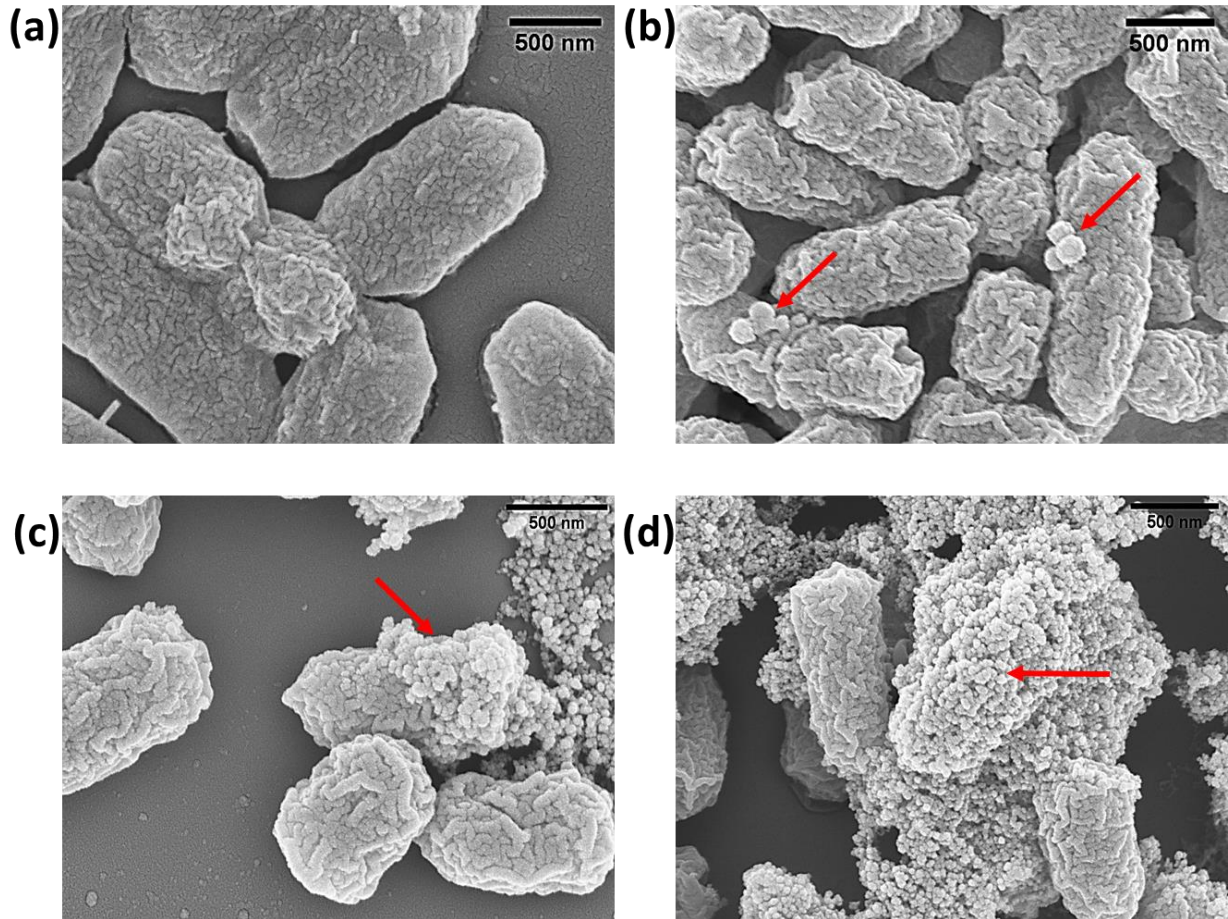


Table 6: List of the cluster genes activated by all three nanoparticles.

Genes	Description	Function	Location	Pathway
glcC	unknown CDS (DNA-binding transcriptional dual regulator)	Regulatory protein/ DNA binding protein	cytosol	Transport and metabolism of glycolate
rssB	response regulator involved in protein turnover, controls stability of RpoS (1st module)	DNA binding transcriptional activator	cytosol	Two-component regulatory system
cysQ	gene product acts on 3'-phosphoadenosine-5'-phosphosulfate	sulfate assimilation/ sulfur compound metabolic process	Cytosol/plasma Membrane	Sulfur metabolism
vacJ	lipoprotein precursor	protein transport	outer membrane	Phospholipid transport system
evgA	response regulator (activator) in two-component regulatory system with EvgS, regulates multidrug	DNA binding transcriptional activator	Cytosol	Two-component regulatory system

	resistance (LuxR/UhpA family)			
sodC	superoxide dismutase precursor (Cu-Zn)	superoxide dismutase activity	Periplasmic space	Oxidative stress response
yhdY	putative ABC superfamily (membrane) amino acid transport protein (2nd module)	membrane transport protein	inner membrane	Amino acid transport
yhhT	putative PerM family permease (1st module)	transmembrane transport	plasma membrane	Transmembrane transport

Verification of the gene expression of the common gene response to all three nanoparticles

We conducted a reverse-transcriptase polymerase chain reaction (qRT-PCR) experiment to verify the gene expression of the 8 genes (Table 6) demonstrated by the reporter gene collection to be part of the common response to all three nanoparticles stimuli. 9 primers were used for this experiment including the 16srRNA which served as internal control (Table 3). The results of the qRT-PCR showed a more dynamic gene expression levels for all 8 genes. Therefore, we observed that all the genes tested were upregulated at least once at different time points during the 4h exposure time. This validated the results obtained by the gene screening experiment. Moreover, the gene expression levels fluctuated from upregulated to downregulated which drastically differed from the upregulated pattern observed with the GFP-reporter gene

library screening results. The gene *glcC* displayed a significant upregulation at the early exposure to gold Nps and PS Nps and an overall similar pattern of expression over the exposure time (Figure 23-A).

The gene *rssB* presented a significant upregulated expression at the early exposure for both gold and PS Nps while showing a late expression in silica Nps (Figure 23-B).

The *cysQ* gene displayed almost an identical pattern of expression with various fold change values over exposure time for both gold and PS Nps while being significantly downregulated in late exposure time to silica Nps (Figure 23-C).

The gene *vacJ* demonstrated a nearly similar expression pattern for all time points except at $t=120\text{min}$ for both gold and PS Nps and were upregulated at early silica Nps exposure (Figure 23-D). The *evgA* gene showed as significant up regulation at the early exposure for both gold and silica Nps and a significant downregulation at $t=60\text{min}$ for PS Nps (Figure 23-E).

The *sodC* gene exhibited a similar pattern of up-and-down regulations with different fold changes during the exposure to both silica and gold Nps. moreover, *sodC* was early upregulated by the presence of PS Nps (Figure 23-F).

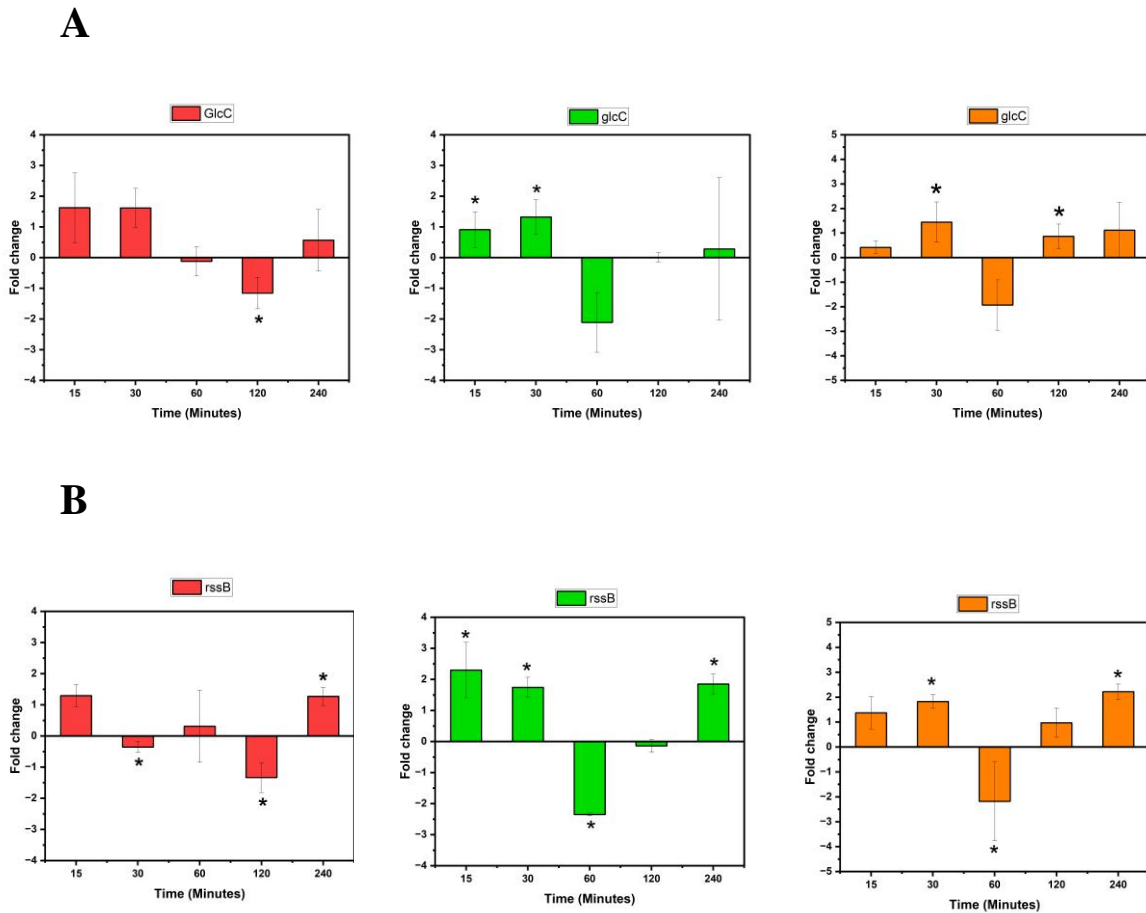
The gene expression of the *yhdY* gene demonstrated a similar trend of expression for both gold and PS Nps. furthermore, this gene was significantly upregulated and downregulated at early and late silica Nps exposure respectively (Figure 23-G).

The *yhhT* gene showed a similar up-and-down expression pattern with different fold changes for both gold and PS Nps. while upregulated at mid- exposure by silica Nps (Figure 23-H).

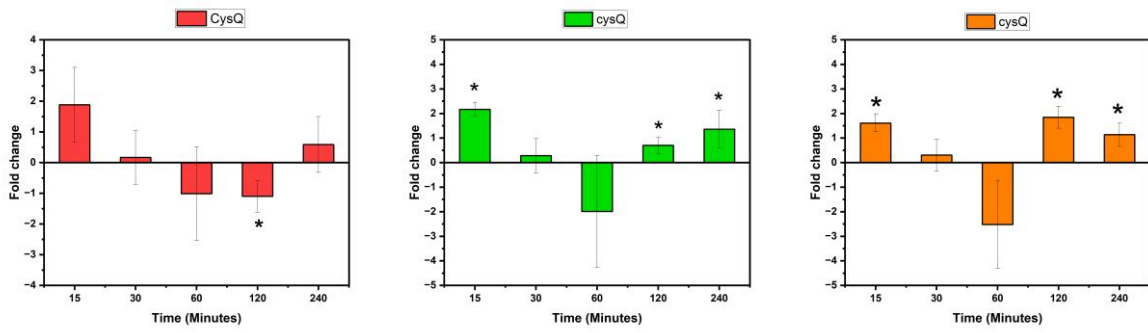
These results demonstrated that the exposure to silica, gold and polystyrene Nps triggered specific gene expression trends from the eight common genetic response genes studied. The

observation of similar gene expression patterns in some of the genes, especially between the metal nanoparticle gold and the polymeric nanoparticle polystyrene suggested potential similarity in signals unleashed by these nanoparticles responsible for that peculiar transcriptomic response pattern in *E. coli*.

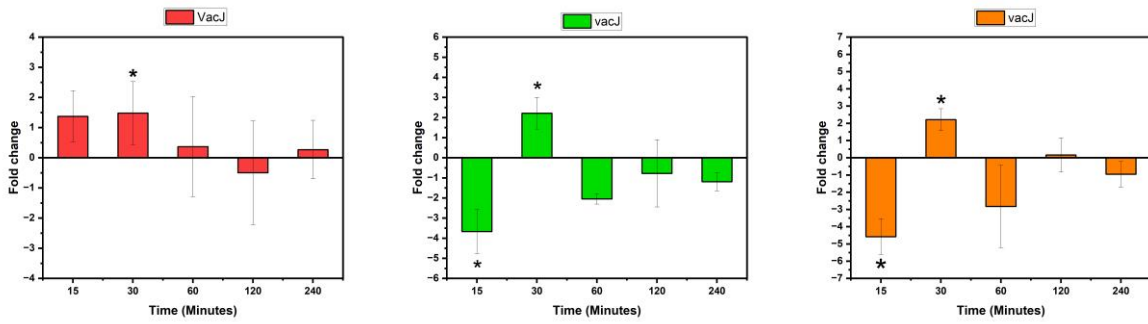
Figure 23: Differential expression of the eight genes after exposure to silica (red), gold (green), and polystyrene (orange) nanoparticles. (*) indicates the statistical significance compared to control.



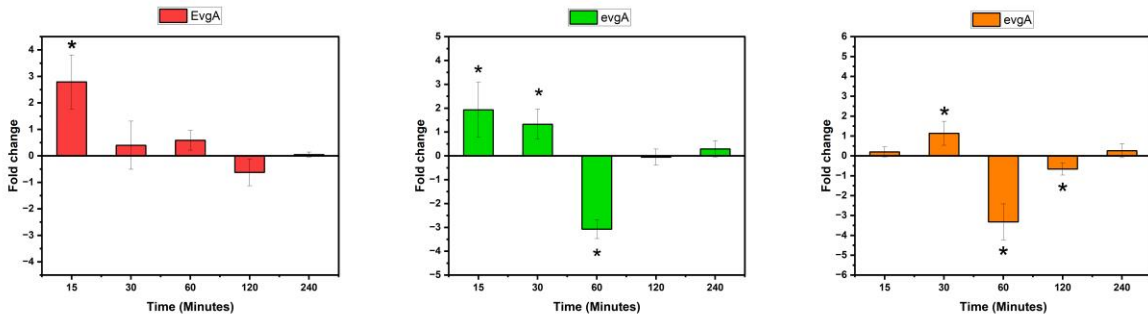
C

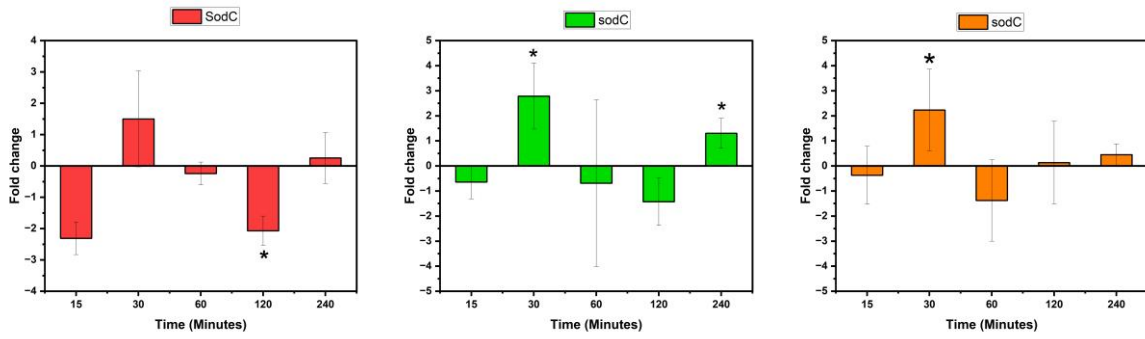
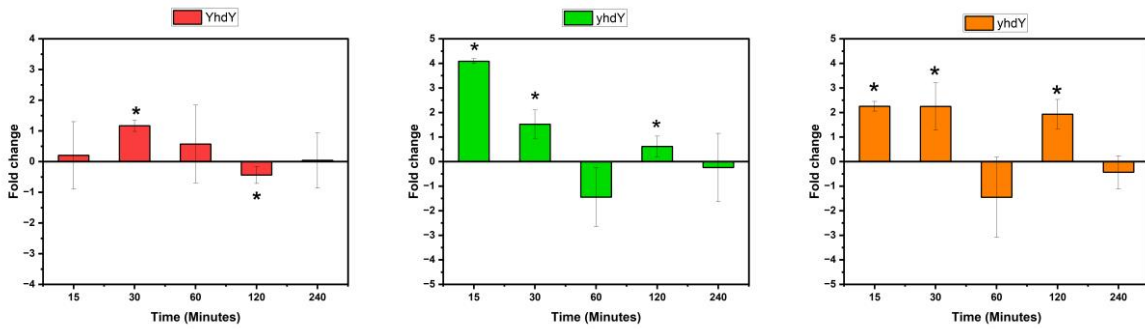
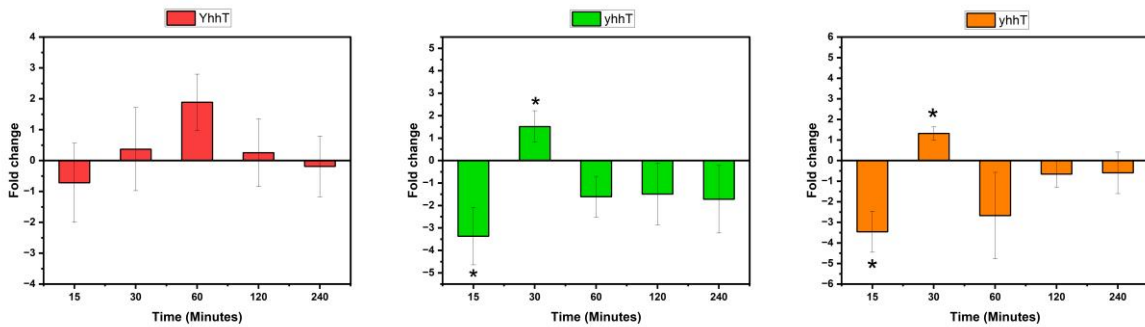


D



E



F**G****H**

***E. coli* mutants' growth curves.**

To determine whether these eight genes that are upregulated by all three nanoparticle conditions are also required for normal growth in the presence of these same nanoparticles, we examine the growth curves of *E. coli* wild type and strains that contain knockout of these genes. We examined three parameters of these growth curves: 1) timing of the lag/log transition, 2) the slope/rate of exponential growth during the log phase, and 3) the OD600 at the stationary phase. The timing lag/log phases indicated the ability of these cells to respond to their local environment resource availability and the ability of these cells to collectively coordinate their metabolism to transition into the exponential phase (Hamill et al., 2020; Schultz & Kishony, 2013). Bacteria prioritize the activation of carbon source utilization enzymes over biomass formation genes as well as metal accumulation (Schultz & Kishony, 2013). For example, *Salmonella enterica serovar Typhimurium* accumulated metal like iron and some minerals like calcium and manganese during the lag phase (Rolfe et al., 2012).

The slope of the log phase indicated the speed of proliferation of the cells and the ability of these cells to process resources into new cellular materials. At this stage, the metabolic activity is at its highest, bacteria cells are multiplying through binary fission (Schultz & Kishony, 2013). For example, in the *Bifidobacterium longum* genes associated with translation, energy generating-metabolic pathways and amino acid synthesis are activated during the log phase (Veselovsky et al., 2022). And finally, the final OD at stationary phase indicates the final cellular concentrations as bacteria deal with multiple physical and chemical stresses that change their gene expression profile for survival (Jaishankar & Srivastava, 2017).

Without any nanoparticle challenge, three mutant strains (Δ GlcC, Δ EvgA, Δ YhdY) exhibited an identical growth habit when compared to the wild-type parental strain. The

remainder strains exhibited slight but statistically significant differences in growth patterns with the wild type *E. coli* control strain. $\Delta vacJ$ and $\Delta rssB$ exhibited differences in the timing of the lag/log transition. This suggests that these genes play a role in quorum sensing mechanisms by enabling the cell-cell interactions during the bacterial growth process (Rolfe et al., 2012). $\Delta sodC$ showed changes in the timing of the lag/log transition and in the rate of proliferation of the log phase (Table 7). Which suggests that *sodC*, an enzyme involved in the intracellular oxidative stress response participate in cell division mechanisms in maintaining “normal” cell growth in log phase. *CysQ* and *YhhT* showed an increase in the final stationary phase OD, suggesting possible compensation of their metabolic functions of both genes in the bacteria growth rate regulation.

The presence of any nanoparticle used in this study did not alter the growth habit of wildtype *E. coli* BW25113 (Table 7). None of the mutant strains of *E. coli* examined in this study showed a difference in the lag/log transition when impacted with any nanoparticle. Suggesting that the differences observed between the parental and knockout strains without nanoparticles is inherent to the mutation and not the extracellular presence of nanomaterials. However, two mutants $\Delta sodC$ and $\Delta CysQ$ exhibited more rapid log phase growth in the presence of all three nanomaterials. The binary fission process seems to be accelerated in absence of these two genes. This suggests that *sodC* and *CysQ* are responsible for attenuating the proliferation rate of *E. coli* in the presence of nanomaterials, however how this is done remains unclear. Some studies showed that *cysQ* is a gene responsible for the conversion of adenosine 3'-phosphate 5'-phosphosulfate (PAPS) to adenosine 5'-phosphosulfate (APS) a critical step in the sulfite synthesis and amino acid (cysteine) biosynthesis (Hatzios et al., 2008; Zhang & Biswas, 2009). In addition, the activity of the gene *cysQ* regulate the level of PAPS which the accumulation is

toxic for the cells. thus, *cysQ* is necessary in aerobic growth conditions in *E. coli* (Neuwald et al., 1992) *sodC* gene encodes for the periplasmic Cu, Zn superoxide dismutase enzyme involved in the bacterial oxidative stress response to superoxide radical anions accumulation (D'Orazio et al., 2001; Keith & Valvano, 2007). Several mutants exhibited alterations to the rate of log phase growth under specific nanomaterial conditions. Δ glcC and Δ yhhT exhibited significant increases in the rate of log phase in presence of polystyrene Nps only. Δ vacJ and Δ rssB exposures to gold Nps showed an increased growth rate in the log phase.

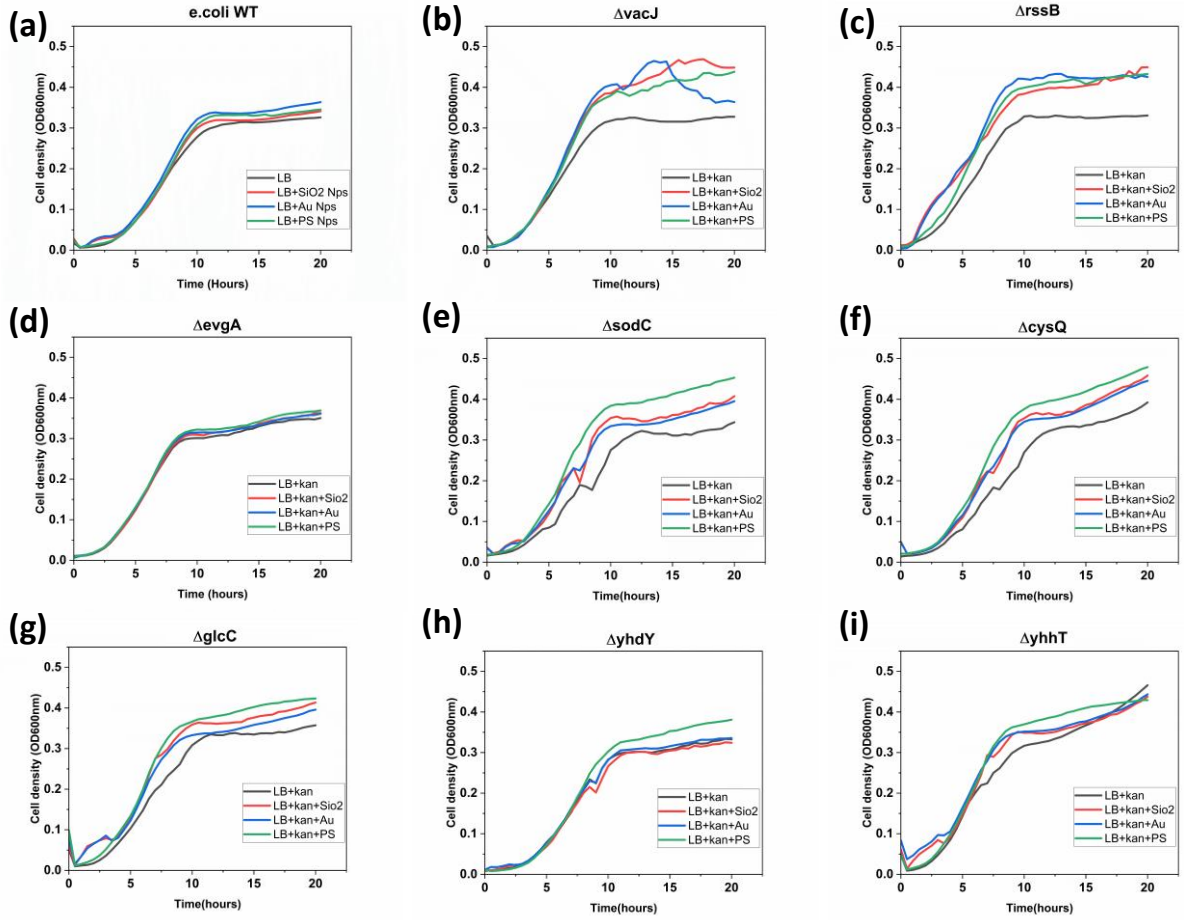
The mutants Δ sodC and Δ cysQ growth curves indicated an increase in cell density compared to the control at the T=15h stationary phase for both silica and polystyrene Nps. three mutants Δ vacJ, Δ glcC and Δ yhhT revealed an increase in cell population at the stationary phase compared to control by a single nanoparticle, polystyrene Nps for both Δ vacJ and Δ yhhT, and silica Nps for Δ glcC. The mutant Δ rssB is the only one to display a significant cellular concentration for both silica and gold Nps. None of the studied mutants showed a significant cell density at the stationary phase for all three nanoparticles.

Table 7: Parameters of the eight *E. coli* mutants' growth curves. (*) represents the statistically significant difference between wild type and mutants and () represents the statistically significant difference between nontreated (control) and nanoparticle-treated *E. coli* mutants.**

Strain	Challenges	Lag/log transition (hours)	Slope log phase	OD stationary at T=15h
<i>E. coli</i> WT	LB	2.62 ± 0.81	0.0378 ± 0.006	0.313 ± 0.022
	SiO2	2.75 ± 0.75	0.0417 ± 0.004	0.320 ± 0.040
	Au	2.68 ± 0.78	0.0444 ± 0.004	0.339 ± 0.024
	PS	2.62 ± 0.64	0.0425 ± 0.004	0.330 ± 0.033
vacJ	LB+Kan	1*	0.0358 ± 0.002	0.315 ± 0.006
	SiO2	1	0.046 ± 0.003**	0.456 ± 0.063
	Au	1.33 ± 0.47*	0.0497 ± 0.003**	0.430 ± 0.155
	PS	1	0.0437 ± 0.003	0.416 ± 0.008**
rssB	LB+Kan	1.33 ± 0.47	0.0379 ± 0.001	0.324 ± 0.015
	SiO2	1	0.0402 ± 0.0006	0.388 ± 0.008**
	Au	1	0.0476 ± 0.002**	0.422 ± 0.032**
	PS	1.33 ± 0.47	0.0499 ± 0.007	0.408 ± 0.047
evgA	LB+Kan	1.66 ± 0.47	0.0415 ± 0.001	0.327 ± 0.007
	SiO2	1.33 ± 0.47	0.0411 ± 0.001	0.336 ± 0.004
	Au	1.33 ± 0.47	0.0418 ± 0.0008	0.333 ± 0.008
	PS	1.66 ± 0.47	0.0435 ± 0.001	0.341 ± 0.004
sodC	LB+Kan	1*	0.0294 ± 0.002*	0.311 ± 0.018
	SiO2	1	0.0388 ± 0.0021**	0.361 ± 0.017**
	Au	1	0.0371 ± 0.002**	0.350 ± 0.008
	PS	2	0.0483 ± 0.002**	0.412 ± 0.020**

cysQ	LB+Kan	2.66 ± 0.47	0.0319 ± 0.002	0.336 ± 0.007*
	SiO2	2.66 ± 0.47	0.0448 ± 0.002**	0.386 ± 0.013**
	Au	2.66 ± 0.47	0.0438 ± 0.0005**	0.378 ± 0.02
	PS	2.33 ± 0.47	0.0482 ± 0.002**	0.419 ± 0.021**
glcC	LB+Kan	2.33 ± 0.47	0.0373 ± 0.001	0.334 ± 0.0009
	SiO2	1	0.0408 ± 0.003	0.376 ± 0.01**
	Au	1.33 ± 0.47	0.0402 ± 0.005	0.358 ± 0.004
	PS	2.33 ± 0.23	0.0529 ± 0.003**	0.408 ± 0.025
yhdY	LB+Kan	3.33 ± 0.23	0.039 ± 0.004	0.307 ± 0.007
	SiO2	3.16 ± 0.23	0.0361 ± 0.003	0.304 ± 0.007
	Au	3	0.0378 ± 0.002	0.315 ± 0.015
	PS	3.33 ± 0.23	0.0444 ± 0.001	0.353 ± 0.017
yhhT	LB+Kan	2.16 ± 0.23	0.0407 ± 0.0002	0.367 ± 0.006*
	SiO2	1.5 ± 0.70	0.0434 ± 0.004	0.372 ± 0.001
	Au	1.33 ± 0.47	0.0434 ± 0.006	0.377 ± 0.012
	PS	2	0.0543 ± 0.0007**	0.41 ± 0.008**

Figure 24: *E. coli* mutants growth curves from exposure to silica, gold, and polystyrene nanoparticles



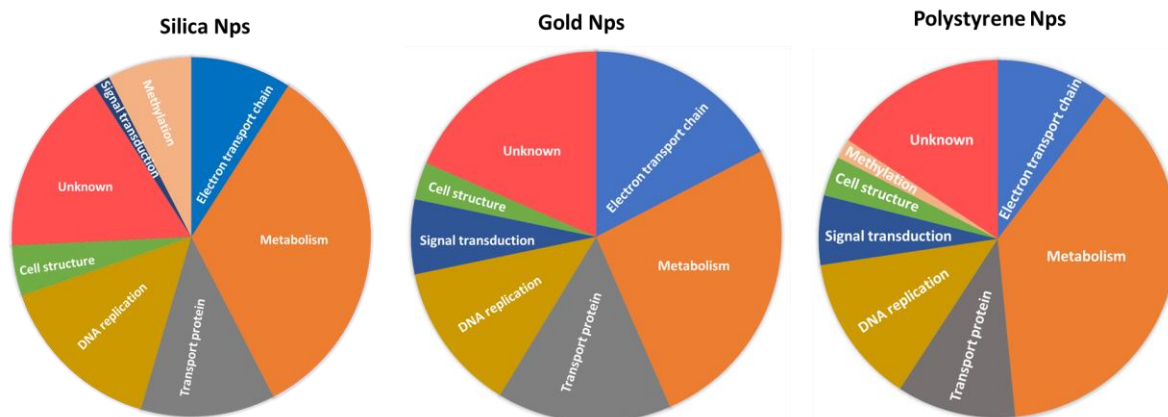
Discussion

The common gene response: Gene expression profile and growth fitness of *E. coli*.

The goal of this study was to determine the transcriptional responses of the bacterium *E. coli* to engineered silica, gold, and polystyrene nanoparticles at nonlethal concentrations. The results obtained through a gene screening analysis showed that 25 genes were upregulated, and 46 genes were downregulated by silica Nps, 96 genes and 222 genes were up regulated by gold and polystyrene Nps respectively. This suggests that there are significant and specific transcriptional profile alterations occurring during the exposure to nanoparticles. This study as well as other studies showed that extracellular assaults of nanoparticles can induce internal metabolic modifications in bacteria (Mortimer et al., 2021; Neal, 2008; Pelletier et al., 2010). This is supported by the gene ontology analysis which demonstrated that metabolic pathways, signal transduction pathways, DNA replication, electron transport chain, transport protein and cell structure are significantly activated by the presence of all three nanoparticles with polystyrene Nps having the highest metabolic alterations among all three nanoparticles (Figure 25). More importantly the gene expression of eight genes part of the common response to all three nanoparticles was evaluated and verified using qRT-PCR. This cluster of genes consists of two two-component regulatory systems response *rssB* (Klauck et al., 2001) and *evgA* (Nishino & Yamaguchi, 2002) that are response regulators in the *rssA/rssB* systems and the *evgS/evgA* system respectively. One gene *sodC*, involved in the regulation of intracellular free radicals' formation (Keith & Valvano, 2007), one gene *cysQ* involved in the sulfur metabolism (Neuwald et al., 1992), another gene *glcC*, is part of the transport and metabolism of glycolate (Pellicer et al., 1996). The gene *yhdY* is speculated to be part of the amino acid transport while the gene

vacJ is involved in phospholipid transport (Xie et al., 2016) and finally yhhT with the molecular function that has not been determined yet, but it is considered as per some unpublished research as a protein transport.

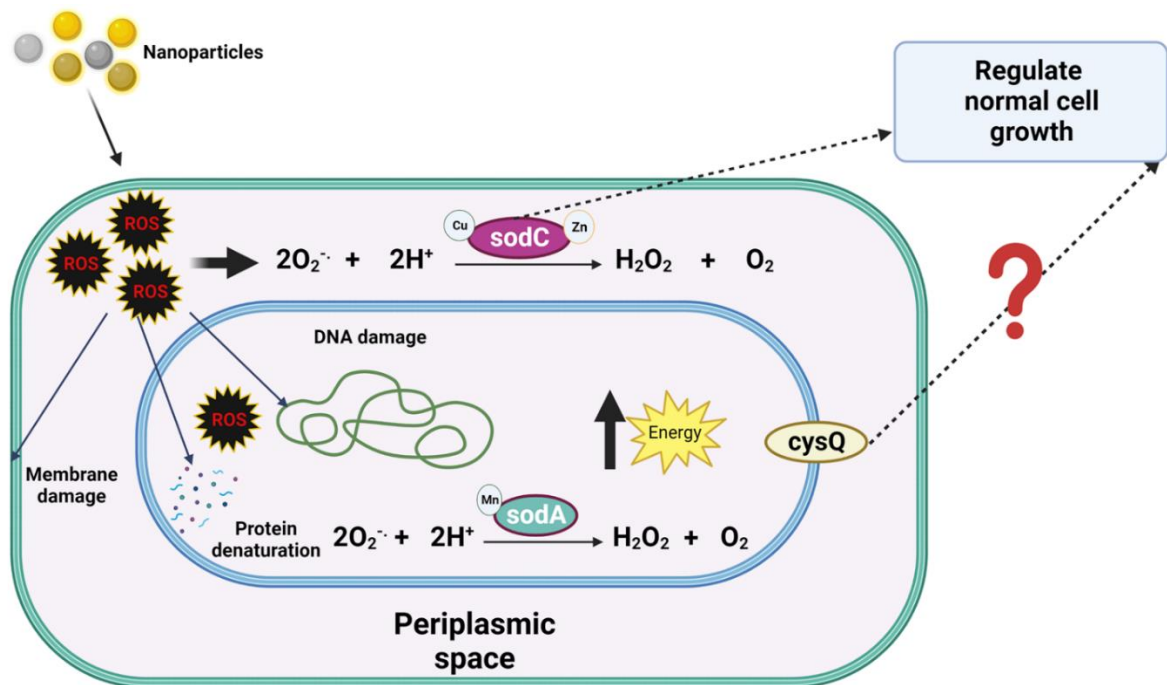
Figure 25: Gene ontology of genes activated by Nanoparticles.



Apparently, there is no established direct connection between all these eight genes that comprise the nanoparticle response, I have discovered. There is a distant connection that exists between evgA and rssB signal transduction systems through the phoQ/phoP system and a small protein B1500 (Eguchi et al., 2007). Some studies reported that production of ROS occurred during the interaction of bacteria with nanoparticles that induced an increase in production of scavenger enzymes to control the concentration of intracellular ROS (Babayevska et al., 2022; Benov & Fridovich, 1994; Joshi et al., 2020). This is corroborated in our study by the upregulation of the gene sodC. The upregulation of the gene vacJ which is involved in the phospholipid transport pathway and also responsible for maintaining the lipid asymmetry in the outer membrane (Xie et al., 2016; Zhao et al., 2017). This indicates a significant activity of the gene vacJ to preserve the integrity of the lipid asymmetry in the outer membrane likely disrupted by the presence of all three nanoparticles as shown in Figure 22 and by other studies (Babayevska et al., 2022; Mortimer et al., 2021; Slavin et al., 2017).

The growth curves of the single gene mutation of the common genetic response demonstrate a possible cell growth promotion in presence of nanoparticles. This suggests that to compensate the absence of the genes, bacteria intensify their metabolic activities while utilizing alternative intracellular enzymes susceptible to continue the cell growth cycle. Several studies reported that metal nanoparticles such as titanium dioxide nanoparticles can promote cell growth in of bacteria (Chavan & Nadanathangam, 2019; Timmusk et al., 2018). Gram-negative bacteria such as *E. coli* may require the activation of genes such as *sodC* and *cysQ* to maintain normal cell growth and cell size during the cell division process as well as assuring the bacterial survival in drastic growth conditions (Figure 26) (Keith & Valvano, 2007; Neuwald et al., 1992).

Figure 26: Proposed model of *sodC* and *cysQ* genes in the regulation of normal cell growth in *E. coli*



Conclusion

The rise in production of engineered nanoparticles comes along with the increasing risk of nanopollution that could likely jeopardize human health and modify the inherent microbiome balance and function in every ecosystem. This study provides a critical insight about the transcriptional responses of bacteria to commercially relevant silica, gold, and polystyrene nanoparticles. Besides the specific gene expression triggered by individual nanoparticle, the existence of a common genetic responses activated by these nanoparticles in *E. coli* enables to understand the interaction between bacteria and nanoparticles. The studied nanoparticles show no inhibitory effects on the single gene knockout of the common gene response revealing the essential role of genes *sodC* and *cysQ* in controlling and regulating the normal bacterial cell growth. This provides critical information about the possible action mechanisms of these nanoparticles when encountering bacteria. However, it is important to further evaluate the real-world ramifications of these bacterial stress response induced by nanoparticle exposure.

CHAPTER IV: EXPRESSION OF OXIDATIVE STRESS RELATED GENES IN *E. COLI* AT THE INTERFACE OF CHARGED GALLIUM NITRIDE SURFACES

This chapter is a reprint of the published paper: Gleco S, Noussi T, Jude A, Reddy P, Kirste R, Collazo R, LaJeunesse D, Ivanisevic A. Oxidative Stress Transcriptional Responses of *Escherichia coli* at GaN Interfaces. *ACS Appl Bio Mater.* 2020 Dec 21;3(12):9073-9081. doi: 10.1021/acsabm.0c01299. Epub 2020 Dec 1. PMID: 35019584.

This study was a collaborative work with the research teams from North Carolina State University, Adroit Materials, and the Joint School of Nanoscience and Nanoengineering. My participation as the second author in this project consisted of determining the gene expressions of the three genes *oxyS*, *KatE* and *sodB* of the RNA samples extracted from the exposure of *E. coli* to gallium Nitride (GaN) surfaces using qRTPCR technique.

Introduction

Microorganisms regulate their physiology at interfaces in response to the physicochemical cues of surfaces in order to adapt to environmental stress and transition to a biofilm lifestyle (Tuson & Weibel, 2013; Y. Wang et al., 2014). Physiological regulation in bacteria is driven by changes in gene expression in response to environmental signals that perturb baseline physiology such as disturbances in membrane potential or increases in reactive oxygen species (ROS) (Bruni et al., 2017; Kim et al., 2019; G. Wang et al., 2017). The efficiency with which microbes respond to environmental cues is dependent on the sensing functions that detect signals. Mechanical signals from surface interactions can be sensed through pathways related to structural components like lipopolysaccharides, flagella, pili, and curli (Muhammad et al., 2020; Rizzello et al., 2011; Song et al., 2017; Tuson & Weibel, 2013). Understanding the

relationship between bacteria sensing functions and their specific involvement with detecting physicochemical cues is important for biomedical and environmental applications.

The surface properties of semiconductors can be modified using approaches such as surface chemistry and light stimuli to engineer surfaces that predictably modulate microbial interactions. The role of surface properties for biointerface applications have been widely studied for biomedical applications such as cell-instructive surfaces, neural interfaces, and *in vitro* sensing applications (Jiang & Tian, 2018; Ross & Lahann, 2015; Snyder, Reddy, Kirste, Collazo, et al., 2018). Although relatively less explored, understanding the interactions of microbes at semiconductor surfaces is important for bioelectronics. The biocompatibility and wide bandgap properties of III-nitride materials are useful for bioelectronics applications including sensing and communication devices (Li & Liu, 2017; Podolska et al., 2012; Snyder, Reddy, Kirste, LaJeunesse, et al., 2018). We have reported on topography and surface chemistry modifications of GaN and $\text{Al}_x\text{Ga}_{1-x}\text{N}$ using wet chemical etching and functionalization with organic adsorbates (Gleco et al., 2019c; Pearce et al., 2015; Snyder et al., 2016; Snyder, LaJeunesse, et al., 2018; Snyder, Reddy, Kirste, LaJeunesse, et al., 2018). Additionally, GaN exhibits persistent photoconductivity (PPC) which is the slow decay of surface charge that accumulated under UV light exposure after the light stimulus is removed. We have demonstrated that surface charge remains for several minutes after the light is removed which enabled noninvasive stimulation of bacteria, yeast, and neurotypical cells at the interface (Gulyuk et al., 2018, 2019; Iyer et al., 2019; Snyder, LaJeunesse, et al., 2018; Snyder, Reddy, Kirste, LaJeunesse, et al., 2018).

The purpose of this study was to identify if the interfacial properties of the substrate triggered an oxidative stress response in *E. coli* at the interface. We analyzed the interactions of *E. coli* at modified GaN interfaces by using quantitative reverse transcriptase polymerase chain

reaction (qRT-PCR) to measure the levels of expression of three oxidative stress related genes – *oxyS*, *katE*, and *sodB*. The PPC properties of GaN were used to analyze the influence of surface charge on regulating the transcription of these genes. The surfaces were also modified using wet chemical treatments that affect the oxides on the surface and have an impact on surface charge (Gleco et al., 2019c, 2020; Snyder, LaJeunesse, et al., 2018; Wilkins et al., 2014). We also evaluated the involvement of structural components on regulating the interfacial interactions using mutated *E. coli* with the *fliC* and *csgG* genes deleted to inhibit the formation of flagella and curli, respectively. The results showed that transcriptional changes related to the target genes could be influenced by surface charge changes. However, there were effects from surface chemistry that changed the transcription of these gene in a way that did not correlate to surface charge. Furthermore, the results differed when flagella and curli were deleted, indicating that they are important structural components for regulating the target pathways at interfaces. The results of this work add to our understanding of the interactions of *E. coli* at interfaces and will be useful for the development of biointerfaces.

Experimental section

Bacteria and growth conditions

The *E. coli* used in this study were from the Keio library and have been used in recent work (Baba et al., 2006; Gleco et al., 2020; Iyer et al., 2019). The parent strain of the single deletion Δ *fliC* and Δ *csgG* mutants was BW25113. The bacterial cultures were grown overnight at 37°C in Tryptic soy broth (Carolina Biological Supply, item #776840) in a shaker incubator before exposure to the surfaces.

Substrate preparation: The GaN wafer used in this work was doped at a concentration of $2 \times 10^{19} \text{ cm}^{-3}$ with Si. The growth process has been described in previous work (Collazo et al.,

2006; Kirste et al., 2013; F. Liu et al., 2007). The details of the substrate preparation have been previously described in depth (Gleco et al., 2019a; Wilkins et al., 2014, 2015) and were the same as those used in recent work (Gleco et al., 2020). Briefly, the 2-inch GaN wafer was diced and cleaned by sonication in acetone, methanol, and water. The substrate pieces were then etched using a 1:1 solution by volume of 85% HCl and diH₂O at 100°C. The samples labeled clean received no further treatment. The substrates labeled “H₂O₂” were soaked for 3 hours in 30% H₂O₂ at room temperature. The substrates labeled “H₃PO₄” were etched in a solution of phosphoric acid at 40°C for 2.5 hours. Last, the substrates labeled “H₃PO₄/C₃H₉O₃P” were soaked in a solution of phosphoric acid and propylphosphonic acid at 40°C for 2.5 hours. The substrate pieces were used multiple times and were autoclaved, cleaned, and retreated prior to bacteria exposure.

Surface exposure protocol and RNA isolation: The protocol for exposing the *E. coli* to the surfaces was used in recent work (Gleco et al., 2020). The surfaces were charged using UV light for 30 minutes. The UV light was then turned off and a 20 µL drop of the overnight bacterial suspension was put in contact with the surface. The bacteria were left on the surface for 5 minutes before pipetting off and transferring into 500 µL of Tryptic soy broth. The suspension was placed into an incubator at 37 °C for 1 hour. Then, a 400 µL portion of the suspension was centrifuged at 13,000 x g for 60 seconds to collect the cells for RNA extraction. The RNA was isolated and purified from the bacteria using the Invitrogen™ RiboPure™ RNA Purification Kit for bacteria (ThermoFisher, cat. AM1925). The manufacturer protocol was followed without modification. Briefly, the bacteria were mechanically lysed using zirconia beads. A phenol-chloroform extraction was used to separate the organic and aqueous phases, which isolates the

nucleic acids from proteins. The nucleic acids were washed and purified using ethanol and a series of washes included with the kit.

qRT-PCR

Quantitative real-time PCR was performed using 20ng of RNA as collected above, amplified using the Luna Universal Probe One-Step RT-qPCR kit (NEB, E3006L) in an Applied Biosystems 7500 Fast PCR System instrument. Gene expression was normalized by the threshold cycle (CT) method.

Table 8: Primer selection for RTPCR

primer set	forward sequence (5'-3')	reverse sequence (5'-3')
16S RNA	TGCCTGATGGAGGGGGATAA	CCGAAGGTACCCCTCTTTGG
oxyS	CCTGGAGATCCGCAAAAGTTC	GCGGCACCTCTTTTAACCCT
katE	TCCGACTGCCCTTACCATA	GTTCGGTTCGTAATTCGCCG
sodB	AAGATGCTCTGGCACGCCACATTT	TAAACTGCGCTTTGAAATCGGCAA

Statistical analysis: One-way ANOVA using Origin 2019 software (version 9.6.0.172) was used for statistical analysis. Tukey's test was used to determine statistically significant differences. All statistics used a significance level of $p < 0.05$ and $n = 3$.

Results and discussion

This work builds off a recent study in which we used *in vitro* assays to measure the intracellular ROS and Ca²⁺ levels of the mutated and WT *E. coli* one-, two-, and three-hours after an initial 5 minute exposure to charged and uncharged surfaces (Gleco et al., 2020). We demonstrated in this previous work that short exposure to charged surfaces did not have a significant impact on the levels of ROS. We found that the Ca²⁺ levels could be stimulated by

surface charge with additional effects from the substrate surface chemistry and the involvement of flagella and curli. Furthermore, the effects measured one-hour after the initial surface exposure were generally gone by the second- and third-hours.

We employed the same protocol to expose the *E. coli* to the substrates in this study. After charging the surfaces using UV light, we utilized the PPC properties to expose the *E. coli* to the charged and uncharged surfaces for 5 minutes in the absence of UV light. The bacteria were removed from the surface and incubated for one hour before the RNA was isolated for qRT-PCR analysis. The only modification to the protocol for this study is that we did not measure the gene expression two- and three-hours after the initial surface exposure because the results from the previous study indicated that initial effects were generally gone by these time points.

Gene-knockouts were used to assess the influence of flagella and curli on regulating the interactions of *E. coli* at the interface. In previous work we have found that the lack of flagella and curli changed the way the *E. coli* responded to charged GaN interfaces (Gleco et al., 2020; Iyer et al., 2019). The flagella-mutated ($\Delta fliC$) *E. coli* had the *fliC* gene deleted and the curli-mutated ($\Delta csgG$) *E. coli* had the *csgG* gene deleted. The *fliC* gene encodes for flagellin which is the primary subunit of flagella (Haiko & Westerlund-Wikström, 2013). Thus, removing this gene prohibits flagella from forming. The *csgG* gene encodes for the CsgG outermembrane lipoprotein that is essential for secretion of the curli subunits CsgA and CsgB. (Barnhart & Chapman, 2006) Prohibiting CsgA and CsgB secretion prevents curli formation. The relative levels of gene expression of the $\Delta fliC$ and $\Delta csgG$ *E. coli* were compared to the wild-type (WT) *E. coli* to determine if the absence of flagella or curli affected the response.

Substrate treatment and properties overview

The GaN substrates were modified using chemical treatments that have been described in previous work (Gleco et al., 2019b, 2020; Wilkins et al., 2014, 2015). Briefly, all surfaces were cleaned then etched using HCl to remove the native surface oxide. The substrates labeled “clean” received no further treatment. The remaining three groups of samples were treated using H₂O₂, H₃PO₄, or H₃PO₄/C₃H₉O₃P and labeled accordingly. The surfaces were characterized in the previous study using atomic force microscopy, Kelvin-probe force microscopy, and contact angle goniometry to determine the effects of chemical treatments and UV light on roughness, surface charge, and wettability, respectively (Gleco et al., 2020). The important characterization result from the previous study is that the clean surface had lower surface charge than the chemically treated surfaces before and after UV exposure. Additionally, there was an increase in surface charge after UV exposure for the clean and H₂O₂-treated surfaces. The UV light did not significantly increase the surface charge of the H₃PO₄ and H₃PO₄/C₃H₉O₃P surfaces as measured by KPFM.

Explanation of the pathways probed

Transcriptomic analyses of *E. coli* have revealed that the genetic expression can be changed in response to external stresses (Aunins et al., 2019; Oladeinde et al., 2018; Partridge et al., 2006; Rizzello et al., 2011; Singh et al., 2019). Using qRT-PCR, we analyzed the expression of three genes related to oxidative stress pathways in *E. coli* – *oxyS*, *katE*, and *sodB*. Analysis of these three genes serves as an indicator of oxidative stress induced by the surface properties of the substrates. The *oxyS* gene is upregulated under oxidative stress to control H₂O₂ levels and has shown to reduce mutagenesis in *E. coli* (Altuvia et al., 1997; González-Flecha & Demple, 1999). The *katE* gene is an indicator of catalase activity which increases when the bacteria are under

oxidative stress from H₂O₂ (Loewen et al., 1985; Nagamiya et al., 2007). Oxidative stress is also indicated by *sodB* levels, which are upregulated to protect the bacteria against superoxide anions (Geslin et al., 2001). The SodB enzyme encoded for by the *sodB* gene catalyzes the reduction of superoxide to H₂O₂.

We compared the relative expression of *oxyS*, *sodB*, and *katE* in *E. coli* one hour after exposure to charged and uncharged GaN surfaces. All measurements were done in triplicate for statistical significance which was verified by performing one-way ANOVA with Tukey’s test to compare the charged and uncharged surfaces. Biologically significant differential gene expression between the charged and uncharged surfaces was assessed by calculating the fold-change in expression. If the charged surface had higher gene expression than the uncharged surface, the fold-change was calculated by dividing the Ct value of the charged surface by the Ct value of the uncharged surface. The inverse of this was done if the uncharged surface had higher gene expression than the charged surface. Furthermore, if the uncharged surface had higher expression than the charged surface, a negative was added to indicate that the genes were expressed less on the charged surface. These values are presented in Table 9.

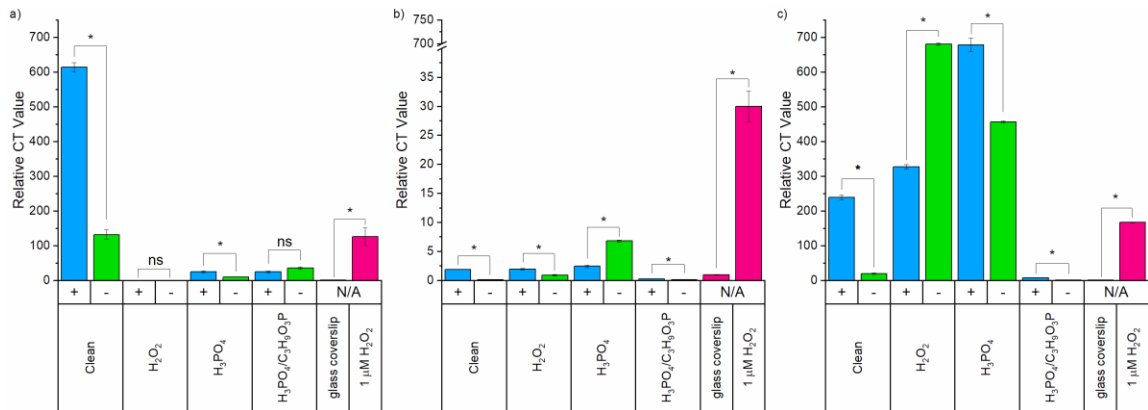
Table 9: Fold-change in gene expression between the charged and uncharged surfaces

	Fold Change Scale	Gene	Surface treatment	WT	Δflic	ΔcsgG
UV- > UV+	-4 and lower	<i>katE</i>	Clean	4.66	15.84	12.38
	-3.50		H ₂ O ₂	1.01	2.14	-2.08
	-3.00		H ₃ PO ₄	2.66	-2.78	1.49
	-2.50		H ₃ PO ₄ /C ₃ H ₉ O ₃ P	-1.45	2.50	22.82
	-2.00		1 μM H ₂ O ₂ vs glass coverslip	136.59	30.83	162.38
UV+ = UV-	-1.50	<i>sodB</i>	Clean	50.49	5.09	1.23
	-2.00		H ₂ O ₂	-1.74	3.37	2.96
	-2.50		H ₃ PO ₄	4.01	1.55	1.07
	-3.00		H ₃ PO ₄ /C ₃ H ₉ O ₃ P	1.08	1.99	-2.84
	-3.50		1 μM H ₂ O ₂ vs glass coverslip	33.43	-1.75	1.54
UV+ > UV-	1.50	<i>oxyS</i>	Clean	7.49	4.07	8.77
	2.00		H ₂ O ₂	-1.45	2.06	-3.85
	2.50		H ₃ PO ₄	4.68	-2.60	-7.46
	3.00		H ₃ PO ₄ /C ₃ H ₉ O ₃ P	1.08	2.08	3.24
	3.50		1 μM H ₂ O ₂ vs glass coverslip	8.39	18.17	2.77
	4 and greater					

katE expression

The relative levels of expression of the *katE* gene are shown in Figure 26. The expression of *katE* was greater in the WT, Δ fliC, and Δ csgG *E. coli* exposed to the 1 μ M H₂O₂ solution compared to the glass coverslip. The WT and Δ csgG *E. coli* had similar levels of *katE* expression after exposure 1 μ M H₂O₂ with 136.59-fold and 162.38-fold increases, respectively. The Δ fliC *E. coli* had lower levels overall and lesser change in expression of 30.82-fold increase when exposed to the 1 μ M H₂O₂ solution compared to the coverslip. This indicates that the flagella are involved with regulating H₂O₂ response in solution. However, when curli were absent the fold-change in expression was slightly greater than the WT, which indicates that the curli are also involved.

Figure 27: Relative Ct values of *katE* expression for the a) WT, b) Δ fliC, and c) Δ csgG *E. coli*



The WT *E. coli* had 4.66-fold increased *katE* expression when exposed to the charged clean surface compared to the uncharged clean surface. There was also 2.66-fold higher expression in the WT *E. coli* exposed to the H₃PO₄-treated surface. There was no statistically significant change in the expression for the H₂O₂-or H₃PO₄/C₃H₉O₃P-treated GaN. Furthermore, the expression of *katE* for WT *E. coli* exposed to the charged and uncharged H₂O₂-, H₃PO₄-, and

H₃PO₄/C₃H₉O₃P-treated GaN were lower than the Ct values of the bacteria exposed to the clean GaN surfaces. This indicates that the surface chemistry of the substrates played a role in the expression of *katE* in a way that reduced transcription. One explanation for this is that the increased surface charge on the chemically treated surfaces compared to the clean surface may have reduced *katE* expression by changing the interactions. Another explanation is that the surface treatments reduced the amount of H₂O₂ generated by the surface.

In contrast to the WT *E. coli*, the Δ fliC *E. coli* had significantly lower levels of *katE* expression when exposed to the clean surface. However, the fold-change in expression was greater with 15.84-fold difference, indicating that there was a response triggered by surface. However, the overall lower levels further support the results from the controls which indicated that flagella are involved with *katE* expression. In general, the levels of expression were similar for each of the surface treatments. The Δ fliC *E. coli* exposed to the charged clean, H₂O₂, and H₃PO₄/C₃H₉O₃P surfaces had higher expression than the bacteria exposed to the same uncharged surfaces with 15.84-, 2.14-, and 2.50-fold higher values, respectively. The bacteria exposed to the H₃PO₄ surfaces had higher levels of *katE* expression after exposure to the uncharged surface compared to the charged surface with -2.78-fold lower expression on the charged surface compared to the uncharged surface. The chemically treated surfaces showed similar levels to the WT *E. coli* but there were differences in the fold-change. These results indicate that the Δ fliC *E. coli* had some response to the differences in surface chemistry. However, the difference compared to the WT on for the clean surface suggests a different interaction of the *E. coli* with the surface when the flagella were deleted.

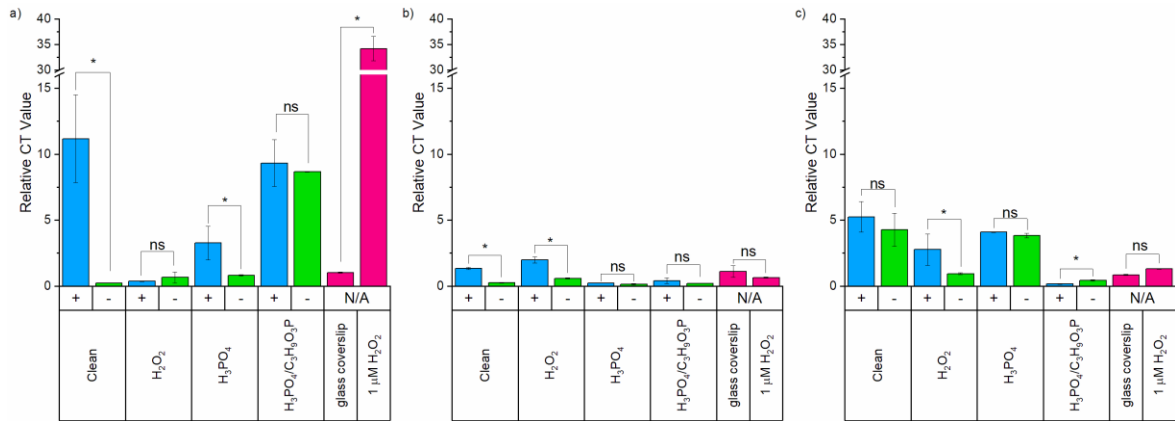
The Δ csgG *E. coli* exposed to the clean GaN had higher expression of *katE* when exposed to the charged surface compared to the uncharged surface with a 12.38-fold difference.

The levels of expression and fold-change were greater than the Δ fliC *E. coli* and lower than the WT *E. coli*. The expression of *katE* for the Δ csgG *E. coli* exposed to the H₃PO₄/C₃H₉O₃P surfaces was greater on the charged surfaces compared to the uncharged surface with a 22.82-fold change which was greater than the WT and Δ fliC *E. coli*. The most significant difference of the Δ csgG *E. coli* compared to the WT and Δ fliC *E. coli* is for the H₂O₂ and H₃PO₄ treated surfaces. Compared to the WT and Δ fliC *E. coli*, the Δ csgG *E. coli* had significantly higher levels of expression for the charged and uncharged surfaces. The fold-change in expression for the Δ csgG *E. coli* exposed to the H₂O₂-GaN was 2.08-fold lower on the charged surface compared to the uncharged surface. The expression of *katE* for the Δ csgG exposed to the H₃PO₄-GaN was 1.49-fold greater on the charged surface compared to the uncharged. This indicates that curli played a role with modulating the interactions at the surface. However, the results do not correlate directly with surface charge differences. Furthermore, the overall greater magnitude in *katE* expression on the surfaces treated with H₂O₂ and H₃PO₄ suggests that surface chemistry played an important role on modulating the interactions.

***sodB* results**

The expression of *sodB* is presented in Figure 27. The expression of *sodB* in the WT *E. coli* exposed to 1 μ M H₂O₂ solution was increased 33.43-fold compared to those exposed to the glass coverslip. The Δ fliC and Δ csgG *E. coli* had no significant difference between the controls, indicating that *sodB* transcription is related to flagella and curli. Additionally, the presence of H₂O₂ in itself is not a trigger for *sodB* transcription as it is involved with removing superoxide anions. Because the transcription of *sodB* was upregulated in response to H₂O₂ for the WT but not the Δ fliC or Δ csgG *E. coli*, the *E. coli* may be more sensitive to lower levels of superoxide through pathways involved with flagella and curli.

Figure 28: Relative Ct values of *sodB* expression for the a) WT, b) Δ fliC, and c) Δ csgG *E. coli*



The WT *E. coli* had no change in *sodB* expression between the charged and uncharged H₂O₂ or H₃PO₄/C₃H₉O₃P surfaces. There was a 50.49-fold increase on the charged clean surface and a 4.01-fold increase on the charged H₃PO₄ surface compared to the uncharged surfaces of the same treatments. Although there was no difference between the charged and uncharged surfaces, the expression of *sodB* in the WT *E. coli* exposed to the H₃PO₄/C₃H₉O₃P was greater than the expression of those exposed to the H₃PO₄ surface. The difference in expression between the charged and uncharged clean GaN suggests that surface charge can stimulate *sodB* transcription in *E. coli* in a way that can be blunted by the surface chemistry.

The Δ fliC *E. coli* showed a different response to the surfaces compared to the WT. There was 5.09-fold greater expression on the charged clean surfaces and 3.37-fold greater expression on the charged H₂O₂ surface compared to the uncharged surfaces. There was no significant difference in *sodB* expression in the Δ fliC *E. coli* exposed to the charged and uncharged H₃PO₄ or H₃PO₄/C₃H₉O₃P surfaces. The overall expression of *sodB* for the Δ fliC *E. coli* was lower than the WT *E. coli* for nearly every surface which indicates that flagella are involved with regulating *sodB* expression at interfaces. The exception is the H₂O₂ surface which had greater expression on

the charged surfaces for the Δ fliC compared to the WT. Furthermore, the WT *E. coli* showed no difference between the charged and uncharged H₂O₂ surfaces. Although the levels of expression were close to the WT, the difference between the Δ fliC and WT for the H₂O₂ surface chemistry suggests that the surface chemistry after H₂O₂ passivation altered the way non-flagellated *E. coli* respond to surface charge.

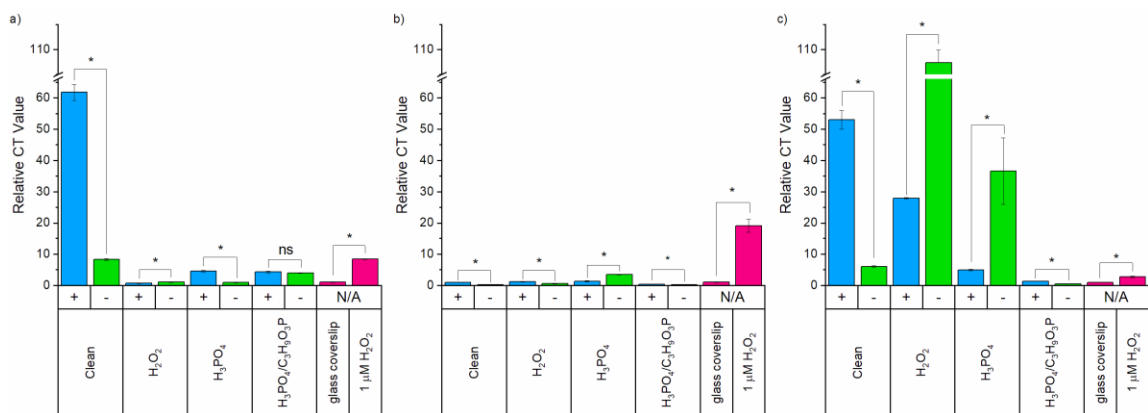
The Δ csgG *E. coli* showed different expression of *sodB* from both the WT and Δ fliC *E. coli*. There was no significant change in expression between the charged and uncharged surfaces for the Δ csgG *E. coli* exposed to the clean or H₃PO₄ surfaces while there was for the WT *E. coli*. Like the Δ fliC mutants, there was greater *sodB* expression of 2.96-fold on the charged H₂O₂ surface compared to the uncharged surface. This suggests that curli have a role in regulating *sodB* at charged interfaces because the WT *E. coli* showed no response. The Δ csgG mutants were the only *E. coli* to show a difference in *sodB* expression for the H₃PO₄/C₃H₉O₃P surface with 2.84-fold lower expression on the charged surface compared to the uncharged surfaces. However, the level of expression was lower than the WT *E. coli* and similar to the Δ fliC *E. coli*. This indicates that the absence of curli and surface chemistry changes the way the *E. coli* respond surface charge. Additionally, the lack of change in expression between the charged and uncharged clean surface indicates that curli are important for regulating the interactions at charged interfaces.

oxyS results

The results of *oxyS* expression are presented in Figure 28. The expression of the *oxyS* gene was greater in the *E. coli* exposed to the 1 μ M H₂O₂ control solution compared to the glass coverslip for the WT, Δ fliC, and Δ csgG *E. coli* with a fold-change of 8.39, 18.17, and 2.77, respectively. Furthermore, the overall levels of expression were relatively similar between them,

indicating that flagella and curli were not essential for *oxyS* expression in response to H₂O₂ in solution.

Figure 29: Relative Ct values of *oxyS* expression for the a) WT, b) Δ fliC, and c) Δ csgG *E. coli*



The WT *E. coli* had 7.49-fold greater expression of *oxyS* when exposed to the charged clean surface compared to the uncharged clean surface. The expression of *oxyS* on the H₂O₂, H₃PO₄ and H₃PO₄/C₃H₉O₃P surfaces was lower than the clean surface indicating that the surface chemistry could blunt the response of *oxyS* in the WT *E. coli*. The change in *oxyS* expression between charged and uncharged surfaces was not significant for the H₃PO₄/C₃H₉O₃P-GaN. There was a significant difference for the H₂O₂- and H₃PO₄-GaN with 1.45-fold lesser and 4.68-fold greater difference between the charged and uncharged surfaces, respectively. These results suggest that in addition to the surface chemistry blunting the response of *oxyS* expression compared to the clean surface, the type of surface chemistry also played a role with regulating the interactions.

The Δ fliC *E. coli* had lower levels of expression compared to the WT for all surfaces. There were small significant differences between the charged and uncharged surfaces for each of the chemical treatments. There was an increase of 4.07-, 2.06-, and 2.08-fold when exposed to

the charged surface compared to the uncharged surface for the clean, H₂O₂, and H₃PO₄/C₃H₉O₃P surfaces, respectively. There was a decrease in *oxyS* expression with a 2.60-fold decrease in the Δ fliC *E. coli* exposed to the charged H₃PO₄ surface compared to the uncharged surface. The overall lower expression of *oxyS* in the Δ fliC *E. coli* compared to the WT *E. coli*, especially for the clean surface, indicates that flagella are involved with triggering *oxyS* expression at surfaces. The magnitude of expression was less significant for the chemically treated surfaces, indicating that the surface chemistry changed the interactions.

The expression of *oxyS* for the Δ csgG *E. coli* was different from the WT and Δ fliC, showing significantly higher levels of expression in some cases. The Δ csgG *E. coli* exposed to the clean surface had 8.77-fold greater levels of *oxyS* expression on the charged compared to the uncharged surface. This result is similar to the WT, indicating that the absence of curli did not impact regulation of *oxyS* at the clean surface. The expression of *oxyS* in the Δ csgG *E. coli* at the H₃PO₄/C₃H₉O₃P surface was 3.24-fold greater on the charged surface compared to the uncharged surface. However, the overall magnitude of *oxyS* was lower than the WT *E. coli*. This is similar to the Δ fliC *E. coli* which had similar magnitude and fold-change on the charged compared to the uncharged surface. This may indicate that curli are similarly affected by the surface chemistry of H₃PO₄/C₃H₉O₃P treatment with regard to *oxyS* expression. The primary difference from the WT *E. coli* for Δ csgG expression is for the H₂O₂ and H₃PO₄ treated surfaces. The Δ csgG *E. coli* showed a decrease in expression on the charged surface compared to the uncharged surface for both treatments with a 3.85-fold change for the H₂O₂ surface and a 7.46-fold change for the H₃PO₄ surface. The magnitude of *oxyS* expression compared to the WT and Δ fliC *E. coli* was significantly greater overall for the Δ csgG *E. coli* for these treatments. Additionally, the Δ csgG *E. coli* showed an opposite response to surface charge for the H₃PO₄ treatment compared to the

WT but the same for the Δ fliC *E. coli*. Conversely, the response to the H₂O₂ treated surface was the same for the WT but the opposite for the Δ fliC *E. coli*. The expression of *oxyS* for the Δ csgG mutants showed clear differences from the WT and Δ fliC, indicating that the regulation of *oxyS* expression at interface depends on curli in some way. However, it is not clear exactly why this is the case. The results do not necessarily correlate with the magnitude of the surface charge because the H₃PO₄/C₃H₉O₃P treated surface had similar magnitude of surface charge as the H₂O₂ and H₃PO₄ treated surfaces. However, the similarities for the H₃PO₄/C₃H₉O₃P and clean surface between the WT and Δ csgG *E. coli* further supports the idea that the interactions with curli and the surfaces play a role in regulating *oxyS* expression that is dependent on specific surface chemistry. It is not clear why there was a decrease in *oxyS* expression at the charged surfaces compared to the uncharged surfaces for H₂O₂ and H₃PO₄ treatments, but it may be that the UV light changes the surface chemistry in a way that affects the interactions.

Summary of gene expression results

The results of this study combined with our previous work indicate that the surface properties of GaN substrates play a role with modulating the stress response of *E. coli* at the interfaces. However, the way the *E. coli* responded to the surface properties did not correlate to surface charge or surface chemistry in a predictable manner. This suggests that the interactions are complex and are dependent on multiple interfacial properties. Furthermore, the deletion of flagella and curli also played a role with modulating the response.

In our previous study we found that the levels of ROS one-hour after exposure to the surfaces were not affected by surface charge changes (Gleco et al., 2020). One explanation for this was that the surfaces did not generate ROS. Another possible explanation was that there may have been a transient response with an initial increase in ROS that was gone by the time we took

our measurements. Finally, there may have also been dilution effects where the cells with increased ROS divided enough times such that the ROS signal was reduced compared to the background. The results presented in this work do not support the explanation that there was no ROS generated by surface exposure because there were changes in transcription in oxidative stress related genes depending on surface charge and surface chemistry. The results do support the explanation that changes in ROS were transient or diluted by division.

The WT *E. coli* showed increased expression of *katE*, *sodB*, and *oxyS* on the charged clean and H₃PO₄ surfaces compared to the uncharged surfaces and insignificant differences on the H₂O₂ and H₃PO₄/C₃H₉O₃P surfaces. The transcription of *katE* and *oxyS* is triggered by H₂O₂ and *sodB* is triggered by superoxide. Therefore, the results indicate that the clean surfaces produced these species when charged using UV light. However, the chemically treated surfaces showed lower levels of expression in most cases except for the expression of *sodB* on the H₃PO₄/C₃H₉O₃P surface which was approximately the same as the clean surface. The surface charge of the chemically treated surface was greater than the surface charge of the clean surface as measured by KPFM in previous work. Additionally, the H₂O₂ treated surface had the greatest increase in surface charge when exposed to UV light compared to the uncharged surface, but the expression of *katE*, *oxyS*, and *sodB* was not significantly different between the charged and uncharged H₂O₂ surfaces. If the transcription response were only because of ROS generation due to surface charge, it would be expected that the expression would be higher on the chemically treated surfaces compared to the clean and on the charged H₂O₂ surface compared to the uncharged surface. However, the results do not correspond with this hypothesis which indicates there were effects from surface chemistry.

There are some possible explanations for this. The first is that the surface chemistry inhibits the quantity of ROS formation of at the surfaces. Additionally, the surface chemistry may also affect the type of ROS formed at the surface because the expression of *katE* and *oxyS* at the clean surface was greater than the chemically treated surfaces, indicating that the clean surface produced more H₂O₂. However, the difference in *sodB* expression was not as significant between the clean and chemically treated surfaces, indicating that superoxide anion formation was less dependent on surface chemistry. Another explanation is that the expression of *katE*, *oxyS*, and *sodB* was lower on the chemically treated surfaces because the surface charge was higher than the clean surface. The higher surface charge of the chemically treated may have changed the way the *E. coli* responded to the surface overall and modified the sensitivity for triggering the corresponding pathways.

The transcription of *katE*, *oxyS*, and *sodB* was also influenced by the absence of flagella or curli compared to the WT *E. coli*. The Δ fliC *E. coli* had significant levels of differential gene expression of *katE* and *oxyS* for each surface with increased expression on the charged clean, H₂O₂, and H₃PO₄/C₃H₉O₃P surface. However, the magnitude of fold-change was lower than the WT *E. coli* except for the clean surface. In comparison to the WT *E. coli*, the expression of *oxyS* and *katE* was lower on the charged H₃PO₄ surface compared to the uncharged surface. The expression of *sodB* was also different for each surface between the WT and Δ fliC *E. coli*. Overall, Δ fliC *E. coli* had less of a transcriptional response compared to the WT *E. coli* and the impact of surface chemistry was not as important because the gene expression of the Δ fliC *E. coli* at the clean surface was not significantly different from the chemically treated surfaces like it was for the WT *E. coli*. The exact reasons for these differences are not clear, but it is not surprising because the primary functions of flagella are motility and surface sensing (O'Toole &

Wong, 2016). Our results suggest that flagella were involved with sensing and regulating the transcription of *E. coli* in response to charged surfaces and surface chemistry.

The results also indicated curli were important for modulating the interactions in a different way than flagella. The expression of *oxyS* in the Δ csgG *E. coli* was nearly identical to the WT *E. coli* for the clean surface. However, there was significantly higher expression on the H₂O₂ and H₃PO₄ treated surfaces in the Δ csgG *E. coli* for *oxyS* and *katE*. The expression of *sodB* was different than the WT but not as significantly different as it was for *oxyS* and *katE*. This suggests that curli are involved interactions toward specific ROS species and subsequent triggering of these pathways. One thing to note is that the Δ csgG *E. coli* had similar levels of *oxyS* and *katE* expression when exposed to the H₂O₂ control solution, indicating that curli were not important for regulating the transcriptional response to H₂O₂ in solution. However, the differences when exposed to the surface indicate that the interactions of curli with the surface may have been important for regulating transcription. It is also interesting that there were higher levels on the H₂O₂ and H₃PO₄ surfaces compared to the WT indicating that there was an interaction with curli that was dependent on surface chemistry. It is not clear why this is the case. Curli are important for adhesion and biofilm formation in *E. coli* (Barnhart & Chapman, 2006). However, the experiment was designed to test short exposures to the surface before biofilm formation occurred. It appears that the surface chemistry after H₂O₂ and H₃PO₄ treatment was a source of stress in the *E. coli* when the curli were deleted.

Conclusions

The results of this study demonstrate that GaN substrates can be modified to change the oxidative stress response of *E. coli* at interfaces. The effects from surface charge and surface chemistry on *E. coli* affected the transcription of three oxidative stress genes – *oxyS*, *katE*, and *sodB*. In the WT *E. coli*, surface charge caused an increase in transcription of these genes when exposed to the clean GaN, indicating that H₂O₂ and superoxide anions were generated. However, the expression at the chemically treated surfaces indicated that the surface chemistry reduced ROS H₂O₂ formation at the surface. There was also an influence on superoxide generation, but the impact was different depending on the surface chemistry. We also observed that flagella and curli play a role with regulating interactions at the interface. The non-flagellated *E. coli* had decreased expression of all genes compared to the WT for the clean surface. There were also differences for the *E. coli* exposed to the chemically treated surfaces, but the results were not significantly different from the WT. In general, the *E. coli* without curli had significantly different expression compared to the WT. The response to the clean surface was relatively similar, but the curli-deleted *E. coli* had significantly higher levels of *oxyS* and *katE* expression on the H₂O₂ and H₃PO₄ treated surfaces indicating that curli are involved with interactions with H₂O₂ at interfaces. Overall, the results of this study demonstrate that short exposure to GaN surfaces can be used to stimulate changes in *E. coli* related to oxidative stress. The results of this work help to understand the interactions of microorganisms at interfaces and the relationship to surface properties which will be useful for biointerface applications.

CHAPTER V: CONCLUSIONS AND FUTURE DIRECTIONS

Conclusions

In this study, the transcriptional responses of the bacterium *E. coli* to the non-lethal exposure of commercially relevant silica, gold and polystyrene engineered nanoparticles were established. Our gene screening results demonstrated that nanoparticles activate specific genes as responses to the nanoparticle assaults. Polystyrene nanoparticles generated the highest number of upregulated genes that are distributed among metabolic pathways, protein transport, signal transduction and DNA replication compared to silica and gold nanoparticles suggesting that polystyrene Nps induced significant genetic machinery alterations that potentially disrupt the cell homeostasis leading to the change in *E. coli* cell behavior. On the other hand, silica and gold Nps exhibit a slight but significant modification of the *E. coli* behavior despite being known as “neutral” and/or “nontoxic” nanoparticles that make them so attractive in the field of biomedicine. More importantly, the qRT-PCR reveal a more dynamic gene expression of the common response genes to all three nanoparticles which include previously identified stress response genes (*rssB*, *evgA*, *sodC*,) genes encoding transports (*yhdY*, *yhhT*, *vacJ/MlaA*), one gene encoding sulfate assimilation (*cysQ*) and one gene (*glcC*) part of the glycolate metabolic pathway. These eight genes with no direct metabolic connections between each other, potentially influence different cellular functions in *E. coli*. Indeed, the up regulations of the gene *sodC* and *vacJ* in this study demonstrate the intracellular production of ROS and disruption of the cell membrane during nanoparticle exposure respectively. The growth curves of the single gene mutations of the common response show that all three nanoparticles promote cell growth in all the mutants suggesting metabolic function compensations of the gene deletion enabling an increase in cell growth to sustain the bacterial survival. Moreover, *sodC* and *cysQ* are essential

genes to maintain bacterial cell growth in normal growth conditions. This study provides a great insight into transcriptional responses to round-shaped nanoparticles of different physicochemical properties. This is critical for the better understanding of the interaction between bacteria and nanoparticles in the context of nanopollution. Furthermore, this study provides additional understanding of potential metabolic mechanisms that could lead to bacteria resistance to nanoparticle-based antibiotics.

Future research recommendations

This work has provided an insightful understanding of the dynamic but complex transcriptomic responses of *e coli* after exposure to roughly same size and shape with different physicochemical properties nanoparticles, by determining a cluster of genes part of the common genetic response to silica, gold and polystyrene Nps. However, more needs to be done to fully elucidate the bacteria-nanoparticle interactions. So, future work could include the transcriptomic analysis of the same set of nanoparticles with *E. coli* for a longer exposure time such as 24 hour or more to verify if the same common gene response is still activated. One important area of focus could be the influence of *E. coli* behavior with changes in size and shape of these three nanoparticles. Moreover, the same set of conditions could be investigated with a different bacterial model organism, preferably a Gram-positive bacteria like *staphylococcus aureus* to evaluate the persistence of the common gene response across different type of bacteria. Another important area of investigation could be the use of smaller sizes and different shapes of these nanoparticles to determine if a similar overlapping genetic response exists in other type of microorganisms such as fungi. These research work will provide a deeper understanding of the complex relationship between nanoparticles and bacteria. This knowledge will have crucial implications in developing new drug treatments to combat bacterial resistance to nanoparticle-

based antibiotics as well as controlling bacteria biofilm. In addition, this will help develop innovative bioremediation strategies through synthetic biology to tackle the nanopollution problem in the future.

REFERENCES

- Abdelraheem, W. M., & Mohamed, E. S. (2021). The effect of Zinc Oxide nanoparticles on *Pseudomonas aeruginosa* biofilm formation and virulence genes expression. *The Journal of Infection in Developing Countries*, *15*(06), 826–832.
<https://doi.org/10.3855/jidc.13958>
- Adel, M., Ahmed, M. A., Elabiad, M. A., & Mohamed, A. A. (2022). Removal of heavy metals and dyes from wastewater using graphene oxide-based nanomaterials: A critical review. *Environmental Nanotechnology, Monitoring & Management*, *18*, 100719.
<https://doi.org/10.1016/j.enmm.2022.100719>
- Adnan, M., Morton, G., Singh, J., & Hadi, S. (2010). Contribution of *rpoS* and *bolA* genes in biofilm formation in *Escherichia coli* K-12 MG1655. *Molecular and Cellular Biochemistry*, *342*(1–2), 207–213. <https://doi.org/10.1007/s11010-010-0485-7>
- Ahangari, A., Mahmoodi, P., & Mohammadzadeh, A. (2022). Biosensors functionalized with nanoparticles for rapid detection of *Brucella*. *Microchemical Journal*, *181*, 107697.
<https://doi.org/10.1016/j.microc.2022.107697>
- Ahangari, A., Mahmoodi, P., & Mohammadzadeh, A. (2023). Advanced nano biosensors for rapid detection of zoonotic bacteria. *Biotechnology and Bioengineering*, *120*(1), 41–56.
<https://doi.org/10.1002/bit.28266>
- Ahmed, B., Rizvi, A., Ali, K., Lee, J., Zaidi, A., Khan, M. S., & Musarrat, J. (2021). Nanoparticles in the soil–plant system: A review. *Environmental Chemistry Letters*, *19*(2), 1545–1609. <https://doi.org/10.1007/s10311-020-01138-y>

- Ajayan, P. M. (1999). Nanotubes from Carbon. *Chemical Reviews*, 99(7), 1787–1800.
<https://doi.org/10.1021/cr970102g>
- Alonso-Caballero, A., Schönfelder, J., Poly, S., Corsetti, F., De Sancho, D., Artacho, E., & Perez-Jimenez, R. (2018). Mechanical architecture and folding of E. coli type 1 pilus domains. *Nature Communications*, 9(1). <https://doi.org/10.1038/s41467-018-05107-6>
- Altuvia, S., Weinstein-Fischer, D., Zhang, A., Postow, L., & Storz, G. (1997). A Small, Stable RNA Induced by Oxidative Stress: Role as a Pleiotropic Regulator and Antimutator. *Cell*, 90(1), 43–53. [https://doi.org/10.1016/S0092-8674\(00\)80312-8](https://doi.org/10.1016/S0092-8674(00)80312-8)
- Ameh, T., Gibb, M., Stevens, D., Pradhan, S. H., Braswell, E., & Sayes, C. M. (2022). Silver and Copper Nanoparticles Induce Oxidative Stress in Bacteria and Mammalian Cells. *Nanomaterials*, 12(14), 2402. <https://doi.org/10.3390/nano12142402>
- An, C., Sun, C., Li, N., Huang, B., Jiang, J., Shen, Y., Wang, C., Zhao, X., Cui, B., Wang, C., Li, X., Zhan, S., Gao, F., Zeng, Z., Cui, H., & Wang, Y. (2022). Nanomaterials and nanotechnology for the delivery of agrochemicals: Strategies towards sustainable agriculture. *Journal of Nanobiotechnology*, 20(1), 11. <https://doi.org/10.1186/s12951-021-01214-7>
- An, P., Zhao, L., Zhang, S., Liu, L., Duan, R., Wei, X., Lu, H., Wang, J., & Li, J. (2016). Growth and optical properties of gallium nitride film on glass substrates: Growth and optical properties of gallium nitride film on glass substrates. *Physica Status Solidi (c)*, 13(5–6), 200–204. <https://doi.org/10.1002/pssc.201510207>

- Arakha, M., Pal, S., Samantarrai, D., Panigrahi, T. K., Mallick, B. C., Pramanik, K., Mallick, B., & Jha, S. (2015). Antimicrobial activity of iron oxide nanoparticle upon modulation of nanoparticle-bacteria interface. *Scientific Reports*, 5(1), 14813.
<https://doi.org/10.1038/srep14813>
- Aruguete, D. M., & Hochella, M. F. (2010). Bacteria—Nanoparticle interactions and their environmental implications. *Environmental Chemistry*, 7(1), 3.
<https://doi.org/10.1071/EN09115>
- Aunins, T. R., Eller, K. A., Courtney, C. M., Levy, M., Goodman, S. M., Nagpal, P., & Chatterjee, A. (2019a). Isolating the *Escherichia coli* Transcriptomic Response to Superoxide Generation from Cadmium Chalcogenide Quantum Dots. *ACS Biomaterials Science & Engineering*. <https://doi.org/10.1021/acsbiomaterials.9b01087>
- Aunins, T. R., Eller, K. A., Courtney, C. M., Levy, M., Goodman, S. M., Nagpal, P., & Chatterjee, A. (2019b). Isolating the *Escherichia coli* Transcriptomic Response to Superoxide Generation from Cadmium Chalcogenide Quantum Dots. *ACS Biomaterials Science & Engineering*, 5(9), 4206–4218.
<https://doi.org/10.1021/acsbiomaterials.9b01087>
- Awet, T. T., Kohl, Y., Meier, F., Straskraba, S., Grün, A.-L., Ruf, T., Jost, C., Drexel, R., Tunc, E., & Emmerling, C. (2018). Effects of polystyrene nanoparticles on the microbiota and functional diversity of enzymes in soil. *Environmental Sciences Europe*, 30(1), 11.
<https://doi.org/10.1186/s12302-018-0140-6>

- Baba, T., Ara, T., Hasegawa, M., Takai, Y., Okumura, Y., Baba, M., Datsenko, K. A., Tomita, M., Wanner, B. L., & Mori, H. (2006). Construction of Escherichia coli K-12 in-frame, single-gene knockout mutants: The Keio collection. *Molecular Systems Biology*, 2(1), 2006.0008. <https://doi.org/10.1038/msb4100050>
- Babayevska, N., Przysiecka, Ł., Iatsunskyi, I., Nowaczyk, G., Jarek, M., Janiszewska, E., & Jurga, S. (2022). ZnO size and shape effect on antibacterial activity and cytotoxicity profile. *Scientific Reports*, 12(1), 8148. <https://doi.org/10.1038/s41598-022-12134-3>
- Barchiesi, J., Castelli, M. E., Di Venanzio, G., Colombo, M. I., & García Vescovi, E. (2012). The PhoP/PhoQ System and Its Role in Serratia marcescens Pathogenesis. *Journal of Bacteriology*, 194(11), 2949–2961. <https://doi.org/10.1128/JB.06820-11>
- Barhoum, A., García-Betancourt, M. L., Jeevanandam, J., Hussien, E. A., Mekkawy, S. A., Mostafa, M., Omran, M. M., S. Abdalla, M., & Bechelany, M. (2022). Review on Natural, Incidental, Bioinspired, and Engineered Nanomaterials: History, Definitions, Classifications, Synthesis, Properties, Market, Toxicities, Risks, and Regulations. *Nanomaterials*, 12(2), 177. <https://doi.org/10.3390/nano12020177>
- Barnhart, M. M., & Chapman, M. R. (2006a). Curli Biogenesis and Function. *Annual Review of Microbiology*, 60(1), 131–147. <https://doi.org/10.1146/annurev.micro.60.080805.142106>
- Barnhart, M. M., & Chapman, M. R. (2006b). Curli Biogenesis and Function. *Annual Review of Microbiology*, 60(1), 131–147. <https://doi.org/10.1146/annurev.micro.60.080805.142106>
- Barshishat, S., Elgrably-Weiss, M., Edelstein, J., Georg, J., Govindarajan, S., Haviv, M., Wright, P. R., Hess, W. R., & Altuvia, S. (2018). OxyS small RNA induces cell cycle arrest to allow DNA damage repair. *The EMBO Journal*, 37(3), 413–426. <https://doi.org/10.15252/emj.201797651>

- Benov, L. T., & Fridovich, I. (1994a). Escherichia coli expresses a copper- and zinc-containing superoxide dismutase. *Journal of Biological Chemistry*, 269(41), 25310–25314.
[https://doi.org/10.1016/S0021-9258\(18\)47248-1](https://doi.org/10.1016/S0021-9258(18)47248-1)
- Benov, L. T., & Fridovich, I. (1994b). Escherichia coli expresses a copper- and zinc-containing superoxide dismutase. *Journal of Biological Chemistry*, 269(41), 25310–25314.
[https://doi.org/10.1016/S0021-9258\(18\)47248-1](https://doi.org/10.1016/S0021-9258(18)47248-1)
- Bhatia, R. P., Kirit, H. A., Predeus, A. V., & Bollback, J. P. (2022). Transcriptomic profiling of Escherichia coli K-12 in response to a compendium of stressors. *Scientific Reports*, 12(1), 8788. <https://doi.org/10.1038/s41598-022-12463-3>
- Białaś, N., Sokolova, V., van der Meer, S. B., Knuschke, T., Ruks, T., Klein, K., Westendorf, A. M., & Epple, M. (2022). Bacteria (*E. coli*) take up ultrasmall gold nanoparticles (2 nm) as shown by different optical microscopic techniques (CLSM, SIM, STORM). *Nano Select*, 3(10), 1407–1420. <https://doi.org/10.1002/nano.202200049>
- Bianchi, M., & Carnevale, G. (2022). Innovative Nanomaterials for Biomedical Applications. *Nanomaterials*, 12(9), 1561. <https://doi.org/10.3390/nano12091561>
- Biswas, P., Polash, S. A., Dey, D., Kaium, Md. A., Mahmud, A. R., Yasmin, F., Baral, S. K., Islam, Md. A., Rahaman, T. I., Abdullah, A., Ema, T. I., Khan, D. A., Bibi, S., Chopra, H., Kamel, M., Najda, A., Fouda, M. M. A., Rehan, U. M., Mheidat, M., ... Hasan, Md. N. (2023). Advanced implications of nanotechnology in disease control and environmental perspectives. *Biomedicine & Pharmacotherapy*, 158, 114172.
<https://doi.org/10.1016/j.biopha.2022.114172>

- Braz, V. S., Melchior, K., & Moreira, C. G. (2020). Escherichia coli as a Multifaceted Pathogenic and Versatile Bacterium. *Frontiers in Cellular and Infection Microbiology*, *10*, 548492. <https://doi.org/10.3389/fcimb.2020.548492>
- Bruni, G. N., Weekley, R. A., Dodd, B. J. T., & Kralj, J. M. (2017). Voltage-gated calcium flux mediates Escherichia coli mechanosensation. *Proceedings of the National Academy of Sciences*, *114*(35), 9445 LP – 9450. <https://doi.org/10.1073/pnas.1703084114>
- Busscher, H. J., & Mei, H. C. (2012). How Do Bacteria Know They Are on a Surface and Regulate Their Response to an Adhering State? *PLoS Pathogens*, *8*(1), e1002440. <https://doi.org/10.1371/journal.ppat.1002440>
- Cano, A., Ettcheto, M., Espina, M., López-Machado, A., Cajal, Y., Rabanal, F., Sánchez-López, E., Camins, A., García, M. L., & Souto, E. B. (2020). State-of-the-art polymeric nanoparticles as promising therapeutic tools against human bacterial infections. *Journal of Nanobiotechnology*, *18*(1), 156. <https://doi.org/10.1186/s12951-020-00714-2>
- Castellano, J. J., Shafii, S. M., Ko, F., Donate, G., Wright, T. E., Mannari, R. J., Payne, W. G., Smith, D. J., & Robson, M. C. (2007). Comparative evaluation of silver-containing antimicrobial dressings and drugs. *International Wound Journal*, *4*(2), 114–122. <https://doi.org/10.1111/j.1742-481X.2007.00316.x>
- Cerjak, H. (2009). Nanomaterials: An introduction to synthesis, properties and applications. *Materials Technology*, *24*(2), 74–74. <https://doi.org/10.1179/175355509X454827>
- Chatterjee, S., Bandyopadhyay, A., & Sarkar, K. (2011). Effect of iron oxide and gold nanoparticles on bacterial growth leading towards biological application. *Journal of Nanobiotechnology*, *9*(1), 34. <https://doi.org/10.1186/1477-3155-9-34>

- Chaud, M., Souto, E. B., Zielinska, A., Severino, P., Batain, F., Oliveira-Junior, J., & Alves, T. (2021). Nanopesticides in Agriculture: Benefits and Challenge in Agricultural Productivity, Toxicological Risks to Human Health and Environment. *Toxics*, 9(6), 131. <https://doi.org/10.3390/toxics9060131>
- Chavali, M. S., & Nikolova, M. P. (2019). Metal oxide nanoparticles and their applications in nanotechnology. *SN Applied Sciences*, 1(6), 607. <https://doi.org/10.1007/s42452-019-0592-3>
- Chavan, S., & Nadanathangam, V. (2019). Effects of Nanoparticles on Plant Growth-Promoting Bacteria in Indian Agricultural Soil. *Agronomy*, 9(3), 140. <https://doi.org/10.3390/agronomy9030140>
- Chehreh Chelgani, S., Rudolph, M., Kratzsch, R., Sandmann, D., & Gutzmer, J. (2016). A Review of Graphite Beneficiation Techniques. *Mineral Processing and Extractive Metallurgy Review*, 37(1), 58–68. <https://doi.org/10.1080/08827508.2015.1115992>
- Chiang, S. M., & Schellhorn, H. E. (2012a). Regulators of oxidative stress response genes in *Escherichia coli* and their functional conservation in bacteria. *Archives of Biochemistry and Biophysics*, 525(2), 161–169. <https://doi.org/10.1016/j.abb.2012.02.007>
- Chiang, S. M., & Schellhorn, H. E. (2012b). Regulators of oxidative stress response genes in *Escherichia coli* and their functional conservation in bacteria. *Archives of Biochemistry and Biophysics*, 525(2), 161–169. <https://doi.org/10.1016/j.abb.2012.02.007>
- Chockalingam, S., Packirisamy, G., & Paulmurugan, R. (2022). Editorial: Nanomaterials for targeted delivery of therapeutic and imaging agents. *Frontiers in Cell and Developmental Biology*, 10, 978690. <https://doi.org/10.3389/fcell.2022.978690>

- Christoforidis, J. B., Chang, S., Jiang, A., Wang, J., & Cebulla, C. M. (2012). Intravitreal Devices for the Treatment of Vitreous Inflammation. *Mediators of Inflammation*, 2012, 1–8. <https://doi.org/10.1155/2012/126463>
- Chung, H. J., Bang, W., & Drake, M. A. (2006). Stress Response of Escherichia coli. *Comprehensive Reviews in Food Science and Food Safety*, 5(3), 52–64. <https://doi.org/10.1111/j.1541-4337.2006.00002.x>
- Chwalibog, Chwalibog, Sawosz, Hotowy, Szeliga, Mitura, S, Mitura, K, Grodzik, MSc Orłowski, & Professor Sokolowska. (2010). Visualization of interaction between inorganic nanoparticles and bacteria or fungi. *International Journal of Nanomedicine*, 1085. <https://doi.org/10.2147/IJN.S13532>
- Collazo, R., Mita, S., Aleksov, A., Schlessner, R., & Sitar, Z. (2006). Growth of Ga- and N- polar gallium nitride layers by metalorganic vapor phase epitaxy on sapphire wafers. *Journal of Crystal Growth*, 287(2), 586–590. <https://doi.org/10.1016/j.jcrysgro.2005.10.080>
- Connell, I., Agace, W., Klemm, P., Schembri, M., Marild, S., & Svanborg, C. (1996). Type 1 fimbrial expression enhances Escherichia coli virulence for the urinary tract. *Proceedings of the National Academy of Sciences*, 93(18), 9827–9832. <https://doi.org/10.1073/pnas.93.18.9827>
- Datta, A., Priyam, A., Bhattacharyya, S. N., Mukherjea, K. K., & Saha, A. (2008a). Temperature tunability of size in CdS nanoparticles and size dependent photocatalytic degradation of nitroaromatics. *Journal of Colloid and Interface Science*, 322(1), 128–135. <https://doi.org/10.1016/j.jcis.2008.02.052>

- Datta, A., Priyam, A., Bhattacharyya, S. N., Mukherjea, K. K., & Saha, A. (2008b). Temperature tunability of size in CdS nanoparticles and size dependent photocatalytic degradation of nitroaromatics. *Journal of Colloid and Interface Science*, *322*(1), 128–135.
<https://doi.org/10.1016/j.jcis.2008.02.052>
- Dawan, J., & Ahn, J. (2022). Bacterial Stress Responses as Potential Targets in Overcoming Antibiotic Resistance. *Microorganisms*, *10*(7), 1385.
<https://doi.org/10.3390/microorganisms10071385>
- Deka, B., Babu, A., Baruah, C., & Barthakur, M. (2021). Nanopesticides: A Systematic Review of Their Prospects With Special Reference to Tea Pest Management. *Frontiers in Nutrition*, *8*, 686131. <https://doi.org/10.3389/fnut.2021.686131>
- Dekkers, S., Wagner, J. G., Vandebriel, R. J., Eldridge, E. A., Tang, S. V. Y., Miller, M. R., Römer, I., de Jong, W. H., Harkema, J. R., & Cassee, F. R. (2019). Role of chemical composition and redox modification of poorly soluble nanomaterials on their ability to enhance allergic airway sensitisation in mice. *Particle and Fibre Toxicology*, *16*(1), 39.
<https://doi.org/10.1186/s12989-019-0320-6>
- Dong, Y., Zhu, H., Shen, Y., Zhang, W., & Zhang, L. (2019a). Antibacterial activity of silver nanoparticles of different particle size against *Vibrio Natriegens*. *PLOS ONE*, *14*(9), e0222322. <https://doi.org/10.1371/journal.pone.0222322>
- Dong, Y., Zhu, H., Shen, Y., Zhang, W., & Zhang, L. (2019b). Antibacterial activity of silver nanoparticles of different particle size against *Vibrio Natriegens*. *PLOS ONE*, *14*(9), e0222322. <https://doi.org/10.1371/journal.pone.0222322>
- D’Orazio, M., Folcarelli, S., Mariani, F., Colizzi, V., Rotilio, G., & Battistoni, A. (2001). Lipid modification of the Cu,Zn superoxide dismutase from. *M. D.*

- Dörr, T., Moynihan, P. J., & Mayer, C. (2019). Editorial: Bacterial Cell Wall Structure and Dynamics. *Frontiers in Microbiology*, *10*, 2051.
<https://doi.org/10.3389/fmicb.2019.02051>
- Dworkin, M., Falkow, S., Rosenberg, E., Schleifer, K.-H., & Stackebrandt, E. (Eds.). (2006). *The Prokaryotes*. Springer New York. <https://doi.org/10.1007/0-387-30742-7>
- Eguchi, Y., Itou, J., Yamane, M., Demizu, R., Yamato, F., Okada, A., Mori, H., Kato, A., & Utsumi, R. (2007). B1500, a small membrane protein, connects the two-component systems EvgS/EvgA and PhoQ/PhoP in *Escherichia coli*. *Proceedings of the National Academy of Sciences*, *104*(47), 18712–18717. <https://doi.org/10.1073/pnas.0705768104>
- Ermolin, M. S., & Fedotov, P. S. (2016). Separation and characterization of environmental nano- and submicron particles. *Reviews in Analytical Chemistry*, *35*(4), 185–199.
<https://doi.org/10.1515/revac-2016-0006>
- Fang, F. C., Frawley, E. R., Tapscott, T., & Vázquez-Torres, A. (2016). Bacterial Stress Responses during Host Infection. *Cell Host & Microbe*, *20*(2), 133–143.
<https://doi.org/10.1016/j.chom.2016.07.009>
- Farr', S. B., & Kogoma, T. (1991). Oxidative Stress Responses in *Escherichia coli* and *Salmonella typhimurium*. *MICROBIOL. REV.*, *55*.
- Friedlander, R. S., Vogel, N., & Aizenberg, J. (2015). Role of Flagella in Adhesion of *Escherichia coli* to Abiotic Surfaces. *Langmuir*, *31*(22), 6137–6144.
<https://doi.org/10.1021/acs.langmuir.5b00815>

- Fringer, V. S., Fawcett, L. P., Mitrano, D. M., & Maurer-Jones, M. A. (2020). Impacts of Nanoplastics on the Viability and Riboflavin Secretion in the Model Bacteria *Shewanella oneidensis*. *Frontiers in Environmental Science*, 8, 97. <https://doi.org/10.3389/fenvs.2020.00097>
- Gammoudi, I., Ndeye Rokhaya Faye, Moroté, F., Moynet, D., Grauby-Heywang, C., & Cohen-Bouhacina, T. (2013). *Characterization of Silica Nanoparticles in Interaction with Escherichia coli Bacteria*. <https://doi.org/10.13140/RG.2.1.2606.9202>
- Ganguly, P., Breen, A., & Pillai, S. C. (2018). Toxicity of Nanomaterials: Exposure, Pathways, Assessment, and Recent Advances. *ACS Biomaterials Science & Engineering*, 4(7), 2237–2275. <https://doi.org/10.1021/acsbomaterials.8b00068>
- Geslin, C., Llanos, J., Prieur, D., & Jeanthon, C. (2001). The manganese and iron superoxide dismutases protect *Escherichia coli* from heavy metal toxicity. *Research in Microbiology*, 152(10), 901–905. [https://doi.org/10.1016/S0923-2508\(01\)01273-6](https://doi.org/10.1016/S0923-2508(01)01273-6)
- Giese, B., Klaessig, F., Park, B., Kaegi, R., Steinfeldt, M., Wigger, H., von Gleich, A., & Gottschalk, F. (2018). Risks, Release and Concentrations of Engineered Nanomaterial in the Environment. *Scientific Reports*, 8(1), 1565. <https://doi.org/10.1038/s41598-018-19275-4>
- Giuliodori, A. M., Gualerzi, C. O., Soto, S., Vila, J., & Tavio, M. M. (2007). Review on Bacterial Stress Topics. *Annals of the New York Academy of Sciences*, 1113(1), 95–104. <https://doi.org/10.1196/annals.1391.008>

- Gleco, S., Noussi, T., Jude, A., Reddy, P., Kirste, R., Collazo, R., LaJeunesse, D., & Ivanisevic, A. (2020). Oxidative Stress Transcriptional Responses of *Escherichia coli* at GaN Interfaces. *ACS Applied Bio Materials*, 3(12), 9073–9081.
<https://doi.org/10.1021/acsabm.0c01299>
- Gleco, S., Reddy, P., Kirste, R., Collazo, R., LaJeunesse, D. R., & Ivanisevic, A. (2020). Modulating the stress response of E. coli at GaN interfaces using surface charge, surface chemistry, and genetic mutations. *ACS Applied Bio Materials*.
<https://doi.org/10.1021/acsabm.0c01007>
- Gleco, S., Romanyuk, O., Gordeev, I., Kuldová, K., Paskova, T., & Ivanisevic, A. (2019a). Modification of the Surface Properties of Al_xGa_{1-x}N Substrates with Gradient Aluminum Composition Using Wet Chemical Treatments. *ACS Omega*, 4(7). <https://doi.org/10.1021/acsomega.9b01467>
- Gleco, S., Romanyuk, O., Gordeev, I., Kuldová, K., Paskova, T., & Ivanisevic, A. (2019b). Modification of the Surface Properties of Al_xGa_{1-x}N Substrates with Gradient Aluminum Composition Using Wet Chemical Treatments. *ACS Omega*, 4(7), 11760–11769. <https://doi.org/10.1021/acsomega.9b01467>
- Gleco, S., Romanyuk, O., Gordeev, I., Kuldová, K., Paskova, T., & Ivanisevic, A. (2019c). Modification of the Surface Properties of Al_xGa_{1-x}N Substrates with Gradient Aluminum Composition Using Wet Chemical Treatments. *ACS Omega*, 4(7), 11760–11769. <https://doi.org/10.1021/acsomega.9b01467>
- Gleiter, H. (n.d.). NANOSTRUCTURED MATERIALS: BASIC CONCEPTS AND MICROSTRUCTURE p. *NANOSTRUCTURED MATERIALS*, 29.

- Gonçalves, J. M., & Bebianno, M. J. (2021). Nanoplastics impact on marine biota: A review. *Environmental Pollution*, 273, 116426. <https://doi.org/10.1016/j.envpol.2021.116426>
- González-Flecha, B., & Demple, B. (1999). Role for the *oxyS* Gene in Regulation of Intracellular Hydrogen Peroxide in *Escherichia coli*. *Journal of Bacteriology*, 181(12), 3833 LP – 3836.
- Groisman, E. A. (2016). Feedback Control of Two-Component Regulatory Systems. *Annual Review of Microbiology*, 70(1), 103–124. <https://doi.org/10.1146/annurev-micro-102215-095331>
- Gruber, T. M., & Gross, C. A. (2003). Multiple Sigma Subunits and the Partitioning of Bacterial Transcription Space. *Annual Review of Microbiology*, 57(1), 441–466. <https://doi.org/10.1146/annurev.micro.57.030502.090913>
- Guan, N., & Liu, L. (2020). Microbial response to acid stress: Mechanisms and applications. *Applied Microbiology and Biotechnology*, 104(1), 51–65. <https://doi.org/10.1007/s00253-019-10226-1>
- Gulyuk, A. V., LaJeunesse, D. R., Collazo, R., & Ivanisevic, A. (2018). Characterization of *Pseudomonas aeruginosa* Films on Different Inorganic Surfaces before and after UV Light Exposure. *Langmuir*, 34(36), 10806–10815. <https://doi.org/10.1021/acs.langmuir.8b02079>
- Gulyuk, A. V., R. LaJeunesse, D., Collazo, R., & Ivanisevic, A. (2018). Characterization of *Pseudomonas aeruginosa* Films on Different Inorganic Surfaces before and after UV Light Exposure. *Langmuir*, 34(36), 10806–10815. <https://doi.org/10.1021/acs.langmuir.8b02079>

- Gulyuk, A. V., R. LaJeunesse, D., Reddy, P., Kirste, R., Collazo, R., & Ivanisevic, A. (2019). Interfacial Properties of Doped Semiconductor Materials Can Alter the Behavior of *Pseudomonas aeruginosa* Films. *ACS Applied Electronic Materials*, *1*(8), 1641–1652. <https://doi.org/10.1021/acsaelm.9b00347>
- Gumbart, J. C., Beeby, M., Jensen, G. J., & Roux, B. (2014). *Escherichia coli* Peptidoglycan Structure and Mechanics as Predicted by Atomic-Scale Simulations. *PLoS Computational Biology*, *10*(2), e1003475. <https://doi.org/10.1371/journal.pcbi.1003475>
- Häffner, S. M., Parra-Ortiz, E., Browning, K. L., Jørgensen, E., Skoda, M. W. A., Montis, C., Li, X., Berti, D., Zhao, D., & Malmsten, M. (2021). Membrane Interactions of Virus-like Mesoporous Silica Nanoparticles. *ACS Nano*, *15*(4), 6787–6800. <https://doi.org/10.1021/acsnano.0c10378>
- Haiko, J., & Westerlund-Wikström, B. (2013a). *The Role of the Bacterial Flagellum in Adhesion and Virulence*. <https://doi.org/10.3390/biology2041242>
- Haiko, J., & Westerlund-Wikström, B. (2013b). The Role of the Bacterial Flagellum in Adhesion and Virulence. *Biology*, *2*(4), 1242–1267. <https://doi.org/10.3390/biology2041242>
- Hamill, P. G., Stevenson, A., McMullan, P. E., Williams, J. P., Lewis, A. D. R., S, S., Stevenson, K. E., Farnsworth, K. D., Khroustalyova, G., Takemoto, J. Y., Quinn, J. P., Rapoport, A., & Hallsworth, J. E. (2020). Microbial lag phase can be indicative of, or independent from, cellular stress. *Scientific Reports*, *10*(1), 5948. <https://doi.org/10.1038/s41598-020-62552-4>
- Hashimoto, M., & Honda, Y. (2019). *Effect of Gold Nanoparticle Size on Bacterial Cell Attachment and Initial Biofilm Formation*.

- Hatzios, S. K., Iavarone, A. T., & Bertozzi, C. R. (2008). Rv2131c from *Mycobacterium tuberculosis* Is a CysQ 3'-Phosphoadenosine-5'-phosphatase. *Biochemistry*, *47*(21), 5823–5831. <https://doi.org/10.1021/bi702453s>
- Hegde, M., Pai, P., Shetty, M. G., & Babitha, K. S. (2022). Gold nanoparticle based biosensors for rapid pathogen detection: A review. *Environmental Nanotechnology, Monitoring & Management*, *18*, 100756. <https://doi.org/10.1016/j.enmm.2022.100756>
- Hochella, M. F., Mogk, D. W., Ranville, J., Allen, I. C., Luther, G. W., Marr, L. C., McGrail, B. P., Murayama, M., Qafoku, N. P., Rosso, K. M., Sahai, N., Schroeder, P. A., Vikesland, P., Westerhoff, P., & Yang, Y. (2019). Natural, incidental, and engineered nanomaterials and their impacts on the Earth system. *Science*, *363*(6434), eaau8299. <https://doi.org/10.1126/science.aau8299>
- Hochella, M. F., Spencer, M. G., & Jones, K. L. (2015). Nanotechnology: Nature's gift or scientists' brainchild? *Environmental Science: Nano*, *2*(2), 114–119. <https://doi.org/10.1039/C4EN00145A>
- Hollenbeck, E. C., Antonoplis, A., Chai, C., Thongsomboon, W., Fuller, G. G., & Cegelski, L. (2018). Phosphoethanolamine cellulose enhances curli-mediated adhesion of uropathogenic *Escherichia coli* to bladder epithelial cells. *Proceedings of the National Academy of Sciences*, *115*(40), 10106–10111. <https://doi.org/10.1073/pnas.1801564115>
- Hoseinzadeh, A., Ghodduji Johari, H., Anbardar, M. H., Tayebi, L., Vafa, E., Abbasi, M., Vaez, A., Golchin, A., Amani, A. M., & Jangjou, A. (2022). Effective treatment of intractable diseases using nanoparticles to interfere with vascular supply and angiogenic process. *European Journal of Medical Research*, *27*(1), 232. <https://doi.org/10.1186/s40001-022-00833-6>

- Hospenthal, M. K., Zyla, D., Costa, T. R. D., Redzej, A., Giese, C., Lillington, J., Glockshuber, R., & Waksman, G. (n.d.). *The Cryoelectron Microscopy Structure of the Type I Chaperone- Usher Pilus Rod*. 26.
- Huang, X., Yin, Z., Wu, S., Qi, X., He, Q., Zhang, Q., Yan, Q., Boey, F., & Zhang, H. (2011). Graphene-Based Materials: Synthesis, Characterization, Properties, and Applications. *Small*, 7(14), 1876–1902. <https://doi.org/10.1002/sml.201002009>
- Imam, S., Chen, Z., Roos, D. S., & Pohlschröder, M. (2011). Identification of Surprisingly Diverse Type IV Pili, across a Broad Range of Gram-Positive Bacteria. *PLoS ONE*, 6(12), e28919. <https://doi.org/10.1371/journal.pone.0028919>
- Itou, J., Eguchi, Y., & Utsumi, R. (2009). Molecular Mechanism of Transcriptional Cascade Initiated by the EvgS/EvgA System in *Escherichia coli* K-12. *Bioscience, Biotechnology, and Biochemistry*, 73(4), 870–878. <https://doi.org/10.1271/bbb.80795>
- Iyer, D., Gulyuk, A., Reddy, P., Kirste, R., Collazo, R., R. LaJeunesse, D., & Ivanisevic, A. (2019). Behavior of *E. coli* with Variable Surface Morphology Changes on Charged Semiconductor Interfaces. *ACS Applied Bio Materials*, 2(9), 4044–4051. <https://doi.org/10.1021/acsabm.9b00573>
- Iyer, D., Gulyuk, A. V., Reddy, P., Kirste, R., Collazo, R., LaJeunesse, D. R., & Ivanisevic, A. (2019). Behavior of *E. coli* with Variable Surface Morphology Changes on Charged Semiconductor Interfaces. *ACS Applied Bio Materials*, 2(9), 4044–4051. <https://doi.org/10.1021/acsabm.9b00573>
- Jaishankar, J., & Srivastava, P. (2017). Molecular Basis of Stationary Phase Survival and Applications. *Frontiers in Microbiology*, 8, 2000. <https://doi.org/10.3389/fmicb.2017.02000>

- Janczarek, M., Klapiszewski, Ł., Jędrzejczak, P., Klapiszewska, I., Ślosarczyk, A., & Jesionowski, T. (2022). Progress of functionalized TiO₂-based nanomaterials in the construction industry: A comprehensive review. *Chemical Engineering Journal*, 430, 132062. <https://doi.org/10.1016/j.cej.2021.132062>
- Jang, J., Hur, H.-G., Sadowsky, M. J., Byappanahalli, M. N., Yan, T., & Ishii, S. (2017). Environmental *Escherichia coli*: Ecology and public health implications-a review. *Journal of Applied Microbiology*, 123(3), 570–581. <https://doi.org/10.1111/jam.13468>
- Jawahar, N., & Meyyanathan, S. (2012). Polymeric nanoparticles for drug delivery and targeting: A comprehensive review. *International Journal of Health & Allied Sciences*, 1(4), 217. <https://doi.org/10.4103/2278-344X.107832>
- Jiang, Y., & Tian, B. (2018a). Inorganic semiconductor biointerfaces. *Nature Reviews Materials*, 3(12), 473–490. <https://doi.org/10.1038/s41578-018-0062-3>
- Jiang, Y., & Tian, B. (2018b). Inorganic semiconductor biointerfaces. *Nature Reviews Materials*, 3(12), 473–490. <https://doi.org/10.1038/s41578-018-0062-3>
- Joshi, A. S., Singh, P., & Mijakovic, I. (2020). Interactions of Gold and Silver Nanoparticles with Bacterial Biofilms: Molecular Interactions behind Inhibition and Resistance. *International Journal of Molecular Sciences*, 21(20), 7658. <https://doi.org/10.3390/ijms21207658>
- Kalir, S., McClure, J., Pabbaraju, K., Southward, C., Ronen, M., Leibler, S., Surette, M. G., & Alon, U. (2001). Ordering Genes in a Flagella Pathway by Analysis of Expression Kinetics from Living Bacteria. *Science*, 292(5524), 2080–2083. <https://doi.org/10.1126/science.1058758>

- Kaper, J. B., Nataro, J. P., & Mobley, H. L. T. (2004). Pathogenic *Escherichia coli*. *Nature Reviews Microbiology*, 2(2), 123–140. <https://doi.org/10.1038/nrmicro818>
- Kashmiri, Z. N., & Mankar, S. A. (2014). *Free radicals and oxidative stress in bacteria*. 7.
- Kato, A., Ohnishi, H., Yamamoto, K., Furuta, E., Tanabe, H., & Utsumi, R. (2000). Transcription of *emrKY* is Regulated by the EvgA-EvgS Two-Component System in *Escherichia coli* K-12. *Bioscience, Biotechnology, and Biochemistry*, 64(6), 1203–1209. <https://doi.org/10.1271/bbb.64.1203>
- Kawasaki, K., Ernst, R. K., & Miller, S. I. (2005). Inhibition of *Salmonella enterica* Serovar Typhimurium Lipopolysaccharide Deacylation by Aminoarabinose Membrane Modification. *Journal of Bacteriology*, 187(7), 2448–2457. <https://doi.org/10.1128/JB.187.7.2448-2457.2005>
- Kazmierczak, M. J., Wiedmann, M., & Boor, K. J. (2005). Alternative Sigma Factors and Their Roles in Bacterial Virulence. *Microbiology and Molecular Biology Reviews*, 69(4), 527–543. <https://doi.org/10.1128/MMBR.69.4.527-543.2005>
- Keith, K. E., & Valvano, M. A. (2007). Characterization of SodC, a Periplasmic Superoxide Dismutase from *Burkholderia cenocepacia*. *Infection and Immunity*, 75(5), 2451–2460. <https://doi.org/10.1128/IAI.01556-06>
- Keller, A. A., & Lazareva, A. (2014). Predicted Releases of Engineered Nanomaterials: From Global to Regional to Local. *Environmental Science & Technology Letters*, 1(1), 65–70. <https://doi.org/10.1021/ez400106t>
- Kelly, K. L., Coronado, E., Zhao, L. L., & Schatz, G. C. (2003). The Optical Properties of Metal Nanoparticles: The Influence of Size, Shape, and Dielectric Environment. *The Journal of Physical Chemistry B*, 107(3), 668–677. <https://doi.org/10.1021/jp026731y>

- Khan, I., Saeed, K., & Khan, I. (2019). Nanoparticles: Properties, applications and toxicities. *Arabian Journal of Chemistry*, *12*(7), 908–931.
<https://doi.org/10.1016/j.arabjc.2017.05.011>
- Khan, S. T., & Malik, A. (2019). Engineered nanomaterials for water decontamination and purification: From lab to products. *Journal of Hazardous Materials*, *363*, 295–308.
<https://doi.org/10.1016/j.jhazmat.2018.09.091>
- Kik, K., Bukowska, B., & Sicińska, P. (2020). Polystyrene nanoparticles: Sources, occurrence in the environment, distribution in tissues, accumulation and toxicity to various organisms. *Environmental Pollution*, *262*, 114297. <https://doi.org/10.1016/j.envpol.2020.114297>
- Kim, S. Y., Kim, Y. J., Lee, S.-W., & Lee, E.-H. (2022). Interactions between bacteria and nano (micro)-sized polystyrene particles by bacterial responses and microscopy. *Chemosphere*, *306*, 135584. <https://doi.org/10.1016/j.chemosphere.2022.135584>
- Kim, S. Y., Park, C., Jang, H. J., Kim, B. o., Bae, H. W., Chung, I. Y., Kim, E. S., & Cho, Y. H. (2019). Antibacterial strategies inspired by the oxidative stress and response networks. *Journal of Microbiology*, *57*(3), 203–212. <https://doi.org/10.1007/s12275-019-8711-9>
- Kimkes, T. E. P., & Heinemann, M. (2019). How bacteria recognise and respond to surface contact. *FEMS Microbiology Reviews*, fuz029. <https://doi.org/10.1093/femsre/fuz029>
- Kirste, R., Mita, S., Hussey, L., Hoffmann, M. P., Guo, W., Bryan, I., Bryan, Z., Tweedie, J., Xie, J., Gerhold, M., Collazo, R., & Sitar, Z. (2013). Polarity control and growth of lateral polarity structures in AlN. *Applied Physics Letters*, *102*(18), 181913.
<https://doi.org/10.1063/1.4804575>

- Klauck, E., Lingnau, M., & Hengge-Aronis, R. (2001). Role of the response regulator RssB in sigmaS recognition and initiation of sigmaS proteolysis in *Escherichia coli*. *Molecular Microbiology*, *40*(6), 1381–1390. <https://doi.org/10.1046/j.1365-2958.2001.02482.x>
- Kline, K. A., Dodson, K. W., Caparon, M. G., & Hultgren, S. J. (2010). A tale of two pili: Assembly and function of pili in bacteria. *Trends in Microbiology*, *18*(5), 224–232. <https://doi.org/10.1016/j.tim.2010.03.002>
- Kolahalam, L. A., Kasi Viswanath, I. V., Diwakar, B. S., Govindh, B., Reddy, V., & Murthy, Y. L. N. (2019). Review on nanomaterials: Synthesis and applications. *Materials Today: Proceedings*, *18*, 2182–2190. <https://doi.org/10.1016/j.matpr.2019.07.371>
- Krishnamurthi, V. R., Niyonshuti, I. I., Chen, J., & Wang, Y. (2021). A new analysis method for evaluating bacterial growth with microplate readers. *PLOS ONE*, *16*(1), e0245205. <https://doi.org/10.1371/journal.pone.0245205>
- Krogfelt, K. A., Bergmans, H., & Klemm', P. (n.d.). Direct Evidence that the FimH Protein Is the Mannose-Specific Adhesin of *Escherichia coli* Type 1 Fimbriae. *INFECT. IMMUN.*, *4*.
- Lahiani, M. H., Chen, J., Irin, F., Poretzky, A. A., Green, M. J., & Khodakovskaya, M. V. (2015). Interaction of carbon nanohorns with plants: Uptake and biological effects. *Carbon*, *81*, 607–619. <https://doi.org/10.1016/j.carbon.2014.09.095>
- Lam, S. J., Wong, E. H. H., Boyer, C., & Qiao, G. G. (2018). Antimicrobial polymeric nanoparticles. *Progress in Polymer Science*, *76*, 40–64. <https://doi.org/10.1016/j.progpolymsci.2017.07.007>

- Lemmin, T., Soto, C. S., Clinthorne, G., DeGrado, W. F., & Dal Peraro, M. (2013). Assembly of the Transmembrane Domain of E. coli PhoQ Histidine Kinase: Implications for Signal Transduction from Molecular Simulations. *PLoS Computational Biology*, 9(1), e1002878. <https://doi.org/10.1371/journal.pcbi.1002878>
- Lesniak, A., Salvati, A., Santos-Martinez, M. J., Radomski, M. W., Dawson, K. A., & Åberg, C. (2013). Nanoparticle Adhesion to the Cell Membrane and Its Effect on Nanoparticle Uptake Efficiency. *Journal of the American Chemical Society*, 135(4), 1438–1444. <https://doi.org/10.1021/ja309812z>
- Li, X., & Liu, X. (2017). Group III nitride nanomaterials for biosensing. *Nanoscale*, 9(22), 7320–7341. <https://doi.org/10.1039/C7NR01577A>
- Li, Z., Wang, L., Li, Y., Feng, Y., & Feng, W. (2019). Carbon-based functional nanomaterials: Preparation, properties and applications. *Composites Science and Technology*, 179, 10–40. <https://doi.org/10.1016/j.compscitech.2019.04.028>
- Ling, D., & Hyeon, T. (2013). Chemical Design of Biocompatible Iron Oxide Nanoparticles for Medical Applications. *Small*, 9(9–10), 1450–1466. <https://doi.org/10.1002/sml.201202111>
- Liu, C., Sun, D., Zhu, J., & Liu, W. (2019). Two-Component Signal Transduction Systems: A Major Strategy for Connecting Input Stimuli to Biofilm Formation. *Frontiers in Microbiology*, 9, 3279. <https://doi.org/10.3389/fmicb.2018.03279>
- Liu, F., Collazo, R., Mita, S., Sitar, Z., Duscher, G., & Pennycook, S. J. (2007). The mechanism for polarity inversion of GaN via a thin AlN layer: Direct experimental evidence. *Applied Physics Letters*, 91(20), 203115. <https://doi.org/10.1063/1.2815748>

- Liu, J., Du, C., Beaman, H. T., & Monroe, M. B. B. (2020). Characterization of Phenolic Acid Antimicrobial and Antioxidant Structure–Property Relationships. *Pharmaceutics*, *12*(5), 419. <https://doi.org/10.3390/pharmaceutics12050419>
- Liu, P., Duan, W., Wang, Q., & Li, X. (2010). The damage of outer membrane of Escherichia coli in the presence of TiO₂ combined with UV light. *Colloids and Surfaces B: Biointerfaces*, *78*(2), 171–176. <https://doi.org/10.1016/j.colsurfb.2010.02.024>
- Liu, W.-T. (2006a). Nanoparticles and their biological and environmental applications. *Journal of Bioscience and Bioengineering*, *102*(1), 1–7. <https://doi.org/10.1263/jbb.102.1>
- Liu, W.-T. (2006b). Nanoparticles and their biological and environmental applications. *Journal of Bioscience and Bioengineering*, *102*(1), 1–7. <https://doi.org/10.1263/jbb.102.1>
- Liu, Y., Wang, J., Sun, Y., Li, H., Zhai, Z., Guo, S., Ren, T., & Li, C. (2022). Nitrogen-doped carbon nanofibers anchoring Fe nanoparticles as biocompatible anode for boosting extracellular electron transfer in microbial fuel cells. *Journal of Power Sources*, *544*, 231890. <https://doi.org/10.1016/j.jpowsour.2022.231890>
- Loewen, P. C., Switala, J., & Triggs-Raine, B. L. (1985). Catalases HPI and HPII in Escherichia coli are induced independently. *Archives of Biochemistry and Biophysics*, *243*(1), 144–149. [https://doi.org/10.1016/0003-9861\(85\)90782-9](https://doi.org/10.1016/0003-9861(85)90782-9)
- Loos, C., Syrovets, T., Musyanovych, A., Mailänder, V., Landfester, K., Nienhaus, G. U., & Simmet, T. (2014). Functionalized polystyrene nanoparticles as a platform for studying bio–nano interactions. *Beilstein Journal of Nanotechnology*, *5*, 2403–2412. <https://doi.org/10.3762/bjnano.5.250>

- Louro, H., Saruga, A., Santos, J., Pinhão, M., & Silva, M. J. (2019). Biological impact of metal nanomaterials in relation to their physicochemical characteristics. *Toxicology in Vitro*, *56*, 172–183. <https://doi.org/10.1016/j.tiv.2019.01.018>
- Lund, P. A., De Biase, D., Liran, O., Scheler, O., Mira, N. P., Cetecioglu, Z., Fernández, E. N., Bover-Cid, S., Hall, R., Sauer, M., & O'Byrne, C. (2020). Understanding How Microorganisms Respond to Acid pH Is Central to Their Control and Successful Exploitation. *Frontiers in Microbiology*, *11*, 556140. <https://doi.org/10.3389/fmicb.2020.556140>
- Ma, Y., Chu, Y., Lyu, S., He, Y., & Wang, Y. (2022). Injectable Optical System for Drug Delivery, Ablation, and Sampling in Deep Tissue. *Advanced Materials Technologies*, *7*(8), 2101464. <https://doi.org/10.1002/admt.202101464>
- Madannejad, R., Shoaie, N., Jahanpeyma, F., Darvishi, M. H., Azimzadeh, M., & Javadi, H. (2019). Toxicity of carbon-based nanomaterials: Reviewing recent reports in medical and biological systems. *Chemico-Biological Interactions*, *307*, 206–222. <https://doi.org/10.1016/j.cbi.2019.04.036>
- Malakar, A., Kanel, S. R., Ray, C., Snow, D. D., & Nadagouda, M. N. (2021). Nanomaterials in the environment, human exposure pathway, and health effects: A review. *Science of The Total Environment*, *759*, 143470. <https://doi.org/10.1016/j.scitotenv.2020.143470>
- Malinverni, J. C., & Silhavy, T. J. (2009). An ABC transport system that maintains lipid asymmetry in the Gram-negative outer membrane. *Proceedings of the National Academy of Sciences*, *106*(19), 8009–8014. <https://doi.org/10.1073/pnas.0903229106>

- Mammari, N., Lamouroux, E., Boudier, A., & Duval, R. E. (2022a). Current Knowledge on the Oxidative-Stress-Mediated Antimicrobial Properties of Metal-Based Nanoparticles. *Microorganisms*, *10*(2), 437. <https://doi.org/10.3390/microorganisms10020437>
- Mammari, N., Lamouroux, E., Boudier, A., & Duval, R. E. (2022b). Current Knowledge on the Oxidative-Stress-Mediated Antimicrobial Properties of Metal-Based Nanoparticles. *Microorganisms*, *10*(2), 437. <https://doi.org/10.3390/microorganisms10020437>
- Mansor, M., & Xu, J. (2020). Benefits at the nanoscale: A review of NANOPARTICLE-ENABLED processes favouring microbial growth and functionality. *Environmental Microbiology*, *22*(9), 3633–3649. <https://doi.org/10.1111/1462-2920.15174>
- Marles-Wright, J., & Lewis, R. J. (2007). Stress responses of bacteria. *Current Opinion in Structural Biology*, *17*(6), 755–760. <https://doi.org/10.1016/j.sbi.2007.08.004>
- Maruyama, C. R., Guilger, M., Pascoli, M., Bileshy-José, N., Abhilash, P. C., Fraceto, L. F., & de Lima, R. (2016). Nanoparticles Based on Chitosan as Carriers for the Combined Herbicides Imazapic and Imazapyr. *Scientific Reports*, *6*(1), 19768. <https://doi.org/10.1038/srep19768>
- Mathelié-Guinlet, M., Béven, L., Moroté, F., Moynet, D., Grauby-Heywang, C., Gammoudi, I., Delville, M.-H., & Cohen-Bouhacina, T. (2017). Probing the threshold of membrane damage and cytotoxicity effects induced by silica nanoparticles in *Escherichia coli* bacteria. *Advances in Colloid and Interface Science*, *245*, 81–91. <https://doi.org/10.1016/j.cis.2017.04.012>

- Matthews, S., Mai, L., Jeong, C.-B., Lee, J.-S., Zeng, E. Y., & Xu, E. G. (2021). Key mechanisms of micro- and nanoplastic (MNP) toxicity across taxonomic groups. *Comparative Biochemistry and Physiology Part C: Toxicology & Pharmacology*, 247, 109056. <https://doi.org/10.1016/j.cbpc.2021.109056>
- Matuła, K., Richter, Ł., Janczuk-Richter, M., Nogala, W., Grzeszkowiak, M., Peplińska, B., Jurga, S., Wyroba, E., Suski, S., Bilski, H., Silesian, A., Bluysen, H. A. R., Derebecka, N., Wesoly, J., Łoś, J. M., Łoś, M., Decewicz, P., Dziewit, L., Paczesny, J., & Hołyst, R. (2019). Phenotypic plasticity of *Escherichia coli* upon exposure to physical stress induced by ZnO nanorods. *Scientific Reports*, 9(1), 8575. <https://doi.org/10.1038/s41598-019-44727-w>
- Mauter, M. S., & Elimelech, M. (2008). Environmental Applications of Carbon-Based Nanomaterials. *Environmental Science & Technology*, 42(16), 5843–5859. <https://doi.org/10.1021/es8006904>
- Mbayachi, V. B., Ndayiragije, E., Sammani, T., Taj, S., Mbuta, E. R., & Khan, A. Ullah. (2021). Graphene synthesis, characterization and its applications: A review. *Results in Chemistry*, 3, 100163. <https://doi.org/10.1016/j.rechem.2021.100163>
- McNeil, S. E. (Ed.). (2011a). *Characterization of Nanoparticles Intended for Drug Delivery* (Vol. 697). Humana Press. <https://doi.org/10.1007/978-1-60327-198-1>
- McNeil, S. E. (Ed.). (2011b). *Characterization of Nanoparticles Intended for Drug Delivery* (Vol. 697). Humana Press. <https://doi.org/10.1007/978-1-60327-198-1>

- Mejias, J. H., Salazar, F., Pérez Amaro, L., Hube, S., Rodriguez, M., & Alfaro, M. (2021). Nanofertilizers: A Cutting-Edge Approach to Increase Nitrogen Use Efficiency in Grasslands. *Frontiers in Environmental Science*, *9*, 635114. <https://doi.org/10.3389/fenvs.2021.635114>
- Miernicki, M., Hofmann, T., Eisenberger, I., von der Kammer, F., & Praetorius, A. (2019a). Legal and practical challenges in classifying nanomaterials according to regulatory definitions. *Nature Nanotechnology*, *14*(3), 208–216. <https://doi.org/10.1038/s41565-019-0396-z>
- Miernicki, M., Hofmann, T., Eisenberger, I., von der Kammer, F., & Praetorius, A. (2019b). Legal and practical challenges in classifying nanomaterials according to regulatory definitions. *Nature Nanotechnology*, *14*(3), 208–216. <https://doi.org/10.1038/s41565-019-0396-z>
- Milewska-Hendel, A., Gawecki, R., Zubko, M., Stróż, D., & Kurczyńska, E. (2016). Diverse influence of nanoparticles on plant growth with a particular emphasis on crop plants. *Acta Agrobotanica*, *69*(4). <https://doi.org/10.5586/aa.1694>
- Miller, E., Garcia, T., Hultgren, S., & Oberhauser, A. F. (2006). The Mechanical Properties of E. coli Type 1 Pili Measured by Atomic Force Microscopy Techniques. *Biophysical Journal*, *91*(10), 3848–3856. <https://doi.org/10.1529/biophysj.106.088989>
- Miller, S. I., & Salama, N. R. (2018). The gram-negative bacterial periplasm: Size matters. *PLOS Biology*, *16*(1), e2004935. <https://doi.org/10.1371/journal.pbio.2004935>

- Minagawa, S., Ogasawara, H., Kato, A., Yamamoto, K., Eguchi, Y., Oshima, T., Mori, H., Ishihama, A., & Utsumi, R. (2003). Identification and Molecular Characterization of the Mg²⁺ Stimulon of *Escherichia coli*. *Journal of Bacteriology*, *185*(13), 3696–3702. <https://doi.org/10.1128/JB.185.13.3696-3702.2003>
- Mitrophanov, A. Y., & Groisman, E. A. (2008). Signal integration in bacterial two-component regulatory systems. *Genes & Development*, *22*(19), 2601–2611. <https://doi.org/10.1101/gad.1700308>
- Miyake, Y., & Yamamoto, K. (2020). Epistatic Effect of Regulators to the Adaptive Growth of *Escherichia coli*. *Scientific Reports*, *10*(1), 3661. <https://doi.org/10.1038/s41598-020-60353-3>
- Monica, R. C., & Cremonini, R. (2009). Nanoparticles and higher plants. *Caryologia*, *62*(2), 161–165. <https://doi.org/10.1080/00087114.2004.10589681>
- Mortimer, M., Wang, Y., & Holden, P. A. (2021a). Molecular Mechanisms of Nanomaterial-Bacterial Interactions Revealed by Omics—The Role of Nanomaterial Effect Level. *Frontiers in Bioengineering and Biotechnology*, *9*, 683520. <https://doi.org/10.3389/fbioe.2021.683520>
- Mortimer, M., Wang, Y., & Holden, P. A. (2021b). Molecular Mechanisms of Nanomaterial-Bacterial Interactions Revealed by Omics—The Role of Nanomaterial Effect Level. *Frontiers in Bioengineering and Biotechnology*, *9*, 683520. <https://doi.org/10.3389/fbioe.2021.683520>
- Muhammad, M. H., Idris, A. L., Fan, X., Guo, Y., Yu, Y., Jin, X., Qiu, J., Guan, X., & Huang, T. (2020). Beyond Risk: Bacterial Biofilms and Their Regulating Approaches. *Frontiers in Microbiology*, *11*, 928. <https://doi.org/10.3389/fmicb.2020.00928>

- Müller, C. M., Åberg, A., Strasevičiene, J., Emödy, L., Uhlin, B. E., & Balsalobre, C. (2009). Type 1 Fimbriae, a Colonization Factor of Uropathogenic *Escherichia coli*, Are Controlled by the Metabolic Sensor CRP-cAMP. *PLoS Pathogens*, 5(2), e1000303. <https://doi.org/10.1371/journal.ppat.1000303>
- Nagamiya, K., Motohashi, T., Nakao, K., Prophan, S. H., Hattori, E., Hirose, S., Ozawa, K., Ohkawa, Y., Takabe, T., Takabe, T., & Komamine, A. (2007). Enhancement of salt tolerance in transgenic rice expressing an *Escherichia coli* catalase gene, katE. *Plant Biotechnology Reports*, 1(1), 49–55. <https://doi.org/10.1007/s11816-007-0007-6>
- Nagar, S. D., Aggarwal, B., Joon, S., Bhatnagar, R., & Bhatnagar, S. (2016). A Network Biology Approach to Decipher Stress Response in Bacteria Using *Escherichia coli* As a Model. *OMICS: A Journal of Integrative Biology*, 20(5), 310–324. <https://doi.org/10.1089/omi.2016.0028>
- Naqvi, Q.-A., Kanwal, A., Qaseem, S., Naeem, M., Ali, S. R., Shaffique, M., & Maqbool, M. (2019a). Size-dependent inhibition of bacterial growth by chemically engineered spherical ZnO nanoparticles. *Journal of Biological Physics*, 45(2), 147–159. <https://doi.org/10.1007/s10867-019-9520-4>
- Naqvi, Q.-A., Kanwal, A., Qaseem, S., Naeem, M., Ali, S. R., Shaffique, M., & Maqbool, M. (2019b). Size-dependent inhibition of bacterial growth by chemically engineered spherical ZnO nanoparticles. *Journal of Biological Physics*, 45(2), 147–159. <https://doi.org/10.1007/s10867-019-9520-4>
- Neal, A. L. (2008). What can be inferred from bacterium–nanoparticle interactions about the potential consequences of environmental exposure to nanoparticles? *Ecotoxicology*, 17(5), 362–371. <https://doi.org/10.1007/s10646-008-0217-x>

- Neuwald, A. F., Krishnan, B. R., Brikun, I., Kulakauskas, S., Suziedelis, K., Tomcsanyi, T., Leyh, T. S., & Berg, D. E. (1992). CysQ, a gene needed for cysteine synthesis in *Escherichia coli* K-12 only during aerobic growth. *Journal of Bacteriology*, *174*(2), 415–425. <https://doi.org/10.1128/jb.174.2.415-425.1992>
- Niño-Martínez, N., Salas Orozco, M. F., Martínez-Castañón, G.-A., Torres Méndez, F., & Ruiz, F. (2019). Molecular Mechanisms of Bacterial Resistance to Metal and Metal Oxide Nanoparticles. *International Journal of Molecular Sciences*, *20*(11), 2808. <https://doi.org/10.3390/ijms20112808>
- Nishino, K., & Yamaguchi, A. (2002). EvgA of the Two-Component Signal Transduction System Modulates Production of the YhiUV Multidrug Transporter in *Escherichia coli*. *Journal of Bacteriology*, *184*(8), 2319–2323. <https://doi.org/10.1128/JB.184.8.2319-2323.2002>
- Oladeinde, A., Lipp, E., Chen, C.-Y., Muirhead, R., Glenn, T., Cook, K., & Molina, M. (2018). Transcriptome Changes of *Escherichia coli*, *Enterococcus faecalis*, and *Escherichia coli* O157:H7 Laboratory Strains in Response to Photo-Degraded DOM. *Frontiers in Microbiology*, *9*, 882. <https://doi.org/10.3389/fmicb.2018.00882>
- O’Toole, G. A., & Wong, G. C. L. (2016). Sensational biofilms: Surface sensing in bacteria. *Current Opinion in Microbiology*, *30*, 139–146. <https://doi.org/10.1016/j.mib.2016.02.004>
- Otto, K., & Silhavy, T. J. (2002). Surface sensing and adhesion of *Escherichia coli* controlled by the Cpx-signaling pathway. *Proceedings of the National Academy of Sciences*, *99*(4), 2287–2292. <https://doi.org/10.1073/pnas.042521699>

- Paget, M. (2015). Bacterial Sigma Factors and Anti-Sigma Factors: Structure, Function and Distribution. *Biomolecules*, 5(3), 1245–1265. <https://doi.org/10.3390/biom5031245>
- Pajerski, W., Ochonska, D., Brzychczy-Wloch, M., Indyka, P., Jarosz, M., Golda-Cepa, M., Sojka, Z., & Kotarba, A. (2019). Attachment efficiency of gold nanoparticles by Gram-positive and Gram-negative bacterial strains governed by surface charges. *Journal of Nanoparticle Research*, 21(8), 186. <https://doi.org/10.1007/s11051-019-4617-z>
- Parashar, M., Shukla, V. K., & Singh, R. (2020). Metal oxides nanoparticles via sol–gel method: A review on synthesis, characterization and applications. *Journal of Materials Science: Materials in Electronics*, 31(5), 3729–3749. <https://doi.org/10.1007/s10854-020-02994-8>
- Park, I.-S., Mahapatra, C., Park, J. S., Dashnyam, K., Kim, J.-W., Ahn, J. C., Chung, P.-S., Yoon, D. S., Mandakhbayar, N., Singh, R. K., Lee, J.-H., Leong, K. W., & Kim, H.-W. (2020). Revascularization and limb salvage following critical limb ischemia by nanoceria-induced Ref-1/APE1-dependent angiogenesis. *Biomaterials*, 242, 119919. <https://doi.org/10.1016/j.biomaterials.2020.119919>
- Partridge, J. D., Scott, C., Tang, Y., Poole, R. K., & Green, J. (2006). Escherichia coli Transcriptome Dynamics during the Transition from Anaerobic to Aerobic Conditions. *Journal of Biological Chemistry*, 281(38), 27806–27815. <https://doi.org/10.1074/jbc.M603450200>
- Pearce, B. L., Wilkins, S. J., Paskova, T., & Ivanisevic, A. (2015). A review of in situ surface functionalization of gallium nitride via beaker wet chemistry. *Journal of Materials Research*, 30(19), 2859–2870. <https://doi.org/DOI: 10.1557/jmr.2015.132>
- Pelletier, D. A., Suresh, A. K., Holton, G. A., McKeown, C. K., Wang, W., Gu, B., Mortensen, N. P., Allison, D. P., Joy, D. C., Allison, M. R., Brown, S. D., Phelps, T. J., & Doktycz,

- M. J. (2010). Effects of Engineered Cerium Oxide Nanoparticles on Bacterial Growth and Viability. *Applied and Environmental Microbiology*, 76(24), 7981–7989.
<https://doi.org/10.1128/AEM.00650-10>
- Pellicer, M. T., Badía, J., Aguilar, J., & Baldomà, L. (1996). *glc* locus of *Escherichia coli*: Characterization of genes encoding the subunits of glycolate oxidase and the *glc* regulator protein. *Journal of Bacteriology*, 178(7), 2051–2059.
<https://doi.org/10.1128/jb.178.7.2051-2059.1996>
- Phan, D. C., Vazquez-Munoz, R., Matta, A., & Kapoor, V. (2020). Short-term effects of Mn₂O₃ nanoparticles on physiological activities and gene expression of nitrifying bacteria under low and high dissolved oxygen conditions. *Chemosphere*, 261, 127775.
<https://doi.org/10.1016/j.chemosphere.2020.127775>
- Podolska, A., Tham, S., Hart, R. D., Seeber, R. M., Kocan, M., Kocan, M., Mishra, U. K., Pflieger, K. D. G., Parish, G., & Nener, B. D. (2012). Biocompatibility of semiconducting AlGa_N/Ga_N material with living cells. *Sensors and Actuators B: Chemical*, 169, 401–406. <https://doi.org/10.1016/j.snb.2012.04.015>
- Pokropivny, V. V., & Skorokhod, V. V. (2007). Classification of nanostructures by dimensionality and concept of surface forms engineering in nanomaterial science. *Materials Science and Engineering: C*, 27(5–8), 990–993.
<https://doi.org/10.1016/j.msec.2006.09.023>
- Poole, K. (2012a). Bacterial stress responses as determinants of antimicrobial resistance. *Journal of Antimicrobial Chemotherapy*, 67(9), 2069–2089. <https://doi.org/10.1093/jac/dks196>
- Poole, K. (2012b). Bacterial stress responses as determinants of antimicrobial resistance. *Journal of Antimicrobial Chemotherapy*, 67(9), 2069–2089. <https://doi.org/10.1093/jac/dks196>

- Poortinga, A. T., Bos, R., Norde, W., & Busscher, H. J. (2002). Electric double layer interactions in bacterial adhesion to surfaces. *Surface Science Reports*, 47(1), 1–32.
[https://doi.org/10.1016/S0167-5729\(02\)00032-8](https://doi.org/10.1016/S0167-5729(02)00032-8)
- Proft, T., & Baker, E. N. (2009a). Pili in Gram-negative and Gram-positive bacteria—Structure, assembly and their role in disease. *Cellular and Molecular Life Sciences*, 66(4), 613–635.
<https://doi.org/10.1007/s00018-008-8477-4>
- Proft, T., & Baker, E. N. (2009b). Pili in Gram-negative and Gram-positive bacteria—Structure, assembly and their role in disease. *Cellular and Molecular Life Sciences*, 66(4), 613–635.
<https://doi.org/10.1007/s00018-008-8477-4>
- Rahman, M. A., Radhakrishnan, R., & Gopalakrishnan, R. (2018). Structural, optical, magnetic and antibacterial properties of Nd doped NiO nanoparticles prepared by co-precipitation method. *Journal of Alloys and Compounds*, 742, 421–429.
<https://doi.org/10.1016/j.jallcom.2018.01.298>
- Ramos, J. L., Gallegos, M.-T., Marqués, S., Ramos-González, M.-I., Espinosa-Urgel, M., & Segura, A. (2001). Responses of Gram-negative bacteria to certain environmental stressors. *Current Opinion in Microbiology*, 4(2), 166–171.
[https://doi.org/10.1016/S1369-5274\(00\)00183-1](https://doi.org/10.1016/S1369-5274(00)00183-1)
- Rao, S. D., & Igoshin, O. A. (2020). *Overlaid positive and negative feedback loops shape dynamical properties of PhoPQ two-component system.*
- Rastogi, A., Zivcak, M., Sytar, O., Kalaji, H. M., He, X., Mbarki, S., & Brestic, M. (2017). Impact of Metal and Metal Oxide Nanoparticles on Plant: A Critical Review. *Frontiers in Chemistry*, 5, 78. <https://doi.org/10.3389/fchem.2017.00078>

- Rau, M. H., Calero, P., Lennen, R. M., Long, K. S., & Nielsen, A. T. (2016). Genome-wide Escherichia coli stress response and improved tolerance towards industrially relevant chemicals. *Microbial Cell Factories*, *15*(1), 176. <https://doi.org/10.1186/s12934-016-0577-5>
- Rawashdeh, R., & Haik, Y. (n.d.). *Antibacterial Mechanisms of Metallic Nanoparticles: A Review*. 2.
- Ren, E., Zhang, C., Li, D., Pang, X., & Liu, G. (2020). Leveraging metal oxide nanoparticles for bacteria tracing and eradicating. *View*, *1*(3), 20200052. <https://doi.org/10.1002/VIW.20200052>
- Rizzello, L., Sorce, B., Sabella, S., Vecchio, G., Galeone, A., Brunetti, V., Cingolani, R., & Paolo Pompa, P. (2011). Impact of Nanoscale Topography on Genomics and Proteomics of Adherent Bacteria. *ACS Nano*, *5*(3), 1865–1876. <https://doi.org/10.1021/nn102692m>
- Rodriguez Ayala, F., Bartolini, M., & Grau, R. (2020). The Stress-Responsive Alternative Sigma Factor SigB of Bacillus subtilis and Its Relatives: An Old Friend With New Functions. *Frontiers in Microbiology*, *11*, 1761. <https://doi.org/10.3389/fmicb.2020.01761>
- Roier, S., Zingl, F. G., Cakar, F., Durakovic, S., Kohl, P., Eichmann, T. O., Klug, L., Gadermaier, B., Weinzerl, K., Prassl, R., Lass, A., Daum, G., Reidl, J., Feldman, M. F., & Schild, S. (2016). A novel mechanism for the biogenesis of outer membrane vesicles in Gram-negative bacteria. *Nature Communications*, *7*(1), 10515. <https://doi.org/10.1038/ncomms10515>
- Rolfe, M. D., Rice, C. J., Lucchini, S., Pin, C., Thompson, A., Cameron, A. D. S., Alston, M., Stringer, M. F., Betts, R. P., Baranyi, J., Peck, M. W., & Hinton, J. C. D. (2012). Lag Phase Is a Distinct Growth Phase That Prepares Bacteria for Exponential Growth and

- Involves Transient Metal Accumulation. *Journal of Bacteriology*, 194(3), 686–701.
<https://doi.org/10.1128/JB.06112-11>
- Ross, A. M., & Lahann, J. (2015). Current Trends and Challenges in Biointerfaces Science and Engineering. *Annual Review of Chemical and Biomolecular Engineering*, 6(1), 161–186.
<https://doi.org/10.1146/annurev-chembioeng-060713-040042>
- Rui, M., Ma, C., Hao, Y., Guo, J., Rui, Y., Tang, X., Zhao, Q., Fan, X., Zhang, Z., Hou, T., & Zhu, S. (2016). Iron Oxide Nanoparticles as a Potential Iron Fertilizer for Peanut (*Arachis hypogaea*). *Frontiers in Plant Science*, 7. <https://doi.org/10.3389/fpls.2016.00815>
- Russo, T. (2003). Medical and economic impact of extraintestinal infections due to *Escherichia coli*: Focus on an increasingly important endemic problem. *Microbes and Infection*, 5(5), 449–456. [https://doi.org/10.1016/S1286-4579\(03\)00049-2](https://doi.org/10.1016/S1286-4579(03)00049-2)
- Sakimoto, K. K., Wong, A. B., & Yang, P. (2016). Self-photosensitization of nonphotosynthetic bacteria for solar-to-chemical production. *Science*, 351(6268), 74–77.
<https://doi.org/10.1126/science.aad3317>
- Saleh, T. A. (2020a). Nanomaterials: Classification, properties, and environmental toxicities. *Environmental Technology & Innovation*, 20, 101067.
<https://doi.org/10.1016/j.eti.2020.101067>
- Saleh, T. A. (2020b). Nanomaterials: Classification, properties, and environmental toxicities. *Environmental Technology & Innovation*, 20, 101067.
<https://doi.org/10.1016/j.eti.2020.101067>

- Santos, A. C. de M., Santos, F. F., Silva, R. M., & Gomes, T. A. T. (2020). Diversity of Hybrid- and Hetero-Pathogenic *Escherichia coli* and Their Potential Implication in More Severe Diseases. *Frontiers in Cellular and Infection Microbiology*, *10*, 339. <https://doi.org/10.3389/fcimb.2020.00339>
- Schultz, D., & Kishony, R. (2013). Optimization and control in bacterial Lag phase. *BMC Biology*, *11*(1), 120. <https://doi.org/10.1186/1741-7007-11-120>
- Selvarajan, V., Obuobi, S., & Ee, P. L. R. (2020). Silica Nanoparticles—A Versatile Tool for the Treatment of Bacterial Infections. *Frontiers in Chemistry*, *8*, 602. <https://doi.org/10.3389/fchem.2020.00602>
- Sengupta, R., Bhattacharya, M., Bandyopadhyay, S., & Bhowmick, A. K. (2011). A review on the mechanical and electrical properties of graphite and modified graphite reinforced polymer composites. *Progress in Polymer Science*, *36*(5), 638–670. <https://doi.org/10.1016/j.progpolymsci.2010.11.003>
- Setty, Y., Mayo, A. E., Surette, M. G., & Alon, U. (2003). Detailed map of a cis-regulatory input function. *Proceedings of the National Academy of Sciences*, *100*(13), 7702–7707. <https://doi.org/10.1073/pnas.1230759100>
- Shaikh, S., Nazam, N., Rizvi, S. M. D., Ahmad, K., Baig, M. H., Lee, E. J., & Choi, I. (2019). Mechanistic Insights into the Antimicrobial Actions of Metallic Nanoparticles and Their Implications for Multidrug Resistance. *International Journal of Molecular Sciences*, *20*(10), 2468. <https://doi.org/10.3390/ijms20102468>
- Shang, Y., Hasan, Md. K., Ahammed, G. J., Li, M., Yin, H., & Zhou, J. (2019). Applications of Nanotechnology in Plant Growth and Crop Protection: A Review. *Molecules*, *24*(14), 2558. <https://doi.org/10.3390/molecules24142558>

- Sharma, P., Pandey, V., Sharma, M. M. M., Patra, A., Singh, B., Mehta, S., & Husen, A. (2021). A Review on Biosensors and Nanosensors Application in Agroecosystems. *Nanoscale Research Letters*, 16(1), 136. <https://doi.org/10.1186/s11671-021-03593-0>
- Shende, S. S., Rajput, V. D., Gorovtsov, A. V., Harish, Saxena, P., Minkina, T. M., Chokheli, V. A., Jatav, H. S., Sushkova, S. N., Kaur, P., & Kizilkaya, R. (2021). Interaction of Nanoparticles with Microbes. In P. Singh, R. Singh, P. Verma, R. Bhadouria, A. Kumar, & M. Kaushik (Eds.), *Plant-Microbes-Engineered Nano-particles (PM-ENPs) Nexus in Agro-Ecosystems* (pp. 175–188). Springer International Publishing. https://doi.org/10.1007/978-3-030-66956-0_12
- Shiau, B.-W., Lin, C.-H., Liao, Y.-Y., Lee, Y.-R., Liu, S.-H., Ding, W.-C., & Lee, J.-R. (2018). The characteristics and mechanisms of Au nanoparticles processed by functional centrifugal procedures. *Journal of Physics and Chemistry of Solids*, 116, 161–167. <https://doi.org/10.1016/j.jpics.2018.01.033>
- Singh, N., Paknikar, K. M., & Rajwade, J. (2019). RNA-sequencing reveals a multitude of effects of silver nanoparticles on *Pseudomonas aeruginosa* biofilms. *Environmental Science: Nano*, 6(6), 1812–1828. <https://doi.org/10.1039/C8EN01286E>
- Sivakumar, P., Lee, M., Kim, Y.-S., & Shim, M. S. (2018). Photo-triggered antibacterial and anticancer activities of zinc oxide nanoparticles. *Journal of Materials Chemistry B*, 6(30), 4852–4871. <https://doi.org/10.1039/C8TB00948A>
- Slavin, Y. N., Asnis, J., Häfeli, U. O., & Bach, H. (2017). Metal nanoparticles: Understanding the mechanisms behind antibacterial activity. *Journal of Nanobiotechnology*, 15(1), 65. <https://doi.org/10.1186/s12951-017-0308-z>

- Snyder, P. J., Kirste, R., Collazo, R., & Ivanisevic, A. (2016a). Nanoscale topography, semiconductor polarity and surface functionalization: Additive and cooperative effects on PC12 cell behavior. *RSC Advances*, 6(100), 97873–97881.
<https://doi.org/10.1039/C6RA21936E>
- Snyder, P. J., Kirste, R., Collazo, R., & Ivanisevic, A. (2016b). Nanoscale topography, semiconductor polarity and surface functionalization: Additive and cooperative effects on PC12 cell behavior. *RSC Advances*, 6(100), 97873–97881.
<https://doi.org/10.1039/C6RA21936E>
- Snyder, P. J., LaJeunesse, D. R., Reddy, P., Kirste, R., Collazo, R., & Ivanisevic, A. (2018a). Bioelectronics communication: Encoding yeast regulatory responses using nanostructured gallium nitride thin films. *Nanoscale*, 10(24), 11506–11516.
<https://doi.org/10.1039/C8NR03684E>
- Snyder, P. J., LaJeunesse, D. R., Reddy, P., Kirste, R., Collazo, R., & Ivanisevic, A. (2018b). Bioelectronics communication: Encoding yeast regulatory responses using nanostructured gallium nitride thin films. *Nanoscale*, 10(24), 11506–11516.
<https://doi.org/10.1039/C8NR03684E>
- Snyder, P. J., Reddy, P., Kirste, R., Collazo, R., & Ivanisevic, A. (2018). Bulk and Surface Electronic Properties of Inorganic Materials: Tools to Guide Cellular Behavior. *Small Methods*, 2(9), 1800016. <https://doi.org/10.1002/smt.201800016>
- Snyder, P. J., Reddy, P., Kirste, R., LaJeunesse, D. R., Collazo, R., & Ivanisevic, A. (2018a). Noninvasive Stimulation of Neurotypic Cells Using Persistent Photoconductivity of Gallium Nitride. *ACS Omega*, 3(1), 615–621. <https://doi.org/10.1021/acsomega.7b01894>

- Snyder, P. J., Reddy, P., Kirste, R., LaJeunesse, D. R., Collazo, R., & Ivanisevic, A. (2018b). Noninvasive Stimulation of Neurotypic Cells Using Persistent Photoconductivity of Gallium Nitride. *ACS Omega*, 3(1), 615–621. <https://doi.org/10.1021/acsomega.7b01894>
- Sohal, I. S., O’Fallon, K. S., Gaines, P., Demokritou, P., & Bello, D. (2018). Ingested engineered nanomaterials: State of science in nanotoxicity testing and future research needs. *Particle and Fibre Toxicology*, 15(1), 29. <https://doi.org/10.1186/s12989-018-0265-1>
- Song, F., E. Brasch, M., Wang, H., H. Henderson, J., Sauer, K., & Ren, D. (2017). How Bacteria Respond to Material Stiffness during Attachment: A Role of Escherichia coli Flagellar Motility. *ACS Applied Materials & Interfaces*, 9(27), 22176–22184. <https://doi.org/10.1021/acscami.7b04757>
- Soppimath, K. S., Aminabhavi, T. M., Kulkarni, A. R., & Rudzinski, W. E. (2001). Biodegradable polymeric nanoparticles as drug delivery devices. *Journal of Controlled Release*, 70(1–2), 1–20. [https://doi.org/10.1016/S0168-3659\(00\)00339-4](https://doi.org/10.1016/S0168-3659(00)00339-4)
- Sun, C., Hu, K., Mu, D., Wang, Z., & Yu, X. (2022). The Widespread Use of Nanomaterials: The Effects on the Function and Diversity of Environmental Microbial Communities. *Microorganisms*, 10(10), 2080. <https://doi.org/10.3390/microorganisms10102080>
- Svenningsen, M. S., Svenningsen, S. L., Sørensen, M. A., & Mitarai, N. (2022). Existence of log-phase *Escherichia coli* persists and lasting memory of a starvation pulse. *Life Science Alliance*, 5(2), e202101076. <https://doi.org/10.26508/lsa.202101076>
- Tasis, D., Tagmatarchis, N., Bianco, A., & Prato, M. (2006). Chemistry of Carbon Nanotubes. *Chemical Reviews*, 106(3), 1105–1136. <https://doi.org/10.1021/cr050569o>

- Timmusk, S., Seisenbaeva, G., & Behers, L. (2018a). Titania (TiO₂) nanoparticles enhance the performance of growth-promoting rhizobacteria. *Scientific Reports*, 8(1), 617.
<https://doi.org/10.1038/s41598-017-18939-x>
- Timmusk, S., Seisenbaeva, G., & Behers, L. (2018b). Titania (TiO₂) nanoparticles enhance the performance of growth-promoting rhizobacteria. *Scientific Reports*, 8(1), 617.
<https://doi.org/10.1038/s41598-017-18939-x>
- Tipler, P. A., & Llewellyn, R. A. (2008). *Modern physics* (5th ed). W.H. Freeman.
- Tiwari, S., Jamal, S. B., Hassan, S. S., Carvalho, P. V. S. D., Almeida, S., Barh, D., Ghosh, P., Silva, A., Castro, T. L. P., & Azevedo, V. (2017). Two-Component Signal Transduction Systems of Pathogenic Bacteria As Targets for Antimicrobial Therapy: An Overview. *Frontiers in Microbiology*, 8, 1878. <https://doi.org/10.3389/fmicb.2017.01878>
- Tripathi, L., Zhang, Y., & Lin, Z. (2014). Bacterial Sigma Factors as Targets for Engineered or Synthetic Transcriptional Control. *Frontiers in Bioengineering and Biotechnology*, 2. <https://doi.org/10.3389/fbioe.2014.00033>
- Tuson, H. H., & Weibel, D. B. (2013). Bacteria–surface interactions. *Soft Matter*, 9(17), 4368. <https://doi.org/10.1039/c3sm27705d>
- Tyagi, N., & Kumar, A. (2020). Understanding effect of interaction of nanoparticles and antibiotics on bacteria survival under aquatic conditions: Knowns and unknowns. *Environmental Research*, 181, 108945. <https://doi.org/10.1016/j.envres.2019.108945>
- Utsumi, R. (2017). Bacterial signal transduction networks via connectors and development of the inhibitors as alternative antibiotics. *Bioscience, Biotechnology, and Biochemistry*, 81(9), 1663–1669. <https://doi.org/10.1080/09168451.2017.1350565>

- Velali, E., Pantazaki, A., Basis, A., Choli-Papadopoulou, T., & Samara, C. (2019). Oxidative stress, DNA damage, and mutagenicity induced by the extractable organic matter of airborne particulates on bacterial models. *Regulatory Toxicology and Pharmacology*, *104*, 59–73. <https://doi.org/10.1016/j.yrtph.2019.03.004>
- Veselovsky, V. A., Dyachkova, M. S., Bespiatykh, D. A., Yunes, R. A., Shitikov, E. A., Polyayeva, P. S., Danilenko, V. N., Olekhnovich, E. I., & Klimina, K. M. (2022). The Gene Expression Profile Differs in Growth Phases of the Bifidobacterium Longum Culture. *Microorganisms*, *10*(8), 1683. <https://doi.org/10.3390/microorganisms10081683>
- Vila, J., Sáez-López, E., Johnson, J. R., Römling, U., Dobrindt, U., Cantón, R., Giske, C. G., Naas, T., Carattoli, A., Martínez-Medina, M., Bosch, J., Retamar, P., Rodríguez-Baño, J., Baquero, F., & Soto, S. M. (2016). *Escherichia coli*: An old friend with new tidings. *FEMS Microbiology Reviews*, *40*(4), 437–463. <https://doi.org/10.1093/femsre/fuw005>
- Vorob'eva, L. I. (2004). Stressors, Stress Reactions, and Survival of Bacteria: A Review. *Applied Biochemistry and Microbiology*, *40*(3), 217–224. <https://doi.org/10.1023/B:ABIM.0000025941.11643.19>
- Wang, G., Jin, W., Qasim, A. M., Gao, A., Peng, X., Li, W., Feng, H., & Chu, P. K. (2017). Antibacterial effects of titanium embedded with silver nanoparticles based on electron-transfer-induced reactive oxygen species. *Biomaterials*, *124*, 25–34. <https://doi.org/10.1016/j.biomaterials.2017.01.028>
- Wang, J., Ma, W., & Wang, X. (2021). Insights into the structure of *Escherichia coli* outer membrane as the target for engineering microbial cell factories. *Microbial Cell Factories*, *20*(1), 73. <https://doi.org/10.1186/s12934-021-01565-8>

- Wang, P., Lombi, E., Zhao, F.-J., & Kopittke, P. M. (2016). Nanotechnology: A New Opportunity in Plant Sciences. *Trends in Plant Science*, 21(8), 699–712.
<https://doi.org/10.1016/j.tplants.2016.04.005>
- Wang, R., Li, H., Sun, J., Zhang, L., Jiao, J., Wang, Q., & Liu, S. (2021). Nanomaterials Facilitating Microbial Extracellular Electron Transfer at Interfaces. *Advanced Materials*, 33(6), 2004051. <https://doi.org/10.1002/adma.202004051>
- Wang, Y., Lee, S. M., & Dykes, G. (2014). The physicochemical process of bacterial attachment to abiotic surfaces: Challenges for mechanistic studies, predictability and the development of control strategies. *Critical Reviews in Microbiology*, 41(4), 452–464.
<https://doi.org/10.3109/1040841X.2013.866072>
- Wilkins, S. J., Greenough, M., Arellano, C., Paskova, T., & Ivanisevic, A. (2014). In Situ Chemical Functionalization of Gallium Nitride with Phosphonic Acid Derivatives during Etching. *Langmuir*, 30(8), 2038–2046. <https://doi.org/10.1021/la404511b>
- Wilkins, S. J., Paskova, T., Reynolds Jr., C. L., & Ivanisevic, A. (2015). Comparison of the Stability of Functionalized GaN and GaP. *ChemPhysChem*, 16(8), 1687–1694.
<https://doi.org/10.1002/cphc.201500105>
- Xie, F., Li, G., Zhang, W., Zhang, Y., Zhou, L., Liu, S., Liu, S., & Wang, C. (2016). Outer membrane lipoprotein VacJ is required for the membrane integrity, serum resistance and biofilm formation of *Actinobacillus pleuropneumoniae*. *Veterinary Microbiology*, 183, 1–8. <https://doi.org/10.1016/j.vetmic.2015.11.021>

- Xu, J., Guo, L., Zhao, N., Meng, X., Zhang, J., Wang, T., Wei, X., & Fan, M. (2022). Response mechanisms to acid stress of acid-resistant bacteria and biotechnological applications in the food industry. *Critical Reviews in Biotechnology*, 1–17.
<https://doi.org/10.1080/07388551.2021.2025335>
- Yang, W., Shen, C., Ji, Q., An, H., Wang, J., Liu, Q., & Zhang, Z. (2009). Food storage material silver nanoparticles interfere with DNA replication fidelity and bind with DNA. *Nanotechnology*, 20(8), 085102. <https://doi.org/10.1088/0957-4484/20/8/085102>
- Yaqoob, A. A., Parveen, T., Umar, K., & Mohamad Ibrahim, M. N. (2020). Role of Nanomaterials in the Treatment of Wastewater: A Review. *Water*, 12(2), 495.
<https://doi.org/10.3390/w12020495>
- Yoon, Y., Truong, P. L., Lee, D., & Ko, S. H. (2022). Metal-Oxide Nanomaterials Synthesis and Applications in Flexible and Wearable Sensors. *ACS Nanoscience Au*, 2(2), 64–92.
<https://doi.org/10.1021/acsnanoscienceau.1c00029>
- Zaslaver, A., Bren, A., Ronen, M., Itzkovitz, S., Kikoin, I., Shavit, S., Liebermeister, W., Surette, M. G., & Alon, U. (2006). A comprehensive library of fluorescent transcriptional reporters for Escherichia coli. *Nature Methods*, 3(8), 623–628.
<https://doi.org/10.1038/nmeth895>
- Zeiner, S. A., Dwyer, B. E., & Clegg, S. (2012). FimA, FimF, and FimH Are Necessary for Assembly of Type 1 Fimbriae on Salmonella enterica Serovar Typhimurium. *Infection and Immunity*, 80(9), 3289–3296. <https://doi.org/10.1128/IAI.00331-12>
- Zhang, J., & Biswas, I. (2009). 3'-Phosphoadenosine-5'-Phosphate Phosphatase Activity Is Required for Superoxide Stress Tolerance in *Streptococcus mutans*. *Journal of Bacteriology*, 191(13), 4330–4340. <https://doi.org/10.1128/JB.00184-09>

- Zhang, P., Qiu, Y., Wang, Y., Xiao, L., Yu, S., Shi, M., Ni, Y., Miron, R. J., Pu, Y., & Zhang, Y. (2022). Nanoparticles Promote Bacterial Antibiotic Tolerance via Inducing Hyperosmotic Stress Response. *Small*, *18*(19), 2105525. <https://doi.org/10.1002/sml.202105525>
- Zhao, L., Gao, X., Liu, C., Lv, X., Jiang, N., & Zheng, S. (2017). Deletion of the *vacJ* gene affects the biology and virulence in *Haemophilus parasuis* serovar 5. *Gene*, *603*, 42–53. <https://doi.org/10.1016/j.gene.2016.12.009>
- Zheng, M., Wang, X., Templeton, L. J., Smulski, D. R., LaRossa, R. A., & Storz, G. (2001). DNA Microarray-Mediated Transcriptional Profiling of the *Escherichia coli* Response to Hydrogen Peroxide. *Journal of Bacteriology*, *183*(15), 4562–4570. <https://doi.org/10.1128/JB.183.15.4562-4570.2001>
- Zhu, X., Su, T., Wang, S., Zhou, H., & Shi, W. (2022). New Advances in Nano-Drug Delivery Systems: *Helicobacter pylori* and Gastric Cancer. *Frontiers in Oncology*, *12*, 834934. <https://doi.org/10.3389/fonc.2022.834934>
- Zielińska, A., Carreiró, F., Oliveira, A. M., Neves, A., Pires, B., Venkatesh, D. N., Durazzo, A., Lucarini, M., Eder, P., Silva, A. M., Santini, A., & Souto, E. B. (2020). Polymeric Nanoparticles: Production, Characterization, Toxicology and Ecotoxicology. *Molecules*, *25*(16), 3731. <https://doi.org/10.3390/molecules25163731>

APPENDIX A: FUNCTIONS OF GENES DIFFERENTIALLY EXPRESSED BY THE
NANOPARTICLES

Silica Nanoparticles Up-regulated genes

Functions	Genes
Cell structure	vacJ, emrA, yhdY, yhhT
DNA replication	glcC, mhpR, rssB, envy, evgA, ylbG
Electron Transport	cbdA, sodC, borD
Metabolism	yrbL, fdhD, cysQ, prpC, allA, fdrA, hscB, lacZ, yniA, yidR
Unknown	yccE, yiaF

Gold nanoparticles Up-regulated genes

Functions	Genes
Cell structure	yhcA, flgH, ycbR
DNA replication	galS, glcC, fear, torT, yjhU, yfjR, yjh, envy, polB, b0582, b0373, yejH
Electron Transport	ydiQ, yhbW, norV, poxB, glpD, cybC, pflA, wrbA, nrfA, yebR, ykgC, guaC, yliI, fold, sodC, yagT
Metabolism	yeaU, yedX, uidA, fucR, ygbJ, aldH, aldA, yjjU, yhfP, galU, yhhY, ackA, fsaA, adhE, cysQ, cfa, deoA, deoD, ygiH, deoC, ycjM, ymdB, dcd, gpp, fkpA
Signal transduction	narQ, zraS, rssB, evgA, borD, ydeI
Transport protein	citT, yjdB, nrfE, yhiP, mdtN, yjdf, yhfK, vacJ, brnQ, yhdY, yhhT, yjiJ

unknown	gatR_1, yjcH, yhfL, yjiT, phnQ, yjdI, yjgR, ydfO, yebF, b1998, yqaC, yjiH, ykgH, yagB, yahC, ygeF, yfbM, yhhZ, b0332
---------	--

Polystyrene nanoparticles Up-regulated genes

Functions	Genes
Cell structure	yhcA, nrfE, flk, eaeH, flgH, vacJ, yiaT, rpmB
DNA replication	crp, leuS, yeaT, pdhR, intA, yhgA, sohA, dhaR, glcC, feaR, b0582, yjhU, ygbI, yjhi, b1331, yiiF, csiE, yfjR, greA, rpmE, ygiU, ligA, gltX, ybaV, yafM, uxuR, yafN, nanR, ydcI, rcsA
Electron Transport	glpD, wrbA, yhbW, norV, nrfA, ydiQ, fdnG, dmsA, cbdA, ndh, narZ, nuoM, hydN, fhuF, yebR
Metabolism	tyrB, glyA, alsI, talA, sdhC, ycbZ, eutB, yeaU, yjdB, yhfP, yhcG, fucR, feaB, galR, bglA, yhhY, yhhN, fsaA, yedX, poxB, fdhD, lacZ, uidA, galU, ssuE, fdhF, nudeE, adhE, serA, chiA, yedQ, pepD, guaB, prlC, cysQ, cfa, pgk, upp, add, amn, cdd, metF, deoA, deoB, deoD, yfbJ, ygiH, guaA, pdxY, yghU, folX, gloA, appA, pldA, fold, yejH, yhbT, yhaM, lpxC, map, cysD, dfp, pyrC, pyrB, panE, eco, yaiE, sodC, ycjG, ymdb, ybiV, yniA, ppiA, yncG, dcd, thiL, nrdB, yjiM, gpp, gmk, ackA, ttdA, aldH, aldA
Methylation	ygjO, smtA, yfiC
Signal transduction	torT, yrfF, narQ, zraS, fh1A, norR, torS, dcuS, torR, rssB, osmC, phoP, rbfA, evgA

Transport protein	setB, yhiP, citT, mdtO, sirA, tolC, sgcC, btuB, yajC, ybaT, emrA, lolA, yhdY, potF, sstT, fepB, ybaE, yhhT, corA, codB, yidK, mdtH, malF, gudP
unknown	renD, pagB, yjcH, mdtN, yjdF, yhfL, yhhZ, yjdI, yjgR, hycB, yhhM, yhiD, yejG, bax, b1998, ydfO, yafS, aspU, yraQ, nohB, ymgC, ybbC, b0501, ykiA, ygeA, yccE, ybjH, ymcC, ydiL, ycgI, ymgE, ygeF, yjiJ, yfbM, yafZ

Silica Nanoparticles Down-regulated genes

Functions	Genes
DNA replication	cspG, pspB, sbcB, yjeI
Electron Transport	ygiD, pdxB, ycaK
Metabolism	yjaB, ansB, ybhJ, yhbU, thiI, rihA, rssA, mpaA, yjdK, yfhM, relA
rRNA methylation	yhiR
Signal transduction	qseB
Stress response	inaA
Transport protein	pqiA, yohM, znuC, yddA, yccM, ytfQ, ygjI
tRNA processing	ykfA, valT, glyU, glnU
unknown	yaeH, ybdN, ybcV, ydfZ, ydfE, b1172, ydcJ, yciW, yfjW, ypfG

APPENDIX B: LIST OF GENES TESTED FROM THE E. COLI PROMOTER LIBRARY

Plate Number	Well	Gene Name	Description
AZ01	A1	rihC	putative purine nucleoside hydrolase
AZ01	A2	yabP	unknown CDS
AZ01	A3	yabI	putative integral membrane protein (1st module)
AZ01	A4	ilvI	acetolactate synthase III, valine sensitive, large subunit FAD and thiamine PPi binding (1st module)
AZ01	A5	secM	secretion monitor that regulates SecA translation
AZ01	A6	yacL	conserved hypothetical protein
AZ01	A7	proB	gamma-glutamate kinase
AZ01	A8	aroL	shikimate kinase II
AZ01	A9	serC	3-phosphoserine aminotransferase / phosphohydroxythreonine transaminase
AZ01	A10	cysB	transcriptional regulator for biosynthesis of L-cysteine (LysR family) (1st module)

AZ01	A11	aroH	3-deoxy-D-arabinoheptulosonate-7-phosphate synthase (DAHP synthetase), tryptophan repressible
AZ01	A12	Empty	Empty well
AZ01	B1	hisL	his operon leader peptide
AZ01	B2	cysK	subunit of cysteine synthase A and O-acetylserine sulfhydrylase A, PLP-dependent enzyme
AZ01	B3	pheL	leader peptide of chorismate mutase-P-prephenate dehydratase
AZ01	B4	dapF	diaminopimelate epimerase
AZ01	B5	tyrB	tyrosine aminotransferase , tyrosine repressible, PLP-dependent
AZ01	B6	cueO	conserved protein, cupredoxin-like
AZ01	B7	argA	N-alpha-acetylglutamate synthase (amino-acid acetyltransferase) (1st module)
AZ01	B8	lysR	transcriptional activator for lysine biosynthesis (LysR family)
AZ01	B9	metC	cystathionine beta-lyase, PLP-dependent (beta-cystathionase)

AZ01	B10	yjgG	putative acetylornithine aminotransferase, PLP-dependent (2nd module)
AZ01	B11	argG	argininosuccinate synthetase
AZ01	B12	asnA	asparagine synthetase A
AZ01	C1	ilvL	ilvGEDA operon leader peptide
AZ01	C2	ilvC	ketol-acid reductoisomerase, NAD(P)-binding
AZ01	C3	serA	D-3-phosphoglycerate dehydrogenase
AZ01	C4	metE	5- methyltetrahydropteroyltriglutamate -homocysteine S-methyltransferase
AZ01	C5	metB	cystathionine gamma-synthase, PLP-dependent
AZ01	C6	argC	N-acetyl-gamma-glutamylphosphate reductase, NAD(P)-binding
AZ01	C7	metA	homoserine transsuccinylase
AZ01	C8	serB	3-phosphoserine phosphatase
AZ01	C9	trpR	transcriptional repressor for tryptophan biosynthesis (TrpR family)
AZ01	C10	U139	promoterless strain

AZ01	C11	pheS	phenylalanine tRNA synthetase, alpha-subunit
AZ01	C12	ybgS	putative homeobox protein
AZ01	D1	amiC	N-acetylmuramoyl-L-alanine amidase (2nd module)
AZ01	D2	lysA	diaminopimelate decarboxylase, PLP-binding (2nd module)
AZ01	D3	b3007	unknown CDS
AZ01	D4	aer	aerotaxis sensor receptor, flavoprotein
AZ01	D5	asnC	transcriptional regulator of asparagine biosynthesis (AsnC family)
AZ01	D6	yifB	putative enzyme (1st module)
AZ01	D7	ilvY	transcriptional activator for isoleucine and valine synthesis (LysR family)
AZ01	D8	metR	transcriptional regulator for methionine biosynthesis (LysR family)
AZ01	D9	metJ	transcriptional repressor for methionine biosynthesis (MetJ family)

AZ01	D10	argE	acetylornithine deacetylase (1st module)
AZ01	D11	yjaB	putative acyltransferase
AZ01	D12	ytjB	membrane protein, transcribed divergently from serB
AZ01	E1	argI	ornithine carbamoyltransferase 1
AZ01	E2	yaaA	putative membrane protein
AZ01	E3	yaaH	putative regulator, integral membrane protein
AZ01	E4	yaaI	unknown CDS
AZ01	E5	yacH	putative membrane protein (3rd module)
AZ01	E6	argF	CP4-6 prophage; ornithine carbamoyltransferase 2, catalytic chain F (1st module)
AZ01	E7	aspC	aspartate aminotransferase, PLP-dependent
AZ01	E8	wrbA	flavodoxin-like protein, trp repressor binding protein
AZ01	E9	prmB	putative methyltransferase (2nd module)
AZ01	E10	cysP	ABC superfamily (peri_bind) thiosulfate transport protein

AZ01	E11	dapA	dihydrodipicolinate synthase
AZ01	E12	glyA	serine hydroxymethyltransferase (2nd module)
AZ01	F1	glnB	regulatory protein (P-II) for nitrogen assimilation by glutamine synthetase (ATase)
AZ01	F2	aroF	3-deoxy-D-arabinoheptulosonate-7- phosphate synthase (DAHP synthetase), tyrosine repressible
AZ01	F3	U66	promoterless strain
AZ01	F4	serA	D-3-phosphoglycerate dehydrogenase (1st module)
AZ01	F5	argD	acetylornithine transaminase (NAcOATase and DapATase), PLP- dependent
AZ01	F6	aroK	shikimate kinase I
AZ01	F7	glnL	sensory kinase (phosphatase) in two-component regulatory system with GlnG (nitrogen regulator II, NRII)
AZ01	F8	fruL	fruR leader peptide
AZ01	F9	lpd	dihydrolipoamide dehydrogenase, FAD/NAD(P)-binding ; component

			of 2-oxodehydrogenase and pyruvate complexes; L protein of glycine cleavage complex second part (2nd module)
AZ01	F10	wrbA	flavodoxin-like protein, trp repressor binding protein
AZ01	F11	ptsG	multimodular PtsG: PTS family enzyme IIC, glucose-specific (1st module)
AZ01	F12	malE	ABC superfamily (peri_bind) maltose transport protein, substrate recognition for transport and chemotaxis (2nd module)
AZ01	G1	tktB	transketolase 2, thiamin-binding, isozyme
AZ01	G2	pfkA	6-phosphofructokinase I
AZ01	G3	edd	6-phosphogluconate dehydratase
AZ01	G4	ylbE	conserved protein
AZ01	G5	ylbF	unknown CDS
AZ01	G6	renD	DLP12 prophage;
AZ01	G7	ybcK	DLP12 prophage; putative recombinase

AZ01	G8	ybcL	DLP12 prophage; protein with phosphatidylethanolamine binding domain
AZ01	G9	glxK	glycerate kinase II
AZ01	G10	flgA	flagellar biosynthesis; assembly of basal-body periplasmic P ring
AZ01	G11	gnd	gluconate-6-phosphate dehydrogenase, decarboxylating (1st module)
AZ01	G12	mgo	malate dehydrogenase
AZ01	H1	lacZ	beta-galactosidase, lac operon
AZ01	H2	eno	enolase
AZ01	H3	rpiA	ribosephosphate isomerase, constitutive
AZ01	H4	glcB	malate synthase G
AZ01	H5	rpe	D-ribulose-5-phosphate 3-epimerase
AZ01	H6	gntR	transcriptional repressor for gluconate utilization (GalR/LacI family)
AZ01	H7	tpiA	triosephosphate isomerase
AZ01	H8	ykfI	CP4-6 prophage;
AZ01	H9	yggG	conserved protein (2nd module)

AZ01	H10	fliC	flagellar biosynthesis; flagellin, filament structural protein (1st module)
AZ01	H11	icd	isocitrate dehydrogenase in e14 prophage, specific for NADP+ (2nd module)
AZ01	H12	yegT	putative MFS family transport protein (2nd module)
AZ02	A1	alsI	ribose 5-phosphate isomerase B, also acts on allose (allose 6-phosphate isomerase)
AZ02	A2	talB	transaldolase B (2nd module)
AZ02	A3	talA	transaldolase A (2nd module)
AZ02	A4	pfkB	6-phosphofructokinase II
AZ02	A5	setB	MFS transporter
AZ02	A6	crp	transcriptional regulator, catabolite activator protein (CAP), cyclic AMP receptor protein (CAMP-binding family), interacts with RNAP
AZ02	A7	pdhR	transcriptional repressor for pyruvate dehydrogenase complex (GntR family) (1st module)

AZ02	A8	pykF	pyruvate kinase I (formerly F), fructose stimulated (2nd module)
AZ02	A9	sdhC	succinate dehydrogenase , cytochrome b556
AZ02	A10	mngR	transcriptional repressor for TCA cycle, fatty acyl responsive transcriptional regulator (GntR family)
AZ02	A11	tktA	transketolase 1 thiamin-binding, isozyme
AZ02	A12	Empty	Empty well
AZ02	B1	leuS	leucine tRNA synthetase (1st module)
AZ02	B2	rluE	putative ribosomal large subunit pseudouridine synthase
AZ02	B3	alsR	transcriptional repressor of ribose catabolism (RpiR/YebK family)
AZ02	B4	maeB	multimodular MaeB: putative malic oxidoreductase (1st module)
AZ02	B5	frdA	fumarate reductase, anaerobic, catalytic and NAD/flavoprotein subunit
AZ02	B6	ydiY	conserved hypothetical protein

AZ02	B7	uvrA	UvrA with UvrBC is a DNA excision repair enzyme (2nd module)
AZ02	B8	fruB	Sugar Specific PTS family, fructose-specific enzyme IIA/FPr component (1st module)
AZ02	B9	yhfA	conserved hypothetical protein
AZ02	B10	msrB	putative methionine sulfoxide reductase/regulator
AZ02	B11	yacH	putative membrane protein (3rd module)
AZ02	B12	dps	stress response DNA-binding protein; starvation induced resistance to H ₂ O ₂ , ferritin-like
AZ02	C1	aroP	APC family, aromatic amino acid transporter (2nd module)
AZ02	C2	ydhZ	conserved hypothetical protein
AZ02	C3	serA	D-3-phosphoglycerate dehydrogenase
AZ02	C4	b0360	IS21 protein 1
AZ02	C5	gltA	citrate synthase
AZ02	C6	pgi	Phospho glucose isomerase
AZ02	C7	caiC	crotonobetaine/carnitine-CoA ligase

AZ02	C8	lacZ	beta-D-galactosidase (1st module)
AZ02	C9	cyoA	cytochrome o ubiquinol oxidase subunit II
AZ02	C10	U139	promoterless strain
AZ02	C11	tdcG_2	L-serine deaminase 3
AZ02	C12	cysH	3'-phosphoadenosine 5'-phosphosulfate (PAPS) reductase
AZ02	D1	ansB	periplasmic L-asparaginase II
AZ02	D2	tdcG_2	L-serine deaminase 3
AZ02	D3	intA	CP4-57 prophage; integrase
AZ02	D4	tdcB	threonine dehydratase, catabolic, PLP-dependent enzyme (1st module)
AZ02	D5	atpI	membrane-bound ATP synthase subunit, F1-F0-type proton-ATPase
AZ02	D6	adiA	arginine decarboxylase
AZ02	D7	cadA	lysine decarboxylase 1
AZ02	D8	emrR	transcriptional repressor of for multidrug resistance pump (MarR family)
AZ02	D9	idnR	IdnR transcriptional regulator
AZ02	D10	hdeB	unknown CDS

AZ02	D11	gadW	putative transcriptional regulator (AraC/XylS family) (2nd module)
AZ02	D12	yhjG	conserved protein
AZ02	E1	yhjJ	putative peptidase
AZ02	E2	yhjK	conserved protein (2nd module)
AZ02	E3	b3044	IS2 protein
AZ02	E4	rhsB	RhsB protein in RhsB element (4th module)
AZ02	E5	yiaW	unknown CDS
AZ02	E6	yidE	putative transport protein (1st module)
AZ02	E7	yihR	putative aldose-1-epimerase
AZ02	E8	glpX	putative enzyme in glycerol metabolism
AZ02	E9	yijF	unknown CDS
AZ02	E10	yijO	putative transcriptional regulator (AraC/XylS family) (2nd module)
AZ02	E11	pagB	unknown CDS
AZ02	E12	hfq	host factor I for bacteriophage Q beta replication, a growth-related protein
AZ02	F1	ansA	cytoplasmic L-asparaginase I
AZ02	F2	yqjF	putative membrane protein

AZ02	F3	U66	promoterless strain
AZ02	F4	yqjG	putative enzyme with S-transferase domain
AZ02	F5	yhaH	putative membrane protein
AZ02	F6	fixC	related to carnitine metabolism (1st module)
AZ02	F7	sdaA	multimodular SdaA: L-serine dehydratase I I (1st module)
AZ02	F8	exuR	transcriptional repressor for carbon degradation (GntR family)
AZ02	F9	tnaC	tryptophanase leader peptide
AZ02	F10	wrbA	flavodoxin-like protein, trp repressor binding protein
AZ02	F11	intB	prophage P4 integrase (1st module)
AZ02	F12	macA	putative membrane protein
AZ02	G1	cspG	low-temperature-responsive gene, nucleic acid-binding domain
AZ02	G2	intZ	CPZ-55 prophage; putative integrase
AZ02	G3	sscR	putative synthase
AZ02	G4	idnK	gluconokinase II
AZ02	G5	somA	conserved hypothetical protein
AZ02	G6	ycbZ	putative ATP-dependent protease

AZ02	G7	eutB	ethanolamine ammonia-lyase, heavy chain (2nd module)
AZ02	G8	cysJ	sulfite reductase, beta (flavoprotein) subunit (1st module)
AZ02	G9	ygjH	putative tRNA synthetase
AZ02	G10	b4283	IS911 protein
AZ02	G11	yqjC	conserved protein
AZ02	G12	ycjK	putative glutamine synthetase (2nd module)
AZ02	H1	lacZ	beta-galactosidase, lac operon
AZ02	H2	ycjW	putative transcriptional repressor (GalR/LacI family) (2nd module)
AZ02	H3	yncD	putative outer membrane porin/receptor (1st module)
AZ02	H4	yneI	putative aldehyde dehydrogenase (2nd module)
AZ02	H5	ydiP	putative transcriptional regulator (AraC/XylS family) (2nd module)
AZ02	H6	yeaM	putative transcriptional regulator (AraC/XylS family) (2nd module)
AZ02	H7	yeaT	putative transcriptional regulator (LysR family) (1st module)

AZ02	H8	yedW	putative transcriptional regulator (OmpR family)
AZ02	H9	yaaJ	putative AGCS family, alanine/glycine transport protein (2nd module)
AZ02	H10	acnB	aconitate hydratase 2 (2nd module)
AZ02	H11	fumB	fumarase B (fumarate hydratase class I), anaerobic isozyme (1st module)
AZ02	H12	ykfG	CP4-6 prophage; putative DNA repair protein
AZ03	A1	ycjL	putative glutamine amidotransferase (1st module)
AZ03	A2	ycjX	conserved hypothetical protein
AZ03	A3	yncE	conserved hypothetical protein
AZ03	A4	yneJ	putative transcriptional regulator (LysR family) (1st module)
AZ03	A5	ydiQ	putative electron transfer flavoprotein
AZ03	A6	yeaU	putative tartrate dehydrogenase
AZ03	A7	yedX	transthyretin-like protein
AZ03	A8	ypdA	putative sensor protein (1st module)
AZ03	A9	yjiT	conserved protein (1st module)

AZ03	A10	citT	DASS family, citrate:succinate transport (antiport) protein (2nd module)
AZ03	A11	galE	UDP-galactose 4-epimerase (1st module)
AZ03	A12	Empty	Empty well
AZ03	B1	poxB	pyruvate dehydrogenase/oxidase FAD and thiamine P _i binding, cytoplasmic in absence of cofactors (1st module)
AZ03	B2	uidA	beta-D-glucuronidase
AZ03	B3	gatY	tagatose 6-phosphate aldolase 2, subunit with GatZ
AZ03	B4	galS	transcriptional repressor for galactose utilization (GalR/LacI family)
AZ03	B5	yjcH	conserved hypothetical protein
AZ03	B6	yjcO	conserved hypothetical protein
AZ03	B7	mdtO	putative transporter (Pit family) (2nd module)
AZ03	B8	mdtN	putative multidrug resistance efflux pump protein, membrane protein
AZ03	B9	phnQ	conserved hypothetical protein

AZ03	B10	yjdB	putative transmembrane protein (1st module)
AZ03	B11	aniC	putative APC family, putrescine/ornithine transport protein, cryptic
AZ03	B12	yjdF	unknown CDS
AZ03	C1	yhbW	putative monooxygenase
AZ03	C2	yjjU	putative transcriptional regulator (2nd module)
AZ03	C3	serA	D-3-phosphoglycerate dehydrogenase
AZ03	C4	yhfK	hypothetical protein
AZ03	C5	yhfL	unknown CDS
AZ03	C6	yhfP	conserved protein
AZ03	C7	yhgA	putative transposase (1st module)
AZ03	C8	yrbL	unknown CDS
AZ03	C9	yhcA	putative periplasmic chaperone protein
AZ03	C10	U139	promoterless strain
AZ03	C11	yhcG	unknown CDS
AZ03	C12	sohA	putative protease; htrA suppressor protein
AZ03	D1	ybcW	DLP12 prophage

AZ03	D2	galU	glucose-1-phosphate uridylyltransferase
AZ03	D3	gutM	transcriptional activator for glucitol utilization
AZ03	D4	srlR	transcriptional repressor for glucitol utilization (DeoR family) (2nd module)
AZ03	D5	fucR	transcriptional activator for L- fucose utilization (DeoR family) (2nd module)
AZ03	D6	dhaR	putative regulator in two-component regulatory system (EBP family), FIS-like domain (1st module)
AZ03	D7	feaB	phenylacetaldehyde dehydrogenase (2nd module)
AZ03	D8	galR	transcriptional repressor for galactose utilization (GalR/LacI family)
AZ03	D9	bglA	6-phospho-beta-glucosidase A
AZ03	D10	glcC	transcriptional activator for glycolate utilization (GntR family)

AZ03	D11	mhpR	transcriptional activator for 3-hydroxyphenylpropionate degradation (IclR family)
AZ03	D12	feaR	transcriptional activator of 2-phenylethylamine catabolism (AraC/XylS family) (2nd module)
AZ03	E1	gatR_1	split transcriptional repressor for galactitol utilization, fragment 1
AZ03	E2	hcaR	multimodular HcaR: transcriptional activator of hca cluster (LysR family) (1st module)
AZ03	E3	yciK	putative oxoacyl-(acyl carrier protein) reductase
AZ03	E4	yfdZ	putative PLP-dependent aminotransferase
AZ03	E5	sohB	putative peptidase (2nd module)
AZ03	E6	yrfF	conserved hypothetical protein
AZ03	E7	yhhY	putative acyltransferase
AZ03	E8	yhhN	unknown CDS
AZ03	E9	yhhQ	putative integral membrane protein (1st module)
AZ03	E10	norV	putative flavodoxin

AZ03	E11	ygbJ	putative dehydrogenase, NAD(P)-binding
AZ03	E12	fsaA	putative transaldolase
AZ03	F1	torT	periplasmic sensor in multi-component regulatory system with TorS (sensory kinase) and TorR (regulator), regulates trimethylamine n-oxide reductase respiratory system
AZ03	F2	fdnG	formate dehydrogenase-N, alpha subunit, nitrate inducible (1st module)
AZ03	F3	U66	promoterless strain
AZ03	F4	ylcE	DLP12 prophage
AZ03	F5	ackA	acetate kinase A (propionate kinase 2)
AZ03	F6	narQ	sensory histidine kinase in two-component regulatory system with NarP (NarL) (2nd module)
AZ03	F7	ttdA	L-tartrate dehydratase
AZ03	F8	glpD	sn-glycerol-3-phosphate dehydrogenase FAD/NAD(P)-binding (aerobic)

AZ03	F9	fdhD	formate dehydrogenase formation protein
AZ03	F10	wrbA	flavodoxin-like protein, trp repressor binding protein
AZ03	F11	zraS	ZraSR Two-Component Signal Transduction System
AZ03	F12	nrfA	nitrite reductase periplasmic cytochrome c(552):
AZ03	G1	yjdl	conserved hypothetical protein
AZ03	G2	dmsA	anaerobic dimethyl sulfoxide reductase, subunit A (1st module)
AZ03	G3	cbdA	putative third cytochrome oxidase, subunit I
AZ03	G4	ndh	respiratory NADH dehydrogenase 2; cupric reductase (2nd module)
AZ03	G5	aldH	aldehyde dehydrogenase, prefers NADP over NAD
AZ03	G6	aldA	aldehyde dehydrogenase A, NAD-linked
AZ03	G7	fhlA	transcriptional activator for induction of formate hydrogen-lyase (EBP family) (2nd module)

AZ03	G8	nrfE	formate-dependent nitrite reductase; involved in attachment of haem c to cytochrome c552
AZ03	G9	cybC	cytochrome b(562)
AZ03	G10	yhhZ	conserved protein
AZ03	G11	yhiP	putative POT family, peptide transport protein
AZ03	G12	b0582	IS186 protein
AZ03	H1	lacZ	beta-galactosidase, lac operon
AZ03	H2	yjfQ	putative transcriptional repressor (DeoR family) (2nd module)
AZ03	H3	ytfE	conserved hypothetical protein
AZ03	H4	ytfF	putative cationic amino acid transporter (1st module)
AZ03	H5	ytfL	putative hemolysin-related protein (1st module)
AZ03	H6	yjgH	putative translation factor
AZ03	H7	yjgR	putative enzyme contains P-loop containing nucleotide triphosphate hydrolase domain
AZ03	H8	yjhU	putative transcriptional regulator
AZ03	H9	mltD	membrane-bound lytic murein transglycosylase D

AZ03	H10	fldA	flavodoxin 1
AZ03	H11	pflA	pyruvate formate lyase activating enzyme 1
AZ03	H12	narZ	nitrate reductase 2, alpha subunit (1st module)
AZ04	A1	nuoM	NADH dehydrogenase I chain M, membrane subunit (2nd module)
AZ04	A2	insB_4	IS1 protein InsB
AZ04	A3	hydN	electron transport protein (FeS center) from formate to hydrogen
AZ04	A4	hycB	hydrogenase-3, iron-sulfur subunit (part of FHL complex)
AZ04	A5	fdhF	formate dehydrogenase H, selenopolypeptide subunit
AZ04	A6	nudE	conserved protein, MutT-like
AZ04	A7	yhhM	unknown CDS
AZ04	A8	sirA	small ubiquitous protein required for normal growth
AZ04	A9	norR	putative transcriptional regulator (EBP family) (2nd module)
AZ04	A10	ygbI	putative transcriptional repressor (DeoR family) (1st module)

AZ04	A11	ssuE	NAD(P)H dependent FMN reductase, sulfate starvation-induced protein
AZ04	A12	Empty	Empty well
AZ04	B1	torS	sensory kinase in multi-component regulatory system with TorR (regulator) and TorT (periplasmic sensor), regulates trimethylamine n-oxide reductase respiratory system (2nd module)
AZ04	B2	torR	response regulator in multi-component regulatory system with TorS (sensory kinase) and TorT (periplasmic sensor), regulates trimethylamine n-oxide reductase respiratory system (TorR family)
AZ04	B3	adhE	multifunctional multimodular AdhE: acetaldehyde-CoA dehydrogenase (1st module)
AZ04	B4	b2192	IS5 protein
AZ04	B5	yfbV	conserved hypothetical protein
AZ04	B6	aegA	putative oxidoreductase, Fe-S subunit

AZ04	B7	ygiP	putative transcriptional regulator (LysR family)
AZ04	B8	glpE	thiosulfate/cyanide sulfurtransferase (rhodanese)
AZ04	B9	fdoG	formate dehydrogenase-O, major subunit (1st module)
AZ04	B10	zraP	zinc homeostasis protein
AZ04	B11	dcuS	sensory histidine kinase in two- component regulatory system with DcuR, regulator of anaerobic fumarate respiration
AZ04	B12	deoR	transcriptional repressor for nucleotide catabolism (DeoR family) (2nd module)
AZ04	C1	ugd	UDP-glucose 6-dehydrogenase (1st module)
AZ04	C2	rfbA	dTDP-glucose pyrophosphorylase (1st module)
AZ04	C3	serA	D-3-phosphoglycerate dehydrogenase
AZ04	C4	rfbB	dTDP-glucose 4,6 dehydratase, NAD(P)-binding

AZ04	C5	gcvT	glycine cleavage complex protein T, aminomethyltransferase, tetrahydrofolate-dependent
AZ04	C6	kbl	2-amino-3-ketobutyrate CoA ligase (glycine acetyltransferase)
AZ04	C7	glmU	bifunctional multimodular GlmU: N-acetyl glucosamine-1-phosphate uridyltransferase (1st module)
AZ04	C8	fpr	ferredoxin-NADP reductase, N-term FAD, C-term NAD sites
AZ04	C9	yhiD	putative Mg(2+) transport ATPase
AZ04	C10	U139	promoterless strain
AZ04	C11	fhuF	acts in reduction of ferrioxamine B iron
AZ04	C12	pppA	bifunctional prepilin peptidase, cleaves N-terminal peptide off and methylates new N-terminal amino acid (2nd module)
AZ04	D1	b2974	conserved hypothetical protein
AZ04	D2	hybO	hydrogenase-2, small chain, required for membrane targeting and nickel acquisition by of HybC
AZ04	D3	chiA	endochitinase

AZ04	D4	yhfX	conserved protein (1st module)
AZ04	D5	yhfZ	unknown CDS
AZ04	D6	yzgL	conserved protein
AZ04	D7	yhhW	conserved hypothetical protein
AZ04	D8	rna	RNase I, cleaves phosphodiester bond between any two nucleotides
AZ04	D9	recE	Rac prophage; exonuclease VIII, ds DNA exonuclease, 5' --> 3' specific (2nd module)
AZ04	D10	rnd	RNase D, processes tRNA precursor
AZ04	D11	ptrB	protease II
AZ04	D12	clpB	ATP-dependent protease, Hsp 100, part of novel multi-chaperone system with DnaK, DnaJ, and GrpE (2nd module)
AZ04	E1	ftsH	ATP-dependent zinc-metallo protease (2nd module)
AZ04	E2	hslV	peptidase component of the HslUV protease
AZ04	E3	mcrB	component of 5-methylcytosine-specific restriction enzyme McrBC
AZ04	E4	yhgF	conserved protein (3rd module)

AZ04	E5	rssB	response regulator involved in protein turnover, controls stability of RpoS (1st module)
AZ04	E6	rnt	RNase T, degrades tRNA , has exonuclease and ssDNAse activity
AZ04	E7	amyA	cytoplasmic alpha-amylase
AZ04	E8	degQ	serine endoprotease
AZ04	E9	pinE	e14 prophage; inversion of adjacent DNA
AZ04	E10	htrA	periplasmic serine protease Do, heat shock protein (2nd module)
AZ04	E11	yedQ	conserved protein (2nd module)
AZ04	E12	erfK	conserved hypothetical protein
AZ04	F1	yeeA	putative membrane protein, transport (1st module)
AZ04	F2	yejG	conserved hypothetical protein
AZ04	F3	U66	promoterless strain
AZ04	F4	apbE	hypothetical protein with similarity to Salmonella typhimurium thiamine biosynthesis/iron-sulfur cluster metabolism protein
AZ04	F5	ygiR	conserved protein
AZ04	F6	ynjF	putative transferase

AZ04	F7	b1788	unknown CDS
AZ04	F8	yoaF	conserved hypothetical protein
AZ04	F9	yoaA	putative ATP-dependent helicase, SOS repair
AZ04	F10	wrbA	flavodoxin-like protein, trp repressor binding protein
AZ04	F11	yebR	conserved hypothetical protein
AZ04	F12	yohL	conserved hypothetical protein
AZ04	G1	pncB	nicotinate phosphoribosyltransferase
AZ04	G2	pepD	aminoacyl-histidine dipeptidase (peptidase D)
AZ04	G3	xseB	exonuclease VII, small subunit
AZ04	G4	rne	RNase E (1st module)
AZ04	G5	dcp	dipeptidyl carboxypeptidase II
AZ04	G6	guaB	multimodular GuaB: putative membrane protein (2nd module)
AZ04	G7	prlC	oligopeptidase A, (1st module)
AZ04	G8	bax	conserved hypothetical protein
AZ04	G9	rph	RNase PH
AZ04	G10	fadB	multifunctional multimodular FadB: 3-hydroxybutyryl-coa epimerase (EC 5.1.2.3); delta(3)-cis-delta(2)- trans-enoyl-coa-isomerase (EC

			5.3.3.8); enoyl-coa-hydratase (4.2.1.17) (1st module)
AZ04	G11	pepE	(alpha)-aspartyl dipeptidase
AZ04	G12	hsdR	endonuclease R, host restriction (1st module)
AZ04	H1	lacZ	beta-galactosidase, lac operon
AZ04	H2	ybhD	putative transcriptional regulator (LysR family) (1st module)
AZ04	H3	ynfB	unknown CDS
AZ04	H4	rstA	response regulator (activator) in two-component regulatory system with RstB (OmpR family)
AZ04	H5	slyB	putative outer membrane lipoprotein
AZ04	H6	ydhO	putative lipoprotein (1st module)
AZ04	H7	osmC	resistance protein, osmotically inducible
AZ04	H8	flk	cell division protein
AZ04	H9	tolC	outer membrane channel; specific tolerance to colicin E1; segregation of daughter chromosomes, role in organic solvent tolerance
AZ04	H10	yhhF	putative methyltransferase
AZ04	H11	uspA	universal stress protein A

AZ04	H12	ecfI	NA
AZ05	A1	yhiI	putative membrane protein
AZ05	A2	yhiJ	conserved hypothetical protein (2nd module)
AZ05	A3	yeaX	putative oxidoreductase
AZ05	A4	yebU	putative methyltransferase (2nd module)
AZ05	A5	b1966	putative outer membrane porin protein
AZ05	A6	yedY	putative reductase
AZ05	A7	apt	adenine phosphoribosyltransferase
AZ05	A8	add	adenosine deaminase
AZ05	A9	amn	AMP nucleosidase
AZ05	A10	cdd	cytidine/deoxycytidine deaminase
AZ05	A11	rfe	undecaprenyl-phosphate γ -N-acetylglucosaminyl transferase
AZ05	A12	Empty	Empty well
AZ05	B1	yifM_2	4-acetamido-4,6-dideoxy-D-galactose transferase
AZ05	B2	metF	5,10-methylenetetrahydrofolate reductase
AZ05	B3	deoA	thymidine phosphorylase
AZ05	B4	deoB	phosphopentomutase

AZ05	B5	deoD	purine-nucleoside phosphorylase
AZ05	B6	yodB	putative cytochrome
AZ05	B7	yeeJ	putative transcriptional regulator (1st module)
AZ05	B8	yeeU	CP4-44 prophage; putative structural protein
AZ05	B9	yeiT	putative glutamate synthase (1st module)
AZ05	B10	yeiP	putative elongation factor
AZ05	B11	b1331	IS5 protein
AZ05	B12	sieB	Rac prophage; phage superinfection exclusion protein
AZ05	C1	spr	suppresses thermosensitivity of pre mutants at low osmolality (lipoprotein)
AZ05	C2	yfbJ	unknown CDS
AZ05	C3	serA	D-3-phosphoglycerate dehydrogenase
AZ05	C4	elaD	conserved hypothetical protein
AZ05	C5	yfbR	conserved protein
AZ05	C6	yfcC	putative integral membrane protein
AZ05	C7	intS	putative prophage Sf6-like integrase
AZ05	C8	b2394	putative transposase

AZ05	C9	hyfR	transcriptional activator for expression of hydrogenase 4 genes, interacts with sigma 54 (EBP family) (2nd module)
AZ05	C10	U139	promoterless strain
AZ05	C11	yiiF	unknown CDS
AZ05	C12	csiE	stationary phase inducible protein
AZ05	D1	yfjP	CP4-57 prophage; putative GTP-binding factor
AZ05	D2	yfjR	CP4-57 prophage; putative transcriptional repressor (DeoR family)
AZ05	D3	yqaC	putative glycosyltransferase
AZ05	D4	ygdQ	putative transmembrane protein, transport
AZ05	D5	yqeI	conserved protein
AZ05	D6	ygeH	putative invasion (regulator) protein
AZ05	D7	ygeY	putative deacetylase (1st module)
AZ05	D8	ygiL	putative fimbrial-like protein (1st module)
AZ05	D9	eaeH	outer membrane protein important for attachment, pathogenesis factor

AZ05	D10	ykgD	putative transcriptional regulator (AraC/XylS family) (2nd module)
AZ05	D11	gsk	inosine-guanosine kinase
AZ05	D12	smtA	S-adenosylmethionine-dependent methyltransferase (1st module)
AZ05	E1	purM	phosphoribosylaminoimidazole synthetase (AIR synthetase)
AZ05	E2	ygiH	conserved hypothetical protein
AZ05	E3	udp	uridine phosphorylase
AZ05	E4	fxsA	suppress F exclusion of bacteriophage T7
AZ05	E5	cysQ	gene product acts on 3'- phosphoadenosine-5'- phosphosulfate
AZ05	E6	deoC	2-deoxyribose-5-phosphate aldolase, NAD(P)-linked
AZ05	E7	metK	methionine adenosyltransferase 1 (AdoMet synthetase) (2nd module)
AZ05	E8	ykgM	putative ribosomal protein
AZ05	E9	ykgC	putative oxidoreductase, FAD/NAD(P)-binding (2nd module)
AZ05	E10	aes	acetyl-esterase
AZ05	E11	ycbC	putative enzyme

AZ05	E12	upp	uracil phosphoribosyltransferase
AZ05	F1	folB	dihydroneopterin aldolase
AZ05	F2	ysgA	putative diene lactone hydrolase
AZ05	F3	U66	promoterless strain
AZ05	F4	aspA	aspartate ammonia-lyase (aspartase)
AZ05	F5	cpdB	2':3'-cyclic-nucleotide 2'-phosphodiesterase
AZ05	F6	yjiH	conserved protein
AZ05	F7	yjiI	conserved hypothetical protein
AZ05	F8	yqgD	unknown CDS
AZ05	F9	phoP	response regulator in two-component regulatory system with PhoQ, transcribes genes expressed under low Mg ⁺ concentration (OmpR family)
AZ05	F10	wrbA	flavodoxin-like protein, trp repressor binding protein
AZ05	F11	guaA	multimodular GuaA: glutamine aminotransferase of GMP synthetase (1st module)
AZ05	F12	pgk	phosphoglycerate kinase
AZ05	G1	sspA	stringent starvation protein A, regulator of transcription

AZ05	G2	arpA	regulator of acetyl CoA synthetase
AZ05	G3	yjhl	putative transcriptional repressor (IclR family)
AZ05	G4	sgcC	NA
AZ05	G5	yjhS	conserved protein
AZ05	G6	adk	adenylate kinase
AZ05	G7	flgH	flagellar biosynthesis, basal-body outer-membrane L (lipopolysaccharide layer) ring protein
AZ05	G8	fabF	3-oxoacyl-[acyl-carrier-protein] synthase II
AZ05	G9	cfa	cyclopropane fatty acyl phospholipid synthase (unsaturated- phospholipid methyltransferase) (2nd module)
AZ05	G10	ydfO	Qin prophage;
AZ05	G11	yebF	conserved hypothetical protein
AZ05	G12	b1998	CP4-44 prophage; putative outer membrane protein
AZ05	H1	lacZ	beta-galactosidase, lac operon
AZ05	H2	fabZ	(3R)-hydroxymyristol acyl carrier protein dehydratase

AZ05	H3	curl	transcriptional regulator of cryptic genes for curli formation and fibronectin binding
AZ05	H4	yibL	conserved protein
AZ05	H5	yicH	conserved protein
AZ05	H6	yieE	unknown CDS
AZ05	H7	yihL	putative transcriptional repressor (GntR family)
AZ05	H8	yihX	putative dehydratase or phosphatase
AZ05	H9	nadK	conserved protein
AZ05	H10	guaC	GMP reductase (2nd module)
AZ05	H11	barA	bifunctional multimodular BarA: sensory histidine kinase in two component regulatory system, activates OmpR (1st module)
AZ05	H12	ygjO	putative ribosomal RNA small subunit methyltransferase (2nd module)
AZ06	A1	coaE	dephospho-CoA kinase
AZ06	A2	rumA	putative RNA methyltransferase (2nd module)

AZ06	A3	soxS	transcriptional activator of superoxide response regulon (AraC/XylS family)
AZ06	A4	yhcF	putative transcriptional regulator
AZ06	A5	speE	spermidine synthase (putrescine aminopropyltransferase)
AZ06	A6	ykgJ	putative ferredoxin
AZ06	A7	rnk	regulator of nucleoside diphosphate kinase
AZ06	A8	mgsA	methylglyoxal synthase
AZ06	A9	gadB	glutamate decarboxylase, PLP-dependent, isozyme beta
AZ06	A10	hdhA	7alpha-hydroxysteroid dehydrogenase, NAD-dependent
AZ06	A11	pdxY	pyridoxal kinase 2/pyridoxine kinase (2nd module)
AZ06	A12	Empty	Empty well
AZ06	B1	nudB	dATP pyrophosphohydrolase, MutT-like
AZ06	B2	cpsG	phosphomannomutase in colanic acid gene cluster
AZ06	B3	pyrG	CTP synthetase

AZ06	B4	gcvA	transcriptional regulator for cleavage of glycine (LysR family)
AZ06	B5	gcvP	glycine cleavage complex protein P, glycine decarboxylase, PLP-dependent
AZ06	B6	speB	agmatinase
AZ06	B7	phnL	putative ABC superfamily (atp_bind), phosphonate transport protein also putative C-P lyase component
AZ06	B8	nrdG	anaerobic ribonucleotide reductase activating protein
AZ06	B9	yfbS	putative response regulator (1st module)
AZ06	B10	ubiX	3-octaprenyl-4-hydroxybenzoate carboxy-lyase
AZ06	B11	usg	putative aspartate-semialdehyde dehydrogenase, NAD(P)-binding (2nd module)
AZ06	B12	yfcU	putative outer membrane protein
AZ06	C1	yfcV	putative fimbrial-like protein

AZ06	C2	fadI	putative acetyl-CoA acetyltransferase with thiolase domain
AZ06	C3	serA	D-3-phosphoglycerate dehydrogenase
AZ06	C4	yfdL	CPS-53 prophage;
AZ06	C5	yfdV	putative AEC family transporter (2nd module)
AZ06	C6	yfdU	putative oxalyl-CoA decarboxylase, FAD and thiamine PPi binding (1st module)
AZ06	C7	fryB	putative PTS system enzyme IIB component
AZ06	C8	ucpA	putative acetoin dehydrogenase
AZ06	C9	eutN	putative detox protein, ethanolamine utilization
AZ06	C10	U139	promoterless strain
AZ06	C11	der	putative GTP-binding factor (1st module)
AZ06	C12	yfgA	conserved protein (2nd module)
AZ06	D1	sseB	enhances serine sensitivity
AZ06	D2	pepB	aminopeptidase (AP)
AZ06	D3	yfhG	conserved protein

AZ06	D4	yfhK	putative sensory kinase in regulatory system (2nd module)
AZ06	D5	b2639	CP4-57 prophage; putative arsenical pump protein
AZ06	D6	luxS	autoinducer 2 (AI-2) synthase; acts in quorum sensing
AZ06	D7	recX	regulator
AZ06	D8	rhsA	RhsA protein in RhsA element (2nd module)
AZ06	D9	ygcU	putative oxidase, FAD-binding subunit
AZ06	D10	ygdL	putative enzyme, NAD(P)-binding (1st module)
AZ06	D11	yqfA	putative transmembrane protein
AZ06	D12	ygfF	putative oxidoreductase, NAD(P)-binding
AZ06	E1	ygfI	putative transcriptional regulator (LysR family)
AZ06	E2	yggE	conserved protein
AZ06	E3	mscS	putative membrane protein, involved in stability of MscS mechanosensitive channel, (1st module)

AZ06	E4	yggM	conserved protein
AZ06	E5	ydjN	putative transport protein (1st module)
AZ06	E6	asr	acid shock protein
AZ06	E7	ydgI	putative APC family, arginine/ornithine antiporter
AZ06	E8	ydiM	putative MFS family transport protein (1st module)
AZ06	E9	ydiF	putative acetyl-CoA:acetoacetyl-CoA transferase alpha subunit (1st module)
AZ06	E10	ydiS	putative electron transfer flavoprotein, NAD/FAD-binding domain
AZ06	E11	yncC	putative transcriptional regulator (GntR family)
AZ06	E12	tam	trans-aconitate methyltransferase (1st module)
AZ06	F1	folX	D-erythro-7,8-dihydroneopterin triphosphate 2'-epimerase (also has dihydroneopterin aldolase activity)
AZ06	F2	ydfH	putative transcriptional repressor (GntR family)

AZ06	F3	U66	promoterless strain
AZ06	F4	ynfE	putative reductase (1st module)
AZ06	F5	pyrH	uridylate kinase (2nd module)
AZ06	F6	psiF	induced by phosphate starvation
AZ06	F7	glnK	regulatory protein, P-II 2, for nitrogen assimilation by glutamine synthetase, regulates GlnL (NRII) and GlnE (ATase)
AZ06	F8	gcl	glyoxylate carboligase
AZ06	F9	b4285	putative transposase
AZ06	F10	wrbA	flavodoxin-like protein, trp repressor binding protein
AZ06	F11	appA	phytase and phosphoanhydride phosphorylase (pH 2.5 acid phosphatase)
AZ06	F12	phoH	PhoB-dependent, ATP-binding pho regulon component (2nd module)
AZ06	G1	gloA	glyoxalase I, nickel isomerase
AZ06	G2	ybdL	putative PLP-dependent aminotransferase (1st module)
AZ06	G3	rhIE	putative ATP-dependent helicase (2nd module)

AZ06	G4	ybjK	putative transcriptional regulator (DeoR family)
AZ06	G5	yafS	putative methyltransferase
AZ06	G6	dpiB	sensory histidine kinase in two- component regulatory system with DpiA, regulation of citrate fermentation and plasmid inheritance genes (1st module)
AZ06	G7	ydgH	unknown CDS
AZ06	G8	yegE	putative modular sensory transducing histidine kinase (2nd module)
AZ06	G9	yfeN	unknown CDS
AZ06	G10	yqgA	conserved hypothetical protein
AZ06	G11	yghU	putative S-transferase
AZ06	G12	pIdA	outer membrane phospholipase A
AZ06	H1	lacZ	beta-galactosidase, lac operon
AZ06	H2	pIdB	lysophospholipase L(2)
AZ06	H3	ybdH	putative alcohol dehydrogenase
AZ06	H4	ybiH	putative transcriptional repressor (TetR/AcrR family)
AZ06	H5	ybjJ	putative transport protein/putative regulator (1st module) (1st module)

AZ06	H6	insA_7	IS1 protein InsA
AZ06	H7	citC	citrate lyase synthetase (citrate (pro-3S)-lyase ligase)
AZ06	H8	pntA	pyridine nucleotide transhydrogenase (proton pump), alpha subunit (2nd module)
AZ06	H9	udk	uridine/cytidine kinase
AZ06	H10	xapA	xanthosine phosphorylase (purine nucleoside phosphorylase)
AZ06	H11	speC	ornithine decarboxylase isozyme
AZ06	H12	gssA	bifunctional: glutathionylspermidine synthetase; glutathionylspermidine amidase (2nd module)
AZ07	A1	yigI	conserved hypothetical protein
AZ07	A2	rhtB	RhtB homoserine Rht Transporter
AZ07	A3	hemB	5-aminolevulinate dehydratase (porphobilinogen synthase)
AZ07	A4	entD	enterochelin synthetase, component D (phosphopantetheinyltransferase)
AZ07	A5	lipA	lipoate synthase, an iron-sulfur enzyme (2nd module)
AZ07	A6	lipB	putative ligase in lipoate biosynthesis

AZ07	A7	ynfK	putative dethiobiotin synthetase
AZ07	A8	intF	CP4-6 prophage; putative phage integrase (2nd module)
AZ07	A9	menD	bifunctional modular MenD: 2-oxoglutarate decarboxylase (1st module) and SHCHC synthase (1st module)
AZ07	A10	menF	isochorismate synthase (isochorismate hydroxymutase 2), menaquinone biosynthesis
AZ07	A11	folC	multifunctional folylpolyglutamate synthase; dihydrofolate synthase, also has formylTHF polyglutamate synthase activity (2nd module)
AZ07	A12	Empty	Empty well
AZ07	B1	menG	putative methyltransferase in menaquinone biosynthesis protein
AZ07	B2	cobU	bifunctional: cobinamide kinase; cobinamide phosphate guanylyltransferase
AZ07	B3	mcrA	e14 prophage; restriction of DNA at 5-methylcytosine residues

AZ07	B4	yahB	putative transcriptional regulator (LysR family) (1st module)
AZ07	B5	yaiM	putative esterase
AZ07	B6	yaiP	putative enzyme in polysaccharide metabolism (1st module)
AZ07	B7	ybdG	putative transport (1st module)
AZ07	B8	ybeF	putative transcriptional regulator (LysR family) or periplasmic binding protein
AZ07	B9	hscC	putative heatshock protein (Hsp70 family) (1st module)
AZ07	B10	abrB	putative transport protein (1st module)
AZ07	B11	ybgQ	putative outer membrane protein (1st module)
AZ07	B12	mazE	part of proteic killer gene system, suppressor of inhibitory function of ChpA
AZ07	C1	ybgD	putative fimbrial-like protein
AZ07	C2	ybhC	putative pectinesterase (2nd module)
AZ07	C3	serA	D-3-phosphoglycerate dehydrogenase

AZ07	C4	fiu	outer membrane porin protein, putative ferrisiderophore receptor (1st module)
AZ07	C5	ybiO	putative integral membrane protein (2nd module)
AZ07	C6	ybjS	putative dehydrogenase, NAD(P)- binding (1st module)
AZ07	C7	hcp	hybrid-cluster protein with unknown physiological role
AZ07	C8	ybjE	conserved hypothetical protein
AZ07	C9	yccA	putative TEGT family transport protein
AZ07	C10	U139	promoterless strain
AZ07	C11	pspB	phage shock protein; regulatory gene, activates expression of psp operon with PspC
AZ07	C12	solA	putative sarcosine FAD/NAD(P)- binding oxidase (1st module)
AZ07	D1	ycgE	putative transcriptional repressor (MerR family) (1st module)
AZ07	D2	ykgE	putative oxidoreductase
AZ07	D3	yahK	putative dehydrogenase, NAD(P)- binding

AZ07	D4	ybaO	putative transcriptional regulator (AsnC family)
AZ07	D5	cueR	putative heavy metal transcriptional repressor (MerR family)
AZ07	D6	allR	transcriptional repressor of allantoin metabolism (IcIR family)
AZ07	D7	sfmC	putative periplasmic chaperone
AZ07	D8	b0663	NA
AZ07	D9	ubiC	chorismate pyruvate lyase
AZ07	D10	ybhJ	putative hydratase (2nd module)
AZ07	D11	pqiA	paraquat-inducible protein A, membrane (1st module)
AZ07	D12	ymcE	suppresses fabA and ts growth mutation
AZ07	E1	csgC	putative curli production protein
AZ07	E2	mviN	putative virulence factor
AZ07	E3	ycgM	putative isomerase
AZ07	E4	ycjM	putative sucrose phosphorylase (1st module)
AZ07	E5	ycbR	putative periplasmic chaperone
AZ07	E6	ycbB	putative carboxypeptidase (N- terminal)
AZ07	E7	hemG	protoporphyrin flavoprotein oxidase

AZ07	E8	mntR	conserved protein
AZ07	E9	yliI	putative dehydrogenase
AZ07	E10	ybjN	unknown CDS
AZ07	E11	folA	dihydrofolate reductase type I; trimethoprim resistance
AZ07	E12	hemH	ferrochelatase
AZ07	F1	entF	adenosinylation of serine, component F of enterobactin synthetase (nonribosomal peptide synthetase) (3rd module)
AZ07	F2	acpP	acyl carrier protein
AZ07	F3	U66	promoterless strain
AZ07	F4	pabC	4-amino-4-deoxychorismate lyase (aminotransferase) (2nd module)
AZ07	F5	molR_2	split molybdate metabolism regulator, fragment 2 of 3
AZ07	F6	ubiE	S-adenosylmethionine:2-DMK methyltransferase / 2-octaprenyl-6- methoxy-1,4-benzoquinone methylase
AZ07	F7	hemN	O ₂ -independent coproporphyrinogen III oxidase (1st module)

AZ07	F8	mog	putative molybdochetalase in molybdopterine biosynthesis
AZ07	F9	pspE	phage shock protein
AZ07	F10	wrbA	flavodoxin-like protein, trp repressor binding protein
AZ07	F11	sfmA	putative fimbrial-like protein
AZ07	F12	bioB	biotin synthetase (2nd module)
AZ07	G1	moaA	molybdopterin biosynthesis, protein A (1st module)
AZ07	G2	iaaA	putative asparaginase
AZ07	G3	hemA	glutamyl tRNA reductase
AZ07	G4	yeiG	putative esterase
AZ07	G5	ispB	octaprenyl diphosphate synthase
AZ07	G6	yiaD	putative outer membrane protein
AZ07	G7	yihD	conserved hypothetical protein
AZ07	G8	hemL	glutamate-1-semialdehyde aminotransferase (aminomutase), PLP-dependent
AZ07	G9	fold	bifunctional 5,10-methylene-tetrahydrofolate dehydrogenase and 5,10-methylene-tetrahydrofolate cyclohydrolase
AZ07	G10	ybhK	putative phosphatase/sulfatase

AZ07	G11	moeA	molybdopterin biosynthesis protein
AZ07	G12	lolB	outer membrane lipoprotein, localization of lipoproteins in the outer membrane
AZ07	H1	lacZ	beta-galactosidase, lac operon
AZ07	H2	folE	GTP cyclohydrolase I
AZ07	H3	bisC	biotin sulfoxide reductase (1st module)
AZ07	H4	mobA	molybdopterin-guanine dinucleotide synthase
AZ07	H5	yoaH	conserved hypothetical protein
AZ07	H6	aaeR	putative transcriptional regulator (LysR family) (1st module)
AZ07	H7	kbaZ	tagatose 6-phosphate aldolase 1, subunit together with AgaY
AZ07	H8	yhaK	conserved hypothetical protein
AZ07	H9	yhdH	putative dehydrogenase, NAD(P) binding (2nd module)
AZ07	H10	yhcB	conserved hypothetical protein
AZ07	H11	yraM	putative enzyme (1st module)
AZ07	H12	yhbO	putative intracellular proteinase with catalase domain
AZ08	A1	yhbQ	conserved hypothetical protein

AZ08	A2	yhbU	putative protease
AZ08	A3	b0671	NA
AZ08	A4	rhsE	rhsE protein in rhs element (2nd module)
AZ08	A5	prpB	putative carboxyphosphoenolpyruvate mutase
AZ08	A6	hyaA	hydrogenase-1 small subunit
AZ08	A7	ghrA	putative oxidoreductase, NAD(P)-binding (2nd module)
AZ08	A8	valV	valine tRNA 2B
AZ08	A9	yeeI	conserved hypothetical protein
AZ08	A10	asnV	asparagine tRNA
AZ08	A11	yejH	putative ATP-dependent helicase (1st module)
AZ08	A12	Empty	Empty well
AZ08	B1	yfeC	putative negative regulator
AZ08	B2	srmB	ATP-dependent RNA helicase (1st module)
AZ08	B3	trxC	reduced thioredoxin 2
AZ08	B4	metZ	initiator methionine tRNA-f1 (duplicate of metW,V)
AZ08	B5	yaeQ	conserved hypothetical protein

AZ08	B6	proL	proline tRNA 2
AZ08	B7	argW	arginine tRNA 5
AZ08	B8	yibK	putative tRNA/rRNA methyltransferase
AZ08	B9	rhoL	rho operon leader peptide
AZ08	B10	rho	transcription termination factor Rho; polarity suppressor (2nd module)
AZ08	B11	rlmB	putative tRNA/rRNA methyltransferase
AZ08	B12	aspU	aspartate tRNA 1 (duplicate of aspT,V)
AZ08	C1	valT	valine tRNA 1 (duplicate of valU,X,Y)
AZ08	C2	ileV	isoleucine tRNA 1 (duplicate of ileT,U)
AZ08	C3	serA	D-3-phosphoglycerate dehydrogenase
AZ08	C4	dxr	subunit of DXP reductoisomerase
AZ08	C5	yafT	unknown CDS
AZ08	C6	yafJ	conserved hypothetical protein
AZ08	C7	b0257	CP4-6 prophage; IS911, putative transposase

AZ08	C8	yagG	CP4-6 prophage; putative sugar transport protein (3rd module)
AZ08	C9	ygeX	putative dehydratase (deaminase), PLP-dependent enzyme (2nd module)
AZ08	C10	U139	promoterless strain
AZ08	C11	ppdD	putative major component of type IV pilin, prelipin peptidase dependent protein
AZ08	C12	yadN	putative fimbrial-like protein
AZ08	D1	yaeH	unknown CDS
AZ08	D2	ykfA	CP4-6 prophage; putative GTP-binding factor (1st module)
AZ08	D3	yagI	CP4-6 prophage; putative transcriptional regulator (IclR family)
AZ08	D4	yadC	putative fimbrial-like protein (2nd module)
AZ08	D5	serW	serine tRNA 5 (duplicate of serX)
AZ08	D6	hepA	RNA Polymerase (RNAP)-binding ATPase and RNAP recycling factor
AZ08	D7	pcnB	poly(A) polymerase I

AZ08	D8	sufI	suppressor of ftsI, putative periplasmic protein, cupredoxin-like
AZ08	D9	tyrV	tyrosine tRNA 1 (duplicate of tyrT)
AZ08	D10	cysT	cysteine tRNA
AZ08	D11	argQ	arginine tRNA 2 (duplicate of argV,Y,Z)
AZ08	D12	argZ	arginine tRNA 2 (duplicate of argV,Y,Q)
AZ08	E1	glyU	glycine tRNA 1
AZ08	E2	deaD	cold-shock DeaD box ATP-dependent RNA helicase (1st module)
AZ08	E3	pnp	polynucleotide phosphorylase, member of mRNA degradosome (3rd module)
AZ08	E4	rhdD	RhdD protein in RhdD element (3rd module)
AZ08	E5	agaR	transcriptional repressor of N-acetyl galactosamine metabolism (DeoR family)
AZ08	E6	yhaJ	putative transcriptional regulator (LysR family)
AZ08	E7	yhdA	conserved protein (2nd module)

AZ08	E8	yhcM	putative ATPase
AZ08	E9	yraL	putative enzyme with methyltransferase domain
AZ08	E10	yraR	putative NADH dehydrogenase
AZ08	E11	yhbP	conserved protein
AZ08	E12	yhbT	conserved hypothetical protein
AZ08	F1	glnU	glutamine tRNA 1 (duplicate of glnW)
AZ08	F2	glnW	glutamine tRNA 1 (duplicate of glnU)
AZ08	F3	U66	promoterless strain
AZ08	F4	prpR	transcriptional activator of propionate catabolism (EBP family) (2nd module)
AZ08	F5	serX	serine tRNA 5 (duplicate of serW)
AZ08	F6	ydhQ	putative enzyme (2nd module)
AZ08	F7	serU	serine tRNA 2
AZ08	F8	yeeO	putative MATE family transport protein (3rd module)
AZ08	F9	nac	transcriptional repressor for histidine utilization/nitrogen assimilation (LysR family)

AZ08	F10	wrbA	flavodoxin-like protein, trp repressor binding protein
AZ08	F11	rsuA	16S rRNA pseudouridine synthase
AZ08	F12	yfiC	putative methyltransferase (1st module)
AZ08	G1	yfiF	putative tRNA/rRNA methyltransferase (2nd module)
AZ08	G2	rof	Rho-binding antiterminator
AZ08	G3	qseB	putative transcriptional regulator (OmpR family)
AZ08	G4	zupT	conserved protein
AZ08	G5	ecfG	putative membrane protein
AZ08	G6	yqiI	conserved hypothetical protein
AZ08	G7	ybaY	glycoprotein/polysaccharide metabolism
AZ08	G8	pgpB	phosphatidylglycerophosphate phosphatase B
AZ08	G9	yfdC	putative transport
AZ08	G10	ecfD	putative lipoprotein (2nd module)
AZ08	G11	yqiJ	unknown CDS
AZ08	G12	dacB	D-alanyl-D-alanine carboxypeptidase, penicillin-binding protein 4

AZ08	H1	lacZ	beta-galactosidase, lac operon
AZ08	H2	def	peptide deformylase
AZ08	H3	slyX	conserved hypothetical protein
AZ08	H4	kdtA	3-deoxy-D-manno-octulosonic-acid transferase (KDO transferase)
AZ08	H5	yifE	putative LysR type transcriptional regulator with pssR
AZ08	H6	iap	aminopeptidase in alkaline phosphatase isozyme conversion (1st module)
AZ08	H7	dgkA	diacylglycerol kinase
AZ08	H8	efp	elongation factor P (EF-P)
AZ08	H9	fk1B	FKBP-type 22KD peptidyl-prolyl cis-trans isomerase (rotamase)
AZ08	H10	ytfM	putative outer membrane protein
AZ08	H11	pmbA	peptide maturation protein, maturation of antibiotic MccB17, see tld genes ?
AZ08	H12	infA	protein chain initiation factor IF-1
AZ09	A1	cls	cardiolipin synthase
AZ09	A2	nlpC	lipoprotein

AZ09	A3	msbB	myristoyl transferase in lipid A biosynthesis, suppressor of htrB (lpxL)
AZ09	A4	pgsA	phosphatidylglycerophosphate synthetase (CDP-1,2-diacyl-sn-glycero-3-phosphate phosphatidyl transferase)
AZ09	A5	lepA	GTP-binding elongation factor (1st module)
AZ09	A6	nlpD	lipoprotein (2nd module)
AZ09	A7	lgt	phosphatidylglycerol-prolipoprotein diacylglyceryl transferase
AZ09	A8	prfB	peptide chain release factor RF-2 (2nd module)
AZ09	A9	plsC	1-acyl-sn-glycerol-3-phosphate acyltransferase (2nd module)
AZ09	A10	rbfA	ribosome-binding factor, role in processing of 10S rRNA
AZ09	A11	glgB	1,4-alpha-glucan branching enzyme (2nd module)
AZ09	A12	Empty	Empty well
AZ09	B1	tufA	protein chain elongation factor EF-Tu (duplicate of tufB)

AZ09	B2	slyD	FKBP-type peptidyl prolyl cis-trans isomerase (rotamase)
AZ09	B3	rfaZ	lipopolysaccharide core biosynthesis
AZ09	B4	nlpA	lipoprotein-28, possible binding protein
AZ09	B5	blc	outer membrane lipoprotein (lipocalin)
AZ09	B6	ygjN	unknown CDS
AZ09	B7	ygjV	conserved protein
AZ09	B8	yhaM	conserved hypothetical protein
AZ09	B9	yhbC	conserved hypothetical protein
AZ09	B10	yraQ	conserved protein (2nd module)
AZ09	B11	psd	phosphatidylserine decarboxylase
AZ09	B12	yhbX	putative transmembrane protein (1st module)
AZ09	C1	yhbE	putative membrane protein (1st module)
AZ09	C2	yhcO	conserved protein, barnase inhibitor-like
AZ09	C3	serA	D-3-phosphoglycerate dehydrogenase
AZ09	C4	smf	hypothetical protein
AZ09	C5	yhdN	unknown CDS

AZ09	C6	bfd	NA
AZ09	C7	yheO	putative regulator
AZ09	C8	yhfG	conserved hypothetical protein
AZ09	C9	ygjJ	unknown CDS
AZ09	C10	U139	promoterless strain
AZ09	C11	ygjQ	putative integral membrane protein
AZ09	C12	ygjR	putative NAD(P)-binding dehydrogenase (1st module)
AZ09	D1	fkpB	NA
AZ09	D2	lpxC	UDP-3-O-acyl N-acetylglucosamine deacetylase
AZ09	D3	frr	ribosome releasing factor
AZ09	D4	plsX	fatty acid/phospholipid synthesis protein, methyltransferase domain
AZ09	D5	rffC	NA
AZ09	D6	tufB	protein chain elongation factor EF- Tu; possible GTP-binding factor (duplicate of tufA)
AZ09	D7	prfC	peptide chain release factor RF-3; possible GTP-binding factor (1st module)
AZ09	D8	tsf	protein chain elongation factor EF- Ts

AZ09	D9	ygiW	conserved hypothetical protein
AZ09	D10	ygiZ	conserved hypothetical protein
AZ09	D11	ygiD	putative enzyme with dioxygenase domain
AZ09	D12	ygiF	conserved hypothetical protein
AZ09	E1	yqjH	putative enzyme, ferredoxin reductase-like, FAD-linked , NADP-linked
AZ09	E2	map	methionine aminopeptidase
AZ09	E3	tesB	acyl-CoA thioesterase II
AZ09	E4	ribA	GTP cyclohydrolase II
AZ09	E5	vacJ	lipoprotein precursor
AZ09	E6	rluD	23S rRNA pseudouridine synthase
AZ09	E7	rfaH	transcriptional activator affecting biosynthesis, assembly and export of lipopolysaccharide core, F pilin, and haemolysin
AZ09	E8	glgS	glycogen biosynthesis, rpoS dependent
AZ09	E9	greA	transcription elongation factor, cleaves 3' nucleotide of paused mRNA
AZ09	E10	smf_2	hypothetical protein

AZ09	E11	fkpA	FKBP-type peptidyl-prolyl cis-trans isomerase (rotamase)
AZ09	E12	rfaQ	lipopolysaccharide core biosynthesis; modification of heptose region of core (2nd module)
AZ09	F1	hdfR	transcriptional repressor of phosphatidylserine synthase (LysR family), also believed to be regulator HdfR of flhDC operon if joined with b3762
AZ09	F2	cysD	ATP-sulfurylase, subunit 1 (ATP:sulfate adenylyltransferase)
AZ09	F3	U66	promoterless strain
AZ09	F4	plsB	glycerolphosphate acyltransferase (2nd module)
AZ09	F5	yjeK	putative aminomutase
AZ09	F6	ytfB	conserved protein
AZ09	F7	msrA	peptide methionine sulfoxide reductase
AZ09	F8	yjgA	putative ABC superfamily (atp_bind) transport protein
AZ09	F9	ppiC	peptidyl-prolyl cis-trans isomerase C (rotamase C)

AZ09	F10	wrbA	flavodoxin-like protein, trp repressor binding protein
AZ09	F11	rpsB	30S ribosomal subunit protein S2
AZ09	F12	yfcG	putative glutathione S-transferase
AZ09	G1	lpxP	palmitoleoyl-acyl carrier protein (ACP)-dependent acyltransferase, cold induced gene
AZ09	G2	hrpA	helicase, ATP-dependent (1st module)
AZ09	G3	fldB	flavodoxin 2
AZ09	G4	argP	inhibitor of replication initiation, also transcriptional regulator of dnaA and argK (affects arginine transport) (LysR family)
AZ09	G5	dfp	flavoprotein affecting synthesis of DNA and pantothenate metabolism (1st module)
AZ09	G6	nohB	DLP12 prophage; bacteriophage DNA packaging protein
AZ09	G7	rpmE	50S ribosomal subunit protein L31
AZ09	G8	thrU	threonine tRNA 4
AZ09	G9	ygiU	conserved protein
AZ09	G10	pyrC	dihydro-orotase

AZ09	G11	ligA	DNA ligase
AZ09	G12	parC	DNA topoisomerase IV, subunit A
AZ09	H1	lacZ	beta-galactosidase, lac operon
AZ09	H2	hsdM	DNA methylase M, host modification
AZ09	H3	cmk	cytidine monophosphate (CMP) kinase
AZ09	H4	pyrB	aspartate carbamoyltransferase
AZ09	H5	yngC	unknown CDS
AZ09	H6	panE	2-dehydropantoate reductase
AZ09	H7	tolA	tol protein required for outer membrane integrity, uptake of group A colicins, C-terminal is coreceptor with F pilus for filamentous phages, role in translocation of filamentous phage DNA to cytoplasm (1st module)
AZ09	H8	yhjY	putative lipase
AZ09	H9	priA	primosomal protein N' (= factor Y) directs replication fork assembly at D-loops, ATP-dependent (2nd module)
AZ09	H10	yohD	putative integral membrane protein

AZ09	H11	yohJ	putative transmembrane protein
AZ09	H12	cysS	cysteine tRNA synthetase (2nd module)
AZ10	A1	hrpB	helicase, ATP-dependent (1st module)
AZ10	A2	seqA	negative modulator of initiation of replication, inhibits open complex formation, mutation in gene alters cell membrane
AZ10	A3	helD	DNA helicase IV (2nd module)
AZ10	A4	metG	methionine tRNA synthetase (1st module)
AZ10	A5	yejL	conserved hypothetical protein
AZ10	A6	btuB	outer membrane porin, transporter for vitamin B12/cobalamin, receptor for E colicins, and bacteriophage BF23 (1st module)
AZ10	A7	ypjA	putative outer membrane protein (1st module)
AZ10	A8	pinH	homolog of pin/cin, phage invertible sequence
AZ10	A9	yqaB	putative phosphoglucomutase, contains a phosphatase-like domain

AZ10	A10	ygaD	conserved protein
AZ10	A11	ygcB	putative enzyme
AZ10	A12	Empty	Empty well
AZ10	B1	mazG	conserved protein
AZ10	B2	ygeQ	unknown CDS
AZ10	B3	yagK	CP4-6 prophage
AZ10	B4	dksA	dnaK suppressor protein
AZ10	B5	proS	proline tRNA synthetase (1st module)
AZ10	B6	asnS	asparagine tRNA synthetase (2nd module)
AZ10	B7	mfd	transcription-repair ATP-dependent coupling factor (1st module)
AZ10	B8	pheM	phenylalanyl-tRNA synthetase (pheST) operon leader peptide
AZ10	B9	selD	selenophosphate synthase
AZ10	B10	hisS	histidine tRNA synthetase
AZ10	B11	alaS	alanyl-tRNA synthetase
AZ10	B12	selA	selenocysteine synthase (with SelD) (2nd module)
AZ10	C1	lysU	lysine tRNA synthetase, inducible; heat shock protein

AZ10	C2	skp	periplasmic molecular chaperone for outer membrane proteins
AZ10	C3	serA	D-3-phosphoglycerate dehydrogenase
AZ10	C4	tgt	tRNA-guanine transglycosylase
AZ10	C5	hupB	DNA-binding protein HU-beta, NS1 (HU-1)
AZ10	C6	dnaX	DNA polymerase III, tau and gamma subunits; DNA elongation factor III (1st module)
AZ10	C7	rluC	23S rRNA pseudouridine synthase
AZ10	C8	cca	tRNA nucleotidyl transferase
AZ10	C9	hupA	DNA-binding protein HU-alpha (HU-2)
AZ10	C10	U139	promoterless strain
AZ10	C11	dkgB	2,5-diketo-D-gluconate reductase B
AZ10	C12	yfeY	conserved hypothetical protein
AZ10	D1	eutS	putative carboxysome structural protein, ethanol utilization
AZ10	D2	ypfG	unknown CDS
AZ10	D3	yffH	conserved protein, MutT-like
AZ10	D4	ypfH	conserved protein
AZ10	D5	ypfJ	conserved protein

AZ10	D6	hda	putative chromosomal replication initiator, DnaA-type
AZ10	D7	yfgB	putative pyruvate formate lyase activating enzyme (2nd module)
AZ10	D8	iscS	cysteine desulfurase (tRNA sulfurtransferase) PLP-dependent (1st module)
AZ10	D9	iscR	putative protein believed to be involved in assembly of Fe-S clusters, DNA-binding domain
AZ10	D10	yfjL	CP4-57 prophage;
AZ10	D11	ydaQ	Rac prophage;
AZ10	D12	yohC	putative transport protein
AZ10	E1	dusC	conserved protein
AZ10	E2	yeiE	putative transcriptional regulator (LysR family)
AZ10	E3	yejO	putative outer membrane protein (1st module)
AZ10	E4	elaA	putative transferase
AZ10	E5	ppiB	peptidyl-prolyl cis-trans isomerase B (rotamase B)
AZ10	E6	ligT	hypothetical protein
AZ10	E7	yajB	conserved hypothetical protein

AZ10	E8	ybfF	putative enzyme (1st module)
AZ10	E9	yccF	conserved hypothetical protein
AZ10	E10	yecM	conserved hypothetical protein
AZ10	E11	mrp	putative ATP-binding protein
AZ10	E12	yejK	nucleotide associated protein, present in spermidine nucleoids
AZ10	F1	gltX	glutamate tRNA synthetase, catalytic subunit (1st module)
AZ10	F2	stpA	DNA-bending protein with chaperone activity
AZ10	F3	U66	promoterless strain
AZ10	F4	glyQ	glycine tRNA synthetase, alpha subunit
AZ10	F5	trmA	tRNA (uracil-5-)-methyltransferase (2nd module)
AZ10	F6	ycgF	conserved protein (2nd module)
AZ10	F7	yniC	putative enzyme, with a phosphatase- like domain
AZ10	F8	nudG	putative enzyme (MutT-like)
AZ10	F9	yeaL	putative membrane protein
AZ10	F10	wrbA	flavodoxin-like protein, trp repressor binding protein
AZ10	F11	yeaP	conserved protein (2nd module)

AZ10	F12	yoaB	conserved protein
AZ10	G1	yebS	putative membrane protein
AZ10	G2	tolB	tol protein required for outer membrane integrity, uptake of group A colicins, and translocation of phage DNA to cytoplasm, may be part of multiprotein peptidoglycan recycling complex (Two domains) (2nd module)
AZ10	G3	yohM	putative transmembrane protein
AZ10	G4	pepN	aminopeptidase N
AZ10	G5	gpt	guanine-hypoxanthine phosphoribosyltransferase
AZ10	G6	thiI	sulfur transfer protein (from cys to ThiS and from IscS to U8-tRNA) (2nd module)
AZ10	G7	sbcB	exonuclease I, 3' --> 5' specific; deoxyribophosphodiesterase
AZ10	G8	xseA	exonuclease VII, large subunit
AZ10	G9	yhiR	conserved protein
AZ10	G10	malS	alpha-amylase (2nd module)
AZ10	G11	yicC	conserved protein (2nd module)
AZ10	G12	pepQ	proline dipeptidase (2nd module)

AZ10	H1	lacZ	beta-galactosidase, lac operon
AZ10	H2	rluF	putative pseudouridine synthase
AZ10	H3	mrr	restriction of methylated adenine
AZ10	H4	yfaY	putative competence-damage protein
AZ10	H5	elaB	unknown CDS
AZ10	H6	yfbU	conserved hypothetical protein
AZ10	H7	yfcD	putative enzyme (MutT-like)
AZ10	H8	yfcE	putative metallo-dependent phosphatase
AZ10	H9	yfcI	putative transposase (1st module)
AZ10	H10	dedA	putative integral membrane protein
AZ10	H11	yfeA	conserved protein (2nd module)
AZ10	H12	ypjB	conserved protein
AZ11	A1	yfjN	CP4-57 prophage; putative cell division protein (2nd module)
AZ11	A2	tilS	cell cycle protein
AZ11	A3	tig	peptidyl-prolyl cis/trans isomerase, trigger factor; a molecular chaperone involved in cell division
AZ11	A4	dicB	Qin prophage; inhibitor of cell division

AZ11	A5	proX	ABC superfamily (peri_bind) glycine/betaine/proline transport protein
AZ11	A6	cspA	major cold shock protein 7.4, transcription antiterminator of hns,
AZ11	A7	b2680	putative resistance protein, possible transporter
AZ11	A8	ygaZ	putative amino acid transporter
AZ11	A9	ygdR	conserved hypothetical protein
AZ11	A10	yqeH	conserved protein
AZ11	A11	ygeG	conserved hypothetical protein
AZ11	A12	Empty	Empty well
AZ11	B1	ygeI	unknown CDS
AZ11	B2	idi	isopentenyl diphosphate isomerase
AZ11	B3	ydfA	Qin prophage;
AZ11	B4	creB	tolerance to colicin E2
AZ11	B5	yeaS	putative transport protein
AZ11	B6	yeaZ	putative glycoprotein endopeptidase
AZ11	B7	yobF	unknown CDS
AZ11	B8	yebO	conserved hypothetical protein
AZ11	B9	yebE	unknown CDS

AZ11	B10	dacA	D-alanyl-D-alanine carboxypeptidase, penicillin-binding protein 5 (1st module)
AZ11	B11	htpX	heat shock protein, integral membrane protein
AZ11	B12	treA	trehalase, periplasmic
AZ11	C1	osmB	osmotically inducible lipoprotein
AZ11	C2	hslJ	heat shock protein hslJ
AZ11	C3	serA	D-3-phosphoglycerate dehydrogenase
AZ11	C4	otsB	trehalose-6-phosphate phosphatase, biosynthetic
AZ11	C5	nlpI	lipoprotein involved in cell division
AZ11	C6	yjvV	putative hydrolase (1st module)
AZ11	C7	ibpB	small heat shock protein IbpB
AZ11	C8	ftsN	essential cell division protein, epimerase- or mutase-like (2nd module)
AZ11	C9	cutA	periplasmic divalent cation tolerance protein; cytochrome c biogenesis
AZ11	C10	U139	promoterless strain
AZ11	C11	mdbB	phosphoglycerol transferase I,

AZ11	C12	ynfA	putative transmembrane protein
AZ11	D1	ynfC	unknown CDS
AZ11	D2	ydgC	putative membrane protein
AZ11	D3	ydhH	conserved hypothetical protein
AZ11	D4	ydhD	conserved protein
AZ11	D5	yjjJ	conserved protein
AZ11	D6	imp	organic solvent tolerance
AZ11	D7	crcB	protein involved in resistance to camphor-induced chromosome decondensation
AZ11	D8	cspB	Qin prophage; cold shock protein; may regulate transcription
AZ11	D9	agaS	putative tagatose-6-phosphate ketose/aldose isomerase (1st module)
AZ11	D10	inaA	pH inducible protein involved in stress response, protein kinase-like
AZ11	D11	pdxB	erythronate-4-phosphate dehydrogenase
AZ11	D12	nudF	conserved protein, MutT-like
AZ11	E1	ftsJ	23S rRNA m2U2552 methyltransferase

AZ11	E2	ftsY	multimodular FtsY: membrane binding domain of cell division protein (1st module)
AZ11	E3	uspB	ethanol tolerance protein
AZ11	E4	yfjM	CP4-57 prophage;
AZ11	E5	envY	transcriptional activator of envelope proteins; thermoregulation of porin biosynthesis (AraC/XylS family) (2nd module)
AZ11	E6	dhaM	dihydroxyacetone kinase subunit M
AZ11	E7	speF	ornithine decarboxylase isozyme, inducible
AZ11	E8	ykgF	putative dehydrogenase
AZ11	E9	yajC	preprotein translocase IISP family, membrane subunit
AZ11	E10	ybaT	putative APC family, amino-acid transport protein (1st module)
AZ11	E11	yafN	conserved hypothetical protein
AZ11	E12	yjaH	conserved protein
AZ11	F1	ecfE	putative protease
AZ11	F2	yaiW	conserved hypothetical protein
AZ11	F3	U66	promoterless strain
AZ11	F4	ecfK	putative outer membrane antigen

AZ11	F5	trkA	Trk system transport of potassium , NAD(P)-binding (1st module)
AZ11	F6	yahI	putative carbamate kinase
AZ11	F7	b0298	putative transposase-related protein
AZ11	F8	ybbC	unknown CDS
AZ11	F9	b0501	unknown CDS
AZ11	F10	wrbA	flavodoxin-like protein, trp repressor binding protein
AZ11	F11	yaiE	conserved protein
AZ11	F12	paaX	transcriptional repressor for phenylacetic acid degradation
AZ11	G1	yadR	conserved hypothetical protein
AZ11	G2	ybaB	conserved hypothetical protein
AZ11	G3	ybaA	unknown CDS
AZ11	G4	cdaR	SdaR transcriptional regulator
AZ11	G5	adrA	conserved protein (2nd module)
AZ11	G6	ppiD	peptidyl-prolyl cis-trans isomerase, for periplasmic folding of outer membrane proteins (1st module)
AZ11	G7	ybaV	conserved hypothetical protein
AZ11	G8	yafM	conserved hypothetical protein
AZ11	G9	uxuR	transcriptional repressor for uxu operon

AZ11	G10	ykiA	unknown CDS
AZ11	G11	ykfJ	unknown CDS
AZ11	G12	yahM	unknown CDS
AZ11	H1	lacZ	beta-galactosidase, lac operon
AZ11	H2	mraZ	protein encoded by an operon involved in formation of the cell envelope and cell division
AZ11	H3	ybaN	putative phage gene 58
AZ11	H4	yagJ	CP4-6 prophage
AZ11	H5	yehH	unknown CDS
AZ11	H6	yfbE	putative aminotransferase
AZ11	H7	eco	ecotin, a serine protease inhibitor
AZ11	H8	polA	DNA polymerase I, 3' --> 5' polymerase, 5' --> 3' and 3' --> 5' exonuclease (1st module)
AZ11	H9	treF	cytoplasmic trehalase
AZ11	H10	yhgE	unknown CDS
AZ11	H11	yaaW	conserved hypothetical protein
AZ11	H12	priC	primosomal replication protein N"
AZ12	A1	insA_3	CP4-6 prophage; IS1 protein InsA
AZ12	A2	ascG	transcriptional repressor of carbon metabolism (GalR/LacI family)
AZ12	A3	pth	peptidyl-tRNA hydrolase

AZ12	A4	ais	protein induced by aluminum, phosphoglycerate mutase-like domain
AZ12	A5	b1420	unknown CDS
AZ12	A6	yjiY	carbon starvation protein (2nd module)
AZ12	A7	napF	Fe-S ferredoxin-type protein: electron transfer
AZ12	A8	dpbA	putative endonuclease
AZ12	A9	rdoA	conserved hypothetical protein
AZ12	A10	pck	phosphoenolpyruvate carboxykinase
AZ12	A11	b0165	unknown CDS
AZ12	A12	Empty	Empty well
AZ12	B1	yadK	putative adhesin
AZ12	B2	cpdA	cyclic 3',5'-adenosine monophosphate phosphodiesterase
AZ12	B3	yacG	conserved hypothetical protein
AZ12	B4	trmU	catalyzes 2-thiouridine modification of tRNA
AZ12	B5	yadS	conserved hypothetical protein
AZ12	B6	xylB	xylulokinase
AZ12	B7	yggD	putative repressor

AZ12	B8	ydeO	putative transcriptional regulator (AraC/XylS family) (2nd module)
AZ12	B9	eutR	putative ARAC-type regulatory protein
AZ12	B10	yehS	unknown CDS
AZ12	B11	yihN	putative MFS superfamily transport protein (1st module)
AZ12	B12	aldB	aldehyde dehydrogenase B (lactaldehyde dehydrogenase)
AZ12	C1	yafV	putative NAD(P)-binding enzyme
AZ12	C2	cytR	transcriptional repressor for nucleoside catabolism and recycling (GalR/LacI family)
AZ12	C3	serA	D-3-phosphoglycerate dehydrogenase
AZ12	C4	yrbA	putative transcriptional regulator (BolA family)
AZ12	C5	ydeP	multimodular YdeP: putative reductase (2nd module)
AZ12	C6	ompN	outer membrane protein N, non- specific porin (1st module)
AZ12	C7	yafU	unknown CDS
AZ12	C8	ybeB	conserved hypothetical protein

AZ12	C9	yafD	unknown CDS
AZ12	C10	U139	promoterless strain
AZ12	C11	dnaQ	DNA polymerase III, epsilon subunit, 3-5 exonucleolytic proofreading function
AZ12	C12	yafL	putative lipoprotein (2nd module)
AZ12	D1	ybgI	conserved protein
AZ12	D2	lit	e14 prophage; phage T4 late gene expression
AZ12	D3	ycgJ	unknown CDS
AZ12	D4	ycgL	conserved hypothetical protein
AZ12	D5	ydbH	conserved protein
AZ12	D6	nhoA	N-hydroxyarylamine O-acetyltransferase
AZ12	D7	ydeJ	conserved protein
AZ12	D8	dinG	LexA regulated (SOS) repair enzyme (2nd module)
AZ12	D9	xthA	exonuclease III, may repair singlet oxygen induced lesions
AZ12	D10	sppA	protease IV, a signal peptide peptidase (2nd module)
AZ12	D11	purT	phosphoribosylglycinamide formyltransferase 2

AZ12	D12	ung	uracil-DNA-glycosylase
AZ12	E1	mutS	methyl-directed mismatch repair, recognize exocyclic adducts of guanosine (2nd module)
AZ12	E2	mutH	methyl-directed mismatch repair protein
AZ12	E3	mutY	adenine DNA glycosylase (1st module)
AZ12	E4	ileX	isoleucine tRNA 2
AZ12	E5	creA	unknown CDS
AZ12	E6	yccR	conserved protein
AZ12	E7	ecpD	putative periplasmic pilin chaperone similar to PapD
AZ12	E8	ybfE	LexA regulated, possible SOS response
AZ12	E9	yciG	conserved hypothetical protein
AZ12	E10	tyrS	tyrosine tRNA synthetase
AZ12	E11	dcm	DNA cytosine methylase
AZ12	E12	sbmC	DNA gyrase inhibitor
AZ12	F1	ada	bifunctional Ada: transcriptional regulator of DNA repair (AraC/Xyl family) (1st module) and O6-

			methylguanine-DNA methyltransferase
AZ12	F2	ygiS	putative ABC superfamily (peri_bind) oligopeptide transport protein
AZ12	F3	U66	promoterless strain
AZ12	F4	dam	DNA adenine methylase
AZ12	F5	gadX	putative transcriptional regulator (AraC/XylS family)
AZ12	F6	mutM	formamidopyrimidine DNA glycosylase
AZ12	F7	xylE	MFS family, xylose:proton symport protein (1st module)
AZ12	F8	yjiW	LexA regulated, possible SOS response
AZ12	F9	ykgH	conserved protein
AZ12	F10	wrbA	flavodoxin-like protein, trp repressor binding protein
AZ12	F11	yagB	CP4-6 prophage;
AZ12	F12	yagM	CP4-6 prophage
AZ12	G1	yagY	unknown CDS
AZ12	G2	yagZ	unknown CDS
AZ12	G3	ykgI	unknown CDS

AZ12	G4	b0309	unknown CDS
AZ12	G5	yafK	conserved protein
AZ12	G6	mutT	7,8-dihydro-8-oxoguanine-triphosphatase, prefers dGTP
AZ12	G7	dinB	DNA polymerase IV, devoid of proofreading, damage-inducible protein P (1st module)
AZ12	G8	brnQ	LIVCS family, branched chain amino acid transporter system II (LIV-II)
AZ12	G9	ftsK	cell division protein, required for cell division and chromosome partitioning (1st module)
AZ12	G10	ydgL	putative oxidoreductase, inner membrane protein
AZ12	G11	sodB	superoxide dismutase, iron
AZ12	G12	nfo	endonuclease IV
AZ12	H1	lacZ	beta-galactosidase, lac operon
AZ12	H2	recN	protein used in recombination and DNA repair (2nd module)
AZ12	H3	ilvD	dihydroxyacid dehydratase
AZ12	H4	rmuC	conserved protein (1st module)
AZ12	H5	yaiA	unknown CDS

AZ12	H6	aidB	putative acyl-CoA dehydrogenase; adaptive response (transcription activated by Ada) (2nd module)
AZ12	H7	ybfD	conserved protein
AZ12	H8	ybgA	conserved protein
AZ12	H9	b0725	unknown CDS
AZ12	H10	ybgE	unknown CDS
AZ12	H11	ybgC	conserved hypothetical protein
AZ12	H12	ybhL	putative transport protein
AZ13	A1	yafC	putative transcriptional regulator (LysR family) (1st module)
AZ13	A2	rnhA	RNase HI, degrades RNA of DNA- RNA hybrids
AZ13	A3	dinJ	damage-inducible protein J
AZ13	A4	ybgH	putative POT family transport protein (1st module)
AZ13	A5	ybiS	conserved hypothetical protein
AZ13	A6	ymfE	e14 prophage
AZ13	A7	minC	cell division inhibitor; activated MinC inhibits FtsZ ring formation
AZ13	A8	ycgK	unknown CDS
AZ13	A9	ldhA	fermentative D-lactate dehydrogenase, NAD-dependent

AZ13	A10	yddH	putative enzyme
AZ13	A11	ydeI	unknown CDS
AZ13	A12	Empty	Empty well
AZ13	B1	ybiA	conserved protein
AZ13	B2	astC	succinylornithine transaminase, also has acetylornithine transaminase activity, PLP-dependent
AZ13	B3	ydjA	conserved protein
AZ13	B4	yebG	DNA damage-inducible gene in SOS regulon, dependent on cyclic AMP and H-NS
AZ13	B5	yfiE	putative transcriptional regulator (LysR family)
AZ13	B6	ygbA	conserved hypothetical protein
AZ13	B7	nudH	invasion protein, MutT-like
AZ13	B8	yggH	putative methyltransferase
AZ13	B9	mug	DNA glycosylase, G/U mismatch specific
AZ13	B10	yneK	conserved protein
AZ13	B11	rob	transcriptional activator for resistance to antibiotics, organic solvents and heavy metals

			(AraC/XylS family) (right origin binding protein) (1st module)
AZ13	B12	sulA	suppressor of Ion; inhibitor of cell division and FtsZ ring formation upon DNA damage/inhibition, HslVU and Lon involved in its turnover
AZ13	C1	fur	transcriptional repressor of iron transport (Fur family)
AZ13	C2	soxR	soxR transcriptional dual regulator
AZ13	C3	serA	D-3-phosphoglycerate dehydrogenase
AZ13	C4	secE	preprotein translocase IISP family, membrane subunit
AZ13	C5	ybhM	putative integral membrane protein, transport
AZ13	C6	ybjO	unknown CDS
AZ13	C7	ycaL	putative heat shock protein
AZ13	C8	ycaI	putative recombination protein, metallo-hydrolase domain
AZ13	C9	ycbK	conserved hypothetical protein
AZ13	C10	U139	promoterless strain
AZ13	C11	ycbW	unknown CDS

AZ13	C12	ycdN	unknown CDS
AZ13	D1	yagU	unknown CDS
AZ13	D2	yahD	conserved hypothetical protein
AZ13	D3	prpC	methylcitrate synthase (citrate synthase 2)
AZ13	D4	b0374	flagellar protein; similar to 3rd module of ATP-binding components of transporters
AZ13	D5	yaiZ	unknown CDS
AZ13	D6	ybaD	conserved protein
AZ13	D7	ybaQ	conserved protein
AZ13	D8	allA	ureidoglycolate hydrolase
AZ13	D9	nhaA	NhaA family of transport protein, Na ⁺ /H antiporter (1st module)
AZ13	D10	fdrA	putative acyl-CoA synthetase, membrane protein (1st module)
AZ13	D11	ahpC	alkyl hydroperoxide reductase, C22 subunit, thioredoxin-like; detoxification of hydroperoxides
AZ13	D12	yccE	putative hemoglobin-binding protein
AZ13	E1	ycjG	putative chloromuconate cycloisomerase (muconate cycloisomerase) (2nd module)

AZ13	E2	marR	transcriptional repressor for antibiotic resistance and oxidative stress
AZ13	E3	aceB	malate synthase A
AZ13	E4	katE	catalase; hydroperoxidase HPII(III) , RpoS dependent
AZ13	E5	evgA	response regulator (activator) in two-component regulatory system with EvgS, regulates multidrug resistance (LuxR/UhpA family)
AZ13	E6	ypjD	conserved protein
AZ13	E7	yqcD	conserved hypothetical protein
AZ13	E8	nfnB	dihydropteridine reductase/oxygen-insensitive NAD(P)H nitroreductase
AZ13	E9	sodC	superoxide dismutase precursor (Cu-Zn)
AZ13	E10	yaiX	putative acyl transferase
AZ13	E11	pmrD	polymyxin resistance protein B
AZ13	E12	hscB	Hsc20 co-chaperone that acts with Hsc66 in IscU iron-sulfur cluster assembly
AZ13	F1	ygeA	putative aspartate racemase

AZ13	F2	bacA	bacitracin resistance; possibly phosphorylates undecaprenol
AZ13	F3	U66	promoterless strain
AZ13	F4	yhjX	putative oxalate/formate antiporter, MFS family (2nd module)
AZ13	F5	secB	molecular chaperone in protein export
AZ13	F6	secA	preprotein translocase; secretion protein of IISB family
AZ13	F7	emrE	DLP12 prophage; MFP family auxillary multidrug transport protein, methylviologen and ethidium resistance
AZ13	F8	ahpF	alkyl hydroperoxide reductase subunit, FAD/NAD(P)-binding; detoxification of hydroperoxides (2nd module)
AZ13	F9	tatE	subunit of TatABCE protein export complex
AZ13	F10	wrbA	flavodoxin-like protein, trp repressor binding protein

AZ13	F11	lolA	periplasmic protein effects translocation of lipoproteins from inner membrane to outer membrane
AZ13	F12	sanA	vancomycin sensitivity, putative oxidoreductase
AZ13	G1	trmE	GTP-binding protein with a role in modification of tRNA
AZ13	G2	emrA	multidrug resistance secretion protein
AZ13	G3	insA_1	IS1 protein InsA
AZ13	G4	yajO	putative oxidoreductase, NAD(P)- linked
AZ13	G5	ylaB	conserved protein (2nd module)
AZ13	G6	ylaC	unknown CDS
AZ13	G7	ybaK	conserved hypothetical protein
AZ13	G8	ylbG	putative regulator
AZ13	G9	yagT	putative oxidoreductase
AZ13	G10	yahC	conserved protein
AZ13	G11	b0332	conserved hypothetical protein
AZ13	G12	b0373	putative transposase-related protein
AZ13	H1	lacZ	beta-galactosidase, lac operon
AZ13	H2	insA_2	CP4-6 prophage; IS1 protein InsA 2
AZ13	H3	yaiI	conserved hypothetical protein

AZ13	H4	ybaP	conserved hypothetical protein
AZ13	H5	allS	putative transcriptional regulator LYSR-type
AZ13	H6	ydcK	putative LpxA-like enzyme
AZ13	H7	allD	ureidoglycolate dehydrogenase
AZ13	H8	dsbG	periplasmic disulfide isomerase, thiol-disulphide oxidase (1st module)
AZ13	H9	cbpA	curved DNA-binding protein
AZ13	H10	borD	DLP12 prophage; bacteriophage lambda Bor lipoprotein homolog, involved in serum resistance
AZ13	H11	marC	inner membrane protein involved in multiple antibiotic resistance
AZ13	H12	slyA	transcriptional activator for hemolysin (MarR family)
AZ14	A1	syd	interacts with secY
AZ14	A2	nfrB	bacteriophage N4 receptor, subunit, inner membrane protein (2nd module)
AZ14	A3	b0255	CP4-6 prophage; IS911 homolog
AZ14	A4	yagE	CP4-6 prophage; putative synthase

AZ14	A5	b0540	DLP12 prophage; putative transposase-related protein
AZ14	A6	cusC	putative outer membrane protein (possible copper ion efflux system)
AZ14	A7	ybdR	putative dehydrogenase, NAD(P) binding (1st module)
AZ14	A8	ybeR	unknown CDS
AZ14	A9	ybeU	unknown CDS
AZ14	A10	ubiF	2-octoprenyl-3-methyl-6-methoxy-1,4-benzoquinone hydroxylase (1st module)
AZ14	A11	ybhE	putative isomerase
AZ14	A12	Empty	Empty well
AZ14	B1	ybhQ	conserved protein
AZ14	B2	ybiN	putative methyltransferase
AZ14	B3	sbmA	ABC superfamily (membrane module of atp&memb) transporter (2nd module)
AZ14	B4	ybbL	putative ABC superfamily (atp_bind) putrescine/spermidine transport protein
AZ14	B5	kdsB	3-deoxy-D-manno-octulosonate-cytidylyltransferase

AZ14	B6	entS	putative POT family transport protein (1st module)
AZ14	B7	lolC	ABC superfamily (membrane), lipoprotein transmembrane transporter (2nd module)
AZ14	B8	pepT	putative peptidase T(aminotripeptidase), Zn-dependent
AZ14	B9	znuC	ABC superfamily (atp_bind) high affinity Zn transport protein
AZ14	B10	yfhH	multimodular YfhH: putative ABC superfamily (membrane) transport protein (1st module)
AZ14	B11	yrbG	putative CacA family, Na:Ca transport protein
AZ14	B12	yheS	putative ABC superfamily (atp_bind) transport protein (1st module)
AZ14	C1	slt	lytic murein transglycosylase, soluble (2nd module)
AZ14	C2	yadG	putative ABC superfamily (atp_bind) transport protein (1st module)

AZ14	C3	serA	D-3-phosphoglycerate dehydrogenase
AZ14	C4	gltJ	ABC superfamily (membrane), glutamate/aspartate transporter
AZ14	C5	ybeZ	putative phosphate starvation-inducible protein, ATP-binding (2nd module)
AZ14	C6	modF	ABC superfamily (atp_bind) molybdenum transport protein (1st module)
AZ14	C7	artP	ABC superfamily (atp&memb) arginine transport transport protein
AZ14	C8	cydD	bifunctional multimodular CydD: ABC superfamily (membrane), cytochrome-related transporter, Zn sensitive (1st module)
AZ14	C9	yddA	bifunctional multimodular YddA: putative ABC superfamily (membrane) transport protein (1st module)
AZ14	C10	U139	promoterless strain
AZ14	C11	btuC	ABC superfamily (membrane), vitamin B12 transport protein

AZ14	C12	mgIA	ABC superfamily (atp_bind) galactose (methyl-galactoside) transport protein (1st module)
AZ14	D1	yojI	putative ABC superfamily (atp module of atp&membrane) transport protein (2nd module)
AZ14	D2	hisQ	ABC superfamily (membrane) histidine and lysine/arginine/ornithine transport system
AZ14	D3	cysW	ABC superfamily (membrane) thiosulfate permease W protein
AZ14	D4	ugpA	ABC superfamily (membrane) sn- glycerol 3-phosphate transport protein
AZ14	D5	dppB	ABC superfamily (membrane) dipeptide transport protein 1 (2nd module)
AZ14	D6	pstC	ABC superfamily (membrane) high- affinity phosphate transporter
AZ14	D7	alsA	subunit of D-allose ABC transporter
AZ14	D8	phnC	ABC superfamily (atp_bind) phosphonate transport protein

AZ14	D9	ybdF	conserved hypothetical protein
AZ14	D10	ybdN	unknown CDS
AZ14	D11	rihA	putative purine nucleoside hydrolase
AZ14	D12	ycdO	conserved hypothetical protein
AZ14	E1	fhuC	ABC superfamily (atp_bind) hydroxymate-dependent iron transport protein
AZ14	E2	oppB	ABC superfamily (membrane) oligopeptide transport protein (2nd module)
AZ14	E3	ydeA	MFS family, L- arabinose/isopropyl-beta-D- thiogalactopyranoside export protein, contributes to control of arabinose regulon (2nd module)
AZ14	E4	yhdX	putative ABC superfamily (membrane) amino acid transport protein (2nd module)
AZ14	E5	yhdY	putative ABC superfamily (membrane) amino acid transport protein (2nd module)
AZ14	E6	xylG	ABC superfamily (atp_bind) D- xylose transport protein

AZ14	E7	ytfR	putative ABC superfamily (membrane) sugar transport protein (1st module)
AZ14	E8	ycdZ	putative transport protein
AZ14	E9	ymdB	conserved protein
AZ14	E10	yceK	unknown CDS
AZ14	E11	ycfJ	putative membrane protein
AZ14	E12	ycgH	conserved protein (2nd module)
AZ14	F1	ycgN	conserved hypothetical protein
AZ14	F2	ycgY	putative enzyme
AZ14	F3	U66	promoterless strain
AZ14	F4	b1228	unknown CDS
AZ14	F5	rluB	putative pseudouridine synthase
AZ14	F6	yciS	conserved hypothetical protein
AZ14	F7	perR	CP4-6 prophage; putative transcriptional repressor for peroxide resistance (LysR family) (1st module)
AZ14	F8	cusR	response regulator in two- component regulatory system with CusS, transcriptional regulation of copper resistance (1st module)

AZ14	F9	uspG	conserved hypothetical protein with adenine nucleotide-binding domain
AZ14	F10	wrbA	flavodoxin-like protein, trp repressor binding protein
AZ14	F11	ybeQ	conserved hypothetical protein (1st module)
AZ14	F12	ybeT	conserved hypothetical protein
AZ14	G1	ybhA	putative phosphatase
AZ14	G2	ybiM	unknown CDS
AZ14	G3	b0656	IS5 protein
AZ14	G4	ampH	putative enzyme
AZ14	G5	yadF	carbonic anhydrase
AZ14	G6	ygeR	putative lipoprotein
AZ14	G7	fepD	ABC superfamily (membrane), ferric enterobactin (enterochelin) transporter
AZ14	G8	ycfT	putative transport protein (2nd module)
AZ14	G9	potA	ABC superfamily (atp_bind), spermidine/putrescine transport protein
AZ14	G10	znuA	subunit of ZnuA/ZnuB/ZnuC ABC transporter

AZ14	G11	yfhB	unknown CDS
AZ14	G12	yrbF	putative ABC superfamily (atp_bind) transport protein
AZ14	H1	lacZ	beta-galactosidase, lac operon
AZ14	H2	kefG	putative electron transfer flavoprotein-NAD/FAD/quinone oxidoreductase
AZ14	H3	yjK	putative ABC superfamily (atp_bind) transport protein (1st module)
AZ14	H4	racC	Rac prophage; contains recE and oriJ
AZ14	H5	ybaL	putative CPA2 family transport protein (1st module)
AZ14	H6	zitB	putative CDF family transport protein (1st module)
AZ14	H7	sapA	ABC superfamily (peri_bind) peptide transport protein
AZ14	H8	mgIB	ABC superfamily (peri_bind) galactose transport protein (1st module)
AZ14	H9	nupX	putative NUP family transport protein

AZ14	H10	yeiM	putative NUP family transport protein (1st module)
AZ14	H11	hisJ	ABC superfamily (peri_bind) histidine transport protein
AZ14	H12	yphF	putative ABC superfamily (peri_bind) transport protein
AZ15	A1	ugpB	ABC superfamily (peri_bind) sn-glycerol 3-phosphate transport protein (2nd module)
AZ15	A2	dctA	DAACS family, C4-dicarboxylic acids transport protein
AZ15	A3	dppA	ABC superfamily (peri_bind) dipeptide transport protein (1st module)
AZ15	A4	alsB	subunit of D-allose ABC transporter
AZ15	A5	dcuA	Dcu family, anaerobic dicarboxylate transport protein
AZ15	A6	ybfG	conserved hypothetical protein
AZ15	A7	cvpA	membrane protein required for colicin V production
AZ15	A8	ybiJ	unknown CDS

AZ15	A9	nmpC	DLP12 prophage; outer membrane porin protein; at locus of qsr prophage (1st module)
AZ15	A10	ybiU	conserved hypothetical protein
AZ15	A11	ybiV	conserved protein, contains phosphatase-like domain
AZ15	A12	Empty	Empty well
AZ15	B1	ybjH	unknown CDS
AZ15	B2	ymcC	putative synthetase
AZ15	B3	yccM	putative ferredoxin-type protein
AZ15	B4	ybcV	DLP12 prophage; putative envelop protein (nohA?)
AZ15	B5	ybhI	putative DASS family transport protein (1st module)
AZ15	B6	potF	ABC superfamily (peri_bind) putrescine transporter (1st module)
AZ15	B7	oppA	ABC superfamily (peri_bind) , oligopeptide transport protein with chaperone properties
AZ15	B8	ydcS	putative ABC superfamily (peri_bind) transport protein

AZ15	B9	yeaV	putative BCCT family, betaine/choline/glycine transport protein
AZ15	B10	yejA	putative ABC superfamily (peri_bind) oligopeptide transport protein (1st module)
AZ15	B11	sstT	YgjU DAACS transporter
AZ15	B12	ybcY	DLP12 prophage; homolog of phage 21 head protein, putative methylase
AZ15	C1	yiiP	putative CDF family transport protein
AZ15	C2	ybdK	conserved hypothetical protein
AZ15	C3	serA	D-3-phosphoglycerate dehydrogenase
AZ15	C4	yjcE	putative CPA1 family, sodium:hydrogen transport protein (1st module)
AZ15	C5	b1367	Rac prophage;
AZ15	C6	ydbC	putative oxidoreductase, aldo/keto reductase family, NAD(P)-linked (2nd module)
AZ15	C7	ydbD	conserved hypothetical protein (2nd module)

AZ15	C8	ydcF	conserved hypothetical protein
AZ15	C9	yliE	conserved protein (2nd module)
AZ15	C10	U139	promoterless strain
AZ15	C11	ydcL	unknown CDS
AZ15	C12	ydcA	unknown CDS
AZ15	D1	ydcX	unknown CDS
AZ15	D2	stfE	e14 prophage; putative tail fiber protein
AZ15	D3	yncI	conserved protein
AZ15	D4	ydfZ	unknown CDS
AZ15	D5	yceP	unknown CDS
AZ15	D6	pspF	transcriptional activator of phage shock (EBP family) (1st module)
AZ15	D7	ycfS	putative enzyme
AZ15	D8	ycfD	putative enzyme
AZ15	D9	ycgX	putative phage protein
AZ15	D10	b1240	unknown CDS
AZ15	D11	yciA	putative enzyme
AZ15	D12	ybjQ	conserved hypothetical protein
AZ15	E1	ybjM	unknown CDS
AZ15	E2	betT	BCCT family, high-affinity choline transporter (2nd module)

AZ15	E3	entC	isochorismate synthetase, enterochelin biosynthesis (2nd module)
AZ15	E4	ytfQ	putative ABC superfamily (peri_bind), D-ribose transport protein
AZ15	E5	crcA	PagP monomer
AZ15	E6	ybjP	unknown CDS
AZ15	E7	ybjL	putative transport protein (2nd module)
AZ15	E8	yliG	conserved protein (2nd module)
AZ15	E9	fepB	ferric enterobactin ABC transporter
AZ15	E10	ybaE	putative ABC superfamily (peri_bind) transport protein
AZ15	E11	nanR	transcriptional repressor of sialic acid metabolism (GntR family) (1st module)
AZ15	E12	ppa	inorganic pyrophosphatase
AZ15	F1	ynaI	putative transmembrane protein
AZ15	F2	ydfE	Qin prophage;
AZ15	F3	U66	promoterless strain
AZ15	F4	ydgD	putative enzyme
AZ15	F5	ydgA	conserved protein

AZ15	F6	ydgK	putative oxidoreductase
AZ15	F7	ydgR	putative POT family, peptide transport protein (2nd module)
AZ15	F8	ydhR	unknown CDS
AZ15	F9	ydhS	putative oxidoreductase
AZ15	F10	wrbA	flavodoxin-like protein, trp repressor binding protein
AZ15	F11	ydiL	unknown CDS
AZ15	F12	kil	hypothetical protein
AZ15	G1	clpS	conserved hypothetical protein
AZ15	G2	ycaD	putative MFS family transport protein (1st module)
AZ15	G3	ycaK	putative electron transfer flavoprotein-NAD/FAD/quinone oxidoreductase
AZ15	G4	ycaP	conserved hypothetical protein (2nd module)
AZ15	G5	ftsQ	essential cell division protein FtsQ
AZ15	G6	ycdC	putative transcriptional repressor (TetR/AcrR family)
AZ15	G7	ymdE	putative malonyl-CoA:Acyl carrier protein transacylase
AZ15	G8	sraB	small RNA

AZ15	G9	ycfR	unknown CDS
AZ15	G10	ymfI	e14 prophage
AZ15	G11	ycgI	unknown CDS
AZ15	G12	ymgE	conserved hypothetical protein
AZ15	H1	lacZ	beta-galactosidase, lac operon
AZ15	H2	ushA	UDP-sugar hydrolase 5'- nucleotidase
AZ15	H3	ynfM	putative MFS family transport protein (1st module)
AZ15	H4	mdtK	putative MATE family transport protein (1st module)
AZ15	H5	yebQ	putative MFS family transport protein (1st module)
AZ15	H6	setA	MFS transporetr
AZ15	H7	selC	selenocysteinyI tRNA
AZ15	H8	racR	Rac prophage; putative prophage repressor
AZ15	H9	uxuA	mannonate hydrolase
AZ15	H10	lacY	MFS family, galactoside permease (M protein) (1st module)
AZ15	H11	araJ	MFS family, arabinose polymer transporter (1st module)

AZ15	H12	yajR	putative MFS family transport protein (1st module)
AZ16	A1	focA	FNT family transport protein (formate channel 1) (2nd module)
AZ16	A2	mdtG	putative MFS family transport protein (1st module)
AZ16	A3	narU	MFS superfamily, nitrate extrusion protein (1st module)
AZ16	A4	ydjE	putative MFS family transport protein (1st module)
AZ16	A5	yfcJ	putative MFS family transport protein (2nd module)
AZ16	A6	idnT	IdnT idonate Gnt transporter
AZ16	A7	yjhF	putative GntP family transport protein
AZ16	A8	dkgA	2,5-diketo-D-gluconate reductase A
AZ16	A9	yaaU	putative MFS family transport protein (1st module)
AZ16	A10	ygbN	putative GntP family transport protein (1st module)
AZ16	A11	b1403	IS21 protein 2
AZ16	A12	Empty	Empty well
AZ16	B1	yqhH	putative outer membrane lipoprotein

AZ16	B2	gmr	conserved protein (2nd module)
AZ16	B3	ymjA	unknown CDS
AZ16	B4	uspE	conserved protein with adenine nucleotide-binding domain (1st module)
AZ16	B5	ydaO	conserved protein
AZ16	B6	ydaG	Rac prophage;
AZ16	B7	uspF	conserved hypothetical protein with adenine nucleotide-binding domain
AZ16	B8	yncJ	unknown CDS
AZ16	B9	yddE	conserved protein
AZ16	B10	yddM	putative transcriptional regulator (OmpR family)
AZ16	B11	cspD	similar to CspA but not cold shock induced, nucleic acid-binding domain
AZ16	B12	ycaC	putative cysteine hydrolase
AZ16	C1	ycaN	putative transcriptional regulator (LysR family) (1st module)
AZ16	C2	ycaO	conserved hypothetical protein (3rd module)
AZ16	C3	serA	D-3-phosphoglycerate dehydrogenase

AZ16	C4	ycdM	putative enzyme
AZ16	C5	b1027	putative transposase-related protein
AZ16	C6	yceF	conserved protein
AZ16	C7	ycfQ	putative regulator (TetR/AcrR family)
AZ16	C8	b1142	e14 prophage
AZ16	C9	ydhP	putative MFS family transport protein (1st module)
AZ16	C10	U139	promoterless strain
AZ16	C11	b1172	conserved hypothetical protein
AZ16	C12	ycgR	putative regulator (TetR/AcrR family)
AZ16	D1	fsr	MFS family fosmidomycin transport protein (2nd module)
AZ16	D2	ynfL	putative transcriptional regulator (LysR family) (1st module)
AZ16	D3	ydhB	putative transcriptional regulator (LysR family)
AZ16	D4	ribE	riboflavin synthase, alpha chain
AZ16	D5	kdgR	putative transcriptional repressor (IclR family)
AZ16	D6	yabN	putative periplasmic binding protein of transport system (2nd module)

AZ16	D7	yebA	conserved protein
AZ16	D8	ptsA	General PTS family, enzyme I, phosphohistidine domain (1st module)
AZ16	D9	gntP	GntP family, gluconate transport protein, GNT III system (1st module)
AZ16	D10	ydcJ	conserved hypothetical protein
AZ16	D11	rssA	putative transmembrane protein
AZ16	D12	ompW	OmpW, outer membrane protein
AZ16	E1	ycjZ	putative transcriptional regulator (LysR family) (1st module)
AZ16	E2	fes	enterochelin esterase
AZ16	E3	cmr	MFS superfamily transporter, multidrug/chloramphenicol efflux transporter (1st module)
AZ16	E4	tonB	energy transducer; uptake of iron, cyanocobalimin; sensitivity to phages, colicins (1st module)
AZ16	E5	yhhT	putative PerM family permease (1st module)
AZ16	E6	pheP	APC family, phenylalanene transporter (2nd module)

AZ16	E7	chaC	cation transport regulator
AZ16	E8	nupG	MFS family, nucleoside transport (2nd module)
AZ16	E9	yniA	conserved protein, protein kinase- like
AZ16	E10	ydjX	putative YdjX-Z family transport protein
AZ16	E11	yddW	conserved protein with glycosyltransferase domain
AZ16	E12	yneE	putative transmembrane transporter
AZ16	F1	yneH	putative glutaminase
AZ16	F2	nohA	Qin prophage; packaging protein NU1
AZ16	F3	U66	promoterless strain
AZ16	F4	glnH	ABC superfamily (peri_bind) glutamine high-affinity transporter
AZ16	F5	hcaT	putative 3-phenylpropionic acid MFS family transport protein (1st module)
AZ16	F6	nanT	MFS family, sialic acid transport protein (1st module)

AZ16	F7	uhpT	MFS family, hexose phosphate transport protein, possible membrane subunit (1st module)
AZ16	F8	uhpA	response regulator (activator) in two-component regulatory system with UhpB, regulates carbon transport (LuxR/UhpA family)
AZ16	F9	ydcI	putative transcriptional regulator (LysR family) (1st module)
AZ16	F10	wrbA	flavodoxin-like protein, trp repressor binding protein
AZ16	F11	yehJ	conserved hypothetical protein
AZ16	F12	yciC	putative membrane protein (1st module)
AZ16	G1	ycjY	conserved hypothetical protein with alpha/beta-Hydrolase domain
AZ16	G2	fepA	outer membrane porin, receptor for ferric enterobactin (enterochelin) and colicins B and D (1st module)
AZ16	G3	narX	sensory histidine kinase in two component regulatory system with NarL, senses nitrate/nitrite,

			regulates anaerobic respiration and fermentation (2nd module)
AZ16	G4	yciI	conserved hypothetical protein
AZ16	G5	uxaC	uronate isomerase
AZ16	G6	ppiA	peptidyl-prolyl cis-trans isomerase A (rotamase A)
AZ16	G7	shiA	MFS family, shikimate and dehydroshikimate transport protein (1st module)
AZ16	G8	yncG	putative glutathione S-transferase
AZ16	G9	glpA	sn-glycerol-3-phosphate dehydrogenase FAD/NAD(P)-binding (anaerobic), large subunit (1st module)
AZ16	G10	fadL	transport of long-chain fatty acids; sensitivity to phage T2, porin
AZ16	G11	nupC	NUP family, nucleoside transport
AZ16	G12	yqeG	putative HAAAP family transport protein
AZ16	H1	lacZ	beta-galactosidase, lac operon
AZ16	H2	ygfU	putative NCS2 family transport protein (1st module)

AZ16	H3	pitA	PiT family, low-affinity phosphate transporter (1st module)
AZ16	H4	xylF	ABC superfamily (peri_bind) xylose transport protein
AZ16	H5	corA	MIT family, Mg ²⁺ /Ni ²⁺ /Co ²⁺ transport protein (Mg transport system I)
AZ16	H6	cysZ	required for sulfate transport
AZ16	H7	codB	NCS1 family, cytosine transporter (2nd module)
AZ16	H8	mscL	mechanosensitive channel
AZ16	H9	gntT	GntP family, high-affinity gluconate permease in GNT I system
AZ16	H10	zntA	P-type ATPase family, Pb/Cd/Zn/Hg transporting ATPase (2nd module)
AZ16	H11	lctP	LctP transporter, L-lactate permease (1st module)
AZ16	H12	rbsD	D-ribose high-affinity transport system; membrane-associated protein
AZ17	A1	mlc	transcriptional repressor for glucose uptake and glycolysis , global

			repressor of carbohydrate metabolism (NagC/XylR (ROK) family) (2nd module)
AZ17	A2	pitB	PiT family, low-affinity phosphate transporter (1st module)
AZ17	A3	fecA	outer membrane porin, receptor for ferric citrate, in multi-component regulatory system with cytoplasmic FecI (sigma factor) and membrane bound FecR (1st module)
AZ17	A4	ychM	putative SulP family transport protein (1st module)
AZ17	A5	xasA	putative APC family, glutamate:gamma-aminobutyric acid antiporter
AZ17	A6	chbA	Sugar Specific PTS family, cellobiose/arbutin/salicinsugar specific enzyme IIA component
AZ17	A7	b1997	CP4-44 prophage; IS2 protein
AZ17	A8	mtr	HAAAP family, tryptophan-specific transport protein
AZ17	A9	cadB	APC family, lysine/cadaverine transport protein

AZ17	A10	treB	Sugar Specific PTS family, trehalose(maltose)-specific enzyme IIBC component (2nd module)
AZ17	A11	ydiU	conserved protein
AZ17	A12	Empty	Empty well
AZ17	B1	ydiV	conserved protein
AZ17	B2	yeaE	putative oxidoreductase, NAD(P)- linked (1st module)
AZ17	B3	manY	Sugar Specific PTS family, mannose-specific enzyme IIC component
AZ17	B4	ygiI	putative APC family transport protein
AZ17	B5	frlA	putative APC family, methionine transport protein
AZ17	B6	yeeR	CP4-44 prophage; putative membrane protein
AZ17	B7	yeeV	CP4-44 prophage;
AZ17	B8	yegP	conserved hypothetical protein
AZ17	B9	yfaD	putative transposase (1st module)
AZ17	B10	yfdG	CPS-53 prophage, putative integral membrane protein
AZ17	B11	yfdQ	CPS-53 prophage (2nd module)

AZ17	B12	yffS	CPZ-55 prophage, putative transcriptional regulator
AZ17	C1	yfgH	putative outer membrane lipoprotein
AZ17	C2	yfhR	putative methylase or hydrolase (1st module)
AZ17	C3	serA	D-3-phosphoglycerate dehydrogenase
AZ17	C4	yfhL	putative ferredoxin
AZ17	C5	smpA	small membrane protein A
AZ17	C6	yfjI	CP4-57 prophage;
AZ17	C7	yqaD	unknown CDS
AZ17	C8	csiD	conserved protein (2nd module)
AZ17	C9	yncB	putative dehydrogenase, NAD(P) binding (2nd module)
AZ17	C10	U139	promoterless strain
AZ17	C11	ego	putative ABC superfamily (atp_bind) sugar transport protein (1st module)
AZ17	C12	nagE	multimodular NagE: PTS family enzyme IIC, n-acetylglucosamine-specific (1st module)

AZ17	D1	manX	PTS family, mannose-specific enzyme IIA component (1st module)
AZ17	D2	tyrP	HAAAP family, tyrosine-specific transport protein
AZ17	D3	srlA	split PTS system, glucitol/sorbitol-specific IIB component
AZ17	D4	yahO	unknown CDS
AZ17	D5	b1437	unknown CDS
AZ17	D6	yncA	putative antibiotic N-acetyltransferase
AZ17	D7	lsrR	putative transcriptional repressor
AZ17	D8	b0259	CP4-6 prophage; IS5 protein 1
AZ17	D9	nagB	glucosamine-6-phosphate deaminase
AZ17	D10	yoaE	putative transmembrane protein (1st module)
AZ17	D11	yecH	unknown CDS
AZ17	D12	yahN	putative transport protein
AZ17	E1	panB	3-methyl-2-oxobutanoate hydroxymethyltransferase
AZ17	E2	nagA	N-acetylglucosamine-6-phosphate deacetylase (2nd module)

AZ17	E3	grxB	glutaredoxin 2
AZ17	E4	pdxH	pyridoxine 5'-phosphate oxidase
AZ17	E5	dcd	2'-deoxycytidine 5'-triphosphate deaminase
AZ17	E6	thiM	hydroxyethylthiazole kinase (THZ kinase)
AZ17	E7	gshA	gamma-glutamate-cysteine ligase
AZ17	E8	gntK	gluconate kinase 2 in GNT I system, thermoresistant
AZ17	E9	grxC	glutaredoxin 3
AZ17	E10	nrdD	anaerobic ribonucleoside- triphosphate reductase
AZ17	E11	thiG	thiamine biosynthesis enzyme subunit, with ThiH
AZ17	E12	yehF	putative GTP-binding protein
AZ17	F1	kch	putative VIC family potassium channel protein
AZ17	F2	yehW	unknown CDS
AZ17	F3	U66	promoterless strain
AZ17	F4	mpaA	unknown CDS
AZ17	F5	pinR	Rac prophage; putative transposon resolvase

AZ17	F6	yddL	putative outer membrane porin protein
AZ17	F7	ydeQ	putative adhesin; similar to FimH protein
AZ17	F8	ydeV	putative sugar kinase (2nd module)
AZ17	F9	yneF	putative transport protein (1st module)
AZ17	F10	wrbA	flavodoxin-like protein, trp repressor binding protein
AZ17	F11	ydfI	putative mannitol dehydrogenase (2nd module)
AZ17	F12	cspI	Qin prophage; cold shock-like protein
AZ17	G1	grpE	Hsp 24 nucleotide exchange factor (1st module)
AZ17	G2	spy	periplasmic protein related to spheroblast formation
AZ17	G3	ydjF	putative transcriptional regulator (DeoR family) (1st module)
AZ17	G4	ydjL	putative dehydrogenase, NAD(P) binding
AZ17	G5	rrmA	23S rRNA m1G745 methyltransferase

AZ17	G6	proQ	protein that affects activity of ProP transporter
AZ17	G7	pphA	serine/threonine specific protein phosphatase 1, signals protein misfolding
AZ17	G8	torY	cytochrome c-type protein in trimethylamine N-oxide reductase system III with TorZ (1st module)
AZ17	G9	yaiN	conserved hypothetical protein
AZ17	G10	yeeX	conserved protein
AZ17	G11	yeeE	putative membrane component of transport system (1st module)
AZ17	G12	wcaJ	putative UDP-glucose lipid carrier transferase/glucose-1-phosphate transferase in colanic acid gene cluster
AZ17	H1	lacZ	beta-galactosidase, lac operon
AZ17	H2	yegW	putative transcriptional repressor
AZ17	H3	yehD	putative fimbrial-like protein (1st module)
AZ17	H4	yehZ	putative ABC superfamily (peri_bind) transport protein

			(possibly glycine betaine choline transport for osmoprotection)
AZ17	H5	yeiC	putative sugar kinase (2nd module)
AZ17	H6	yciT	putative transcriptional regulator (DeoR family) (2nd module)
AZ17	H7	ydcR	multimodular YdcR; putative transcriptional regulator (GntR family) (1st module)
AZ17	H8	stfR	Rac prophage; putative tail fiber protein (1st module)
AZ17	H9	ynbA	putative enzyme
AZ17	H10	ydcG	putative enzyme
AZ17	H11	ydcM	putative transposase
AZ17	H12	thiC	5'-phosphoryl-5-aminoimidazole = 4-amino-5-hydroxymethyl-2-methylpyrimidine-P
AZ18	A1	yhdJ	putative methyltransferase
AZ18	A2	b3218	IS5 protein
AZ18	A3	kefF	putative electron transfer flavoprotein-NAD/FAD/quinone oxidoreductase, subunit for KefC K ⁺ efflux system
AZ18	A4	dusB	conserved protein

AZ18	A5	ribC	riboflavin synthase, beta chain
AZ18	A6	thiL	thiamin-monophosphate kinase
AZ18	A7	gst	glutathionine S-transferase
AZ18	A8	nrdB	ribonucleoside-diphosphate reductase 1, beta subunit
AZ18	A9	nrdH	glutaredoxin-like protein; hydrogen donor
AZ18	A10	aceK	isocitrate dehydrogenase kinase/phosphatase, also has ATPase activity
AZ18	A11	aphA	subunit of acid phosphatase/phosphotransferase
AZ18	A12	Empty	Empty well
AZ18	B1	yibF	putative glutathione S-transferase (1st module)
AZ18	B2	ampD	N-acetyl-anhydromuramyl-L- alanine amidase
AZ18	B3	dgt	deoxyguanosine triphosphate triphosphohydrolase
AZ18	B4	ybjC	unknown CDS
AZ18	B5	fecI	sigma (19) factor of RNA polymerase, affected by FecR and

			outer membrane receptor FecA (TetR/ArcR family)
AZ18	B6	yfeK	conserved protein
AZ18	B7	yqiC	conserved protein
AZ18	B8	accB	acetylCoA carboxylase, BCCP subunit, carrier of biotin
AZ18	B9	trxA	thioredoxin 1, redox factor
AZ18	B10	yhgN	putative integral membrane protein
AZ18	B11	nadC	quinolinate phosphoribosyltransferase
AZ18	B12	panD	aspartate 1-decarboxylase
AZ18	C1	grxA	glutaredoxin1 redox coenzyme for glutathione-dependent ribonucleotide reductase
AZ18	C2	osmE	transcriptional activator of ntrL gene
AZ18	C3	serA	D-3-phosphoglycerate dehydrogenase
AZ18	C4	yfaL	conserved protein (2nd module)
AZ18	C5	pdxK	pyridoxal-pyridoxamine kinase/hydroxymethylpyrimidine kinase

AZ18	C6	ribB	3,4 dihydroxy-2-butanone-4-phosphate synthase
AZ18	C7	ggt	gamma-glutamyltranspeptidase (1st module)
AZ18	C8	rhlB	putative ATP-dependent helicase (2nd module)
AZ18	C9	asd	aspartate-semialdehyde dehydrogenase, NAD(P)-binding (1st module)
AZ18	C10	U139	promoterless strain
AZ18	C11	hdeD	conserved protein
AZ18	C12	yhjC	putative transcriptional regulator (LysR family) (1st module)
AZ18	D1	bcsE	unknown CDS
AZ18	D2	yiaG	putative transcriptional regulator
AZ18	D3	yiaU	putative transcriptional regulator (LysR family)
AZ18	D4	pgmI	phosphoglycerate mutase III, cofactor independent (3rd module)
AZ18	D5	yidL	putative transcriptional regulator (AraC/XylS family) (2nd module)
AZ18	D6	yidS	putative oxidoreductase with FAD/NAD(P)-binding domain

AZ18	D7	yidI	NA
AZ18	D8	yaiB	unknown CDS
AZ18	D9	bolA	activator of morphogenic pathway (BolA family), important in general stress response
AZ18	D10	ompX	outer membrane protease, receptor for phage OX2
AZ18	D11	yedP	conserved protein with phosphatase-like domain
AZ18	D12	atoS	sensory protein kinase in two-component regulatory system with AtoC (2nd module)
AZ18	E1	amiA	N-acetylmuramoyl-l-alanine amidase I
AZ18	E2	slp	outer membrane protein, induced after carbon starvation
AZ18	E3	rfaD	ADP-L-glycero-D-mannoheptose-6-epimerase, NAD(P)-binding
AZ18	E4	murC	L-alanine adding enzyme, UDP-N-acetyl-muramate:alanine ligase (1st module)

AZ18	E5	mrcB	bifunctional multimodular MrcB: transglycosyl transferase of penicillin- binding protein 1b (2nd module)
AZ18	E6	fhuA	outer membrane porine protein porin, receptor for ferrichrome, colicin M, and phages T1, T5, and phi80 (1st module)
AZ18	E7	ompG	outer membrane protein; novel porin
AZ18	E8	lpp	murein lipoprotein, links outer and inner membranes
AZ18	E9	rcaA	transcriptional activator of capsular/exo- polysaccharide synthesis (LuxR/UhpA family)
AZ18	E10	agn43	CP4-44 prophage; phase-variable outer membrane associated fluffing protein (2nd module)
AZ18	E11	mltC	membrane-bound lytic murein transglycosylase C
AZ18	E12	yidC	preprotein translocase, membrane component
AZ18	F1	murB	UDP-N- acetylenolpyruvoylglucosamine reductase, FAD-binding

AZ18	F2	fimD	outer membrane protein; export and assembly of type 1 fimbriae, interrupted
AZ18	F3	U66	promoterless strain
AZ18	F4	yjbB	putative PNaS family transport protein/regulator/enzyme (1st module)
AZ18	F5	yjbE	conserved hypothetical protein
AZ18	F6	yjbF	putative membrane associated protein
AZ18	F7	psiE	conserved hypothetical protein
AZ18	F8	yjbJ	unknown CDS
AZ18	F9	yjbI	conserved protein
AZ18	F10	wrbA	flavodoxin-like protein, trp repressor binding protein
AZ18	F11	dusA	conserved protein
AZ18	F12	yjbQ	conserved hypothetical protein
AZ18	G1	yjcD	conserved protein (1st module)
AZ18	G2	yjdK	unknown CDS
AZ18	G3	yjeI	conserved protein
AZ18	G4	yjeN	unknown CDS
AZ18	G5	b2861	IS2 protein
AZ18	G6	yjeB	conserved protein

AZ18	G7	yjfl	unknown CDS
AZ18	G8	yjfK	unknown CDS
AZ18	G9	ytfI	conserved hypothetical protein
AZ18	G10	yjgJ	unknown CDS
AZ18	G11	rscF	regulator in colanic acid synthesis; overexpression confers mucoid phenotype, increases capsule synthesis
AZ18	G12	ybbB	conserved hypothetical protein
AZ18	H1	lacZ	beta-galactosidase, lac operon
AZ18	H2	ompT	DLP12 prophage; protease VII; outer membrane protein 3b (a), putative porin
AZ18	H3	ompA	outer membrane protein 3a (II*;G;d) (2nd module)
AZ18	H4	hipB	transcriptional repressor which interacts with HipA
AZ18	H5	uidC	membrane-associated protein
AZ18	H6	cld	regulator of length of O-antigen component of lipopolysaccharide chains

AZ18	H7	pbpG	D-alanyl-D-alanine endopeptidase; penicillin-binding protein 7 and penicillin-binding protein 8
AZ18	H8	cirA	outer membrane porin, receptor for colicin I, requires TonB (1st module)
AZ18	H9	murA	UDP-N-acetylglucosamine 1- carboxyvinyltransferase
AZ18	H10	nanA	N-acetylneuraminate lyase (aldolase)
AZ18	H11	mreC	rod shape-determining protein
AZ18	H12	fadE	putative medium-/long-chain acyl- CoA dehydrogenase (4th module)
AZ19	A1	yhiL	unknown CDS
AZ19	A2	hdeA	conserved protein
AZ19	A3	yhjB	putative transcriptional regulator (LuxR/UhpA family)
AZ19	A4	yhjR	unknown CDS
AZ19	A5	yiaF	conserved protein
AZ19	A6	yiaJ	transcriptional repressor (IclR family)
AZ19	A7	yiaT	putative outer membrane protein, scaffolding protein?

AZ19	A8	yidK	putative SSS family, myo-inositor transporter, C term glycosyltransferase-like
AZ19	A9	yidR	conserved protein (2nd module)
AZ19	A10	yidH	conserved hypothetical protein
AZ19	A11	yajG	putative lipoprotein
AZ19	A12	Empty	Empty well
AZ19	B1	ddlA	D-alanine-D-alanine ligase A (2nd module)
AZ19	B2	ybiF	putative membrane protein
AZ19	B3	mipA	scaffolding protein for murein-synthesizing holoenzyme, outer membrane protein
AZ19	B4	dsrA	anti-sense RNA, silencer of rcsA gene, interact with rpoS translation
AZ19	B5	rscC	sensory histidine kinase in two-component regulatory system with RcsB, regulates colanic capsule biosynthesis (2nd module)
AZ19	B6	ypeA	putative acyltransferase
AZ19	B7	hofM	conserved hypothetical protein
AZ19	B8	b3505	IS5 protein

AZ19	B9	htrL	involved in lipopolysaccharide biosynthesis
AZ19	B10	rplT	50S ribosomal subunit protein L20, also posttranslational autoregulator
AZ19	B11	rpmI	50S ribosomal subunit protein A
AZ19	B12	rrfG	5S rRNA
AZ19	C1	rpsL	30S ribosomal subunit protein S12
AZ19	C2	rrnG	16S rRNA
AZ19	C3	serA	D-3-phosphoglycerate dehydrogenase
AZ19	C4	rpsP	30S ribosomal subunit protein S16
AZ19	C5	rpsO	30S ribosomal subunit protein S15
AZ19	C6	rrfD	5S rRNA
AZ19	C7	rrlD	23S rRNA
AZ19	C8	rpsM	30S ribosomal subunit protein S13
AZ19	C9	rplN	50S ribosomal subunit protein L14
AZ19	C10	U139	promoterless strain
AZ19	C11	yfhM	conserved protein
AZ19	C12	yphG	putative transferase
AZ19	D1	yfjG	conserved hypothetical protein
AZ19	D2	b2641	CP4-57 prophage;
AZ19	D3	yqaE	putative YqaE family transport protein

AZ19	D4	ygcW	putative deoxygluconate dehydrogenase
AZ19	D5	ygcF	putative coenzyme PQQ synthesis protein, nitrogenase iron-molybdenum domain
AZ19	D6	ygdI	unknown CDS
AZ19	D7	yqeK	unknown CDS
AZ19	D8	sseA	putative sulfurtransferase
AZ19	D9	yphH	putative transcriptional repressor (NagC/XylR (ROK) family) (2nd module)
AZ19	D10	smpB	small protein B
AZ19	D11	yfjW	CP4-57 prophage;
AZ19	D12	b2651	unknown CDS
AZ19	E1	ygaQ	unknown CDS
AZ19	E2	ygaV	conserved protein
AZ19	E3	yqcE	putative MFS family transporter (2nd module)
AZ19	E4	csdA	cysteine sulfinatase desulfinate
AZ19	E5	ygeF	conserved hypothetical protein
AZ19	E6	yjiM	putative 2-hydroxyglutaryl-CoA dehydratase
AZ19	E7	yjiA	putative cobalamin synthesis protein

AZ19	E8	yjiX	unknown CDS
AZ19	E9	yjiJ	putative sugar transporter (1st module)
AZ19	E10	yjjL	putative MFS family transport protein, cryptic, joins former yjiZ and yjjL
AZ19	E11	rpsJ	30S ribosomal subunit protein S10
AZ19	E12	rpmB	50S ribosomal subunit protein L28
AZ19	F1	rrlG	23S rRNA
AZ19	F2	rpsG	30S ribosomal subunit protein S7, initiates assembly
AZ19	F3	U66	promoterless strain
AZ19	F4	rmf	ribosome modulation factor (involved in dimerization of 70S ribosomes)
AZ19	F5	rrnH	16S rRNA
AZ19	F6	rrlH	23S rRNA
AZ19	F7	rrfH	5S rRNA
AZ19	F8	rpsA	30S ribosomal subunit protein S1 (3rd module)
AZ19	F9	rimL	acetyl transferase, modifies N-terminal serine of 50S ribosomal subunit protein L7/L12

AZ19	F10	wrbA	flavodoxin-like protein, trp repressor binding protein
AZ19	F11	rplY	50S ribosomal subunit protein L25
AZ19	F12	ssrA	10Sa RNA, non-ribosomal RNA, mediates tagging and proteolysis of incomplete polypeptides
AZ19	G1	rrfC	5S rRNA
AZ19	G2	rrnA	16S rRNA
AZ19	G3	rrlA	23S rRNA
AZ19	G4	rrnB	16S rRNA
AZ19	G5	rrfB	5S rRNA
AZ19	G6	rplL	50S ribosomal subunit protein L7/L12
AZ19	G7	rrfE	5S rRNA
AZ19	G8	rrlB	23S rRNA
AZ19	G9	rrlE	23S rRNA
AZ19	G10	yidX	unknown CDS
AZ19	G11	yieH	putative enzyme with a phosphatase-like domain
AZ19	G12	fabR	putative regulator (TetR/AcrR family)
AZ19	H1	lacZ	beta-galactosidase, lac operon
AZ19	H2	yiiR	conserved protein

AZ19	H3	nudC	conserved hypothetical protein, MutT-like protein
AZ19	H4	rimJ	acetylation of N-terminal alanine of 30S ribosomal subunit protein S5
AZ19	H5	rpsU	30S ribosomal subunit protein S21
AZ19	H6	rrnC	16S rRNA
AZ19	H7	dgoR	putative transcriptional repressor (GntR family)
AZ19	H8	yieG	conserved protein (1st module)
AZ19	H9	yihU	putative oxidoreductase (1st module)
AZ19	H10	yiiQ	conserved protein
AZ19	H11	sthA	pyridine nucleotide transhydrogenase
AZ19	H12	rsd	regulator of sigma D, has binding activity to the major sigma subunit of RNAP
AZ20	A1	mdtH	putative MFS superfamily transport protein
AZ20	A2	ygjD	putative O-sialoglycoprotein endopeptidase
AZ20	A3	yjfY	unknown CDS
AZ20	A4	rrnD	16S rRNA

AZ20	A5	ftsZ	tubulin-like GTP-binding protein and GTPase, forms circumferential ring in cell division
AZ20	A6	fliF	flagellar biosynthesis; basal-body MS(membrane and supramembrane)-ring and collar protein
AZ20	A7	phoR	sensory kinase in two-component regulatory system with PhoB, regulates pho regulon (2nd module)
AZ20	A8	clpX	specificity component of clpA-clpP ATP-dependent serine protease, chaperone
AZ20	A9	yebB	unknown CDS
AZ20	A10	fliE	flagellar biosynthesis; basal-body component
AZ20	A11	gyrB	DNA gyrase, subunit B (type II topoisomerase) (1st module)
AZ20	A12	Empty	Empty well
AZ20	B1	malF	ABC superfamily (membrane) maltose transport protein (2nd module)

AZ20	B2	flgM	anti-FliA (anti-sigma) factor; also known as RflB protein
AZ20	B3	rhaT	DMT Superfamily, L-rhamnose:H ⁺ symporter protein (1st module)
AZ20	B4	relA	(p)ppGpp synthetase I (GTP pyrophosphokinase)
AZ20	B5	uvrC	UvrC with UvrAB is a DNA excision repair enzyme (1st module)
AZ20	B6	ihfB	IHF transcriptional dual regulator
AZ20	B7	cynT	carbonic anhydrase
AZ20	B8	flgB	flagellar biosynthesis, cell-proximal portion of basal-body rod
AZ20	B9	htpG	chaperone Hsp90, heat shock protein C 62.5
AZ20	B10	yjjY	hypothetical protein
AZ20	B11	cynR	transcriptional regulator of cyanate metabolism (LysR family) (1st module)
AZ20	B12	ydfV	Qin prophage;
AZ20	C1	lacZ	beta-D-galactosidase (1st module)
AZ20	C2	motA	proton conductor component of motor, torque generator

AZ20	C3	serA	D-3-phosphoglycerate dehydrogenase
AZ20	C4	ompR	transcriptional regulator in two-component regulatory system with EnvZ, affects outer membrane protein synthesis (OmpR family) (1st module)
AZ20	C5	relB	Qin prophage; part of two-component toxin-antitoxin system with RelE, transcriptional repressor of relBE operon
AZ20	C6	uvrY	putative transcriptional regulator for damaged DNA repair (LuxR/UhpA family)
AZ20	C7	cyaA	adenylate cyclase
AZ20	C8	rhaS	positive regulator for L-rhamnose catabolism (AraC/XylS family) (2nd module)
AZ20	C9	chaB	cation transport regulator
AZ20	C10	U139	promoterless strain
AZ20	C11	argU	arginine tRNA 4
AZ20	C12	garD	galactarate dehydratase

AZ20	D1	oxyR	transcriptional regulator of oxidative stress, regulates intracellular hydrogen peroxide (LysR family)
AZ20	D2	araE	MFS family, L-arabinose: proton symport protein (low-affinity transporter) (1st module)
AZ20	D3	rhaD	rhamnulose-1-phosphate aldolase (2nd module)
AZ20	D4	tar	subunit of MCP-II
AZ20	D5	ompC	outer membrane protein 1b (ib;c), porin (1st module)
AZ20	D6	ndk	nucleoside diphosphate kinase
AZ20	D7	ruvA	Holliday junction helicase subunit A (1st module)
AZ20	D8	rpoD	sigma D (sigma 70) factor of RNA polymerase, major sigma factor during exponential growth (2nd module)
AZ20	D9	dsdX	Gnt family transport protein (1st module)
AZ20	D10	fliL	flagellar biosynthesis
AZ20	D11	greB	transcription elongation factor and transcript cleavage

AZ20	D12	katG	catalase; hydroperoxidase HPI(I)
AZ20	E1	araB	L-ribulokinase (2nd module)
AZ20	E2	glnA	glutamine synthetase (2nd module)
AZ20	E3	ligB	putative DNA ligase
AZ20	E4	araD	L-ribulose-5-phosphate 4-epimerase (1st module)
AZ20	E5	gpp	guanosine pentaphosphatase and exopolyphosphatase
AZ20	E6	polB	DNA polymerase II and and 3' --> 5' exonuclease
AZ20	E7	uvrD	DNA-dependent ATPase I and helicase II (1st module)
AZ20	E8	dnaK	chaperone Hsp70 in DNA biosynthesis/cell division (1st module)
AZ20	E9	gmk	guanylate kinase
AZ20	E10	ybeL	conserved hypothetical protein
AZ20	E11	sodA	superoxide dismutase, manganese
AZ20	E12	rhaB	rhamnulokinase
AZ20	F1	leuA	2-isopropylmalate synthase
AZ20	F2	rpoH	sigma H (sigma 32) factor of RNA polymerase; transcription of heat

			shock proteins induced by cytoplasmic stress
AZ20	F3	U66	promoterless strain
AZ20	F4	hlyE	hemolysin E
AZ20	F5	yiiU	conserved hypothetical protein
AZ20	F6	araC	transcriptional regulator of arabinose catabolism (AraC/XylS family)(2nd module)
AZ20	F7	gltB	glutamate synthase, large subunit (2nd module)
AZ20	F8	dnaJ	chaperone with DnaK; heat shock protein
AZ20	F9	groE	GroES, 10 Kd chaperone binds to Hsp60 in pres. Mg-ATP, suppressing its ATPase activity
AZ20	F10	wrbA	flavodoxin-like protein, trp repressor binding protein
AZ20	F11	lexA	transcriptional repressor for SOS response (signal peptidase of LexA family)
AZ20	F12	rpoS	sigma S (sigma 38) factor of RNA polymerase, major sigma factor during stationary phase

AZ20	G1	hemC	hydroxymethylbilane synthase (porphobilinogen deaminase)
AZ20	G2	pstS	ABC superfamily (peri_bind) high-affinity phosphate transporter
AZ20	G3	fliA	sigma F (sigma 28) factor of RNA polymerase, transcription of late flagellar genes (class 3a and 3b operons)
AZ20	G4	rpoE	sigma E (sigma 24) factor of RNA polymerase, response to periplasmic stress (TetR/ArcR family)
AZ20	G5	recA	DNA strand exchange and recombination protein with proteiase and nuclease activity (1st module)
AZ20	G6	arcB	multimodular ArcB: membrane part of sensory histidine kinase in two-component regulatory system with ArcA, senses redox conditions (1st module)
AZ20	G7	malX	Sugar Specific PTS family, maltose and glucose-specific IIC (1st module)

AZ20	G8	phoA	modular PhoA: alkaline phosphatase (2nd module)
AZ20	G9	lon	DNA-binding, ATP-dependent protease Ia; cleaves RcsA and Sula, heat shock k-protein (ATP ase activity) (2nd module)
AZ20	G10	yecF	unknown CDS
AZ20	G11	umuD	component of DNA polymerase V, signal peptidase with UmuC
AZ20	G12	trpL	trp operon leader peptide
AZ20	H1	lacZ	beta-galactosidase, lac operon
AZ20	H2	lacI	transcriptional repressor of lactose catabolism (GalR/LacI family)
AZ20	H3	dsdC	transcriptional regulator of D-serine dehydratase (deaminase) (LysR family) (1st module)
AZ20	H4	fliY	cysteine binding periplasmic transport protein, sulfate starvation induced
AZ20	H5	malI	transcriptional repressor of maltose regulon (GalR/LacI family)
AZ20	H6	galP	MFS family, galactose:proton symporter (1st module)

AZ20	H7	rpsT	30S ribosomal subunit protein S20
AZ20	H8	ubiG	3-demethylubiquinone-9 3-methyltransferase and 2-octaprenyl-6-hydroxy phenol methylase
AZ20	H9	phoB	response regulator in two-component regulatory system with PhoR (or CreC) , regulates Pi uptake (OmpR family) (1st module)
AZ20	H10	clpP	proteolytic subunit of clpA-clpP ATP-dependent serine protease, heat shock protein F21.5
AZ20	H11	yeaH	conserved hypothetical protein
AZ20	H12	ssb	ssDNA-binding protein controls activity of RecBCD nuclease
AZ21	A1	yoaD	conserved protein (2nd module)
AZ21	A2	yfbM	conserved protein
AZ21	A3	yafZ	hypothetical protein
AZ21	A4	gudP	YgcZ MFS transporter
AZ21	A5	cvrA	YcgO CPA1 Transporter
AZ21	A6	ybjG	putative permease
AZ21	A7	aqpZ	AqpZ - water MIP channel
AZ21	A8	yebF	unknown CDS

AZ21	A9	lacA	galactoside O-acetyltransferase monomer, subunit of galactoside O-acetyltransferase
AZ21	A10	araF	arabinose ABC transporter